Nuclear Factor I and Calpain Signaling in Glioblastoma

by

Minh The Vo

A thesis submitted in partial fulfillment of the requirements for the degree of

Doctor of Philosophy

in

Cancer Sciences

Department of Oncology
University of Alberta

Abstract

Glioblastoma (GBM), classified as WHO grade IV astrocytoma, is the most common and lethal adult primary brain tumour. Despite recent advances in treatment, GBM prognosis remains largely unchanged with most patients succumbing to the disease within ~15 months of diagnosis. This dismal outcome can be attributed in part to its highly infiltrative nature, with tumour cells spreading into normal brain parenchyma at early stages of the disease. We and others have shown that the expression of brain fatty acid-binding protein (FABP7) correlates with increased GBM cell migration *in vitro* and a worse prognosis. In GBM, *FABP7* is regulated by the Nuclear factor I (NFI) family of four transcription factors: NFIA, B, C, X. These transcription factors, specifically NFIA and NFIB, have been shown to play key roles in regulating neural cell migration and gliogenesis.

We have also demonstrated that NFI transcriptional activity is dependent on its phosphorylation state, with hypophosphorylated NFI associated with FABP7 expression. NFIs are dephosphorylated by the calcineurin phosphatase in GBM cells. Calcineurin, in turn, is cleaved and activated by calpain proteases. Ubiquitously-expressed calpain 1 and calpain 2, the best characterized members of the calpain family, have been shown to be master regulators of cell migration, with functions spanning all major steps of this process. Importantly, calpain 2 is essential for the infiltration of GBM cells in a zebrafish model. Calpain proteolytic activity is tightly regulated by the cell, with the most well-known mechanisms being autoproteolysis and regulation by its endogenous inhibitor, calpastatin (encoded

by the *CAST* gene). Previous work from our lab has identified *CAST* as a putative target of NFI in GBM cells.

Here, we confirm NFI binding to a *de novo CAST* alternative promoter. We show that binding of hypophosphorylated NFI to *CAST* intron 3 results in increased utilization of the alternative promoter and a higher ratio of class 2 (encoding for XL-less calpastatin isoforms) to class 1 (encoding for full-length calpastatin) *CAST* variants, which ultimately leads to altered subcellular distribution of calpastatin. Our findings provide a foundation for further investigations into the possibility of regulatory crosstalk between NFI and the calpain pathway.

To this end, we identify two NFI-calpain positive feedback loops with opposing effects in GBM: NFIB-calpain 1 and NFIA-calpain 2. We provide evidence for two distinctive mechanisms by which differentially phosphorylated NFIB can increase calpain 1 activity. In turn, calpain 1, via calcineurin, promotes NFIB dephosphorylation, a process that is accompanied by altered subnuclear distribution and transcriptional activity of NFIB. We also show that the NFIB-calpain 1 positive feedback loop acts to suppress cell migration while having little to no effect on GBM cell viability. In contrast, we found only one mechanism by which NFIA can increase calpain 2 activity. Like calpain 1, calpain 2 cleaves and activates calcineurin, which dephosphorylates NFIA and causes an increase in FABP7 expression. The NFIA-calpain 2 crosstalk acts to increase GBM cell migration and survival. These NFI-calpain positive feedback loops can be exploited with calpain inhibitors to reduce GBM cell survival.

Preface

The research presented hereafter was conducted with assistance or in collaboration as noted below.

Chapter 2 has been published as **Vo TM,** Burchett R, Brun M, Monckton EA, Poon HY, Godbout R. *Effects of nuclear factor I phosphorylation on calpastatin (CAST) gene variant expression and subcellular distribution in malignant glioma cells*. **Journal of Biological Chemistry**, **(2019)** 294(4):1173-88. The majority of RT-qPCR and immunofluorescence experiments were performed by R. Burchett who worked under my supervision as a project and summer student. This chapter was based on the findings of M. Brun. Many of the gel shifts and western blots were carried out by E. Monckton and H.Y. Poon. I was responsible for forming hypothesis, designing and performing experiments, interpreting results and writing the manuscript.

Chapter 3 has been accepted for publication as **Vo TM,** Jain S, Burchett R, Monckton EA, and Godbout R. *A positive feedback loop involving nuclear factor IB and calpain 1 suppresses glioblastoma cell migration*. **Journal of Biological Chemistry**, **(2019)** Jul 1. pii: jbc.RA119.008291. The majority of GBM cell migration and survival experiments were carried out by S. Jain. Some of the RT-qPCR experiments were carried out by R. Burchett. Most of the nuclear and cytoplasmic fractionations were carried out by E. Monckton E and were based on my instructions. I was responsible for forming hypothesis, designing and performing experiments, interpreting results and writing the manuscript.

Chapter 4 is being prepared for publication as **Vo TM**, Jain S, Burchett R, Monckton EA, and Godbout R. *Nuclear Factor IA and calpain 2 positive feedback loop positively regulates glioblastoma cell migration and cell survival*. The majority of GBM cell migration and survival experiments were carried out by S. Jain. Some of the RT-qPCR experiments were carried out by R. Burchett. Nuclear and cytoplasmic fractionations were carried out by E. Monckton based on my instructions. I was responsible for forming hypothesis, designing and performing experiments, interpreting results and writing the manuscript.

Dedication

"*Aut viam inveniam aut faciam*"

Hannibal Barca (247-182 BCE)

To my parents, Võ Ngọc Minh (1964-2009) and Nguyễn Thị Liên, for their unconditional love, selfless sacrifice, invaluable guidance and unwavering faith.

To my brothers, Võ Minh Thanh and Võ Minh Thuận, for their lifetime support.

Acknowledgements

First and foremost, I would like to express my deepest gratitude to my supervisor Dr. Roseline Godbout, whose insights and guidance have made my study of “pain” an enthralling intellectual journey. Without her continued assistance and support, above and beyond the academic realm, I would not have been able to achieve my Canadian dream. Dr. Godbout’s excellence in research and mentorship, as well as her integrity and honesty, will serve as the standard against which my actions as a scientist, or simply as a person, shall be measured.

I would like to thank all other members of the Godbout Lab: Miranda Brun, for initiating the NFI/calpain line of investigation; Rebecca Burchett, for identifying and optimizing myriad of experimental conditions; Saket Jain, for handling the cell migration and survival assays; Elizabeth Monckton, for generating DNA constructs, performing routine experiments and troubleshooting technical difficulties; Stanley Poon, for teaching and carrying out multiple western blot experiments; Lei Li and Rong-Zong Liu for teaching me a variety of experimental procedures and answering countless number of questions; and finally my fellow students, Jack Wang, Xia Xu and Daniel Choi, for accompanying me through this unforgettable journey.

I sincerely thank members of my supervisory committee, Dr. Gordon Chan and Dr. David Eisenstat, for their continued support and insightful feedbacks on my research objectives and techniques. I am also grateful for the Department of Oncology office personnel, including Yvette Labiuk and Jennifer Freund, for providing an excellent support for us, Cancer Sciences students. I am indebted to

Dr. Sun and Gerry of the CCI Cell Imaging Facility for their invaluable support with immunofluorescence analysis. Finally, I would like to thank all faculty members of the Division of Experimental Oncology for their generosity in providing necessary reagents and technical expertise.

Table of Contents

List of Figures

List of Tables

Abbreviations

2-HG	2-Hydroxyglutarate
5’-RLM RACE	5' - RNA Ligase-Mediated Rapid Amplification of cDNA Ends
AA	Anaplastic Astrocytoma
ACM	Aclacinomycin A, Aclarubicin
ACTB	Beta-Actin
AIF	Apoptosis-Inducing Factor
Akt	Protein Kinase B
ALLN	Calpain Inhibitor I
ALT	Alternative Promoter
AMPA	Alpha-Amino-3-Hydroxy-5-Methylisoxazole-4-Propionate
AP2	Activating Protein 2
ATRX	ATP-Dependent Helicase X-Linked Helicase II
Bax	Bcl-2-Like Protein 4
BBB	Blood-Brain-Barrier
BCL-2	B-Cell Lymphoma 2
BCNU	Carmustine
Bid	Bax-Like BH3
BSA	Bovine Serum Albumin
CaMKII/IV	Ca2+/Calmodulin-Dependent Protein Kinase Type II/IV
cAMP	Cyclic Adenosine Monophosphate
CAPN1/2	Large Subunit of Calpain 1/2
CAPSN1	Calpain 1/2 Small Subunit
Cas9	CRISPR-Associated Protein 9
CAST	Calpastatin
CCNU	Lormustin
CDK	Cyclin-Dependent Kinases
CDKN	Cyclin Dependent Kinase Inhibitor
cDNA	Complementary DNA
ChIP	Chromatin Immunoprecipitation
CIP	Calf Intestinal Alkaline Phosphatase
CNA	Calcineurin A
CNB	Calcineurin B
CNS	Central Nervous System
CNT	Control
CP	Canonical Promoter
CRISPR	Clustered Regularly Interspaced Short Palindromic Repeats
CsA	Cyclosporin A
CT	Computed Tomography

CTF	CCAAT-Binding Transcription Factor
DAPI	4,6-Diamino-2-Phenylindole
dCTP	Deoxycytidine Triphosphate
DMEM	Dulbecco's Modified Eagle Medium
DMSO	Dimethylsulfoxide
DNA	Deoxyribonucleic Acid
EDTA	Ethylenediaminetetraacetic Acid
EGFR	Epidermal Growth Factor Receptor
ERK	Extracellular Signal-Regulated Kinase
ESCC	Esophageal Squamous Cell Carcinoma
EZH2	Enhancer of Zeste 2 Polycomb Repressive Complex 2 Subunit
FABP7, B-FABP	Brain Fatty Acid-Binding Protein
FAK	Focal Adhesion Kinase
FBS	Fetal Bovine Serum
FDA	U.S. Food and Drug Administration
FGFR3	Fibroblast Growth Factor Receptor 3
FK506	Tacrolimus
GABRA6	Gamma-Aminobutyric Acid Type A Receptor 6
GAPDH	Glyceraldehyde 3-Phosphate Dehydrogenase
GBM	Glioblastoma
G-CIMP	Glioma-CpG Island Methylator Phenotype
GFAP	Glial Fibrillary Acidic Protein
GLAST	Glutamate Aspartate Transporter Gene
HA	Hemagglutinin
HCl	Hydrochloric Acid
HEPES	4-(2-Hydroxyethyl)-1-Piperazineethanesulfonic Acid
HER2	Epidermal Growth Factor Receptor 2
HGFR	Hepatocyte Growth Factor Receptor
HRP	Horseradish Peroxidase
IDH	Isocitrate Dehydrogenase
IgE/G	Immunoglobulin E/G
IκBα	Inhibitor ff NF-κB
JAK2	Janus Kinase 2
K_d	Dissociation Constant
kDa	Kilo Dalton
KLF4	Krüppel-Like Factor 4
LTP	Long-Term Potentiation
MARCKS	Myristoylated Alanine-Rich C-Kinase Substrate
m-calpain	Calpain 2
MDM2/4	Mouse Double Minute 2/4 Homolog
MG	Malignant Glioma

MGMT	O6-Methylguanine-Dna Methyl Transferase
MMP2	Matrix Metalloproteinase 2
M-MuLV	Moloney Murine Leukemia Virus
MRI	Magnetic Resonance Imaging
mRNA	Messenger RNA
mTOR	Mechanistic Target of Rapamycin
NAD	Nicotinamide Adenine Dinucleotide
NADPH	Nicotinamide Adenine Dinucleotide Phosphate
NE	Nuclear Extract
NFAT	Nuclear Factor of Activated T Cells
NFI	Nuclear Factor I
NF-κB	Nuclear Factor Kappa-Light-Chain-Enhancer of Activated B Cells
NLS	Nuclear Localization Signal
NOS	Not-Otherwise-Specified
NPC	Neural Progenitor Cells
OLIG2	Oligodendrocyte Transcription Factor 2
PBS	Phosphate Buffered Saline
PDGFRA	Platelet Derived Growth Factor Alpha
PEI	Polyethyleneimine
PI	Phosphatidylinositol
PI3K	Phosphatidylinositol 3-Kinase
PKA	Protein Kinase A
PKC_{δ}	Protein Kinase C Isoform delta
PP2B	Protein Phosphatase 2B
PPP3	Protein Phosphatase 3
PTEN	Suppressor Phosphatase and Tensin Homolog
RB	Retinoblastoma
RCAN	Regulator of Calcineurin
RhoA	Ras Homolog Gene Family, Member A
RLU	Relative Light Unit
RNA	Ribonucleic Acid
RNA Pol II	RNA Polymerase Ii
ROS	Reactive Oxygen Species
RT	Radiotherapy
RTK	Receptor Tyrosine Kinase
RT-qPCR	Real-Time Quantitative Polymerase Chain Reaction
SCLC	Small Cell Lung Cancer
SDS-PAGE	Sodium Dodecyl Sulfate Polyacrylamide Gel Electrophoresis
siRNA	Small Interfering RNA
SOX	SRY-Related HMG Box

STAT3	Signal Transducer and Activator Of Transcription 3
SV40	Simian Virus 40
TAP	Tobacco Acid Pyrophosphatase
TBE	Tris/Borate/EDTA
TCGA	The Cancer Genome Atlas Research Network
TGF-β	Transforming Growth Factor Beta
TNF-α	Tumour Necrosis Factor Alpha
TMZ	Temozolomide
VEGF-A	Vascular Endothelial Growth Factor A
WBRT	Whole-Brain Radiotherapy
WCE	Whole Cell Lysate
WHO	World Health Organization
α-KG	α-Ketoglutarate
αPIX	PAK-Interacting Exchange Protein
λ-phosphatase	Lambda Phosphatase
μ-calpain	Calpain 1

CHAPTER 1: INTRODUCTION

1.1 Glioma

1.1.1 Glioma classification and epidemiology

The central nervous system (CNS) is comprised of two broad classes of cells: neurons which are responsible for information processing and glia which provide support for neurons (1). CNS tumours have traditionally been classified largely based on their histopathological features (2). Gliomas, believed to arise from glial or glial-like cells, account for ~80% of all primary malignant brain tumours (3). Gliomas can be divided into sub-categories based on cell type, including but not limited to tumours of astrocytic (astrocytomas), oligodendroglial (oligodendrogliomas) and ependymal (ependymomas) origins (2). Astrocytic tumours can be further stratified into four different grades (I to IV), with lower grades (I-II) indicating more differentiated and benign tumours, whereas higher grades (III and IV) indicate less differentiated and more malignant tumours (4,5). The prognosis for high-grade tumours is generally worse than that of low-grade tumours (6). However, recent advances in whole genome sequencing have led to the reconsideration of the classification scheme of CNS tumours (7).

As of 2016, CNS tumours have been classified based not only on their phenotypic but also on genotypic parameters (8). In fact, genetic signatures may outweigh histological features to reach a more unified diagnostic scheme (Figure 1.1). Due to the importance of accurate tumour classification, reflected by the ability to predict biological behaviour and recommend appropriate treatment, neurooncologists are encouraged to append the genetic features of CNS tumours to the histopathological diagnoses (8). Some of the common genetic tests include

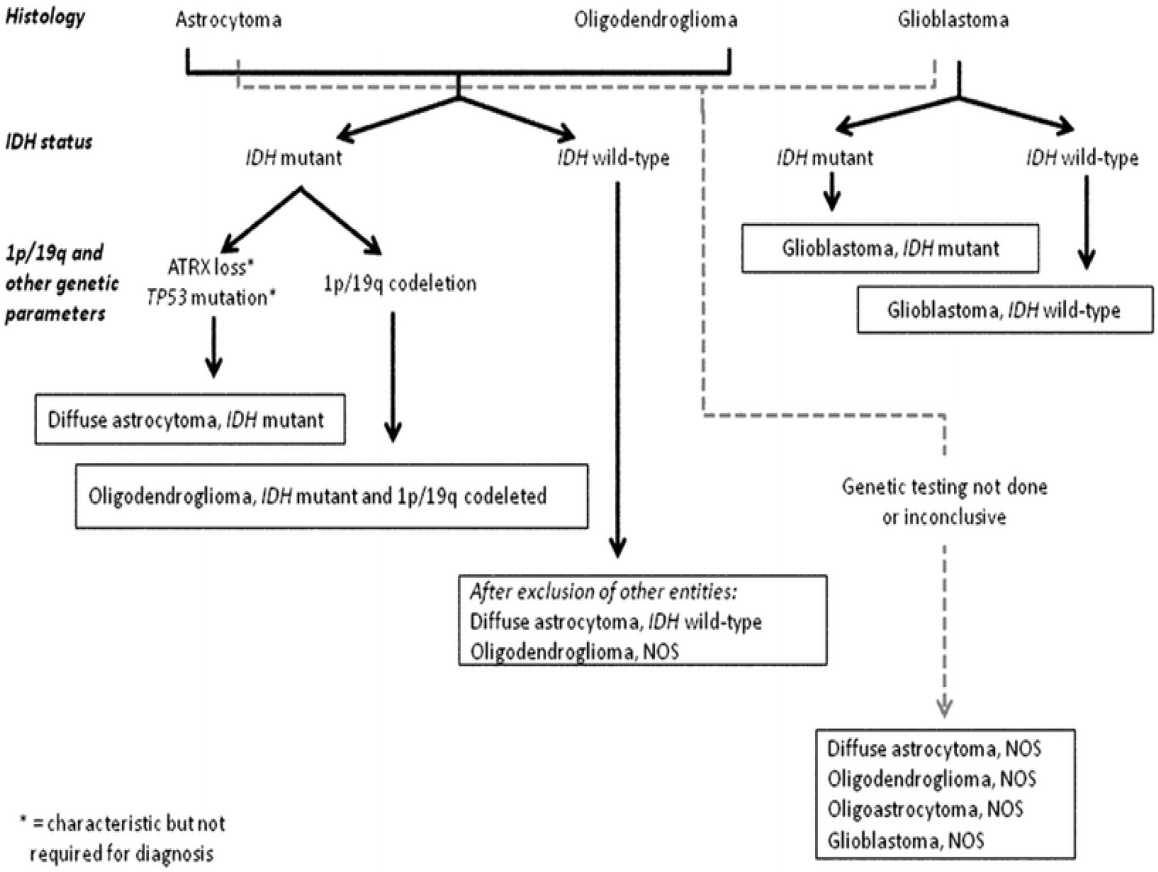

Figure 1.1. Use of histological and genotypic characteristics in the classification of gliomas

IDH, isocitrate dehydrogenase; ATRX, ATP-dependent helicase X-linked helicase II; NOS, not-otherwise-specified. Reproduced from Louise *et al.* (8) with permission from the Acta Neuropathologica Journal.

isocitrate dehydrogenase (*IDH*) (9) and *TP53* mutations (10), 1p/19q co-deletion (11), as well as epidermal growth factor receptor (*EGFR*) amplification and/or mutation (12). Besides providing terminological accuracy in both clinical and research contexts, as well as consistency for international communications, these molecular signatures reflect advances in our understanding of CNS tumours, the etiology of which remain largely unknown.

Despite advances in the field of glioma epidemiology, few risk factors associated with these tumours have been identified. Only one type of environmental factor, high doses of ionizing radiation, has been directly linked to glioma tumorigenesis (13). Exposure to high doses of radiation is common when cancers are treated with radiation, including that used to treat children with leukemia (14). These children may develop gliomas at later stages in life (15). A second confirmed glioma risk factor is hereditary mutations in highly penetrant genes, which tend to be associated with rare genetic syndromes (16). One example is germline mutation of *TP53* (encoding p53 – the guardian of the genome), a defining characteristic of Li-Fraumeni syndrome. These hereditary mutations predispose affected individual to a wide variety of malignancies, 10% of which are gliomas (17,18). Preliminary evidence obtained from recent studies have demonstrated an inverse correlation between glioma incidence rate and high levels of serum IgE, typically observed in individuals with allergic conditions (19). Risk factors for specific subcategories of glioma are currently unknown.

1.1.2 Astrocytomas and malignant glioma

Amongst gliomas, astrocytic tumours (Figure 1.2) are the most frequently encountered in the clinical setting (20). Grade I astrocytomas including pilocytic astrocytoma and subependymal giant cell astrocytoma are defined as well-circumscribed tumours with a low proliferative index (21). These tumours typically occur in children or young adults and can be cured with surgery alone as they seldomly recur or transform into higher grades (22). In contrast, grade II astrocytomas, encompassing diffuse astrocytoma and the less commonly known pleomorphic xanthoastrocytoma, are often more infiltrative and may transform into higher grade tumours (8,23). However, their proliferative potential remains comparable to that of grade I tumours (5). Anaplastic astrocytoma (AA) together with the rare anaplastic pleomorphic xanthoastrocytoma make up grade III astrocytomas (8). These tumours often have a high proliferative index and nuclear atypia in conjunction with extensive infiltration (3).

Based on genetic features, grades II (diffuse astrocytoma) and III (anaplastic astrocytoma) astrocytic tumours can be subdivided into *IDH*-wildtype or *IDH*-mutant, with the majority of these tumours falling into the latter category (24). Although the exact mechanism is not clear, patients with *IDH*-mutant grade II and III astrocytomas typically survive longer than those with *IDH*-wildtype tumours, indicating the prognostic power of this genetic marker (25,26). Moreover, *IDH* status carries a significant diagnostic power. *IDH*-wildtype anaplastic astrocytoma is so rare that its diagnosis is routinely re-evaluated to avoid misdiagnosis of glioblastoma (GBM), also known as grade IV astrocytoma (7,24).

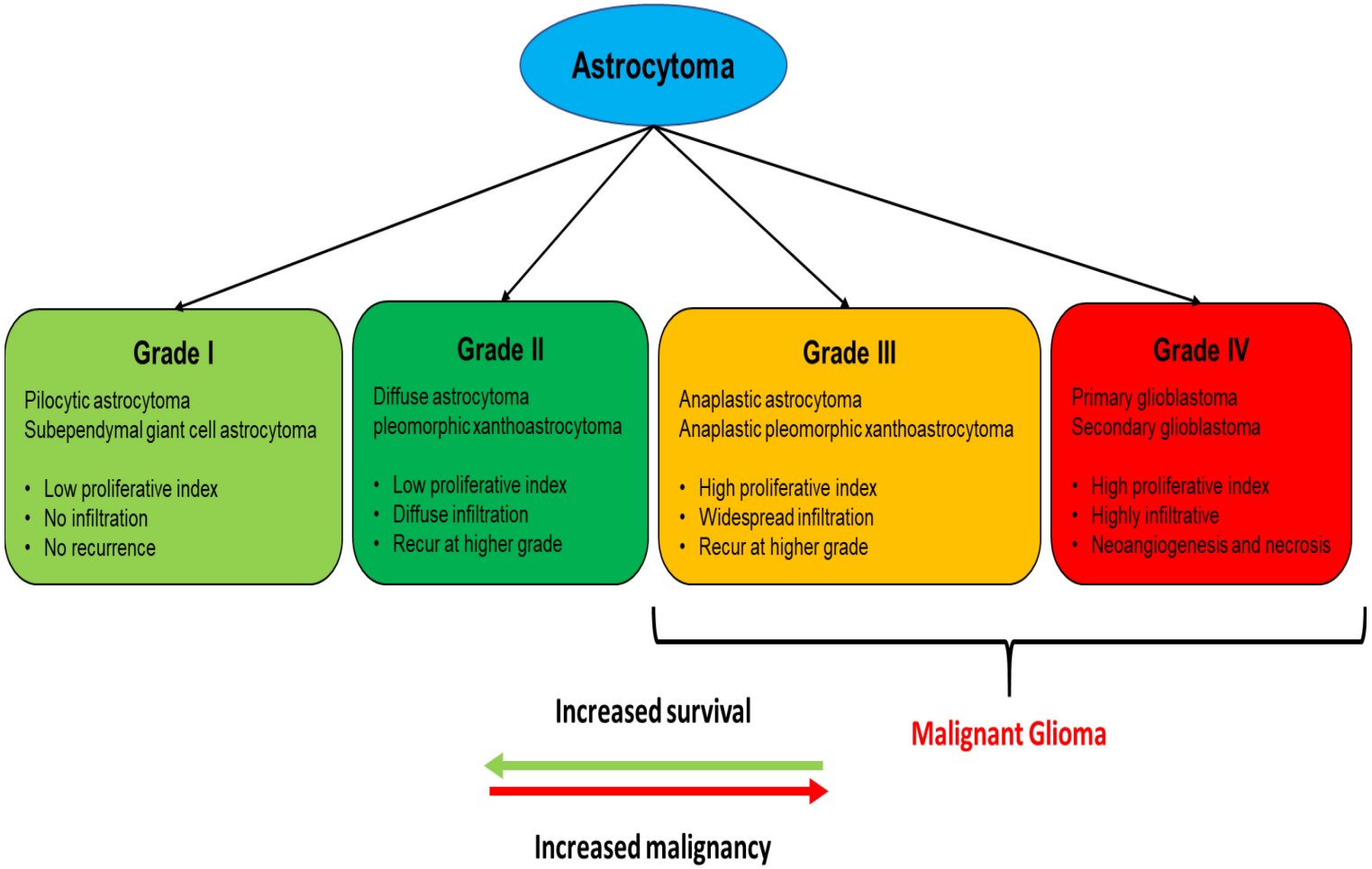

Figure 1.2. Astrocytoma classification

Similar to grade II and grade III astrocytomas, adult GBM is divided into *IDH*-wildtype and *IDH*-mutant, with the former accounting for ~90% of GBM diagnosis (27). *IDH*-wildtype GBM, clinically known as primary GBM, arises *de novo* in patients over 55 years old without prior evidence of lower grade tumours and typically carries the worst prognosis amongst astrocytomas (28). In contrast, *IDH*-mutant or secondary GBM, frequently observed in younger patients, results from the progression of diffuse or anaplastic astrocytomas and carries better prognosis compared to *IDH*-wildtype GBM (29). If IDH testing is not available, grade II-IV astrocytomas will be classified based on their histopathological characteristics, followed by NOS (not-otherwise-specified) designation (8).

Grades III and IV astrocytic tumours, collectively referred to as malignant glioma (MG), represent the most common and aggressive form of primary adult brain cancers, with the majority of patients succumbing to the disease within 5 years (grade III astrocytoma) or 1.5 years (grade IV astrocytoma) of diagnosis (23). In the United States, approximately 17,000 new MG cases are reported each year, most of which affect patients 60 to 80 years of age with a ratio of 3 males to 2 females (20,30). MG is twice as likely to occur in Caucasians than Africans, with Asians and American Indians being less likely to be diagnosed with the disease (31). Age-adjusted analysis of glioma rates over the 1979-2008 period in Nordic countries revealed that MG incidence remains relatively stable, with no noticeable increasing or decreasing trend (15).

1.1.3 Glioblastoma: diagnosis, treatment, survival and challenges

GBM is the most commonly diagnosed form of all glioma tumours, and has a median survival time of ~15 months with a 5-year survival probability of less than 5% (3,32). As a result, GBM is the primary focus of both research and clinical investigative efforts dedicated to brain cancer. Research in the field of GBM has resulted in a sounder understanding of many aspects of this disease including epidemiology, etiology, diagnosis, treatment and palliative care.

Patients with primary GBM often present at late stages of the disease when symptoms, including neural deficits, cognitive impairment, headaches and seizures, are apparent (33). GBM is diagnosed on the basis of imaging, including invasive techniques and non-invasive techniques such as computed tomography (CT) and magnetic resonance imaging (MRI) (34). Following tumour visualization and confirmation, surgical resection is often prescribed to: (i) alleviate the effect of the mass by removing the bulk of the tumour, (ii) provide samples for a more accurate diagnosis with definitive histopathological and genetic characteristics, and (iii) insert local therapeutic agent if desired (35). However, the inherently infiltrative and heterogenous nature of GBM cells undermines the curative effects of surgery. Furthermore, the location of some GBM tumours may render resection impossible (35). In instances where surgery is possible, gross total resection is advised, with strong consideration given to the maintenance of normal brain function, as there is a strong correlation between a more complete removal of the tumour and increased survival time (36-39). Despite its infiltrative capacity, GBM tumours rarely metastasize from the CNS (40).

In the late 1970's, whole-brain radiotherapy (WBRT) following surgical resection was shown to significantly improve patient survival time compared to supportive care alone (41-43). Although technological advances now allow fractionated (~2 Gy over 6 weeks) delivery of external radiation beams, the total dose is still limited to 60 Gy (44-46). Beyond this threshold, RT failed to improve patient survival while inflicting damage to normal brain tissue (47,48). In fact, a pioneering clinical trial done here at the Cross Cancer Institute has demonstrated that hypofractionated RT (40 Gy in 15 fractions over 3 weeks), while offering no improvement in survival time for elderly GBM patients, has a more favourable toxicity profile compared to standard course RT, laying the foundation for the potential use of abbreviated RT course for the treatment of GBM (49). Beyond the alteration of radiation doses and schedule, more accurate delivery mechanisms of radiation beams are being explored. The LINAC-MR project, an MRI-guided linear accelerator also being developed at the Cross Cancer Institute, allows for a more precise field of treatment by monitoring and compensating for real-time movements of the intended target (50).

In addition to radiation, GBM patients were traditionally treated with DNA alkylating drugs including nitrosourea-based compounds, carmustine (BCNU) and lomustine (CCNU), amongst other chemotherapeutic agents (41). However, these drugs are highly toxic and offer little to no improvement over RT alone (51). In 2005, a landmark study demonstrated the superiority of RT with concomitant and adjuvant temozolomide (TMZ), an oral DNA-alkylating agent, in improving patient survival compered to RT alone (12.1 months versus 14.6 months) (52). Also, 2-

year and 5-year survival rates of GBM patients increased from 10.4% to 26.5% and from 1.9% to 9.8%, respectively (53) for patients who received radiotherapy and temozolomide compared to patients who received radiotherapy alone. As a result, the current standard-of-care for GBM in most countries, including Canada, includes concurrent administration of TMZ (75 mg/m^2 over 42 days) followed by six cycles of adjuvant TMZ (150-200 mg/m^2/day for 5 consecutive days every 28 days) (54,55). TMZ induces its genotoxicity by alkylating DNA mainly at the O^6 guanine position, creating the cytotoxic O^6-methylguanine lesion, which can be reversed by the O^6-methylguanine-DNA methyl transferase (MGMT). When treated with TMZ, GBM patients whose *MGMT* promoter is methylated (and silenced) have higher median survival times compared to those carrying the unsilenced *MGMT* gene (21.7 months vs 15.3 months) (56). Unfortunately, most patients will eventually develop resistance to TMZ, allowing the tumour to progress. Without effective second-line treatment, GBM recurrence often results in death.

Due to their inability to cross the blood-brain-barrier (BBB), most conventional orally- and intravenously-administered chemotherapeutic agents are ineffective against GBM. However, the emergence of molecular-targeted therapies raises new, perhaps overly optimistic, hope for a better approach to GBM treatment. One of the defining characteristics of GBM tumour is its abnormal network of neovasculature, the formation of which can be targeted with anti-angiogenic drugs (57). To this end, bevacizumab, a humanized monoclonal antibody against vascular endothelial growth factor A (VEGF-A), is currently being used for recurrent GBM (54). Unfortunately, the clinical benefits of bevacizumab

are limited in the case of GBM, with no improvement in overall survival for newly diagnosed patients (58). Other low molecular weight molecules targeting a variety of relevant signaling pathways in GBM are being investigated (59). However, signaling pathways redundancy together with the heterogenous nature of GBM cells pose a significant barrier toward the successful development of these agents (60).

The most exciting field of investigation in tumour biology at this time is immunotherapy. The brain was previously thought to be an immune-privileged site due to the BBB and lack of a typical lymphatic drainage system (61). However, recent findings have challenged this notion. It has been shown that brain tumour-derived antigens can be drained into cervical lymph nodes and presented to specific T-cells, which subsequently can migrate into the CNS and kill the tumour cells (62,63). Consequently, a wide range of therapies aimed at activating the immune system, including antigen-specific vaccines and immune checkpoint blockade, are being developed for GBM (64).

1.1.4 Glioblastoma molecular biology and tumourigenesis

The greatest barrier toward effective treatment of GBM may be our lack of understanding of the diversity of this disease, which is further complicated by intratumour heterogeneity. Recent efforts by The Cancer Genome Atlas Research Network (TCGA) have resulted in the identification of four adult GBM molecular subtypes: proneural, neural, mesenchymal and classical (65). Each subtype carries a specific genetic profile (Figure 1.3), and thus may respond differently to

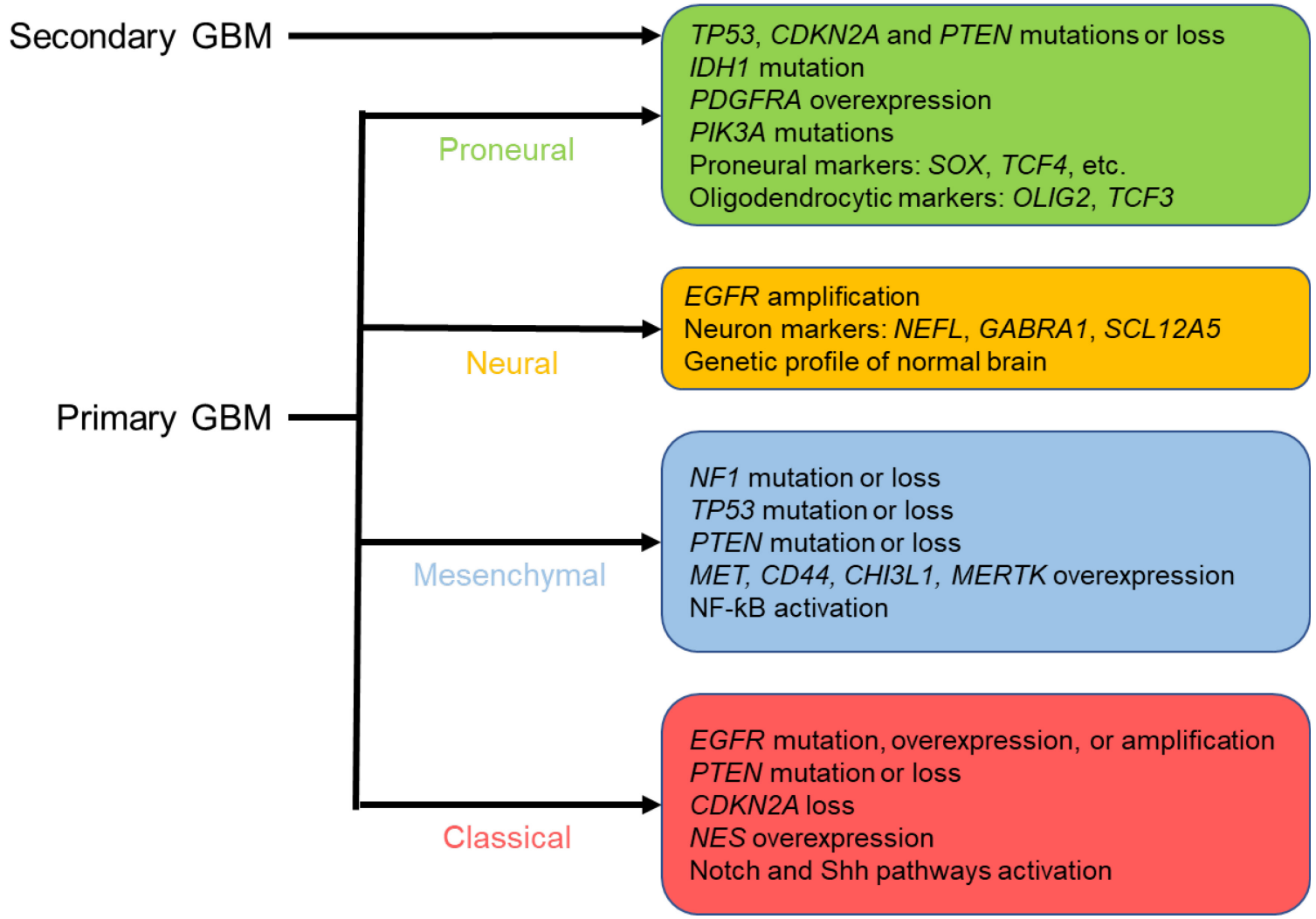

Figure 1.3. Glioblastoma molecular subtypes

the current standard-of-care for GBM. Decades of research have identified numerous signaling pathways relevant to GBM tumourigenesis. However, almost three-quarters of GBM tumours carry concurrent alterations in the following three pathways: p53, retinoblastoma (pRB) and receptor tyrosine kinase (RTK)/phosphatidylinositol 3-kinase (PI3K) (66-68). Aberrant signaling in these three core pathways grants GBM important hallmarks of cancer, including increased cell survival and proliferation as well as compromised cell cycle checkpoints and apoptotic signaling (69).

Disruption in the p53 signaling pathway is observed in 87% of GBM (66,70). The importance of the p53 pathway in GBM tumourigenesis is expected because p53, a well-known tumour suppressor, is encoded by the most commonly mutated gene in all malignancies. As the guardian of the genome, p53 induces cell cycle arrest and apoptosis in response to genotoxic and cytotoxic stress (71). In the absence of stress stimuli, p53 is directly bound and its transcriptional activity inhibited by mouse double minute 2 homolog (MDM2) (72). Furthermore, as an E3 ubiquitin ligase, MDM2 ubiquitinates and targets p53 for subsequent proteasomal degradation (72,73). Similarly, MDM4 – another negative regulator of p53 – has been found to be overexpressed in GBM (74). In addition, the $p14^{ARF}$ tumour suppressor, an upstream positive regulator of p53, is frequently mutated or deleted in GBM (66). As a result, suppression of p53 activity can be achieved through the overexpression of MDM2/4 or loss of $p14^{ARF}$, without having to alter p53 or its encoding gene *TP53* (66,74,75). Beside its relevance in primary GBM, *TP53* mutations are detected in 65% of diffuse (grade II) astrocytoma, indicating that

disruption in p53 signaling may be the driver for the development of secondary GBM (10,70).

Mutations in the *RB1* gene (encoding pRB) occur in at least 20% of high-grade gliomas and loss of RB protein (pRB) is commonly detected in primary GBM (76,77). The association between *RB1* mutations and GBM tumourigenesis can be attributed to pRB's role as a master regulator of cell proliferation. By interacting and inhibiting the activity of E2F transcription factors, pRB prevents the activation of genes involved in cell cycle growth and division (78). Progression of the cell cycle from G1 to S phase is contingent on the phosphorylation of pRB by cyclin-dependent kinases (CDK) 4 and 6 and subsequent release of E2F from pRB (78). Consequently, CDK inhibitors including CDKN2B, CDKN2C, and $p16^{INK4A}$ can prevent G1-S progression by keeping pRB in a dephosphorylated state and bound to E2F transcription factors (78). As observed for the p53 pathway, dysregulation of pRB signaling can occur through multiple mechanisms: mutation or deletion of the *RB1* gene, amplification of CDKs or loss of CDK inhibitors (66,79). Although mechanistically different, these alterations lead to uncontrolled proliferation of GBM cells.

Alteration in the PI3K signaling pathway occurs in ~70% of GBMs (77). Whereas p53 and pRB functions primarily involve intrinsic signaling pathways, the PI3K complex links extracellular growth factor with internal processes of the cell, including survival, metabolism, differentiation and proliferation (80). Of all the different types of disruptions in the RTK/PI3K pathway, amplification of EGFR signaling remains one of the most frequently encountered alterations in GBM

(81,82). Aberrant EGFR/PI3K signaling can be induced by overexpression of wildtype EGFR (~45% of GBMs) or the expression of EGFRvIII, a constitutively active and ligand-independent EGFR mutant (~50% of GBMs) (70,83-85). Besides EGFR, other RTKs are able to activate the PI3K pathway in GBM including epidermal growth factor receptor 2 (HER2), platelet derived growth factor alpha (PDGFRA*)* and hepatocyte growth factor receptor (HGFR) (66). Of various downstream effectors of PI3K, the tumour suppressor phosphatase and tensin homolog (*PTEN)* appears to be the most commonly affected, with 36% of GBM tumours carrying mutations in, or deletion of, this gene (66,82). Loss of PTEN activity results in further upregulation of PI3K signaling, which leads to increased tumour cell proliferation and invasion (80,81).

In addition to the three core pathways (p53, pRB1 and PI3K), advances in whole genome/transcriptome sequencing have shone light on other signaling pathways that are frequently altered in GBM. As previously described, *IDH* is fundamental to the classification of astrocytomas including GBM and is mutated in 12-20% of GBM tumours, with higher incidence in secondary (85%) compared to primary GBM (5%) tumours (9,68,86). Although little is known about how *IDH* mutation contributes to GBM tumourigenesis, GBM patients with *IDH* mutation have improved survival compared to *IDH* wildtype patients (82). IDH1 catalyzes NAD^+-dependent decarboxylation of isocitrate to α-ketoglutarate (α-KG) (87). All *IDH1* mutations in glioma are characterized by a missense mutation at residue 132, with >85% of these resulting in an arginine to histidine substitution (9,88). Analogous mutations in *IDH2* at arginine position 172 (R172H) have also been

documented (88). IDH1 R132H and IDH2 R172H mutants can no longer convert isocitrate into α-KG, but instead convert isocitrate into 2-hydroxyglutarate (2-HG) (82,89). By competing with α-KG, 2-HG can inhibit the activity of several histone demethylases and cause widespread methylation of CpG islands, also known as the glioma-CpG island methylator phenotype (G-CIMP) (68,90). Virtually all G-CIMP GBM tumours carry *IDH* mutations and have a significantly better prognosis (68,91). With further technological advances, one can safely predict that our understanding of molecular pathways underlying glioma tumourigenesis will only become more complex and may lead to reclassification of these tumours.

1.2 The Nuclear Factor I (NFI) family

1.2.1 The NFI family and its expression in embryogenesis

Nuclear Factor I (NFI) transcription factor, also called CCAAT-binding transcription factor (CTF) due to its affinity for CCAAT elements, was initially known for its role in the replication of viral genomes (92-95). NFI is sequence-specific and has been shown to bind the palindromic consensus sequence: TTGGC(N_{3-6})GCCAA (96-99). DNA sequence analyses have identified putative NFI-binding elements in a large number of genes, many of which are tissue-specific including lung, muscle and brain (100-104). So far, four NFI genes have been identified in vertebrates (*NFIA*, *NFIB*, *NFIC* and *NFIX*), the transcripts of which undergo further alternative splicing, creating a diverse array of NFI isoforms with different transcriptional activity (Figure 1.4) (105-110). Each NFI is comprised of a highly conserved N-terminal domain responsible for DNA binding and

dimerization and a variable C-terminal domain responsible for transactivation or repression of target genes (Figure 1.4) (111,112). NFIs function as either homo- or hetero-dimers, with similar *in vitro* affinities and specificities (112-115).

Different NFI members exert unique transcriptional control on a single promoter, likely because of the variability in the C-terminal transactivation domain (116). How NFI activates transcription is not fully understood although a proline-rich domain identified in all four NFIs has been shown to induce transcription of NFI target genes (111,115,117). The NFIC proline-rich domain contains an heptapeptide repeat (PTSPSYS), similar to that observed in RNA polymerase II, allowing NFI to interact with the general transcription factor TFIIB and TATA-box binding protein (118-120). Despite the lack of a well-conserved heptapeptide repeat, other NFI members can still function as transcription factors, suggesting other mechanisms for NFI-mediated transcriptional regulation (117,121). For example, NFI can alter chromatin structure by interacting with histone proteins (122,123). Importantly, NFI can act as a master regulator of gene expression, especially during development, through its interaction with other transcription factors including but not limited to forkhead box A1 (124), thyroid transcription factor 1 (125), and Sry-related HMG box (Sox) 9 and 10 (126,127).

The expression profiles of the four NFI genes are complex, with both unique and overlapping patterns observed during mouse embryogenesis. *Nfia* is first to be expressed in the developing brain, followed by *Nfic* in the dorsal root ganglia (128). Subsequently, expression of *Nfib* and *Nfix* is detected in both the neocortex and ventricular zone (128). *NFI* knockout models further reveal roles for NFIA,

Figure 1.4. NFI members, isoforms, general domain structure and phosphorylation sites

Adapted from Chen *et al.* (129) with permission from the Cancer Letters Journal.

NFIB and NFIX in the developing mouse brain (130-132). Knockout of *Nfia* in mice results in perinatal lethality, with further examination of *Nfia-/-* brains revealing partial or complete loss of the corpus callosum, accumulation of cerebrospinal fluid (hydrocephalus), midline glial structural abnormality, and delayed brain maturation (130,131,133). In addition to the phenotypes observed in *Nfia*-/- mice, *Nfib-/-* brains exhibit loss of neural progenitor cells (NPCs), resulting in abnormal cerebral cortex neurogenesis (134-137). *Nfix-/-* mice are characterized by postnatal lethality, with hyperproliferation of NPCs and delayed neuronal and glial differentiation (132,138-140). In contrast, *Nfic* knockout mice are viable although they demonstrate disruption in tooth root development (141). Further genetic analysis of *Nfi*-/- mice also identified complex compensatory pathways for different NFI genes. For example, *Nfia* expression is increased in *Nfib-/-* mice and higher levels of *Nfib* are observed in *Nfia-/-* brains, demonstrating crosstalk between different NFI members (133,137).

1.2.2 Role of NFI in gliogenesis and neuronal development

Given the frequency and severity of neural defects, especially the delay in glial differentiation and maturation observed upon knocking out different members of the NFI family, it is evident that NFI plays an important role in regulating gliogenesis. In addition, NFI has been shown to regulate the expression of the glial fibrillary acidic protein (*GFAP*) gene, a specific marker for differentiated astrocytes (142). Based on *in situ* hybridization analysis of murine embryonic spinal cord, *Nfia* and *Nfib* expression is induced in the ventricular zone at the onset of gliogenesis,

concomitant with that of the glutamate aspartate transporter gene (*GLAST*) – an early marker of gliogenesis (143). Misexpression of NFIA and NFIB results in premature induction of glial-specific genes, including *GLAST* and fibroblast growth factor receptor 3 (*FGFR3*) (143,144). Notch-induced Sox9 signaling induces the expression of NFIA, followed by demethylation and expression of astrocytic genes in differentiating neural precursor cells (142,145). Also, misexpression of NFIA and NFIB leads to accelerated expression of *GFAP*, suggesting that these two NFIs promote terminal differentiation of astrocytes (143). In contrast, NFIA has been shown to suppress the differentiation of neural progenitor cells into oligodendrocytes by counteracting the effects of Sox10 (127,146). By interacting with NFIA, Sox10 negatively regulates NFIA-dependent astrocyte-specific genes including *GFAP* and thereby promotes the differentiation of glial precursors into oligodendrocytes (146) (127). These findings indicate that NFI, particularly NFIA, promotes the commitment of glial precursors to the astrocytic lineage over the oligodendroglial lineage.

In addition to its functions in gliogenesis, NFI also plays important roles in neuronal development. NFIB expression is detected in both neuronal cells of developing murine olfactory bulbs and excitatory neurons of the subventricular zone in adult brain (147). NFI activates the expression of gamma-aminobutyric acid type a receptor 6 (GABRA6), a specific marker for mature granular neurons in the cerebellum (148,149). In maturing cerebellar granular neurons, NFI target genes are often occupied by the nuclear factor of activated T cells (NFAT) due to the close proximity of their binding elements, preventing NFI from inducing the

terminal differentiation of these neurons (150). As a result, when NFAT binding to these genes is reduced, NFI can induce the maturation of cerebellar granular neurons, including axon extension, migration, dendritogenesis, and synapse formation (150-153).

Other studies have also demonstrated a role for NFI in the maintenance of neural precursor cells. NFIA knockdown leads to reduced numbers of astrocytic (FGFR3-expressing) and oligodendroglial [oligodendrocyte transcription factor (Olig) 2-expressing)] progenitor cells (143). NFIA depletion also reduces the expression of *Hes5*, a Notch effector gene essential for the self-renewal of neural precursor cells (154). In fully-developed brain, NFI is expressed in the subventricular zone, which is enriched in stem cells (138,147). Genetic and epigenetic analyses reveal that NFI binding motifs are enriched and occupied in self-renewing and quiescent neural stem cells (155,156). These findings indicate that the role of NFI in the CNS is dynamic, such that NFI promotes glial and neuronal differentiation during embryogenesis but acts to maintain the neural stem cell population in adult brain (156,157).

1.2.3 Regulation of NFI transcriptional activity

Mechanisms underlying the regulation of NFI transcriptional activity are not completely understood. In 1988, NFI was reported to be post-translationally modified with O-glycosylation (158). Two years later, NFI was reported to be phosphorylated by DNA-dependent protein kinase (159). Subsequently, NFI was found to be phosphorylated by CDK1; however, this phosphorylation does not

appear to affect the binding affinity of NFI to DNA, suggesting that phosphorylation may have unknown effects on NFI (160). Early empirical evidence implicating post-translational phosphorylation in the regulation of NFI transcriptional activity was obtained in c-Myc overexpressing 3T3-L1 cells (161). Whereas only one form of NFI was detected in wildtype quiescent 3T3-L1 adipocytes, three differentially phosphorylated forms of NFI were observed upon overexpression of c-Myc in these cells (161). Although different forms of phosphorylated NFI have similar DNA binding affinities, overexpression of c-Myc results in decreased transcription from NFI-dependent promoters, indicating that NFI phosphorylation is important for regulating its transcriptional activity (161).

NFI is phosphorylated by Janus kinase 2 (Jak2) in mammary epithelial cells, preventing NFI from being degraded and thereby increasing levels of NFI transcriptional activity (162). As a result, phosphorylation appears to activate NFI transcriptional activity. In contrast, our group has demonstrated that NFI is differentially phosphorylated in a panel of 10 GBM cell lines, with hypophosphorylated NFI correlated to the expression of NFI target genes: *FABP7* and *GFAP* (163). Of considerable interest, we have previously shown that NFI dephosphorylation is mediated by the calcium-dependent calcineurin phosphatase (164). Consequently, phosphorylation seems to suppress NFI activity in GBM cells. These findings suggest that post-translational phosphorylation may serve as a modulatory mechanism for NFI activity rather than being a simple on/off switch.

Besides phosphorylation, other mechanisms underlying the regulation of NFI transcriptional activity have been reported. A transforming growth factor beta

(TGF-β)-responsive element was identified in the proline-rich domain of NFIC (123). Binding of TGF-β to this domain results in induction of NFIC activity. However, occupation of the proline-rich domain by the tumour necrosis factor alpha (TNF-α) leads to suppression of NFIC activity (165). Importantly, mutation of phosphorylation sites located in the proline-rich domain to which TGF-β and TNF-α bind did not affect their ability to alter NFIC transcriptional activity (165). Together, these observations suggest that NFI activity can be altered through phosphorylation-independent mechanisms, including protein-protein interaction.

1.2.4 Role of NFI in malignant glioma

Because of its extensive involvement in normal development, including gliogenesis, abnormal expression of NFI and dysregulation of its regulatory network are commonly observed in many cancers, including GBM (Figure 1.5). Whereas NFIA expression is barely detectable in other forms of brain tumours, NFIA is highly expressed in all grades of astrocytoma (166,167). In fact, ectopic expression of NFIA in oligodendrogliomas is sufficient to induce an astrocytic-shift in these tumours (168), in agreement with the role of NFIA in promoting terminal differentiation of astrocytes during development (167). In addition, *NFIA* mRNA is significantly upregulated in GBM tumours compared to normal brain, with most of the NFIA-positive cells being detected in infiltrative GBM cells (167). However, the functional consequence of increased NFIA expression in GBM remains controversial. NFIA has been shown to promote GBM tumourigenesis through the negative regulation of both *TP53* and *CDKN1A* genes (169). Moreover, NFIA forms

NFIA

Role in development	*Role in cancer*
Brain	
Driver of astroglial differentiation	TSG/oncogene in astrocytoma
Astroglial-oligodendroglial cell fate determinant and maintains mature oligodendrocytes	TSG in oligodendroglioma
Driver of postmitotic CGN differentiation	TSG in medulloblastoma
Bone marrow	
Lineage fate determinant that favours the megakaryocyte-erythroid lineage progression over granulocyte-monocyte lineage progression	TSG in excessive erythroblastosis-type of myeloproliferative disorders, acute erythroid leukemia, and T-cell lymphomas

NFIC

Role in development	*Role in cancer*
Mammary gland	
Driver of epithelial cell differentiation and/or apoptosis, but no known function in maintaining the differentiated cell state	TSG in ER-positive and ER-negative breast carcinomas
Bone	
Regulator of osteoblast proliferation, differentiation, and migration	TSG in osteosarcoma
Bone marrow	
Driver of megakaryocyte differentiation from megakaryocyte-erythroid progenitors	TSG in T-cell lymphomas

NFIX

Role in development	*Role in cancer*
Brain	
Driver of astroglial differentiation	Oncogene in astrocytoma

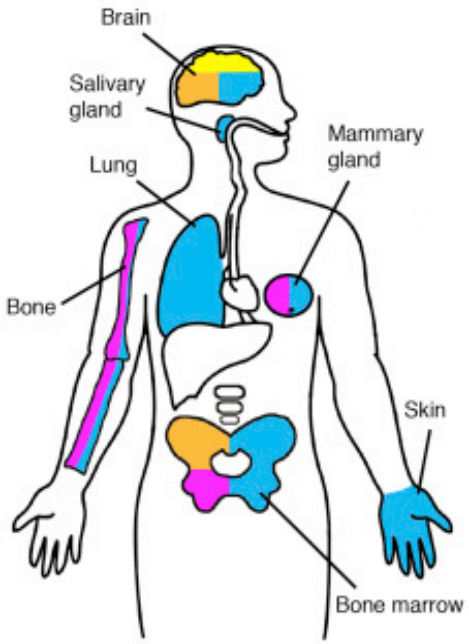

NFIB

Role in development	*Role in cancer*
Brain	
Driver of astroglial differentiation	TSG in astrocytoma
Salivary gland	
Driver of submandibular gland tubule cell differentiation	TSG in AdCC
Lung	
Driver of mesenchymal-to-epithelial differentiation and maintains epithelial cells	TSG in NSCLC
Mammary gland	
Transcriptional regulator of mammary-specific proteins, but no known function in mammary gland epithelial cell differentiation.	Oncogene in ER-negative breast carcinoma
Skin	
Maintains melanocyte stem cell quiescent state	Oncogene/TSG in cutaneous melanoma
	Oncogene in uveal melanoma
Bone marrow	
Driver of megakaryocyte differentiation from megakaryocyte-erythroid progenitors	TSG in excessive erythroblastosis-type of myeloproliferative disorders and T-cell lymphomas
Bone	
Regulator of osteoblast proliferation, differentiation, and migration	TSG in osteosarcoma

Figure 1.5. Role of different NFIs in cancer

Reproduced from Chen *et al.* (129) with permission from the Cancer Letters Journal

a feedforward loop with NF-κB in GBM cells that leads to increased tumour cell survival (170). Surprisingly, NFIA protein expression in astrocytomas is associated with improved survival of GBM patients (167), suggesting that the role of NFIA in GBM tumourigenesis is complex and dependent on other interacting partners.

Similar to NFIA, NFIB plays a paradoxical role in GBM. *NFIB* RNA levels are inversely correlated with astrocytoma grade (171). In addition, higher NFIB RNA levels are associated with improved survival in patients with classical and mesenchymal GBM subtypes (171). Although the mechanism remains to be investigated, NFIB appears to exert its anti-tumour effects through the signal transducer and activator of transcription 3 (STAT3) signaling pathway in these GBM subtypes (171). Oncogenic behaviour for NFIB has also reported, with NFIB expression correlated with increased growth of the neural GBM subtype (171). In addition, *NFIB* expression is upregulated in the aggressive triple-negative breast cancer subtype (172). NFIB has also been shown to act as a driver of tumour metastasis in small cell lung cancer (SCLC) by increasing chromatin accessibility (173,174). Similarly, NFIB acting downstream of the neural transcription factor BRN2 promotes melanoma cell migration and invasion (175). These findings reinforce the idea that NFIB-mediated regulation of target genes has opposing effects on tumourigenesis dependent on the context in which NFIB is examined.

Compared to NFIA and NFIB, the roles of NFIC and NFIX in cancer are less well-characterized. NFIC, through its regulation of Krüppel-like factor 4 (KLF4) and E-cadherin expression, can suppress epithelial-to-mesenchymal transition and invasion of breast cancer cells (176). NFIX depletion has also been shown to

reduce cell proliferation, migration and invasion in lung cancer cells, in support of an oncogenic role for NFIX (177). In the context of GBM, we have previously shown that all four NFI members regulate the expression of the *GFAP* and *FABP7* genes, with hypophosphorylated NFI associated with GFAP/FABP7 expression in GBM cells (178,179). FABP7 is a marker of neural progenitor/stem cells and GFAP is a marker of astrocytic cells (2,180,181). An intact NFI binding consensus site is required for transcriptional activation of the *FABP7* promoter (163). Expression of FABP7 has previously been correlated with increased GBM cell migration and invasion (182) and a worse clinical prognosis (183,184). Similar to the expression of NFIA in GBM, FABP7 is primarily detected in areas of heavy tumour infiltration, including perivascular regions (167,182). Together with the compensatory pathways observed between different members of the NFI family, these findings reveal intricate expression patterns, diverse downstream regulatory networks and even opposing functions for NFI in cancer formation and progression.

1.3 The calpain/calcineurin pathway

1.3.1 The calpain family

Calpain, first identified in 1964 and subsequently purified in 1976, is a family of neural, Ca^{2+}-dependent, non-lysosomal cysteine proteases (185,186). Calpain and its homologs are present in a wide variety of living organisms, including prokaryotes (187). To date, 15 calpain-encoding genes, including those encoding conventional and unconventional calpains, have been identified in human tissues (188). This project focuses on the best-characterized conventional calpain 1 (μ-calpain) and calpain 2 (m-calpain), with “μ” and “m” prefixes indicating the micro-

or milli-molar Ca^{2+} concentration required for the activation of these two calpains *in vitro* (189). In fact, whether a calpain member is considered to be a “classical calpain” depends on the similarity of its domain structure to that of calpains 1 and 2 (189). Hereafter, the term “calpain” is used to refer to both calpains 1 and 2, unless otherwise specified. Unlike other proteases, calpain-dependent cleavage of downstream effectors is of a “proteolytic processing” nature, resulting in altered activity of calpain targets rather than their degradation (190). Calpain-mediated cleavage is highly site-specific and dependent on 3D conformation of the polypeptide rather than the primary amino acid sequence of the target (191-193). Also, the specificity of both calpains overlaps to a great degree, leading to compensation of one’s activity by the other (191). However, targets specific to either calpain 1 or calpain 2 have also been reported (194,195).

Calpains function as heterodimers comprised of a shared small subunit (CAPSN1) and a distinctive large subunit (Figure 1.6): CAPN1 (for calpain 1) or CAPN2 (for calpain 2). The large (~80 kDa) subunit, in turn, is divided into four domains: the N-terminal anchor helix domain (I), the CysPc protease domain (II), the C2 domain-like domain (III) and the penta-EF hand domain (IV) (190). The small (~30 kDa) subunit contains an N-terminal glycine-rich domain (V) and a C-terminal penta-EF-hand domain (VI) (190). The N-terminal anchor helix domain of the large subunit is unique to calpain, with no sequence homology to any known protease families (196). The CysPc domain contains the catalytic triad (cysteine, histidine and asparagine) that is similar to other cysteine proteases including papain and cathepsins (196). The remaining sequence of this domain, however,

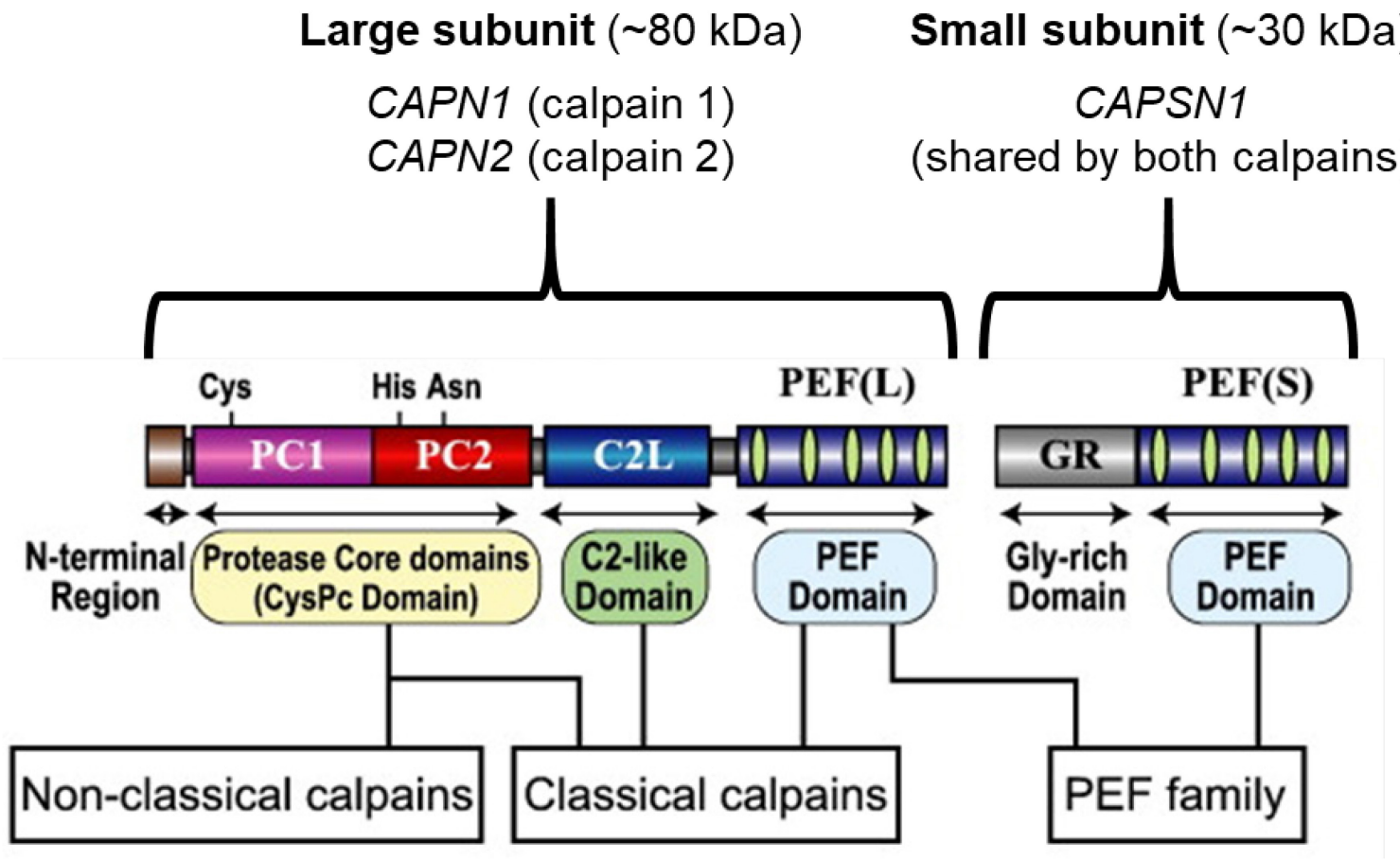

Figure 1.6. Domain composition of conventional calpains 1 and 2

PC1 and PC2, Protease core; PEF, penta-EF-hand. Adapted from Ono and Sorimachi (188) with permission from the Biochimica et Biophysica Acta (BBA) - Proteins and Proteomics Journal.

shares little homology with other cysteine proteases (196). Importantly, both N-terminal domains I (large subunit) and V (small subunit) have been shown to undergo autoproteolysis, which will be discussed in greater detail (196). X-ray crystallographic analysis reveals that domain II can be further divided into two subdomains IIa and IIb, each of which can bind one Ca^{2+} atom (197,198). Domain III of the large subunit is responsible for joining domains II and IV and is unique to calpain (196). In addition, domain III has been shown to bind phospholipids in a Ca^{2+}-dependent manner and thus targets calpain to various intracellular membrane-bound structures as well as the plasma membrane (199). The glycine-rich domain of the small subunit has also been suggested to interact with phospholipids, and based on its disordered structure, is believed to tether calpain to other molecules (196). Domains III and V therefore may play important roles in calpain subcellular localization and substrate specificity as well as the regulation of calpain activity. Both penta-EF-hand domains (IV and VI) share some homology with calmodulin and are responsible for additional binding of Ca^{2+} (190).

1.3.2 Calpain functions in cell migration and survival/death

Since all tissues examined express at least one of the two calpains (194), they are believed to have fundamental roles in the normal operation of the cell. In fact, knocking down *CAPSN1*, which results in the loss of both calpains 1 and 2, is embryonic lethal (200). Although the full extent of its functions is currently unknown, calpain has been directly or indirectly implicated in a wide range of cellular processes including but not limited to cell cycle, cell motility, signaling

transduction pathways, cell differentiation, cell death and survival, and synaptic plasticity. Only the functions of calpain in cell motility/migration and death/survival will be discussed here.

Calpain is frequently referred to as the master regulator of cell motility/migration because of its extensive involvement in most, if not all, major steps of this process such as adhesion complex turnover, cell spreading, and membrane protrusion (Figure 1.7) (201). Calpain's role in cell migration was first demonstrated in 1997, with calpain inhibition leading to decreased integrin-dependent cell migration (202). Mechanistically, pharmacological inhibition of calpain results in reduced cell migration by stabilizing adhesion complexes at the rear-end of the cell and thus lowering their detachment and turnover rates (203). In addition, calpain-dependent cleavage of talin 1 has been shown to increase binding of talin 1 to integrin β leading to the activation of the latter, which is essential for the formation of adhesion complexes (204-206). Loss of calpain activity also inhibits microtubule-mediated disassembly of adhesion complexes (207). Together, these findings suggest that calpain is involved in all aspects of adhesion complex dynamic: formation, disassembly and turnover.

General calpain inhibition can also lead to reduced cell spreading in vascular smooth muscle cells (208), pancreatic β cells (209), T cells (210) and platelets (211). More specifically, calpain 2 appears to promote this process in fibroblasts through the regulation of actin remodeling (212). In contrast, calpain 1 has been shown to cleave and generate a dominant negative fragment of RhoA, which can inhibit spreading of bovine aortic endothelial cells (213). These

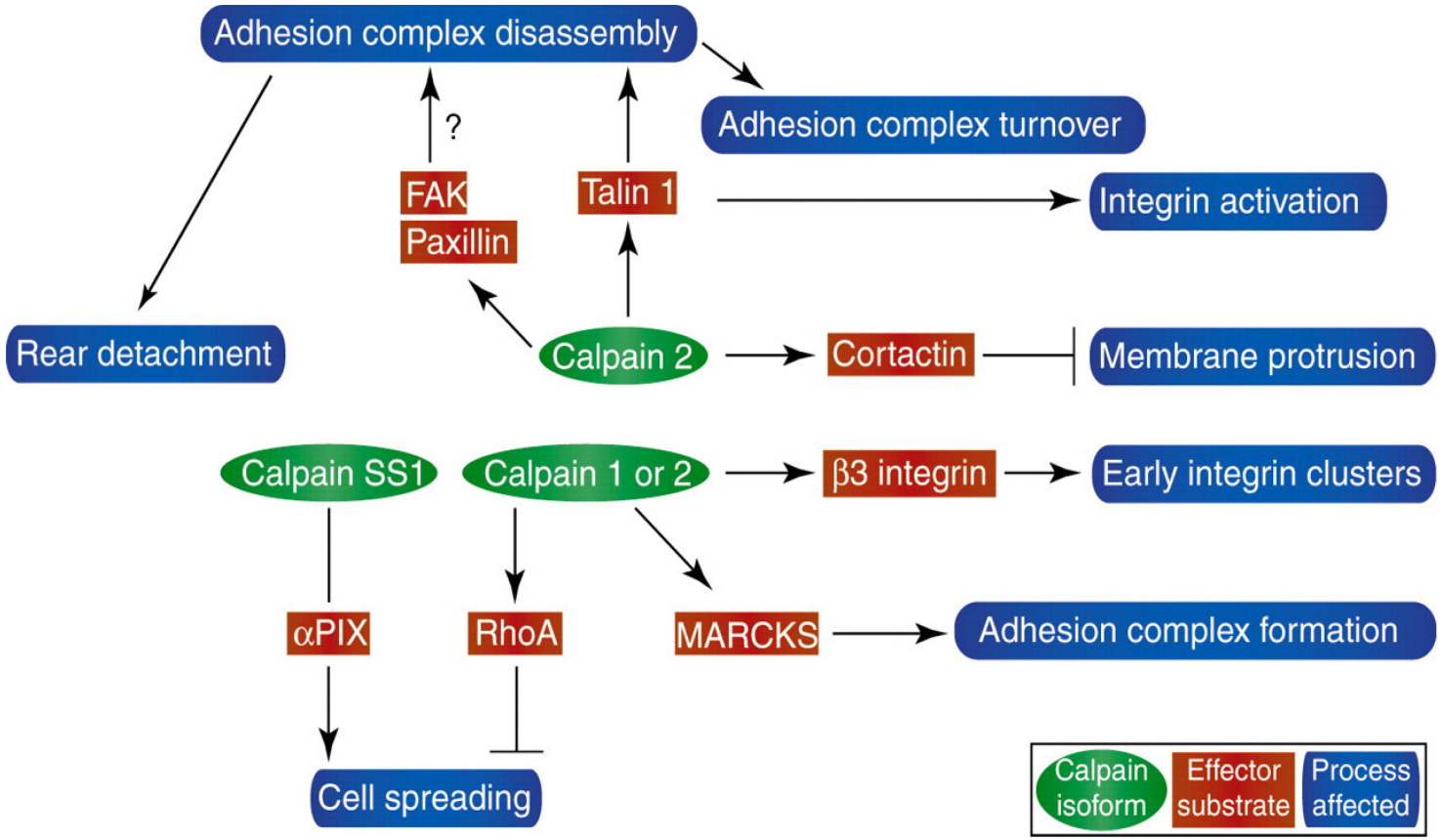

Figure 1.7. Opposing role of calpain in cell migration

Calpain SS1, calpain small subunit; FAK, focal adhesion kinase; RhoA, Ras homolog gene family, member A; αPIX, PAK-interacting exchange protein; MARCKS; Myristoylated alanine-rich C-kinase substrate. Reproduced from Franco *et al.* (201) with permission from the Journal of Cell Science.

observations indicate that the role of calpains 1 and 2 in cell spreading is not only specific to each calpain but also dependent on the biological context. Although rare, calpains 1 and 2 can exert opposite functions on the same cellular process (214,215). Artificial inhibition of calpains induces abnormal formation of membrane protrusions, including lamellipodia and filopodia (212). Calpain 2 appears to be responsible for calpain-mediated regulation of membrane protrusions as depletion of this calpain leads to destabilization of leading-edge protrusions (194). Interestingly, knocking down the calpain target, cortactin - a regulator of actin, produces similar phenotypes to calpain 2 depletion, suggesting that cleavage of cortactin is important for calpain-mediated regulation of membrane protrusions (201).

The functions of calpain in cell survival and death are not as well characterized as its role in cell migration. However, calpain is known to promote both cell survival and apoptosis, a programmed cell death that is dependent on biological context (Figure 1.8). The pro-survival role of calpain is best illustrated by its regulation of p53 stability, with calpain shown to cleave and degrade p53 (216). As a result, inhibition of calpain leads to increased levels of p53 and p21 as well as activation of caspase, resulting in cell death by apoptosis (217). Calpain further contributes to cell survival by degrading the inhibitor of NF-κB (IκBα), resulting in the activation of NF-κB signaling (218). Calpain can also destroy pro-apoptotic proteins, including the transcription factor MYC (219,220). Consequently, inhibition of calpain in MYC-positive fibroblasts leads to anoikis, an apoptotic process induced by detachment of cells from the extracellular matrix (221).

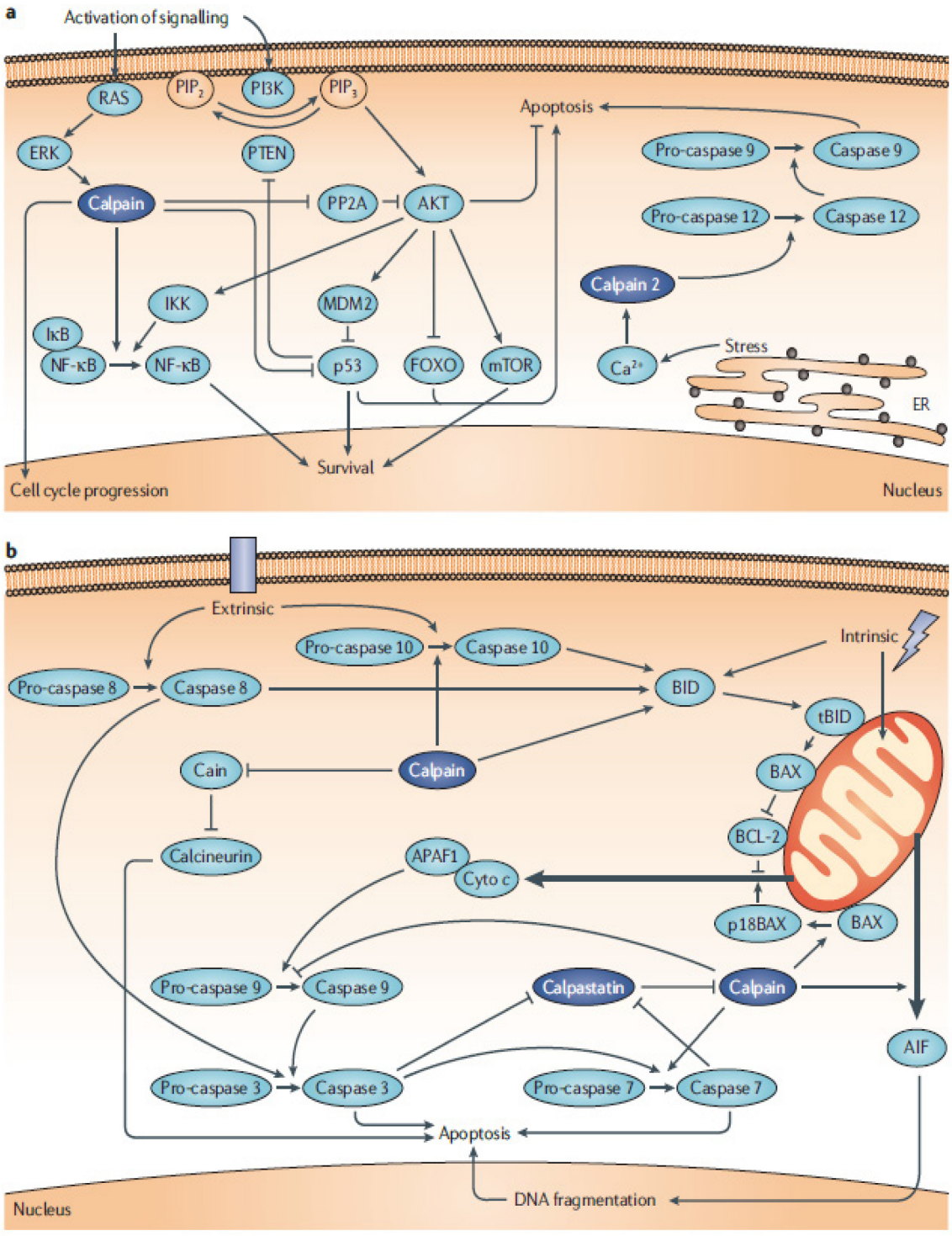

Figure 1.8. Calpain can induce both cell survival (a) and apoptosis (b)

Reproduced from Storr *et al.* (218) with permission from Nature Reviews Cancer.

In contradiction with the above-noted roles for calpains in cell survival, calpain has been shown to cleave and activate p53 upon DNA damage in neuronal cells, leading to apoptosis (219). Calpain also cleaves and activates a variety of caspases including caspase 7, caspase 10 and caspase 12 (218). Calpain-mediated cleavage of caspase 7 produces an even more active form of this protease compared to that generated by caspase 3-mediated cleavage, suggesting that calpain may be a more potent apoptotic activator than apoptosis repressor (222). Calpain cleaves and activates caspase 12 in response to endoplasmic reticulum stress, leading to the activation of apoptosis (223). Calpain can also promote apoptosis in a caspase-independent manner (218). Calpain has been reported to cleave and activate pro-apoptotic members of the B-cell lymphoma 2 (BCL-2) family, including the Bax-like BH3 (Bid) (224) and bcl-2-like protein 4 (Bax) (225) proteins, resulting in cytochrome c release from the mitochondria. These findings demonstrate diverse functions for calpain in the regulation of cell death and survival.

1.3.3 Calpain and cancer, with a focus on GBM

Due to its multifaceted functions, dysregulation of calpain expression and calpain-mediated proteolysis of downstream effectors have been documented in many diseases including but not limited to neurodegenerative diseases, muscular dystrophy, diabetes and cardiomyopathy. In cancer, upregulation of calpain 1 expression has been observed in renal cell carcinoma, schwannoma and meningioma (226,227). High calpain 1 levels contribute to pancreatic cancer progression and poor clinical prognosis (228). Increased calpain 2 levels were also

reported in colorectal adenocarcinoma (229). Moreover, calpain 2 has been shown to enhance progression and chemo-resistance of non-small cell lung cancer cells (230). Beyond the typical calpains 1 and 2, other members of the calpain family have been implicated in tumourigenesis. Immunohistochemical analysis reveals that calpain 6 expression is significantly increased in uterine and cervical malignancies (231,232). In contrast, calpain 3 expression is reduced in melanoma (233). Similarly, decreased calpain 9 levels were observed in gastric cancer (234). These findings represent only a small body of evidence from the literature demonstrating the extensive involvement of calpain in a wide range of neoplastic conditions.

Although there are many different molecular pathways through which calpain can regulate malignant transformation and progression, calpain-mediated regulation of tumour cell migration/invasion and apoptosis are most relevant to this thesis (Figure 1.9). Calpain 2 is essential for the invasion of prostate cancer cells (235). Similarly, silencing of calpain results in decreased metastatic potential of osteosarcoma cells (236). With respect to cell death, calpain 1 is the predominant mediator of apoptosis in human lung adenocarcinoma cells treated with cisplatin (237,238). In contrast, calpain-mediated proteolysis of pRB induces proteasomal degradation of pRB, enhancing survival of HeLa cells (239). These findings suggest that, mirroring calpain functions in normal cell migration and apoptosis, calpain's role in either promoting or inhibiting these processes is dependent on specific cancer types, or even subtypes.

10

Calpains	Cancer	Implications
Calpain 1	Bladder carcinoma	Cell migration, invasion
Calpain 2	Brain tumors	Cell death
	Breast cancer	Invadopodia dynamics, invasion
	Breast cancer	Cyclin E truncation
	Lung cancer	Cell migration, invasion
	Melanoma	Degradation of $p27^{Kip1}$
	Meningioma	Degradation merlin, adhesion, contact inh.
	Neuroblastoma	Regulation of NO production
	Osteosarcoma	Invasion, metastasis formation
	Prostate cancer	Cell migration, invasion
	Prostate cancer	Degradation of E-cadherin
	Renal carcinoma	Metastasis formation
	Rhabdomyosarcoma	Cell migration, invasion

Figure 1.9. Calpain-mediated regulation of tumour cell migration/invasion and death/survival

Adapted from Leloup and Wells (240) with permission from Expert Opinion on Therapeutic Targets

In GBM, calpain has been shown to mediate the apoptotic-inducing effects of a variety of chemical compounds. Curcumin, a polyphenolic compound, induces apoptosis in U87 GBM cells by activating calpain signaling (241). In curcumin-treated cells, α-spectrin (270 kDa) was found to be cleaved into a 145 kDa fragment, which is specific to calpain-mediated proteolysis of this protein (242). Similarly, silibinin – a polyphenolic flavonoid – also induces calpain-dependent apoptosis in GBM cells (243). In the latter study, activation of calpain by silibinin treatment was followed by the generation of reactive oxygen species (ROS) concomitant with the activation of protein kinase C isoform δ (PKC_{δ}) (243). Unlike other PKC isoforms, PKC_{δ} promotes apoptosis (244). In addition, cleavage of Bax and nuclear translocation of apoptosis-inducing factor (AIF) was also observed, with the former inducing release of cytochrome c from the mitochondria and the latter causing DNA fragmentation in the nucleus (243). As a result, treating U87 GBM cells with calpain blocks silibinin-induced ROS generation, resulting in decreased levels of apoptosis (244). Besides apoptosis, calpain also induces necrosis, a form of cell death caused by noxious stimuli, in response to chemical treatment (245). These findings suggest the potential use of calpain activators to induce GBM cell death. While radiation therapy and chemotherapy have already been demonstrated to effectively induce GBM cell death, leading to shrinkage of the tumour mass (53,246), current GBM treatment fails to target infiltrative tumour cells, which ultimately results in GBM recurrence.

Due to its extensive involvement in the regulation of cell migration, calpain is essential for the infiltration of GBM cells *in vitro* and *in vivo*. To this end, only the

role of calpain 2, but not calpain 1, has been elucidated. It has long been noted that calcium flux induced by autocrine glutamate signaling is important for the invasive phenotype of GBM cells (247,248). However, the exact molecular mechanism underlying this observation remained unclear until 2010, when calpain 2 was shown to be the key mediator of GBM cell invasion in response to calcium influx (249). Knocking down calpain 2 or pharmacological inhibition of calpain activity leads to a 90% reduction in GBM cell invasion upon treatment of these cells with A23187, a calcium ionophore (249). Mechanistically, depletion of calpain 2 results in reduced levels of extracellular matrix metalloproteinase 2 (MMP2) in response to A23187 treatment (249). MMPs, including MMP2, are responsible for degradation of extracellular matrix proteins, thereby facilitating tumour cell invasion (250). Increased MMP2 expression has been correlated with higher grade astrocytomas and a worse clinical prognosis (251,252). Calpain 2 has also been shown to be essential for the infiltration of GBM cells in a zebrafish brain model (253). Calpain 2-depleted GBM cells were able to form a tumour mass when transplanted into the zebrafish brain but exhibited a ~3-fold reduction in long-distance migration compared to control cells (253). This study also showed that calpain 2 knockdown was associated with decreased formation of new blood vessels, suggesting that calpain 2 positively regulates neoangiogenesis, a defining characteristic of GBM tumours (253). A related finding is that the angiogenic effects of VEGF are facilitated by calpain-induced reorganization of the actin cytoskeleton in endothelial cells (254).

1.3.4 Calpain substrates, in particular calcineurin

To date, more than 100 substrates of calpain have been identified *in vitro*, with a subset of these verified as calpain targets *in vivo* (196). Mirroring the diverse functions of calpain, its substrates are involved in a wide array of cellular processes and can be classified, with some exceptions, into four general groups: cytoskeletal proteins (group 1), membrane-bound proteins (group 2), kinases/phosphatases (group 3) and transcription factors (group 4) (196). For example, calpain-mediated proteolysis of vimentin (group 1 substrate), an intermediate filament protein, results in increased sprouting of endothelial cells upon the formation of new blood vessels (255). Calpain has also been shown to cleave the alpha-amino-3-hydroxy-5-methylisoxazole-4-propionate (AMPA) receptor (group 2 substrate), an important transmembrane glutamate receptor, resulting in dampened neuronal excitability in ischemia and epilepsy (256). With respect to group 3 substrates, calpain cleaves calcium/calmodulin-dependent (CAM) protein kinase II to a smaller fragment that is still active in the absence of calmodulin (257). Finally, calpain can cleave the transcription factor USF (group 4 substrate), resulting in the inability of USF to activate transcription (258). Beyond the four general categories of substrates, calpain can cleave other proteins including enzymes such as the calmodulin-dependent cyclic nucleotide phosphodiesterase, abolishing its dependence on calmodulin (259). Although the majority of calpain functions take place inside the cell, calpain can also be secreted into the extracellular environment. One example would be the release of calpain from activated human lymphoid cells, which leads to the degradation of myelin (260).

Amongst all known calpain substrates, calcineurin phosphatase is perhaps the best characterized downstream effector of calpain. Calcineurin, otherwise known as protein phosphatase 3 (PPP3) or protein phosphatase 2B (PP2B), is a Ca^{2+}/calmodulin-dependent serine/threonine phosphatase, comprised of two subunits: the catalytic subunit calcineurin A (CNA) and a regulatory subunit calcineurin B (CNB) (261,262). Although calcineurin is involved in various signaling pathways, it is best known for its role in the regulation of the immune response, particularly in T-cell activation. Calcineurin, when activated, dephosphorylates the NFAT transcription factor at multiple serine residues (263,264). Dephosphorylation of NFAT by calcineurin results in the nuclear translocation of this transcription factor, allowing it to bind DNA and activate the transcription of genes involved in the activation of T-cells (265,266). As a result, inhibitors of calcineurin such as cyclosporin A (CsA) and FK506 (Tacrolimus) are routinely used in the clinic as immunomodulatory agents (266-269).

Binding of calcineurin to calcium leads to a change in conformation of the former, exposing the calmodulin binding domain in the CNA subunit (270,271). In turn, binding of calmodulin to CNA results in the displacement of the autoinhibitory domain from the catalytic subunit and thus the activation of calcineurin (264,272). Calcineurin activity is controlled by a family of Regulator of Calcineurin (RCAN) proteins, which can either promote or inhibit calcineurin phosphatase activity (273-276). Subcellular localization is another regulatory mechanism for calcineurin activity. In resting cells, calcineurin remains chiefly in the cytoplasm (277,278). Upon activation, calcineurin can translocate into the nucleus and dephosphorylate

its targets (279). In the context of GBM, we have previously shown that calcineurin is primarily located in the cytoplasm of NFI-hyperphosphorylated cells. Upon treating these cells with ionomycin A, a calcium ionophore, calcineurin is activated and translocates into the nucleus where it dephosphorylates NFI.

Calpain has been shown to cleave CNA (~60 kDa) at three locations, with cleavage at amino acids 501, 424 and 392 resulting in 57 kDa, 48 kDa and 45 kDa fragments, respectively (Figure 1.10). The 57 kDa form of CNA, detected in Alzheimer Disease brains, still retains the C-terminal auto-inhibitory domain but is more active than the full-length form of CNA (280). The 48 kDa form of CNA, detected in hypertrophic myocardium, no longer contains the autoinhibitory domain and thus is a constitutively active fragment (278,281). Similarly, the 45 kDa, detected in excitotoxic neurodegeneration, is constitutively active due to absence of the autoinhibitory domain (282). Importantly, both the 45 kDa and 48 kDa forms of CNA also lose the nuclear export signal located adjacent to the autoinhibitory domain and thus predominantly localize to the nucleus (281). These findings suggest that calpain-mediated proteolysis of calcineurin plays an important role in the regulation of calcineurin activity and subcellular localization, particularly in pathological conditions.

1.3.5 Regulation of calpain proteolytic activity

Although calpain activity is essential for a wide range of physiological processes, hyperactivation of calpain may have lethal consequences on the cell. For example, it has been suggested that all Z-disks, marking the boundaries of

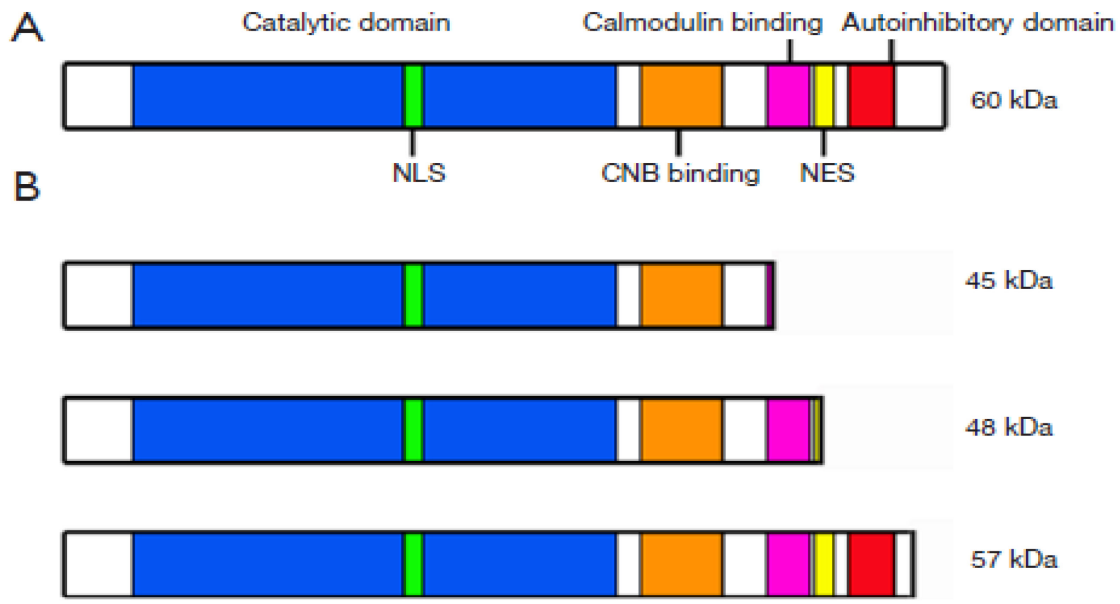

Figure 1.10. Calpain-mediated proteolysis of calcineurin catalytic subunit

Calpain 1 cleaves calcineurin at three distinct sites, generating three truncated forms ranging from 45 to 57 kDa. The 45 and 48-kDa isoforms no longer contain the NES, which prevents them from being exported from the nucleus. NLS, nuclear localizing signal; CNB, calcineurin regulatory subunit, NES, nuclear export signal. Reproduced from Brun and Godbout (283) with permission from Translational Cancer Research.

adjacent sarcomeres in a myofibril, would be proteolytically degraded within 5 min if all calpain in that myofibril was active (196). Consequently, the majority of calpain molecules remain inactive in resting cells. Calpain activation occurs only if required and must be tightly controlled by a variety of mechanisms to ensure optimal operation of the cell.

Calpain is a calcium-dependent protease and thus calcium influx is required for its activation. However, it has long been realized that the amount of calcium required for half-maximal activity of calpain 1 (3-50 μM) and calpain 2 (400-800 μM) greatly exceed the physiological range of calcium concentration (50-300 nM) in most cells (196,284). Shortly after their successful purification, both the large and the small subunits of calpain were reported to undergo autoproteolysis, hereafter abbreviated as autolysis, in the presence of calcium *in vitro* (285,286). Autolyzed calpains require significantly lower calcium concentrations to reach half-maximal proteolytic activity compared to non-autolyzed forms of calpain: 0.5-2 μM for autolyzed calpain 1 and 50-150 μM for autolyzed calpain 2 (287). This discovery raised the question of whether full-length calpain, similar to other cysteine proteases, is synthesized as a proenzyme and subsequently activated by autolysis. Many *in vitro* kinetic and mutagenesis studies, however, have demonstrated that even though autolysis precedes proteolytic activity of calpain (288-290), full-length calpains are still active proteases (291-293). Therefore, the physiological significance of autolysis in the regulation of calpain activity remains obscure. Nevertheless, we know the following facts about calpain autolysis: (i) the *in vitro* calcium concentrations required for calpain autolysis is slightly lower than

that needed for calpain activation (288,294), (ii) autolysis occurs concomitant with *in vivo* activation of calpain activity, preceding calpain-mediated proteolysis of downstream targets (295-298), and (iii) autolyzed calpain reaches half-maximal activity faster than full-length calpain, but is more prone to degradation or aggregation than full-length calpain (299). Consequently, whether full-length calpain is proteolytically active or not is of little physiological relevance and autolysis has therefore been used as a marker for the initiation of calpain proteolytic activity.

Based on the calcium requirements for non-autolyzed and autolyzed calpains, it appears that only autolyzed calpain 1 can achieve meaningful levels of proteolytical activity under physiological calcium concentrations of 50-300 nM. It is therefore evident that the cell must have other ways of lowering the calcium concentrations required for calpain activation. To this end, binding of calpain to phospholipids, especially phosphatidylinositol (PI), has been shown to lower the *in vitro* calcium requirements for calpain autolysis by ~8-fold (300). Phospholipids are found in cell membranes, including the plasma and ER membranes, where calcium channels are also located. As a result, binding of calpains to biological membranes may expose calpains to transient calcium flux that may reach the micromolar levels required for full activation of calpain. In addition, various proteins are able to reduce the calcium concentrations required for calpain activation. For example, in human neutrophils or rat skeletal muscles, a ~40 kDa heat-stable polypeptide can lower the calcium requirements for calpain 2 half-maximal activity (301,302). Similarly, a ~15 kDa monomeric protein, which functions as a ~30 kDa homodimer, reduces

the calcium concentrations needed for half-maximal activity of calpain 1 in multiple cell types (303). Interestingly, endogenous calpain activators have failed to gain much attention to date, with little known about these proteins including their identity. This is likely due to the fact that most calpain-related diseases result from pathological activation of calpain, rather than absence or inhibition of calpain activity.

Besides being regulated by other macromolecules, post-translational modifications of calpain, including but not limited to phosphorylation, also play a role in the regulation of calpain activity. Using phospho-specific antibodies in combination with mass spectrometry, calpain 1 was found to be phosphorylated at nine residues and calpain 2 at eight residues, with most of these sites located on the large subunit of both calpains (196). EGF-induced phosphorylation of calpain 2 at serine 50 by extracellular signal-regulated kinase (ERK) activates calpain both *in vitro* and *in vivo* (304,305). Also, Protein Kinase A (PKA)-mediated phosphorylation of calpain 2 prevents its binding to PI at the plasma membrane and 'freezes' calpain 2 in an inactive state (306,307). These findings indicate that phosphorylation of calpain affects not only its proteolytic activity but also its subcellular distribution and substrate specificity. Calpain activity is also regulated by the small subunit that is shared by both calpains 1 and 2. This subunit has been shown to have chaperone activity required for the proper folding of the large subunit (308). It has also been reported that the large and small subunits of calpain can dissociate upon autolysis (299). The dissociated large subunits, however,

quickly aggregate and become inactive, suggesting that the small subunit is essential for maintenance of calpain proteolytic activity (299).

It is important to note that the intricate network of regulatory mechanisms described so far constitutes only a part of the control that a cell may exert on calpain. As described in Section 1.4, there is an entire family of proteins dedicated to the control of calpain activity.

1.4 Calpastatin: Endogenous inhibitor of calpain

1.4.1 The calpastatin family

During the purification of calpain from porcine skeletal muscle, it was noted that calpain remained inactive in the crude extract until it was precipitated at pH 6.2 (186). Further examination of the supernatant revealed that the inhibition of calpain was mediated by a heat-stable (up to 100^{o}C) and trypsin-labile factor (186). Although the exact identity of this factor was unknown at the time, the name “calpastatin” was first proposed in 1979 to describe its calpain inhibiting function (309). It was not until 1982 that calpastatin was successfully purified from human erythrocytes as a 70 kDa protein (310). Initial attempts to purify calpastatin produced highly variable results, with polypeptides ranging from 34 to 300 kDa reported: 107 kDa in human liver (311), 145 kDa in bovine heart (312), 50 kDa in rabbit skeletal muscle (313), 172 kDa in porcine skeletal muscle (314), 115 kDa in bovine cardiac muscle (315), and 125 kDa in bovine brain (316). A number of reasons were proposed to explain these variations in molecular mass.

First, calpastatin is highly prone to proteolytic degradation (312,315). The use of harsh extraction conditions, often including heating in earlier studies, likely led to degradation of calpastatin. Second, circular dichroism and nuclear magnetic resonance revealed that the calpastatin polypeptide assumes virtually complete coil formation in solution (317,318). As a result, analysis of calpastatin using size exclusion chromatography, which significantly overestimates the size of molecules with coiled formation, generated the high molecular weights associated with certain calpastatin polypeptides. Third, calpastatin has been reported to migrate anomalously in SDS-PAGE gels, making it difficult to reconcile calpastatin size based on denaturing gel electrophoresis (319,320). For example, the previously mentioned 70 kDa calpastatin identified by SDS-PAGE in human erythrocytes actually has a molecular weight of 46 kDa (310). However, the diversity of the calpastatin family is largely an inherent product of its complex transcriptional regulation.

There is only one calpastatin gene, named *CAST*, in each mammalian species examined so far (196). In human, the *CAST* gene is located on chromosome 5 (321). The use of alternative promoters in combination with alternative splicing results in a large family of *CAST* transcripts and calpastatin isoforms. Currently, >44 transcript variants of *CAST* (Ensembl database, gene ID: ENSG00000153113) and 21 calpastatin isoforms (NCBI database, gene ID: 831) have been reported in humans. However, the bulk of calpastatin studies has been performed in species other than human. Both murine and bovine *CAST* genes have 5 exons (1xa, 1xb, 1y, 1z and 1u) upstream of exon 2, with three alternative

promoters located upstream of exons 1xa, 1xb and 1u (322-325). In addition, another alternative promoter upstream of exon 15 directs the expression of a much shorter *CAST* transcript variant (326). Not counting alternatively spliced variants, *CAST* transcripts can be classified into four general types, which correspondingly encode four different types of calpastatin isoforms (Figure 1.11). Murine type I and II variants, the homologs of which have not been directly identified in human, start with exons 1xa and 1xb, respectively (323,325). Type III *CAST* variants, starting at exon 1u, have been found in all mammalian species examined to date (320,322-325,327). Type IV variants, starting from the alternative exon 14t, were first identified in human testis and are expressed in this tissue alone (326). It is currently unclear if the alternative promoters previously identified in bovine and murine *CAST* genes are present in human

At the protein level, the longest calpastatin isoforms (encoded by type I and II variants) are comprised of 4 calpain inhibitory repeats (domain I-IV) and 2 N-terminal extensions (domain XL and L). These two isoforms differ in the aa sequence of the XL domain (Figure 1.11) (320). The prototypical calpastatin (encoded by type III variants) lacks the XL domain, whereas the testis-specific isoform (encoded by type IV variants) only contains domain II to IV (310,326). Variants of each type are further subjected to alternative splicing and thus can produce different calpastatin isoforms with distinct migrating rates in SDS-PAGE gels. For example, type III *CAST* variants have been shown to undergo alternative splicing resulting in exon 3 and/or exon 6 being removed from the coding sequence (328,329). This exon skipping results in different calpastatin isoforms that migrate

at a faster rate (110-125 kDa) in SDS-PAGE gels compared to the typical type III calpastatin isoform (135 kDa) (Figure 1.11). Also, a single tissue often expresses more than one type of *CAST* variants and thus calpastatin isoforms, resulting in further complications when interpreting data obtained from calpastatins isolated from tissues (330). As a result, the physiological significance of different calpastatin isoforms remains a mystery.

1.4.2 Calpastatin-mediated inhibition of calpain

In contradiction to the diverse expression profiles of *CAST* transcripts variants and calpastatin isoform, intact calpastatin appears to have only one known function: to regulate calpain. Reflecting its highly specific role, the amino acid sequence of calpastatin is unique and shares no homology with any known polypeptides, including that of cystatins, inhibitors of many cysteine proteases other than calpains (331). Furthermore, calpastatin does not inhibit any other proteases tested to date, including cysteine proteases (cathepsin B, ficin, papain and bromelin) and non-cysteine proteases (chymotrypsin, thermolysin, thrombin, trypsin, pepsin, plasmin and cathepsin D) (331). Although each of the four inhibitory domains of calpastatin can bind and inhibit one calpain 1 or calpain 2 molecule, they do so with different efficacy: domain II < domain III < domain IV < domain I, ranging from the least to the most effective domain (332). Different affinities of calpastatin inhibitory domains for specific calpains have also been reported; however, results are inconsistent, with some studies suggesting that calpain 2 is more efficiently inhibited by calpastatin compared to calpain 1 while

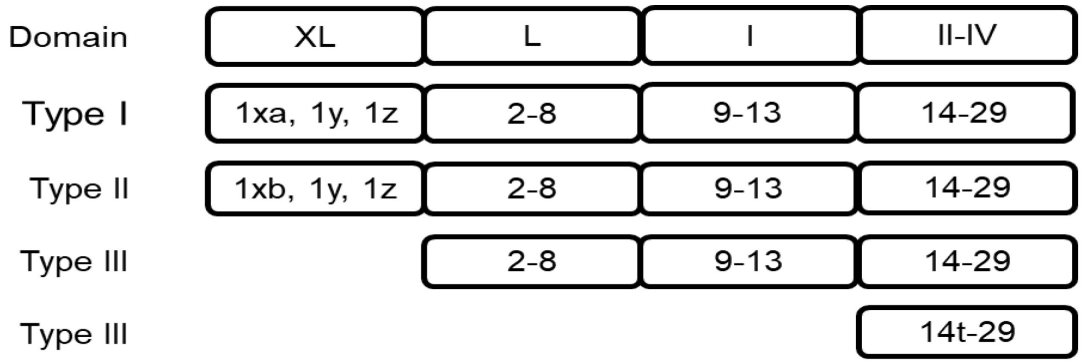

Nature of Transcript	Properties of Protein
Type I; contains 1xa, 1y, 1z, exons for domain L and all four repeats; 85-kDa polypeptide	Rate of migration in SDS-PAGE and sites of tissue expression are unknown; 172 kDa in porcine skeletal muscle??
Type II; contains 1xb, 1y, 1z, exons for domain L and all four repeats; 84-kDa polypeptide	Migrates as 145 kDa in SDS-PAGE; XL domain contains three protein kinase A phosphorylation sites in some species; present in cardiac muscle; other tissues?
Type III; prototypical; contains exons for domain L and all four repeats; 77–78 kDa	Migrates as 135 kDa in SDS-PAGE; mammalian skeletal muscle; other distribution not characterized
Deletion of exon 3 in domain L; contains all four repeats; 74–75 kDa	Migrates as 125 kDa in SDS-PAGE; mammalian skeletal muscle; other distribution not characterized
Deletion of exons 3 and 6 in domain L; 72–73 kDa	Rate of migration in SDS-PAGE unknown (110–115 kDa?); tissue distribution has not been characterized
Lacks domains L and I; 46-kDa polypeptide	Migrates as 70 kDa in SDS-PAGE; human, pig, rabbit erythrocytes; possibly also in cells
Type IV; lacks domains L and I and part of domain II; ?? kDa	Rate of migration in SDS-PAGE is unknown; transcript found only in testis
Lacks domain L and domains I, II, and III; 18.7 kDa	Rate of migration in SDS-PAGE unknown; found in human testis

Figure 1.11. Four types of murine *CAST* transcript variants and their corresponding calpastatin isoforms

Domain I-IV: calpain inhibitory domains. Adapted from Goll *et al*. (196) with permission from Physiological Reviews

others indicate the opposite (333-335). Each of the four domains (I-IV) can be further divided into three subdomains: A, B and C. Function-structure analysis has revealed that a highly conserved 12-aa motif in domain B is essential for calpain inhibition, with mutation in just two amino acids resulting in a near total loss of calpain inhibitory activity of calpastatin (336,337). An intact calpastatin molecule, containing all four calpain inhibitory repeats, is a potent inhibitor of calpain, with a dissociation constant (K_d) of <3 nM (331).

It has long been known that binding of calpastatin to calpain is dependent on calcium (338). This interaction is reversible, with recovery of proteolytically active calpain observed upon addition of calcium chelators (339). The calcium concentration needed for calpastatin and calpain binding is below that required for calpain to reach half-maximal activity. As a result, calpastatin is able to inhibit calpain upon calcium influx before calpain can become activated (315). Both full-length and autolyzed forms of calpains bind calpastatin at lower calcium concentrations than those required for their half-maximal activity (340). As calpastatin does not appear to bind calcium, the dependency of the calpain-calpastatin interaction on calcium is thought to be specific to calpain (196). Subsequent studies have shown that subdomain A of calpastatin interacts with domain IV of the large subunit of calpain (K_d of 3.1 nM) and that subdomain C of calpastatin binds to domain VI of the small subunit of calpain (K_d of 31 nM), with both of these interactions dependent on calcium (341,342). Binding of subdomain B to the region close to the active site of calpain has also been assumed to be dependent on calcium although this assumption is not supported by empirical

evidence (196,337). Interestingly, subdomain A or subdomain C alone does not have any inhibitory activity and is unable to prevent calpain autolysis but can block the binding of calpain to cell membranes (341-343). In contrast, subdomain B by itself cannot block the interaction between calpain and cell membranes, but is able to reduce calpain autolysis (343). These findings suggest that different subdomains of the inhibitory repeat of calpastatin are used to control specific aspects of calpain activity, including calpain activation and subcellular distribution.

It is important to note that most if not all studies on calpain/calpastatin interaction have been carried out using either calpain 1 or calpain 2. Thus, the role of calpastatin in regulating other members of the calpain family, specifically unconventional calpains, is currently unclear. Given that: (i) calpastatin is such a potent inhibitor of calpain, (ii) binding of calpastatin to calpain occurs at a lower calcium concentration than that required for calpain activity, and (iii) calpain and calpastatin are almost always co-expressed in any given cell, there must be ways for the cell to induce the disassociation between calpain and calpastatin to allow initiation of calpain proteolytic activity. In fact, the regulation of calpastatin activity may be as important for calpain-mediated proteolysis as the regulation of the protease itself; however, little is known about the molecular mechanisms underlying the regulation of calpastatin.

1.4.3 Regulation of calpastatin

So far, the functions of calpastatin domain XL and domain L have not been discussed as they are not well understood. However, they do not possess any inhibitory capacity towards either calpain 1 or calpain 2 (334). Research carried

out over the last few decades has pointed to roles for these two domains in the regulation of calpastatin activity, and by extension, calpain activity. The XL domain of bovine full-length calpastatin (encoded by type II *CAST* variants) contains three PKA phosphorylation sites (325). *In vivo* phosphorylation of calpastatin by PKA results in an increase in the amount of membrane-related calpastatin, from 6% to 30% (344). Furthermore, immunofluorescence analysis shows that calpain and calpastatin often co-localize in the cytoplasm of resting cells (345). However, upon calcium influx resulting from treatment of cells with a calcium ionophore, calpain translocates to the plasma membrane. In contrast, calpastatin remains in the cytoplasm (345,346). Given that calpain can localize to the membrane fraction of the cell through its interaction with phospholipids (300), these findings suggest that PKA-mediated phosphorylation of domain XL may be a mechanism by which the cell can target calpastatin to or away from membrane-localized calpain, resulting in the suppression or activation of calpain, respectively.

Compared to our limited understanding of domain XL's significance, functions of domain L are better characterized. Domain L is where the majority of known *CAST* alternative splicing events occur (Figure 1.11). Of 7 exons encoding the L domain, splicing events at 4 different exons have been reported including exons 3, 4, 5 and 6 (196). The physiological significance of splicing of exons 3 and 6 has been addressed in a number of studies. Expression of exon 3, or lack thereof, appears to have a significant impact on tissue-specific expression of calpastatin. In the porcine model, both exon 3-containing and exon 3-deleted *CAST* transcripts are found in the heart; however, only exon 3-spliced transcripts

are expressed in skeletal muscle (347). Although its function is unclear, exon 3 encodes the most basic stretch of amino acids in domain L (324). Consequently, it has been proposed that this exon is responsible for the targeting of calpastatin to cell membranes. In erythrocytes, a free domain L fragment lacking exon 3-encoded amino acids prevents the autolysis of calpain (348). More importantly, the interaction between calpain and this exon 3-less domain L occurs in the absence of calcium, indicating that calpastatin can bind calpain in its inactive state (348). The region of domain L encoded by exons 4-7 was subsequently shown to be responsible for calcium-independent interaction between calpain and calpastatin, which can be disrupted by PKC-mediated phosphorylation of domain L (349). These findings suggest that calpastatin may not only inhibit the proteolytic activity of active calpain but also prevent calpain autolysis and activation.

Exon 6 of domain L has been directly implicated in the regulation of calpastatin intracellular distribution. The amino acid sequence encoded by exon 6 contains multiple phosphorylation sites that are required for the reversible localization of calpastatin from cytosolic soluble fraction to aggregated clusters, with the latter condition reducing the availability of calpastatin to bind calpains (350). Treating cells with cAMP results in the near total aggregation of calpastatin, preventing its translocation to the plasma membrane where calpain is localized (350). Consequently, calpain is free to undergo activation, leading to a 2 to 3-fold increase in the degradation of calpain downstream effectors such as talin (350). Although the kinase responsible for the phosphorylation of exon 6-encoded sequences has not been identified, PKA-mediated phosphorylation of domain L-

containing calpastatin reproduces the aggregation phenotype (351). Together, these findings provide insight into one of the few well-defined molecular mechanisms underlying the regulation of calpastatin subcellular distribution and activity. Finally, domain L has also been shown to bind to several types of calcium channels in a variety of cell types (352,353). However, the significance of these observations is unknown.

1.5 Research Objectives

Hypothesis: In GBM cells, NFI cross-signals with calpain through calpastatin and calcineurin.

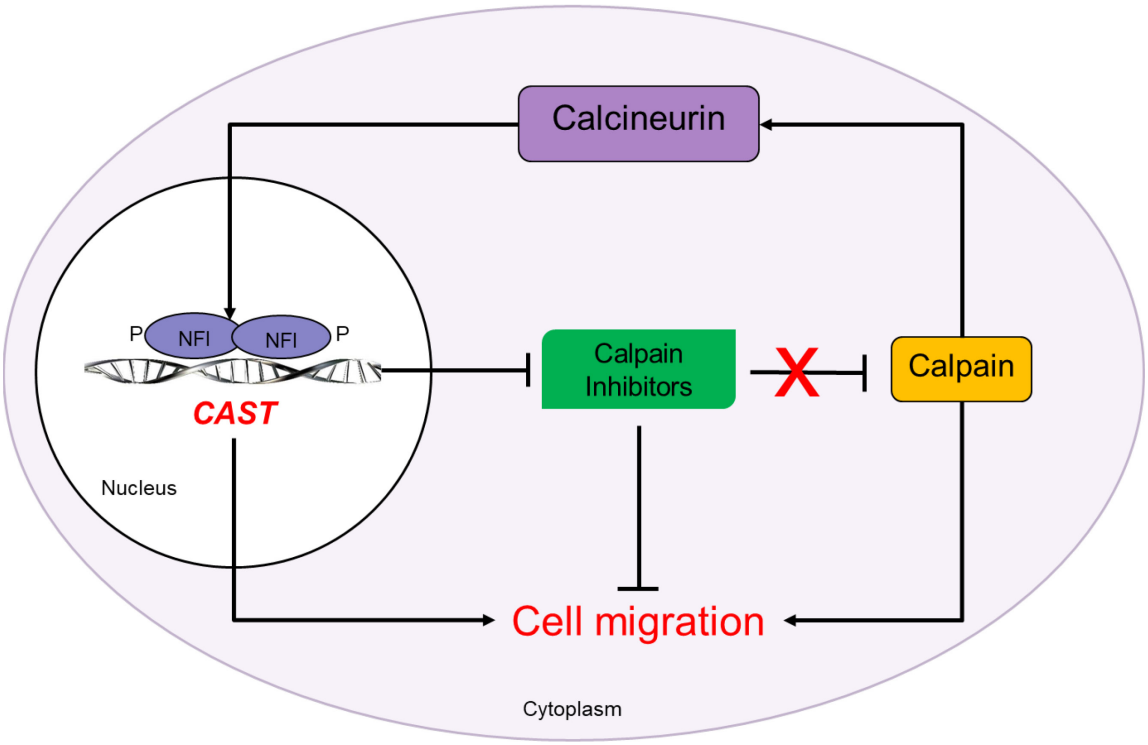

1.5.1 Chapter 2

My first objective was to confirm the regulation of *CAST* by NFI in MG cell lines. In this paper, we presented a complex NFI-mediated mechanism for regulation of *CAST* in MG cells. We identified two NFI binding sites located in human *CAST* intron 3, approximately 4 kb upstream of exon 4 that drive expression of a *CAST* transcript variant that excludes the XL domain of calpastatin. Our results indicate that NFIs control the subcellular localization of calpastatin in MG cells through usage of the newly identified alternative *CAST* promoter. Binding of hypophosphorylated NFI to *CAST* intron 3 results in increased utilization of the alternative promoter and a higher ratio of class 2 (encoding for XL-less calpastatin isoforms) to class 1 (encoding for full-length calpastatin) *CAST* variants. Depletion of NFIs in NFI-hypophosphorylated MG cells results in accumulation of calpastatin at the plasma membrane. Since calpastatin directly binds and inhibits calpain, regulation of *CAST* variant expression by NFI with accompanying alterations in calpastatin subcellular localization may ultimately control calpain activity. Along with the previous findings indicating that NFI activity is regulated by calcineurin, these results provide a foundation for further investigations into the possibility of regulatory crosstalk between NFI and the CAST/calpain/calcineurin signaling pathway in MG cells.

1.5.2 Chapter 3

Having elucidated the regulation of *CAST* by NFI, my second objective was to unravel the crosstalk between NFI and calpain in MG cells. In this manuscript, we demonstrated a positive feedback loop between NFIB and calpain 1 mediated

by calpastatin and calcineurin. We identified two mechanisms by which NFIB can increase calpain 1 activity: (i) hyperphosphorylated NFIB causes a decrease in calpastatin concentration across the cytoplasm so that it cannot effectively inhibit calpain 1 autolysis and activation and (ii) hypophosphorylated NFIB induces differential compartmentalization of calpastatin (cytoplasm) and active calpain 1 (nuclear). In turn, calpain 1, via calcineurin, promotes NFIB dephosphorylation, a process that is accompanied by a more accessible subnuclear localization and has been shown by others to increase NFIB activity. We also showed that the NFIB-calpain 1 positive feedback loop acts mainly to suppress cell migration while having little to no effect on MG cell viability. Inhibition of calpain activity using a pan-specific calpain inhibitor resulted in decreased MG cell survival based on a colony formation assay. Our findings support the potential use of calpain inhibitors in GBM treatment. However, pan-specific calpain antagonists in GBM would have to undergo extensive pre-clinical studies to address their potential side effects in promoting tumour cell migration.

1.5.3 Chapter 4

Besides a NFIB-calpain 1 positive feedback loop, we also observed crosstalk between NFIA and calpain 2 in MG cells. NFIA knockdown resulted in loss of autolyzed calpain 2 in the nucleus in both U87 and U251 MG cells. We found that while NFIA negatively regulates *CAST*, it does not directly regulate the calpain 2 gene. Immunofluorescence analysis using anti-calpain 2 and anti-calcineurin antibodies confirmed the loss of nuclear calpain 2 upon NFIA

knockdown and also revealed the loss of nuclear calcineurin upon NFIA depletion in both U87 and U251 MG cell lines. NFIA depletion also led to reduced calpain activity but, unlike NFIB depletion, did not induce noticeable changes in calpastatin subcellular localization. Together, these results suggest that NFIA, regardless of its phosphorylation state, promotes calpain 2 activity via one mechanism: the negative regulation of *CAST* expression. In addition, we found that depletion of calpain 2 in U251 cells results in the loss of nuclear calcineurin and decreased expression of brain fatty acid binding protein (FABP7), a known target of NFI, suggesting that calpain 2 may enhance NFI transcriptional activity. Knocking down NFIA and/or calpain 2 decreased GBM cell survival and cell migration, indicating the oncogenic nature of this crosstalk. Due to our inability to find a NFIA-specific antibody, we were unable to examine the effect of calpain 2 depletion on NFIA phosphorylation and subcellular localization.

CHAPTER 2: EFFECTS OF NUCLEAR FACTOR I PHOSPHORYLATION ON CALPASTATIN (CAST) GENE VARIANT EXPRESSION AND SUBCELLULAR DISTRIBUTION IN MALIGNANT GLIOMA CELLS

2.1 Introduction

Malignant glioma (MG), encompassing WHO grade III (anaplastic astrocytoma) and IV (glioblastoma) astrocytomas, is the most common and deadly form of adult primary brain tumors (57). Despite aggressive treatment by surgical resection, radiation therapy and adjuvant chemotherapy, patient prognosis remains dismal, with a median survival time of less than 5 years for anaplastic astrocytoma and 15 months for glioblastoma (30,55). Tumor recurrence and inevitable treatment failure are, at least in part, due to the highly infiltrative nature of MG cells (354,355). Post-mortem examination often reveals the dissemination of tumor cells into normal brain parenchyma, frequently found distal from the original tumor mass and at early stages of the disease (356). Early infiltration of tumor cells, together with the inherent resistance of MG cells to cytotoxic drugs and radiation therapy, severely limit the efficacy of conventional focal and systemic treatments (357-359). While targeting infiltrative MG cells would likely be of clinical benefit, molecular mechanisms underlying MG cell migration and infiltration remain poorly characterized.

Our laboratory has previously shown that the expression of brain fatty acid-binding protein (FABP7, B-FABP) is associated with increased MG cell migration *in vitro* (182). FABP7 is found at sites of infiltration in glioblastoma tumors, with elevated levels of FABP7 correlating with decreased survival in glioblastoma patients (184,360,361). *FABP7* expression is regulated by Nuclear Factor I (NFI), a family of four transcription factors (NFIA, NFIB, NFIC and NFIX) (163,362). NFIs bind to the consensus recognition sequence: 5'-TTGGCN$_{(3-6)}$GCCAA-3' as either

homodimers or heterodimers through their highly-conserved N-terminal DNA-binding domains (114,363). NFIs can also interact with half of the consensus palindrome sequence, albeit at reduced affinity (97). The variable C-terminal transactivation domain of NFI can either inhibit or activate its target genes depending on tissue and promoter context (117), with different NFIs able to elicit distinct effects on the same promoter (362). In addition to *FABP7*, a neural progenitor/stem cell marker, NFI regulates genes involved in glial cell differentiation, such as the glial fibrillary acidic protein (*GFAP*) gene (117,362,364).

NFI is differentially phosphorylated in MG cells, with the hypophosphorylated form of NFI correlating with *FABP7* and *GFAP* expression (163). Dephosphorylation of NFI is mediated by calcineurin, a calcium-dependent serine/threonine phosphatase (164). Calcineurin, in turn, is cleaved and activated by calpain, a family of calcium-dependent non-lysosomal cysteine proteases (282,365). The best characterized mechanism for controlling calpain activity is through its endogenous inhibitor, calpastatin, which is encoded by a single gene, *CAST (366)*. Calpastatin has a complex expression profile, both at the RNA and protein levels, a consequence of multiple promoters and alternative splicing (324,325,327). Based on sequence and structure analyses, full-length murine and bovine calpastatins have four repetitive calpain inhibitory domains (I to IV) with each domain able to bind to one calpain molecule (319). The function(s) of two extension regions at the N-terminus of the calpastatin polypeptide, domains XL (encoded by different combinations of exons $1x_a$, $1x_b$, 1y, and 1z) and L (encoded by exons 2-8), remain poorly understood (322,325). Four different types of

calpastatin have been identified to date based on which domains they contain (323). Three major *CAST* RNA variants have been identified by northern blot analysis in bovine heart, including two that encode XL-containing and XL-less calpastatin isoforms (325).

Direct binding is required for calpastatin inhibition of calpain activity, with sequestration of calpastatin away from calpain postulated to control local calpain activity (367). Similar to calpain, calpastatin is often found at the plasma membrane and surrounding the nucleus (196). Aggregation of calpastatin in the perinuclear region may serve as a mechanism through which calpain can escape calpastatin inhibition in other compartments of the cell (351). In contrast, calpastatin localization at the plasma membrane is believed to inhibit calpain activity through direct binding of calpastatin to calpain. As many known targets of calpain involved in cell migration are found at the plasma membrane, a consequence of calpastatin localization to the plasma membrane may be decreased cell migration (368). While nuclear localization of calpastatin has also been described, its significance remains unclear (345).

Chromatin immunoprecipitation-on-chip (ChIP-on-chip) experiments to identify targets of NFI in MG cells revealed *CAST* as a putative NFI target gene. Our data indicate that NFI binds to an alternative promoter located upstream of *CAST* exon 4 and affects the relative levels of *CAST* variants transcribed from the canonical versus alternative promoters. We show that binding of hypophosphorylated NFI to *CAST* intron 3 results in: (i) increased transcriptional activity of *CAST* alternative promoter, (ii) a higher ratio of XL-less to XL-containing

CAST transcript variants, (iii) loss of calpastatin at the plasma membrane and (iv) accumulation of calpastatin in the perinuclear region. These findings suggest a key role for NFI in the transcriptional regulation of different *CAST* variants, with accompanying effects on the subcellular distribution of calpastatin.

2.2 Results

2.2.1 In vitro occupancy of putative CAST NFI binding sites

All four NFIs are expressed in cells of glial origin as well as glioblastoma cells, with a number of NFI targets identified in these glial-like cell types (117,163,362). An antibody that recognizes all four NFIs was used to identify additional NFI targets in MG cells (369). Analysis of ChIP-on-chip data obtained with this pan-specific NFI antibody and FABP7/GFAP-expressing U251 MG cells resulted in the identification of *CAST* as a putative target of NFI (369). Sequence analysis of DNA bound by NFI revealed three putative NFI recognition sites located within the intronic region upstream of exon 4: C1 (-3928 to -3915 bp), C2 (-3663 to -3628 bp), and C3 (-3469 to -3453 bp) with +1 defined as the first nucleotide of exon 4 (Figure 2.1A & B). To verify protein binding to these 3 putative NFI recognition sites, we performed gel shift assays with nuclear extracts prepared from U87 and U251 MG cells. C1, C2, and C3 double-stranded oligonucleotides radiolabeled with [α-^{32}P]dCTP were incubated with (+) or without (-) nuclear extracts and separated on native polyacrylamide gels. Although protein-DNA complexes were detected with all three probes, the shifted bands observed with C1 were considerably weaker than those observed with C2 and C3 probes (see

Figure 2.2A for U87 results). Weak binding to C1 is likely due to poor conservation of the first palindromic half of the NFI consensus sequence, with one of the two conserved guanine residues missing from this site (Figure 2.1Figure 2B). We therefore focused on the C2 and C3 NFI recognition sites in subsequent experiments.

Protein binding to the C2 and C3 oligonucleotides was examined using nuclear extracts prepared from both NFI-hyperphosphorylated U87 and NFI-hypophosphorylated U251 MG cells (163,362). These cell lines express all four NFIs, with similar amounts of *NFIA* RNA and higher levels of *NFIB, NFIC* and *NFIX* RNA in U251 compared to U87 MG cells (Figure 2.9A) (362). Similar overall levels of NFI protein are observed in U87 and U251 MG cells using a pan-specific antibody (362)

As previously observed for the *FABP7* promoter (163,362), protein–DNA complexes are formed using both U87 and U251 nuclear extracts. U87 protein-DNA complexes migrate more slowly than those in U251, in keeping with the hyperphosphorylated state of NFIs in U87 MG cells Figure 2.2B) (362). A 100X molar excess of either cold C2 or C3 oligonucleotide competitor effectively prevented binding of proteins to the C2 probe in both U251 and U87 MG cells. Similar results were obtained with the C3 probe, except that the lower band was competed out with excess C3, but not excess C2, oligonucleotides. Excess mutated C2* oligonucleotides (mutated at two conserved G residues in the first half of the palindrome - Figure 2.2C) competed to some extent with the radiolabeled C2 probe, resulting in a reduced signal compared to cold C2 (wild-

type) competitor (Figure 2.2B). Excess mutated C3* oligonucleotides (mutated at two conserved G residues in the first half of the palindrome and two C residues in the second half of the palindrome - Figure 2.1C) failed to compete with the C3 probe (Figure 2.2B). As expected, oligonucleotides containing a consensus NFI binding site effectively competed with the C2 and C3 probes for protein binding, but oligonucleotides containing a consensus AP2 binding site did not compete with either probe. These data indicate that: (i) an intact NFI consensus binding site is required for protein binding to C2 and C3 probes and (ii) the lower C3-protein complex (indicated by the asterisk), while specific to the C3 oligonucleotide, does not involve NFI binding.

2.2.2 In vitro binding of NFI to C2 and C3 oligonucleotides

To investigate whether NFI is a component of the C2 or C3 oligonucleotide-protein complexes observed in Figure 2.2, we carried out supershift assays using antibodies targeting each of the four NFIs. As there are no reliable sources for some of the NFI antibodies, we generated our own anti-NFI antibodies. These NFI antibodies showed moderate (anti-NFIA, -NFIB and -NFIC) to high specificity (anti-NFIX) toward their intended targets (Figure 2.9B). Importantly, this panel of NFI antibodies did not cross-react with other members of the NFI family (Figure 2.9B). Supershifted bands were observed when anti-NFIC antibody was incubated with either the C2 or C3 probe in the presence of either U87 or U251 nuclear extracts, indicating that NFIC is present in both C2- and C3-protein complexes (Figure

2.3A). Weak supershifted bands were also observed with the anti-NFIX antibody. Although no supershifted band was detected in the presence of anti-NFIA antibody, there was a reduction in the intensity of the protein-DNA complex, suggesting interference with the binding of NFIA to the DNA probe in the presence of anti-NFIA antibody. Addition of anti-NFIB antibody to both U251 and U87 nuclear extracts resulted in faster-migrating C2- and C3-protein complexes, suggesting that binding of NFIB to anti-NFIB antibody results in the dissociation of an NFIB co-factor. Supershift experiments with anti-AP2 antibody had no effect on the migration of either the C2-protein or C3-protein complexes. These results suggest that all four NFIs may bind to C2 and C3 oligonucleotides or interact with protein-C2 or -C3 complexes, in both U87 and U251 MG cells. To verify the binding of NFIs to C2 and C3 oligonucleotides, we transiently transfected U87 and U251 MG cells with siRNA targeting NFIC and repeated the gel shift experiments. NFIC was chosen for this analysis as it produced the strongest supershifted band. Depletion of NFIC resulted in the loss (or reduction in signal intensity) of both the shifted and supershifted bands (Figure 2.10A), supporting the binding of NFIC to both C2 and C3 NFI binding sites located in *CAST* intron 3.

As not all antibodies can supershift, we transiently transfected U87 and U251 MG cells with hemagglutinin (HA)-tagged NFI expression constructs and repeated the supershift assay with an anti-HA antibody. The latter antibody has previously been shown to supershift HA-tagged NFI proteins in gel shift assays (362). Western blot analysis of nuclear extracts prepared from cells transfected with each of the four HA-tagged NFI constructs revealed successful expression of

HA-tagged NFIs (Figure 2.3B). The presence of supershifted bands in extracts prepared from all four NFI transfectants indicates that C2 and C3 oligonucleotides are recognized by all four members of the NFI family in both U87 or U251 MG cells, at least when NFIs are ectopically expressed (Figure 2.3C). The migration patterns of the shifted complexes were similar in both U87 and U251 MG cells, suggesting that exogenous NFIs are not subjected to the same phosphorylation/dephosphorylation process as endogenous NFIs.

2.2.3 Binding of NFI to CAST in intact chromatin

To explore the binding of NFI to *CAST* intron 3 in the context of native chromatin, we performed ChIP analysis using two NFI- hyperphosphorylated (U87 and T98) and two NFI-hypophosphorylated (M049 and U251) MG cell lines (163). Cells were crosslinked with formaldehyde to capture DNA-protein interactions. NFI-bound DNA was then immunoprecipitated with an anti-NFI antibody (Tanese) that preferentially recognizes NFIC but also binds to the other NFIs (362). The rationale for using this antibody is that NFIC appears to be a major component of both the protein-C2 and protein-C3 complexes based on supershift (Figure 2.3C) and NFIC-knockdown experiments (Figure 2.10A). Rabbit IgG served as the negative control for these ChIP experiments. ChIP DNA was purified and PCR-amplified with primers flanking C2 or C3 NFI recognition sites (Table 2.1). DNA bands were detected in all four cell lines using primers flanking C3; however, PCR products were only detected in T98 and U87 using primers flanking C2 (Figure

2.4A). The absence of DNA bands in the IgG control lanes combined with the absence of DNA bands using *GAPDH* primers in the NFI lanes, support specific interaction between the anti-NFI antibody and the C2 and C3 NFI binding sites.

For quantitative analysis of ChIP products, we performed qPCR on chromatin immunoprecipitated DNA using primers flanking C2 and C3 recognition sites (Table 2.1). Primers to the *GAPDH* promoter served as the negative control. In agreement with our qualitative analysis, binding to C3 oligonucleotides was observed in all four cell lines, whereas binding to C2 was only observed in T98 and U87 MG cell lines (Figure 2.10B). As both C2 and C3 reside in intron 3, our results suggest that NFI occupies an alternative promoter upstream of *CAST* exon 4, with NFI binding C3 regardless of its phosphorylation status. In contrast, C2 is only bound by hyperphosphorylated NFI based on both qualitative and quantitative ChIP data.

2.2.4 Binding of RNA polymerase II to CAST canonical promoter and intron 3 region in intact chromatin

To assess the transcriptional states of the *CAST* canonical (CP) and putative alternative (ALT) promoters in U87 (NFI-hyperphosphorylated) versus U251 (NFI-hypophosphorylated) MG cells, we performed ChIP analysis with an antibody to RNA polymerase II (Pol II) that specifically recognizes a phosphorylated Ser 5 residue in its C-terminal domain repeats (YSPTSPS). This phosphorylated form of RNA Pol II occupies the proximal promoter regions of transcriptionally active genes (370). We used mouse IgG as a control for antibody

specificity. We also included two additional controls: a region of the active *GAPDH* proximal promoter that contains the TATA box bound by RNA Pol II (positive control) and an upstream region of the *GAPDH* promoter that is not bound by RNA Pol II (negative control).

In U87 MG cells, RNA Pol II showed significantly increased occupancy at the canonical *CAST* promoter compared to the alternative *CAST* promoter in intron 3. In U251 MG cells, RNA Pol II occupied both the canonical (primers flanking a proximal TATA box upstream of exon 1) and alternative (primers flanking a proximal TATA box upstream of exon 4) *CAST* promoters (Figure 2.4B; primers listed in Table 2.1). These results indicate that the alternative *CAST* promoter located in intron 3 is active primarily in NFI-hypophosphorylated U251 MG cells. Thus, our combined ChIP data suggest that engagement of hypophosphorylated NFI at C3 activates *CAST* intron 3 alternative promoter; whereas occupation of C2 and C3 by hyperphosphorylated NFI inactivates *CAST* intron 3 alternative promoter.

2.2.5 CAST variant expression in MG cells

Our combined gel shift and ChIP data indicate that C2 and C3 are *bona fide* NFI binding sites. To address the possibility of an alternative *CAST* transcription start site downstream of these binding sites, we carried out 5'-RLM RACE using total RNA prepared from T98 (hyperphosphorylated NFI) and U251 (hypophosphorylated NFI) MG cells. cDNAs underwent two rounds of PCR amplification using nested primer pairs designed to amplify transcripts initiating at

exon 1 (class 1 variants) or exon 4 (class 2 variants) (Table 2.1). Two main bands were identified in T98, a strong band at ~340 bp and a weak band at ~60 bp (Figure 2.5A). The only clear band detected in U251 cells was ~60 bp. Based on DNA sequencing analysis, the 340 bp DNA fragment contains exons 1 to 4 sequences whereas the 60 bp band only has exon 4 sequences (Figure 2.5A). These results are consistent with the presence of two *CAST* promoters in MG cells, with the canonical promoter upstream of exon 1 directing the expression of the longer form of *CAST* found (class 1 variant), and the NFI-bound alternative promoter upstream of exon 4 directing the expression of the shorter form of *CAST* (class 2 variant) (Figure 2.5B). As ChIP data demonstrate RNA Pol II occupancy at both the canonical and alternative *CAST* promoters in U251 MG cells, the smear observed at ~350 bp (see square bracket in Figure 2.5A) may represent transcription start site stuttering in NFI-hypophosphorylated U251 cells.

2.2.6 CAST promoter activity in MG cells

To further examine the utilization of the two promoters controlling the expression of class 1 and class 2 *CAST* variants, we transfected T98 and U251 MG cells with pGL3 luciferase reporter gene constructs driven by either the canonical (CP) (-1990 to +50 with +1 indicating the start of exon 1) or alternative (ALT) promoter (-4026 to +20 with +1 indicating the start of exon 4). The empty (promoterless) pGL3 vector served as the negative control. We then assessed the activity of *CAST* canonical and alternative promoters by measuring luciferase activity. In T98 MG cells (hyperphosphorylated NFI), the canonical promoter

generated a 27-fold increase in luciferase activity compared to empty vector (Figure 2.5C). In comparison, luciferase activity driven by the NFI-bound alternative promoter was increased 4.3-fold relative to control levels. In contrast, luciferase activity was increased by 2.7-fold and 3.5-fold when U251 (hypophosphorylated NFI) MG cells were transfected with vector containing the *CAST* canonical promoter and alternative promoter, respectively (Figure 2.5D). These results are generally consistent with our 5'-RLM RACE and ChIP data in that they demonstrate: (i) strong bias towards utilization of the *CAST* canonical promoter in NFI-hyperphosphorylated T98 cells and (ii) similar utilization of both canonical and alternative promoters in NFI-hypophosphorylated U251 MG cells.

Next, we tested the effect of mutating the C2 and C3 NFI binding sites on luciferase activity. For these experiments, we generated luciferase reporter constructs with NFI binding site mutations at C2 (ALT-C2*), C3 (ALT-C3*), or both C2 and C3 (ALT-C2*C3*). In U251 MG cells, luciferase activity driven by the ALT-C2* promoter was not statistically different from that of wild-type alternative promoter, in agreement with our ChIP results indicating that C2 is not bound by NFI in these cells (Figure 2.5E). Mutation of C3 resulted in lower luciferase activity (0.56-fold) compared to wildtype alternative promoter ($p<0.0001$), suggesting that C3 is required for NFI-mediated positive regulation of *CAST* alternative promoter activity. Mutating both the C2 and C3 sites resulted in a slight decrease ($p<0.05$) in luciferase activity compared to mutating C3 alone. These results are in agreement with C3 being the main effector of *CAST* alternative promoter activity

in NFI-hypophosphorylated U251 MG cells, in keeping with our ChIP data (Figure 2.4).

2.2.7 Expression of calpastatin isoforms in MG cells

To understand how the regulation of *CAST* by NFI affects calpastatin protein, we examined expression of different calpastatin isoforms in NFI-hyper- (U87) and NFI-hypophosphorylated (U251) MG cells using a pan-specific anti-calpastatin antibody. U87 MG cells primarily expressed the full-length calpastatin (indicated by the asterisk), which has been shown to migrate as a ~145 kDa band in SDS-PAGE (196). The full-length calpastatin is a translational product of class 1 *CAST* variants, which in turn is directed by the canonical promoter. In contrast, U251 MG cells expressed both the full-length and XL-less isoform (indicated by the arrow), which has been shown to migrate as a ~135 kDa band (196). The absence of the latter in U87 MG cells suggests that the ~135 kDa band is a translational product of class 2 *CAST* variants which is directed by the alternative promoter. The ratio of the 145 kDa to 135 kDa bands is approximately 1:1 (Figure 2.6A). In agreement with our previous observations, these results support: (i) preferential utilization of the *CAST* canonical promoter in NFI-hyperphosphorylated MG cells, and (ii) utilization of both the *CAST* alternative and canonical promoters in MG cells with hypophosphorylated NFI. To test the specificity of the calpastatin antibody, we transfected U251 MG cells with siRNAs targeting different regions of *CAST* RNA (exon 4 or exon 16). Western blot analysis shows one strong band at ~140 kDa, along with several weaker bands, all of which disappear upon *CAST* siRNA transfection (Figure 2.6B).

2.2.8 Regulation of CAST by NFI

We also examined how NFI regulates endogenous *CAST* mRNA levels by depleting U251 and U87 MG cells of specific NFIs using siRNAs to each of the four NFIs (Figure 2.6C). Endogenous *CAST* variant analysis was carried out using primers that span *CAST* exons 1 and 2 (E1-E2) to measure class 1 *CAST* variants, primers that target exons 4 and 5 (E4-E5) to measure levels of combined class 1 and 2 *CAST* variants, and primers that target exons 16 and 18 (E16-E18) to measure levels of all calpastatin variants as this region encodes domain II (second inhibitory domain) of calpastatin which is commonly found in brain calpastatin isoforms (see Table 2.1 for primer sequences).

There was no significant difference in levels of class 1 *CAST* transcripts upon knockdown of any of the NFIs in U87 MG cells (Figure 2.6D). Knockdown of either NFIB or NFIC in U87 MG cells significantly reduced the levels of combined class 1 and 2 *CAST* transcripts, to 0.55-fold ($p<0.0001$) or 0.73-fold ($p<0.001$) of control levels, respectively (Figure 2.6E). Depletion of NFIB, but not NFIA, NFIC or NFIX, reduced total *CAST* RNA levels in U87 MG cells to 0.61-fold ($p<0.0001$) of control levels (Figure 2.6F). These data indicate that NFIB may act as a positive regulator of class 2 *CAST* transcript levels in NFI-hyperphosphorylated U87 MG cells. However, the interpretation of these data is confounded by the following factors: (i) the complex expression profile of *CAST* RNAs, (ii) crosstalk between the different NFIs (e.g. knockdown of NFIB decreases *NFIC* levels) (Figure 2.6C), and (iii) the low levels of NFIB in U87 MG cells based on northern blot analysis

(14) and RT-qPCR (Figure 2.9A)

Depletion of either NFIC or NFIX in NFI-hypophosphorylated U251 MG cells had no significant effect on levels of class 1 *CAST* transcripts (Figure 2.6G). However, NFIA- and NFIB-depleted cells showed a small increase in class 1 transcripts, by 1.48 ($p<0.05$) and 1.22-fold ($p<0.05$), respectively. Depletion of NFIA, but not NFIB, NFIC and NFIX, in U251 MG cells significantly reduced levels of combined class 1 and 2 *CAST* transcripts (0.47-fold decrease compared to control; $p<0.01$) (Figure 2.6H). Knocking down either NFIC or NFIX was accompanied by increased levels of total (E16-E18-containing) *CAST* transcripts, by 1.34-fold ($p<0.05$) and 1.99-fold ($p<0.05$), respectively (Figure 2.6I). Overall, our data in U251 MG cells are consistent with all 4 NFIs playing some role in regulating the complement of *CAST* variants expressed in NFI-hypophosphorylated MG cells. NFIA in particular appears to act as a weak negative regulator of class 1 *CAST* transcripts and a strong positive regulator of class 2 *CAST* transcripts.

2.2.9 Changes in calpastatin subcellular localization upon NFI depletion

One of the best characterized roles of calpastatin is inhibition of calpain protease activity. In turn, the subcellular location of calpain determines its physiological functions, with calpain frequently found at the plasma membrane where it cleaves downstream targets, many of which are migration-related effectors (306,371). Since direct binding of calpastatin to calpain is required to inhibit calpain's protease activity (366), we examined the effect of NFI depletion on

calpastatin subcellular localization in NFI-hypophosphorylated U251 MG cells which express both full-length and XL-less calpastatin.

In U251 MG cells, calpastatin was primarily present in the nucleus and cytoplasm, with increased immunostaining in the perinuclear region (Figure 2.7A; Figure 2.11). NFIA- and NFIC-knockdown resulted in increased accumulation of calpastatin at the plasma membrane. NFIB- and NFIX-depleted U251 cells showed increased calpastatin immunostaining at the plasma membrane in structures resembling lamellipodia as well as higher levels of nuclear calpastatin.

To examine the importance of NFI phosphorylation state on calpastatin subcellular localization, we treated U251 MG cells with 1 μM cyclosporin A (CSA), an inhibitor of calcineurin that promotes NFI hyperphosphorylation (164). CSA-treated U251 MG cells showed increased levels of hyperphosphorylated NFI (indicated by the asterisks) (Figure 2.7B). Immunostaining analysis revealed a perinuclear localization for calpastatin in U251 MG cells treated with DMSO vehicle. CSA-treated cells showed a more diffuse calpastatin immunostaining pattern in the cytoplasm with accumulation at the plasma membrane (Figure 2.7C; Figure 2.12A). For comparison, we immunostained U87 MG cells with anti-calpastatin antibody. Calpastatin was found throughout the cytoplasm and at the plasma membrane. (Figure 2.7D; Figure 2.12B). Thus, the subcellular distribution of calpastatin in U251 MG cells with induced NFI hyperphosphorylation shows some similarity with that of NFI-hyperphosphorylated U87 MG cells.

When combined with our NFI promoter analyses, these immunostaining data support a regulatory link between NFI hypophosphorylation and: (i) utilization

of the *CAST* alternative promoter, (ii) transcription of class 2 *CAST* variants, (iii) expression of XL-less calpastatin, (iv) loss of calpastatin at the plasma membrane, and (v) perinuclear localization of calpastatin

2.3 Discussion

Many studies have demonstrated the importance of NFIs in the development of the central nervous system including the regulation of neural cell differentiation and gliogenesis (143,145). In particular, NFIA and NFIB are required for the initiation of gliogenesis and later promote the differentiation of astrocytes (112,126). In MG, NFI regulates *FABP7*, the expression of which coincides with increased tumor cell migration, tumor infiltration and worse clinical prognosis (182,360,361,372). In the context of MG cells, NFI transcriptional activity is regulated by its phosphorylation state (373), with dephosphorylation of NFI mediated by the calcineurin phosphatase, a well-known target of calpain (164,374,375).

We show here that NFI regulates transcription of the *CAST* gene, which encodes calpastatin, a highly specific inhibitor of calpain (366). Similar to NFI, the calpains also play a role in brain development, with μ-calpain (calpain 1) suppressing neural differentiation, and m-calpain (calpain 2) inducing glial differentiation (215). Furthermore, limited proteolysis of calpain targets is required for many aspects of tumor cell migration including focal adhesion turnover (376), cytoskeleton remodeling (377), invadopodia formation (378), and lamellipodia stabilization at the migration edge (194). Notably, m-calpain is

essential for MG infiltration of the brain in zebrafish (253). The convergence of NFI and calpastatin/calpain in normal brain development and regulation of cell migration suggests possible crosstalk between these two pathways, with NFI regulating expression of specific *CAST* variants, and calcineurin regulating NFI activity.

Overexpression of calpastatin protects cells from both calpain-mediated oxidative and proteolytic stress (379,380), whereas depletion of calpastatin is associated with human neurodegenerative disorders including Alzheimer's disease (381). While these reports highlight the importance of calpastatin, little is known about the regulation of calpastatin itself in the cell. Our combined data, including gel shift assays, supershift assays, ChIP analysis, reporter gene assays and analysis of *CAST* mRNA variants and calpastatin isoform expression, reveal a complex NFI-mediated mechanism for regulation of *CAST* in human MG cells. In particular, we identified two NFI binding sites located in human *CAST* intron 3, approximately 4 kb upstream of exon 4 that drive expression of a *CAST* transcript variant that excludes the XL domain of calpastatin.

Bovine and murine *CAST* genes have five exons ($1x_a$, $1x_b$, 1y, 1z, and 1u) located upstream of exon 2, with the latter showing homology with human exon 4 (NCBI, NG_029490, NC_000079, AC_000164). Human exons 1, 2, and 3 share sequence homology with exons $1x_b$, 1y, and 1z, respectively. A functional promoter has been identified upstream of exons $1x_b$ in both bovine and murine species (323,325). The location of NFI binding sites upstream of human *CAST* exon 4 suggests that this intronic region may also contain an NFI-bound alternative

promoter. We present evidence that the two NFI binding sites (C2 and C3) located upstream of exon 4 are differentially occupied by NFIs in different MG cell lines. NFI binding to C2 is confined to MG cell lines with hyperphosphorylated NFI, whereas NFI binding to C3 is observed in both NFI hyper- and hypophosphorylated cell lines. The core binding palindromic sequence is identical in both C2 and C3; however, the two sites differ in the spacing between the two halves of the palindrome: 5 bp for C2 and 6 bp for C3. The length of the spacer region has been shown to influence the binding affinity of NFI to its target genes (382), and may explain differential NFI binding to C2 and C3 binding sites.

Data from RNA Pol II ChIP, luciferase reporter gene and western blot analyses indicate that differential utilization of NFI-binding sites in *CAST* intron 3 results in a significantly higher ratio of XL-less calpastatin (a translational product of class 2 variants directed by the alternative promoter), versus full-length calpastatin (a translational product of class 1 variants directed by the canonical promoter) in migratory NFI-hypophosphorylated (U251) MG cells compared to non-migratory NFI-hyperphosphorylated (T98 and U87) MG cells. The subcellular localization of calpastatin isoforms encoded by these variants may help explain what drives increased cell migration in MG cells. It has already been shown that calpain and calpastatin co-localize in the cytoplasm (345). When cells are treated with a Ca^{2+} ionophore, calpain relocates to the plasma membrane where it regulates many migratory processes; however, calpastatin remains in the cytoplasm (345,346). These findings suggest that release of calpain from calpastatin is important for calpain activation. Full-length human calpastatin, which

contains domains XL, L, and four inhibitory repeats (I-IV), is encoded by class 1 variant and shares homology with the ~145 kDa type II bovine calpastatin. The latter harbors 3 protein kinase A (PKA) phosphorylation sites in the XL domain (325). Phosphorylation of calpastatin by PKA *in vivo* increases the amount of membrane-associated calpastatin from 6 to 30% (383). Thus, one would predict that calpastatin isoforms that contain domain XL (encoded by class 1 variants; Figure 2.5B) are more likely to localize to and inhibit calpain at the plasma membrane compared to the XL-less calpastatin isoform (encoded by class 2 variants), resulting in lower cell migration capacity.

In keeping with the idea that disassociation of calpain from calpastatin at the plasma membrane drives migration, calpastatin was primarily observed in the cytoplasmic perinuclear region of NFI-hypophosphorylated (migratory) U251 MG cells. It is noteworthy that perinuclear localization has been associated with increased calpastatin aggregation, with aggregated calpastatin showing reduced binding to calpain (384). Depletion of NFIs in U251 MG cells (accompanied by reduced class 2 *CAST* variants and increased class 1 *CAST* variants in the case of NFIA depletion) resulted in increased plasma membrane localization of calpastatin. In addition, knockdown of NFIB and NFIX was accompanied by increased nuclear localization of calpastatin (385). Nuclear calpain is believed to promote cell survival through various signaling pathways, including Ku80, NF-κB and PI-3K/Akt (386-388). As calpastatin is a calpain inhibitor, one may reason that the accumulation of calpastatin in the nucleus of MG cells antagonizes the pro-survival effects mediated by nuclear calpain. Thus, NFIB and NFIX may promote

either cell migration or cell death depending on the ratio of membrane to nuclear calpastatin in MG cells. Such an effect would be consistent with NFIB's paradoxical role, either acting as an oncogene or tumor suppressor, in different types of cancer (389).

We propose that there is regulatory crosstalk between NFIs and the calpastatin/calpain signaling pathway in MG cells that involves the following steps (Figure 2.8): (i) calcineurin is cleaved and activated by calpain in the cytoplasm (282), (ii) activated calcineurin translocates to the nucleus and dephosphorylates NFI (164), (iii) hypophosphorylated NFI regulates its target genes (163,362) including *CAST* through its alternative promoter, which enhances the expression of cytosolic XL-less calpastatin with concomitant suppression of plasma membrane-associated full-length calpastatin, and (iv) in the absence of full-length calpastatin at the plasma membrane, calpain cleaves its cell migration-enhancing effectors, resulting in the increased cell migration associated with NFI-hypophosphorylated MG cells.

In summary, our results indicate that NFIs control the subcellular localization of calpastatin in MG cells through usage of an alternative *CAST* promoter located upstream of exon 4. Binding of hypophosphorylated NFI to *CAST* intron 3 results in increased utilization of the alternative promoter and a higher ratio of class 2 (encoding for XL-less calpastatin isoforms) to class 1 (encoding for full-length calpastatin) *CAST* variants. Depletion of NFIs in NFI-hypophosphorylated MG cells results in accumulation of calpastatin at the plasma membrane. Since calpastatin directly binds and inhibits calpain, regulation of

CAST variant expression by NFI with accompanying alterations in calpastatin subcellular localization may ultimately control calpain activity. Future work will involve a more in-depth examination of the NFI-calpain signaling pathway, how it affects MG cell migration and whether it can be exploited to reduce MG infiltration through the inhibition of calpain.

2.4 Experimental Procedures

2.4.1 Cell lines, constructs, transfections and treatments

The origins of the MG cell lines used in this study have been previously described (181,362). Cells were cultured in Dulbecco's modified Eagle's minimum essential medium supplemented with 10% fetal calf serum, streptomycin (50 µg/ml), and penicillin (50 units/ml). NFI expression constructs, including pCH (empty vector), pCHNFIA, pCHNFIB, pCHNFIC, and pCHNFIX, were a gift from Dr. R. Gronostajski (Case Western Reserve University). Constructs were introduced into MG cells using polyethyleneimine-PEI (Polysciences)-mediated transfection with a ratio of 5:1 (µL PEI: µg DNA). The DNA was removed 18 h after transfection, and cells harvested 60 h post-transfection.

For cyclosporin A (CSA) treatment, near confluent U251 MG cells were treated with either DMSO (negative control) or 1 µM CSA for 1 h at 37ºC. Cells were either harvested for western blot analysis or fixed for immunofluorescence analysis as described below.

2.4.2 Gel shift Assay

Gel shift assays were performed as previously described (163,390). Probes (C1, C2, C3) were prepared by annealing complementary oligonucleotides with 5'- and 3'-overhangs, followed by filling-in the overhangs with Klenow polymerase and [α-^{32}P]dCTP. Cold competitors were prepared by annealing complementary oligonucleotides in the absence of [α-^{32}P]dCTP. Cold competitors with mutated NFI binding sites (C2* and C3*) were prepared by replacing the two conserved G residues at positions 3 and 4 with A residues. In addition, C residues at positions 12 and 13 were replaced with A residues in C3* (Figure 2.1). NFI and AP2 consensus competitor oligonucleotides were synthesized by annealing 5'-ATTTTGGCTTGAAGCCAATATG-3' & 5'-CATATTGGCTTCAAGCCAAAAT-3' (NFI consensus binding site is underlined) and 5'-GATCGAACTGACCGCCCGCGGCCCGT-3' & 5'-ACGGGCCGCGGGCGGTCAGTTCGATC-3' (AP2 consensus binding site underlined). U87 and U251 MG cells were transiently transfected with 7 µg of each of the HA-tagged NFI expression constructs (pCH, pCHNFIA, pCHNFIB, pCHNFIC and pCHNFIX) or siRNA targeting NFIC as described in the next section. Nuclear extracts were prepared using NE-PER® Nuclear and Cytoplasmic Extraction reagents (ThermoFisher Scientific). Four µg of nuclear extracts prepared from NFI or pCH-transfected cells were pre-incubated in binding buffer [20 mM Hepes pH 7.9, 1 mM spermidine, 10 mM dithiothreitol, 20 mM KCl, 0.1% Nonidet P-40, 10% glycerol] in the presence of 1 µg polydI-dC for 10 min at room temperature. Where indicated, a 100X molar excess of unlabeled competitor oligonucleotide was added

to the reaction. For supershift experiments, 0.5 µg anti-AP2 (Santa Cruz Biotechnology), anti-HA (Roche Applied Science), pan-specific anti-NFI (obtained from Dr. N. Tanese, NYU Medical Center), anti-NFIA (custom polyclonal antibody, antigen CPDTKPPTTSTEGGA, GenScript), anti-NFIB (custom polyclonal antibody, antigen CSGSPSHNDPAKNPP, GenScript), anti-NFIC (custom polyclonal antibody, antigen CDQEDSKPITLDTTD, GenScript), or anti-NFIX (custom polyclonal antibody, antigen CDGSGQATGQHSQRQ, GenScript) antibodies were included during the preincubation stage. Next, radiolabeled oligonucleotides were added, followed by an incubation period of 20 min at room temperature. Reactions were then electrophoresed in a 6% non-denaturing polyacrylamide gel in 0.5X TBE (Tris-borate EDTA). The gels were dried and exposed to X-ray film.

2.4.3 Knockdown of endogenous NFIs and CAST

U87, T98 and/or U251 MG cells were transfected with the following NFI-targeting Stealth® siRNAs: control scrambled siRNA [Cat. # 12935-200 and 12935-300 (Invitrogen)], NM_005595_stealth_919 (5'-GAAAGUUCUUCAUACUACAGCAUGA-3' of NFIA), NM_005596_stealth_1020 (5'-AAGCCACAAUGAUCCUGCCAAGAAU-3' of NFIB), NM_005597_stealth_1045 (5'-CAGAGAUGGACAAGUCACCAUUCAA-3' of NFIC), NM_002501_stealth_752 (5'-GAGAGUAUCACAGACUCCUGUUGCA-3' of NFIX), NM_001042440.3_stealth_486 (5'-UCCUCUGGUGCAACCAGCAAGUCUU-3' of *CAST*) and NM_00190442.1_stealth_1264 (5'-ACAAUCCCAUCUGAGUACAGAUUAA-3' of

CAST). Cells were transfected with 10 nM of each siRNA using the RNAiMAX Lipofectamine reagent (Invitrogen) according to the manufacturer's protocol. After 48 h, cells were split 1 in 6 and transfected with another round of siRNA. Cells were harvested 60 h after the second transfection.

2.4.4 Reverse transcription (RT) and quantitative polymerase chain reaction (qPCR)

Total RNA was isolated from transfected cells using the TRIzol® reagent (ThermoFisher Scientific). First-strand cDNA was synthesized using Superscript II® reverse transcriptase (Invitrogen). For RT-PCR, cDNAs were amplified using primers to the different NFIs or β-actin which served as the loading control (see Table 2.1 for list of primers). For qPCR, cDNAs were amplified using primer pairs targeting specific regions of the *CAST* gene and the BrightGreen® qPCR master mix (ABM Scientific). qPCR results were normalized to *GAPDH*. Relative fold change was generated by normalizing each treatment to the respective scrambled siRNA control.

2.4.5 Chromatin immunoprecipitation

ChIP was carried out as previously described (391). Briefly, MG cells were crosslinked with 1% formaldehyde for 20 min at room temperature. Crosslinking was terminated using glycine to a final concentration of 0.125 M. Cells were then collected in 1X PBS supplemented with 0.5 mM phenylmethylsulphonyl fluoride (PMSF), washed and resuspended in lysis buffer [44 mM Tris-HCl pH 8.0, 10 mM EDTA, 1% SDS, 1X Complete® protease inhibitors (Roche Applied Science)]. Cells

were sonicated twice at 4°C for 10 cycles (1 min per cycle, 30s power on and 30s power off) with output level set to high (Bioruptor 300® ultrasonic homogenizer, Diagenode). Next, lysates were precleared twice (constant rotation at 4°C for 1 h) with protein G-Sepharose Fast Flow beads (Sigma Aldrich) and SDS diluted to 0.1%. Either 2 µg of rabbit (for NFI) or mouse (for RNA polymerase II) IgG (negative control), 2 µg of a pan-specific anti-NFI antibody (obtained from Dr. Naoko Tanese, NYU Medical Center, NY), or 2 µg of anti-RNA polymerase II antibody (Abcam) were incubated with lysates at 4°C overnight with constant rotation. Protein G-Sepharose beads were added to reactions and incubated at 4°C for 2 h. Beads were washed in buffers of increasing stringency (140 mM NaCl to 500 mM NaCl to 250 mM LiCl). Protein-DNA complexes were eluted in 0.1 M $NaHCO_3$, 5 mM NaCl, 1% SDS and incubated at 65°C overnight to reverse cross-links. DNA was purified by phenol-chloroform extraction, followed by ethanol precipitation. *CAST* NFI binding regions (C2 and C3), as well as *GAPDH* promoter (negative control) were amplified (Table 2.1) using the following parameters**:** 95°C for 3 min; 35 cycles at 95°C for 30 s, 60°C for 30 s, and 72°C for 30 s; 72°C for 7 min. Amplified DNA was resolved in 1.5% agarose gels and visualized using ethidium bromide. For quantitative analysis, chromatin-immunoprecipitated DNA was amplified by qPCR using the primers listed in Table 2.1. Results are presented as relative fold change compared to IgG negative control.

2.4.6 5'-rapid amplification of cDNA ends (RACE)

Total RNA was isolated from T98 and U251 MG cells as described above. *CAST* cDNA was generated using the FirstChoice® RNA ligase-mediated rapid

amplification of cDNA ends (RLM-RACE) kit (Ambion) according to manufacturer's protocol. Briefly, 5 µg of total RNA was digested with calf intestinal alkaline phosphatase (CIP) to remove the 5'-phosphate group from non-messenger RNA molecules as well as degraded mRNAs. Intact mRNA is capped and remains uncleaved by CIP. The 5'-cap was then removed with tobacco acid pyrophosphatase (TAP), yielding a 5'-monophosphate to which an RNA adapter with known sequence was ligated using T4 RNA ligase. *CAST*-specific primer (Table 2.1) was used to reverse transcribe RNA with M-MuLV reverse transcriptase. cDNAs were PCR-amplified using nested primer pairs (Table 2.1). The DNA was electrophoresed in a 3% MetaPhor agarose (FMC Bioproducts, Rockland, USA) gel, excised, purified (Monarch DNA extraction kit, New England Biolabs) and sequenced (BigDye Terminator® v3.1 cycle sequencing kit, ThermoFisher Scientific).

2.4.7 Luciferase reporter gene assay

The following reporter gene constructs were generated using the pGL3 luciferase vector (Promega®) with the SV40 promoter element removed: (i) empty vector control (CNT), (ii) -1990 to +50 bp of the *CAST* promoter linked to the luciferase gene, with +1 denoting the first nucleotide of exon 1 (designated CP for canonical promoter region), and (iii) -4026 to +20 bp relative to exon 4, with +1 denoting the first nucleotide exon 4 (designated ALT for NFI-bound alternative promoter). Site-directed mutagenized ALT-C2*, ALT-C3*, and ALT-C2*3* constructs were generated using the Quickchange® site-directed mutagenesis kit (Agilent Technologies) as indicated in Figure 2.1. Cells were transfected with

luciferase reporter constructs using JetPrime® transfection reagent (VWR) according to the manufacturer's instructions. Transfected cells were lysed directly on the plate using Promega's Cell Culture Lysis Buffer for 20 min at room temperature. Equal amounts of luciferase substrate were added to 20 μL protein lysates and light emitted from the bioluminescent conversion of D-luciferin to oxyluciferin was measured with the FLUOstar OPTIMA (BMG LABTECH) microplate reader. Relative light unit per μg (RLU/μg) was obtained by dividing the amount of light emitted from each sample by their respective protein concentration (measured using the Bradford reagent). Relative fold change was calculated by normalizing the RLU/μg of each promoter construct against that of the empty vector control.

2.4.8 Western blot analysis

Nuclear extracts were prepared using the NE-PER® Nuclear and Cytoplasmic Extraction reagents (ThermoFisher Scientific). Whole cell lysates were prepared by syringing cells 15-20 times (23G needles) at 4°C in lysis buffer [50 mM Tris-HCl pH 7.5, 1% sodium deoxycholate, 1% Triton X-100, 150 mM NaCl, 50 mM sodium fluoride, 1 mM sodium orthovanadate, 10 mM EDTA, 0.1% SDS, 1X Complete protease inhibitor (Roche Applied Science), and 1X PhosSTOP phosphatase inhibitor (Roche Applied Science)]. Proteins were resolved in polyacrylamide-SDS gels and electroblotted onto polyvinylidene fluoride (PVDF) or nitrocellulose membranes. Blots were immunostained with rabbit pan-specific anti-calpastatin antibody (1:10,000, Santa Cruz), mouse anti-β-actin antibody (1:100,000, Sigma Aldrich), mouse anti-HA antibody (1:5000, Roche Applied

Science), mouse pan-specific anti-NFI antibody (1:1000, Santa Cruz), or α-tubulin (1:50,000, Hybridoma Bank) followed by detection with horseradish peroxidase-conjugated secondary antibody (Jackson ImmunoResearch Biotech) using the Immobilon® western chemiluminescent HRP substrate (EMD Millipore).

2.4.9 Immunofluorescence analysis

Cells were transfected with the indicated siRNAs and plated onto glass coverslips 48 h after transfection. Twenty-four h later, cells were fixed with 4% paraformaldehyde for 10 min and permeabilized with 0.25% Triton X-100 for 4 min, followed by blocking with 3% bovine serum albumin (BSA) for 45 min at room temperature. Cells were immunostained with rabbit anti-calpastatin (1:100, Santa Cruz) primary antibody, followed by Alexa 488-conjugated donkey anti-rabbit antibody (1:400, Life Technologies). To reduce background signal, the coverslips were washed with 0.01% Tween-20 in PBS for 5 min followed by two 5 min washes with PBS alone after each antibody incubation. Coverslips were mounted onto microscope slides with polyvinyl alcohol-based medium containing 1 μg/mL 4,6-diamino-2-phenylindole (DAPI) (CalBiochem). Images were acquired with a X40/1.3 oil immersion lens on a Zeiss LSM 710 confocal microscope using the ZEN software (Zeiss).

Assay	Target	Sense Primer	Antisense Primer
RT-(q)PCR	*NFIA*	CTCCACAAAGCGCCTCAAG	CATCAGGGCAGACAAGTTGG
	NFIB	GAAGTCCAAGCCACAATGATC	GATGCAGAGCTGAACAATGG
	NFIC	GATGCAGAGCTGAACAATGG	CATCTCTGTCTTCTTCACCG
	NFIX	GTTCAAACCAGCAAGGAGATG	CGTCATCAACAGGGCTCTC
	ACTB	CTGGCACCACACCTTCTAC	CATACTCCTGCTTGCTGATC
qPCR	*CAST* exon 1 - exon 2	ACAACTGCAAGCTAGATCTG	CTTTCTTTTCTCCTGGTTTGG
	CAST exon 4 - exon 5	GTGTCAGCTTCCTCTGGTG	CTGTTTTTTGTGTTTTTTCTTGTT
	CAST exon 16 - exon 18	AGTGTGGTGAGGATGATGAAA	TTTTCAGTTGGCTTAGATGGTT
	GAPDH	GAGATCCCTCCAAAATCAA	CACACCCATGACGAACAT
ChIP	*CAST* C2	TGTGCCAAGTTCCGAGCCAA	TAGAAGCAGGGGCAGAGGAA
	CAST C3	TGTAGTGGCGCAATGGATGA	CTGGGCAATGTAGTGAGACC
	CAST canonical promoter	GTTCTCCTCCCCATAAAAGTT	AGGAAGCGGATCACAAAAACA
	CAST alternative promoter	ATTCATTATGTGCCAGGGAGT	AAATCTAGTAGGAGGTGGTGT
	GAPDH positive control	TACTAGCGGTTTTACGGGCG	TCGAACAGGAGGAGCAGAGAGCGA
	GAPDH negative control	GAACCAGCACCGATCACC	CCAGCCCAAGGTCTTGAG
RLM RACE	Outer RNA adapter	GCTGATGGCGATGAATGAACACTG	
	Inner RNA adapter	CGCGGATCCGAACACTGCGTTTGCTGGCTTTGATG	
	CAST exon 4		TACTGGAAGACTTGCTGGTTGC
	CAST exon 8		ACTTCCTGTATCTGATGCCTGC
	CAST exon 14		CTTCTCCACCTTTCTTTTCT

Table 2.1. Primer sequences

A

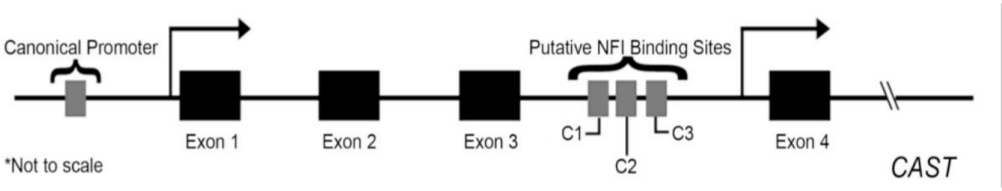

B

NFI Consensus Binding Sequence

TTGGC **(N_{3-6})** **GCCAA**

C1	AGGGAA	*CAT***GC**	ACGCA	**GCCCA**	GTG
	TT	**GTACG**	TGCGT	**CGGGT**	CACAAGAA
C2	GGTGC	**CTGGC**	AAGAG	**GCCAG**	GAGGA
	G	**GACCG**	TTCTC	**CGGTC**	CTCCTGCAC
C3	CCCATC	**CTGGC**	TCACTT	**GCCAG**	GAC
	AG	**GACCG**	AGTGAA	**CGGTC**	CTGGACG

C

C2*	GG TGC	**CTaaC**	AAGAG	**GCCAG**	GAG GA
	G	**GAttG**	TTCTC	**CGGTC**	CTC CTG CAC
C3*	CCC ATC	**CTaaC**	TCACTT	**GaaAG**	GAC
	AG	**GAttG**	AGTGAA	**CttTC**	CTG GAC G
NFI	ATT	**TTGGC**	TTGAA	**GCCAA**	TAT G
	TAA	**AACCG**	AACTT	**CGGTT**	ATA C

AP2 GAT CGA ACT GAC CGC CCG CGG CCC GT
CTA GCT TGA CTG GCG GGC GCC GGG CA

Figure 2.1. Schematic representation of *CAST* promoters and location of predicted NFI binding sites

(A) The canonical and alternative *CAST* promoters located upstream of exon 1 and exon 4, respectively. The relative position of the three putative NFI binding sites (C1, C2, and C3; not to scale) found within intron 3 are shown. (B) Comparison of the three NFI recognition elements and NFI consensus binding site. Conserved nucleotide sequences are indicated in bold. (C) C2* and C3* represent mutated C2 and C3 NFI binding sites, with substitutions indicated in lowercase letters. NFI and AP2 recognition sites are positive and negative competitors, respectively, for gel shift experiments.

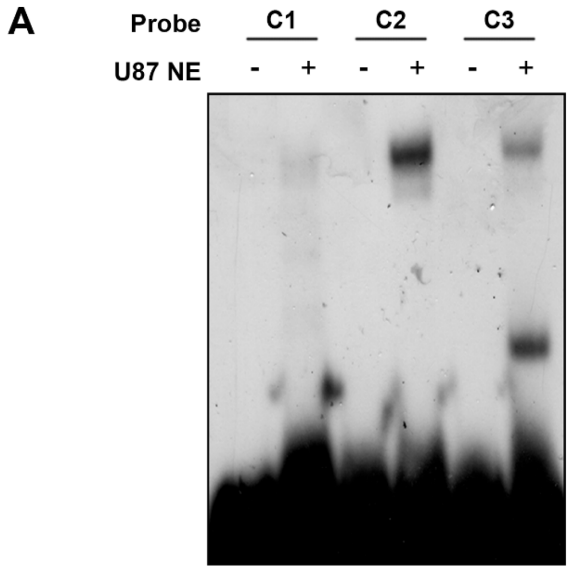
A
Probe
C1
C2
C3
U87 NE
- + - + - +

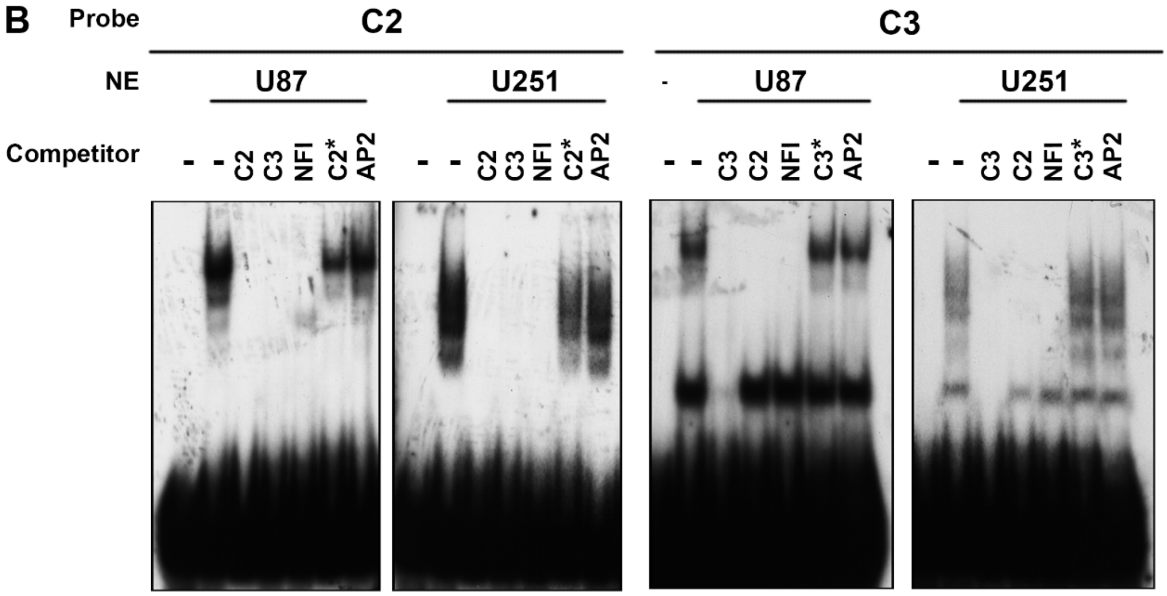
B
Probe
C2
C3
NE
U87
U251
U87
U251
Competitor
- - C2 C3 NFI C2* AP2
- - C2 C3 NFI C2* AP2
- - C3 C2 NFI C3* AP2
- - C3 C2 NFI C3* AP2

Figure 2.2. Gel shifts showing binding of proteins in MG cells to *CAST* NFI recognition sites

(A) Gel shift assay using ^{32}P-labeled C1, C2, and C3 double-stranded oligonucleotides with (+) or without (-) nuclear extracts (1 μg) prepared from U87 MG cells. Samples were electrophoresed in a 6% polyacrylamide gel in 0.5X TBE buffer to separate free DNA probes and DNA-protein complexes. (B) Gel shift assays using nuclear extracts from U87 or U251 MG cells (1 μg per lane) and ^{32}P-labelled C2 and C3 oligonucleotides. When indicated, 100X unlabeled wildtype (C2, C3, NFI, and AP2) or mutated (C2* and C3*) competitors were added to the reaction. Samples were electrophoresed in a 6% polyacrylamide gel in 0.5X TBE buffer to separate free DNA probes and DNA-protein complexes. Gels are representative of three independent experiments.

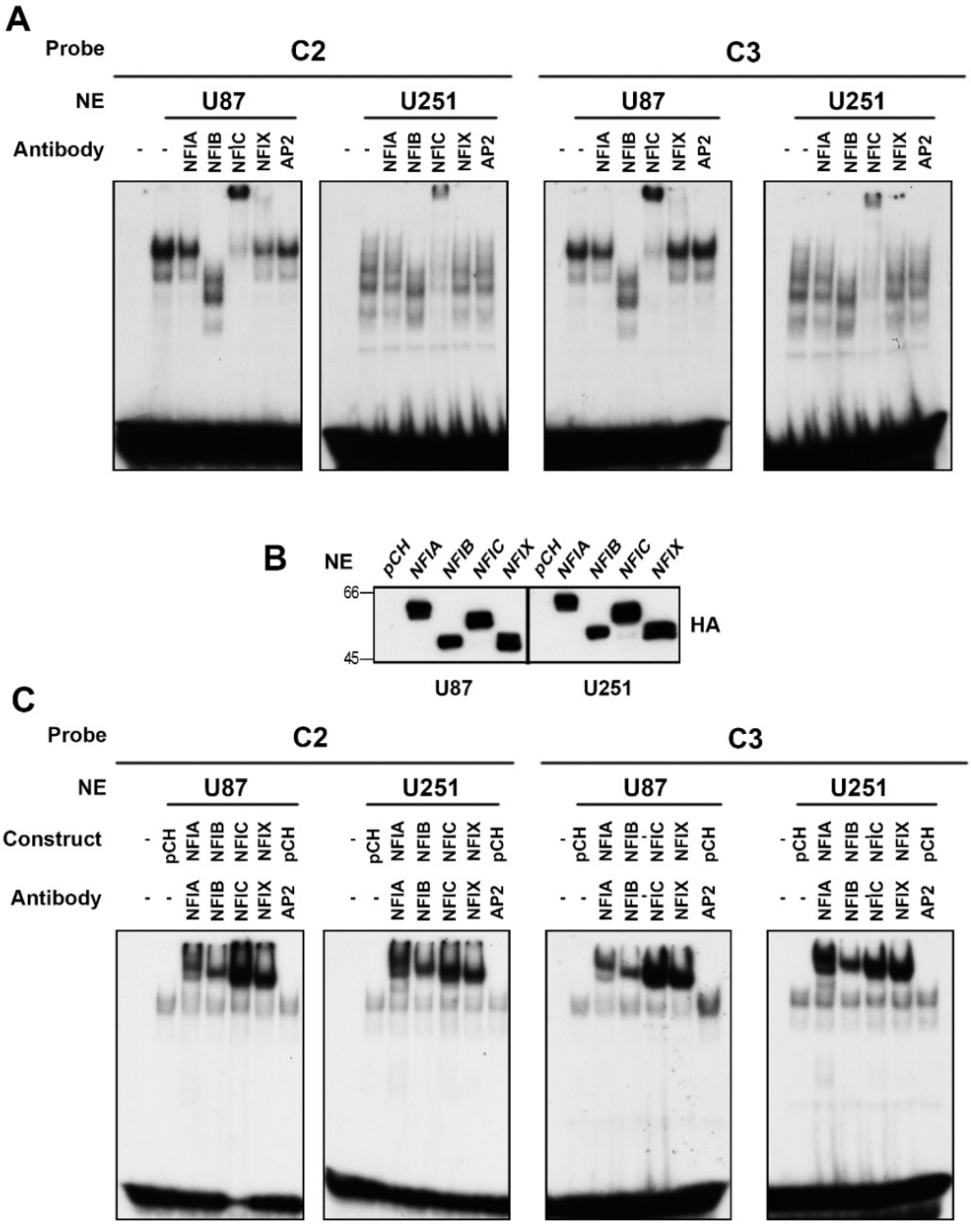
A
Probe
C2
C3
NE
U87
U251
U87
U251
Antibody
- - NFIA NFIB NFIC NFIX AP2
B
NE
pCH NFIA NFIB NFIC NFIX pCH NFIA NFIB NFIC NFIX
66
45
HA
U87
U251
C
Probe
C2
C3
NE
U87
U251
U87
U251
Construct
- pCH NFIA NFIB NFIC NFIX pCH
Antibody
- - NFIA NFIB NFIC NFIX AP2

Figure 2.3. *In vitro* binding of NFIs to the two *CAST* NFI binding sites in intron 3

(A) Supershift assays were carried out with 4 µg of nuclear extracts prepared from U87 or U251 MG cells and ^{32}P-labelled C2 and C3 oligonucleotides. NFIA, NFIB, NFIC, or NFIX antibodies were added to the reactions as indicated. Anti-AP2 antibody served as a non-specific control. Samples were electrophoresed in a 6% polyacrylamide gel in 0.5X TBE buffer to separate free DNA probes and DNA-protein complexes. Gels are representative of three independent experiments. (B) Western blot analysis of U87 and U251 MG cells transiently transfected with HA-tagged NFI expression constructs. Empty vector (pCH) served as negative control. Nuclear extracts were prepared using the NE-PER Nuclear and Cytoplasmic Extraction Kit (ThermoFisher Scientific). Proteins were transferred to nitrocellulose membranes and immunoblotted with anti-HA antibody. (C) Nuclear extracts were prepared from U87 or U251 cells transfected with the indicated HA-tagged NFI expression constructs. Four µg nuclear extracts were incubated with ^{32}P-labelled C2 and C3 oligonucleotides, and anti-HA antibody included where indicated. Anti-AP2 antibody served as a negative control. Samples were electrophoresed in a 6% polyacrylamide gel in 0.5X TBE buffer to separate free DNA probes and DNA-protein complexes. Gels are representative of two independent experiments.

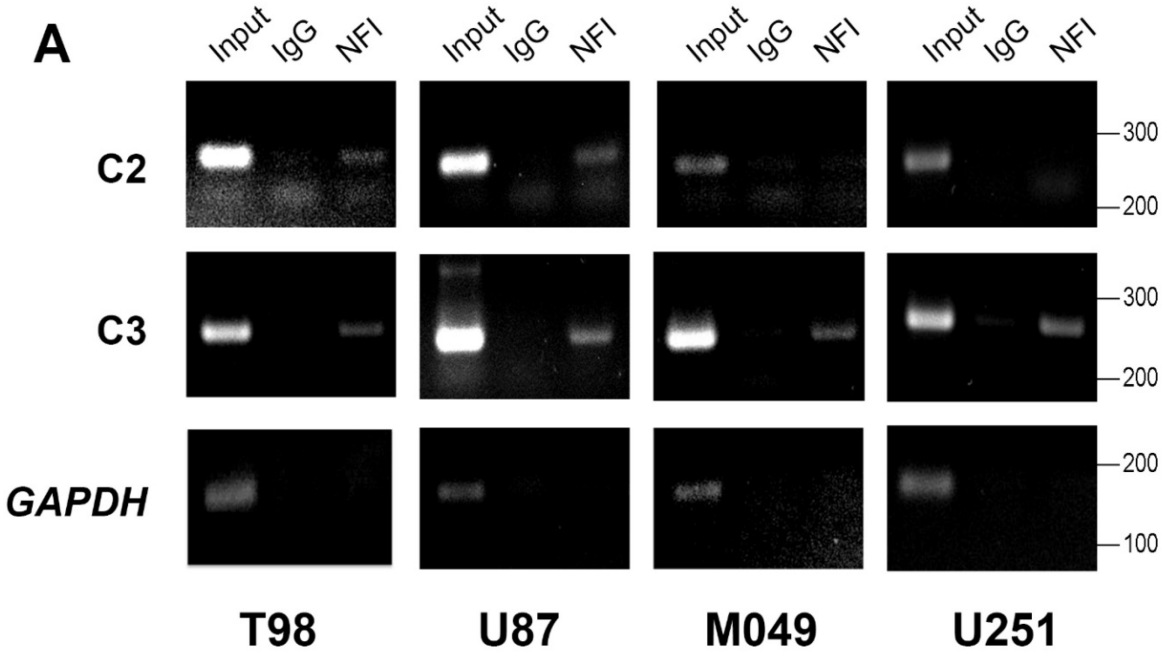
A
Input
IgG
NFI
C2
C3
GAPDH
300
200
100
T98
U87
M049
U251

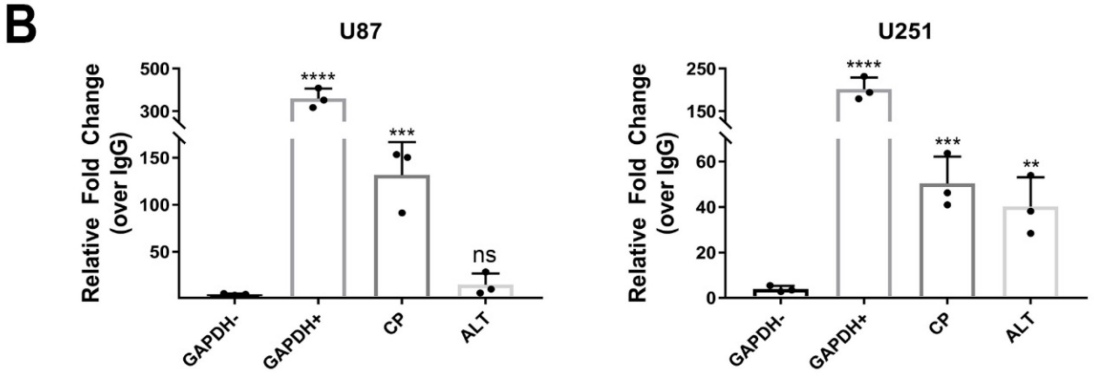
B
U87
U251
Relative Fold Change (over IgG)
GAPDH-
GAPDH+
CP
ALT
ns

Figure 2.4. *In vivo* binding of NFIs to the two *CAST* NFI binding sites in intron 3

ChIP analyses were performed with 2 μg of a pan-specific anti-NFI (Tanese) antibody (A) or an anti-RNA polymerase II antibody (B) using some or all of the following cell lines: NFI-hyperphosphorylated T98 and U87 and NFI-hypophosphorylated M049 and U251 MG cell lines. (A) Primers targeting C2 and C3 were used for PCR amplification of *CAST* NFI binding sites (Table 2.1). Primers to a non-relevant region of *GAPDH* promoter served as a negative control. Input consists of genomic DNA obtained after sonication but before immunoprecipitation. The band in input DNA is of the expected size and serves as a positive control. (B) Specific primers were used to qPCR amplify either the *CAST* canonical (CP) or alternative (ALT) promoter region, each of which contains a TATA box (Table 2.1). Primers to an upstream region of the *GAPDH* proximal promoter served as a negative control (Table 2.1). Primers to the *GAPDH* proximal promoter region containing the TATA box served as a positive control (Table 2.1). Scatter plots in panel B were generated by normalizing signals obtained with NFI or RNA Pol II antibodies against those generated by IgG. Each ChIP experiment was carried out three times. qPCR data are presented as mean ± S.D. (*p-value<0.05, **p-value <0.01, ***p-value <0.001, ****p-value <0.0001).

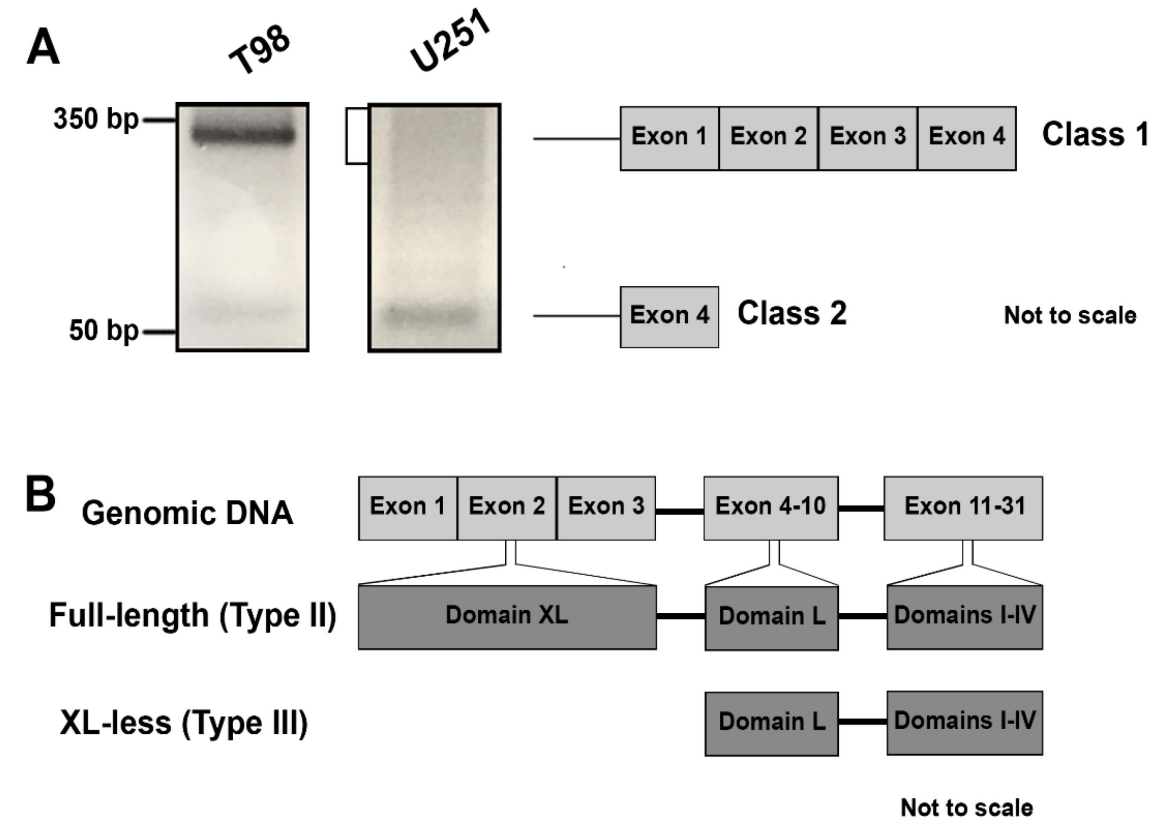
A
T98
U251
350 bp
50 bp
Exon 1
Exon 2
Exon 3
Exon 4
Class 1
Exon 4
Class 2
Not to scale
B
Genomic DNA
Exon 1
Exon 2
Exon 3
Exon 4-10
Exon 11-31
Full-length (Type II)
Domain XL
Domain L
Domains I-IV
XL-less (Type III)
Domain L
Domains I-IV
Not to scale
C
T98
Relative Fold Change
CNT
CP
ALT
D
U251
Relative Fold Change
CNT
CP
ALT
E
U251
Relative Fold Change
ns
CNT
ALT
ALT-2*
ALT-3*
ALT-2*3*

Figure 2.5. *CAST* promoter activity and calpastatin isoform expression in MG cells

(A) 5'-RLM RACE was carried out using 5 µg of total RNA isolated from NFI-hyperphosphorylated (T98) or NFI-hypophosphorylated (U251) MG cells. Antisense primer targeting exon 14 of the *CAST* gene was used for reverse transcription. Nested PCR amplification was carried out with 5'-ligated outer and inner primers and antisense primers targeting exons 8 and 4 of the *CAST* gene, respectively. PCR products were electrophoresed in 3% Metaphor (FMC Bioproducts) agarose gel, visualized with ethidium bromide, excised, purified, and sequenced using the BigDye Terminator v3.1 cycle sequencing kit (ThermoFisher Scientific). Exon composition of the isolated DNA products based on sequence analysis is indicated on the right. (B) Domain composition of XL-containing (Full-length/Type II) and XL-less (Type III) calpastatin isoforms. (C) T98 and (D) U251 MG cells were transiently transfected with luciferase reporter constructs containing the canonical promoter (CP) (~2000 bp upstream of *CAST* exon 1), alternative promoter (ALT in intron 3 containing the NFI binding sites (~4000 bp upstream of *CAST* exon 4), or empty vector (CNT). Luciferase activity was measured using the Luciferase Assay System (Promega) and the FLUOstar microplate reader (BMG LABTECH). Relative fold change was calculated relative to the empty vector control. Scatter plots show data from 3 independent experiments. (E) U251 MG cells were transiently transfected with luciferase reporter constructs containing the wildtype ALT or constructs containing mutation at C2 (ALT-C2*), C3 (ALt-C3*), or both C2 and C3 (ALT-C2*C3*) NFI binding sites. Luciferase activity was measured

48 h post-transfection as described above. P-values were obtained from one-way ANOVA statistical analysis of three independent experiments. (*p-value<0.05, **p-value <0.01, ***p-value <0.001, ****p-value <0.0001).

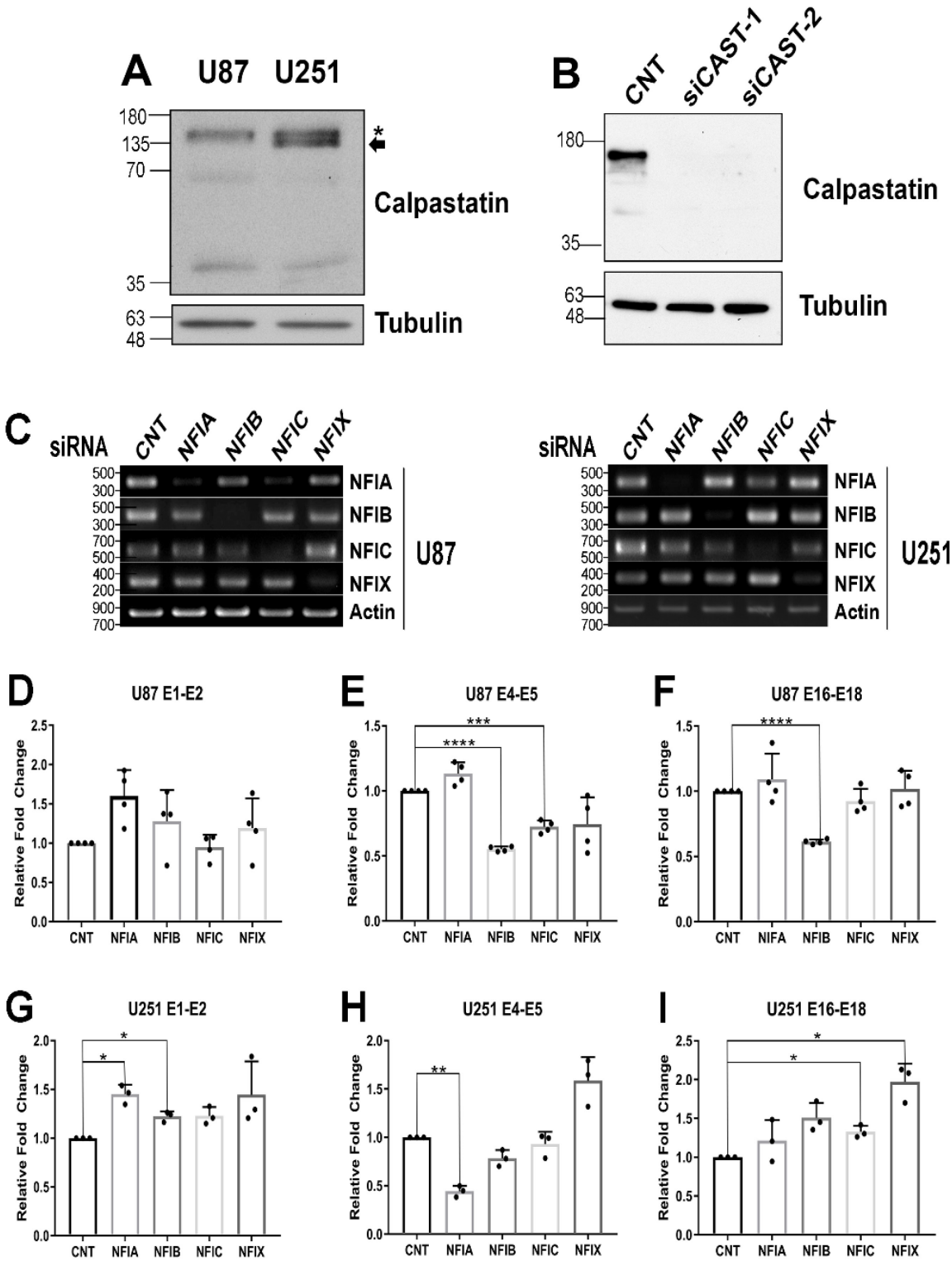
A
U87
U251
180
135
70
35
63
48
*
Calpastatin
Tubulin
B
CNT
siCAST-1
siCAST-2
180
35
63
48
Calpastatin
Tubulin
C
siRNA
CNT
NFIA
NFIB
NFIC
NFIX
500
300
500
300
700
500
400
200
900
700
NFIA
NFIB
NFIC
NFIX
Actin
U87
U251
D
U87 E1-E2
E
U87 E4-E5
F
U87 E16-E18
Relative Fold Change
CNT
NFIA
NFIB
NFIC
NFIX
NIFA
***
****
G
U251 E1-E2
H
U251 E4-E5
I
U251 E16-E18
**

Figure 2.6. *CAST* variants and calpastatin isoform expression in MG cells

Whole cell extracts from (A) non-transfected U87 and U251 or (B) U251 MG cells transiently transfected with scrambled (control; CNT) or siRNAs targeting *CAST* exon 4 (si-CAST-1) and exon 16 (siCAST-2) were electrophoresed in a 15% SDS-polyacrylamide gel at 180 V for 75 min and then transferred to a nitrocellulose membrane. Blots were immunostained with rabbit polyclonal anti-calpastatin antibody (1:10,000, Santa Cruz) or mouse anti-α-tubulin antibody (1:100,000, Hybridoma Bank) followed by horseradish peroxidase-conjugated secondary antibody (1:50,000). The signal was detected using the Immobilon western detection reagent. (C) RT-PCR showing the knockdown efficiencies of siRNAs targeting specific NFIs in U87 and U251 MG cells. (D-I) Quantitative PCR analysis using cDNAs prepared from U87 (D-F) or U251 (G-I) MG cells transiently transfected with siRNAs targeting specific NFIs as indicated. cDNAs were amplified with primers targeting exons 1 and 2 (D, G), exons 4 and 5 (E, H), or exons 16 and 18 (F, I) of the *CAST* gene. *GAPDH* was used as a control for variation in cDNA concentration. Scatter plots show fold changes relative to scrambled siRNA control (set at 1) in three independent experiments. Bars represent the mean ± s.d. for three independent experiments (*p-value<0.05, **p-value <0.01, ***p-value <0.001, ****p-value <0.0001).

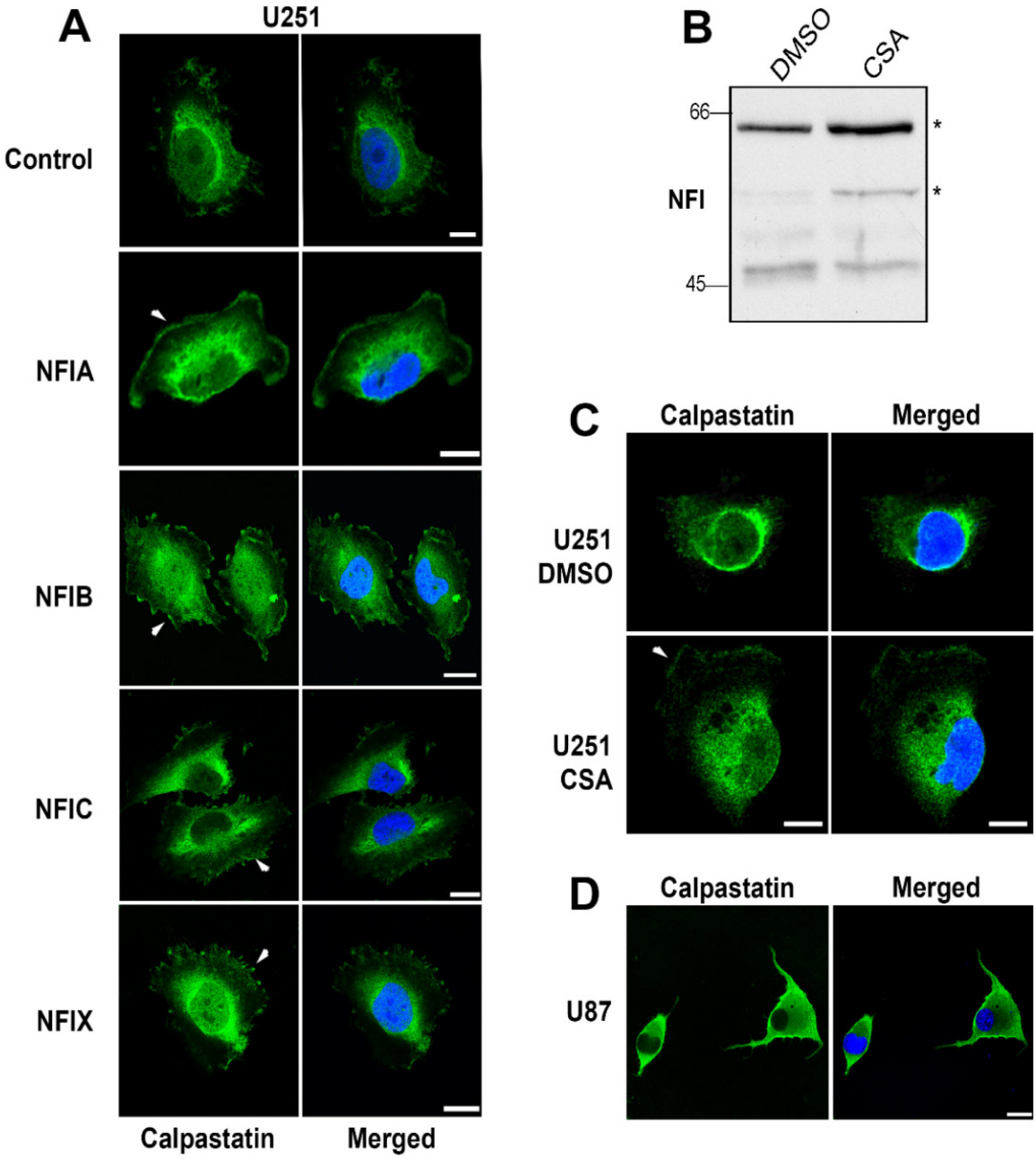
A
U251
Control
NFIA
NFIB
NFIC
NFIX
Calpastatin
Merged
B
DMSO
CSA
66
45
NFI
*
*
C
Calpastatin
Merged
U251
DMSO
U251
CSA
D
Calpastatin
Merged
U87

Figure 2.7. Changes in calpastatin subcellular localization upon NFI knockdown or modification of NFI phosphorylation

(A) U251 MG cells were transiently transfected with siRNAs targeting the indicated NFIs, then plated on coverslips. After 48 h, cells were fixed with 4% paraformaldehyde and immunostained with a polyclonal anti-calpastatin antibody (1:100, Santa Cruz Biotechnologies) followed by Alexa 488-conjugated secondary antibody (green signal). Nuclei were stained with DAPI (blue) and images acquired by confocal microscopy using a 40X/1.3 oil immersion lens. Bars, 10 μm. All images are representative of the majority of cells observed under each condition. The arrowheads point to the calpastatin signal at the plasma membrane. (B) U251 MG cells were treated with 1 μM of cyclosporin A (CSA) for 1 h at 37ºC. Nuclear extracts were electrophoresed in polyacrylamide-SDS gels and electroblotted onto nitrocellulose membranes. Blots were immunostained with a mouse pan-specific anti-NFI antibody (1:1,000, Santa Cruz Biotechnologies), followed by horseradish peroxidase-conjugated secondary antibody (1:50,000). The signal was detected using the Immobilon western detection reagent. The asterisks point to hyperphosphorylated forms of NFI. (C) CSA-treated U251 MG cells or (D) U87 MG cells transfected with scrambled (control) siRNAs were fixed, immunostained and visualized as described in A. Bars, 20 μm (C) or 10 μm (D). All images are representative of three independent experiments.

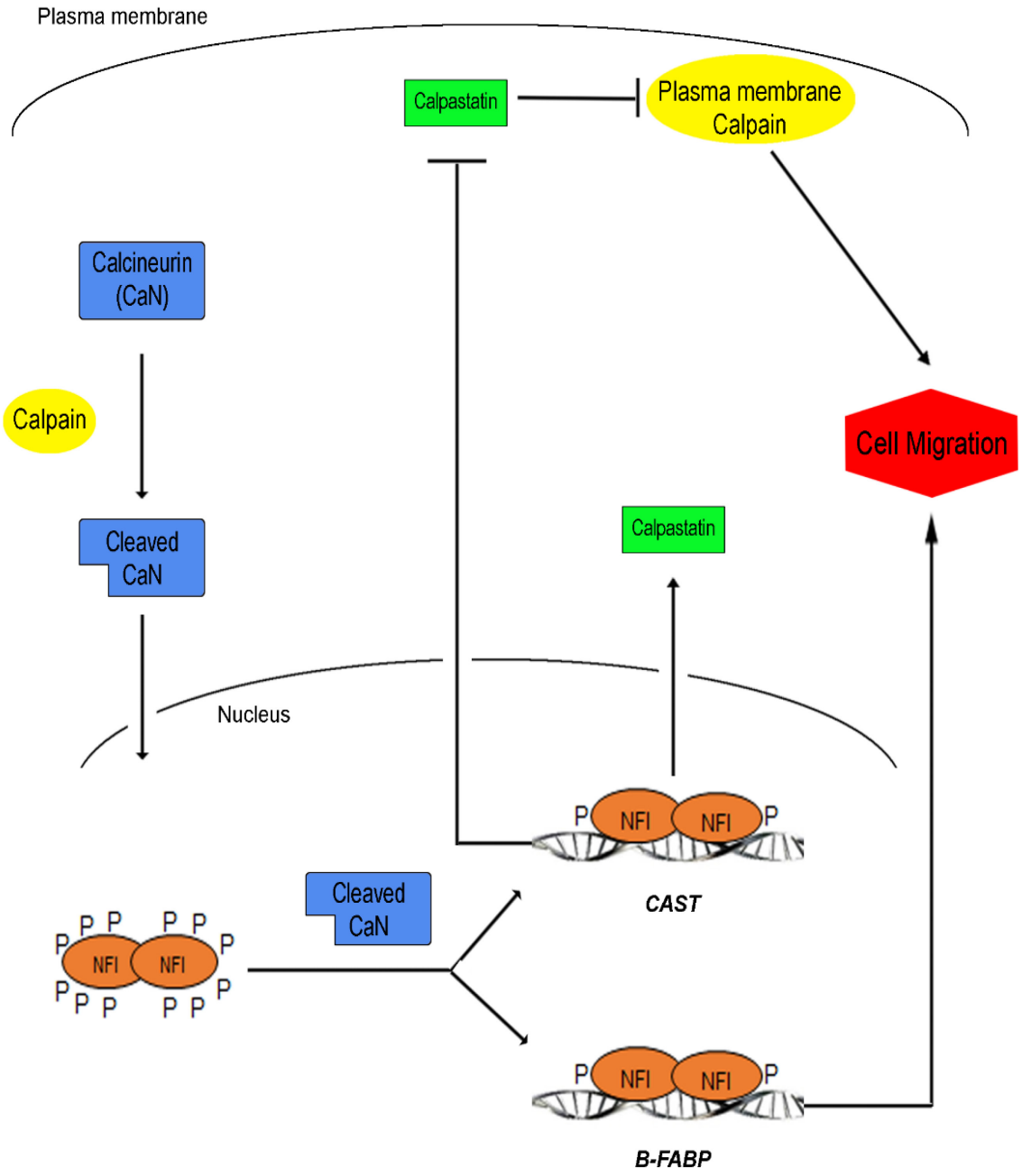
Plasma membrane
Calpastatin
Plasma membrane Calpain
Calcineurin (CaN)
Calpain
Cell Migration
Cleaved CaN
Calpastatin
Nucleus
P NFI NFI P
CAST
Cleaved CaN
P P P P P NFI NFI P P P P P P
P NFI NFI P
B-FABP

Figure 2.8. Model of the regulatory crosstalk between the calpain/calpastatin pathway and NFI in MG cells

In the cytoplasm, calcineurin is cleaved and activated by calpain. Activated calcineurin translocates to the nucleus, dephosphorylates and activates NFI. Hypophosphorylated NFI upregulates cell migration-promoting *FABP7* as well as *CAST* variants that exclude the XL domain and preferentially localize to the cytoplasm. NFI also negatively affects the expression of plasma membrane-associated full-length calpastatin. As a consequence, calpastatin-calpain interaction at the plasma membrane is reduced, calpain remains active, calpain target effectors are cleaved, and MG cell migration is enhanced.

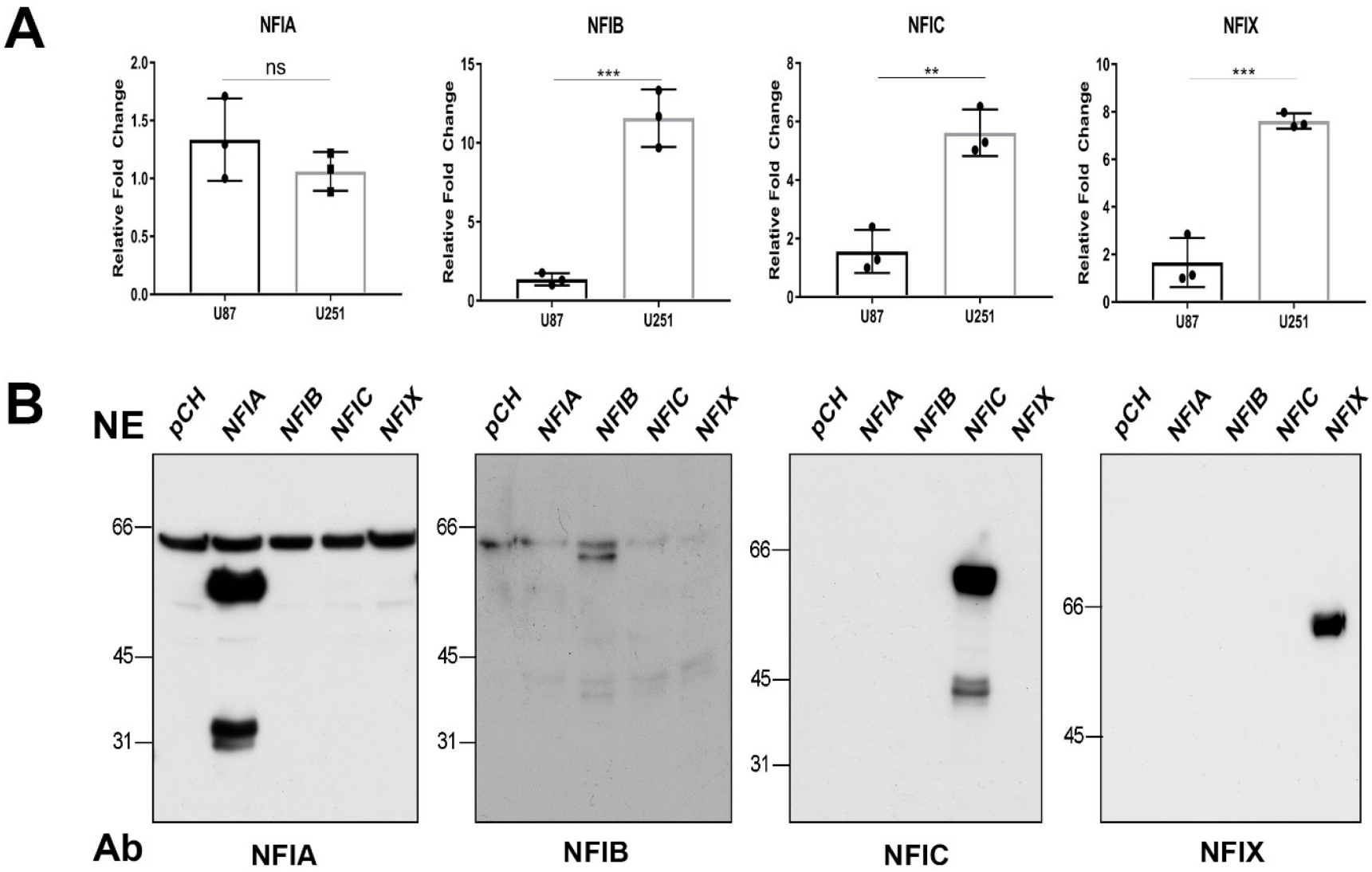
A
NFIA
NFIB
NFIC
NFIX
Relative Fold Change
ns
***
**
***
U87
U251
B
NE
pCH
NFIA
NFIB
NFIC
NFIX
66
45
31
Ab
NFIA
NFIB
NFIC
NFIX

Figure 2.9. Endogenous NFI levels and specificity of anti-NFI antibodies

Anti-NFI antibodies (GenScript) were generated to unique regions of each NFI. (A) RT-qPCR was performed using RNA isolated from U87 and U251 MG cells with primers targeting the indicated NFIs (Table 2.1). Expression of each NFI in U251 was normalized against that of U87 MG cells. *GAPDH* was amplified as a control for amount of cDNA. Each experiment was carried out three independent times. Data are presented as mean ± S.D. (*p-value<0.05, **p-value <0.01, ***p-value <0.001, ****p-value <0.0001). (B) U251 MG cells were transiently transfected with the indicated HA-tagged NFI expression constructs. Empty vector (pCH) served as negative control. Nuclear extracts were prepared using the NE-PER Nuclear and Cytoplasmic Extraction Kit (ThermoFisher Scientific). Proteins were transferred to nitrocellulose membranes, immunoblotted with the indicated GenScript anti-NFI antibodies (1:1000) followed by horseradish peroxidase-conjugated secondary antibody (1:50,000). The signal was detected using the Immobilon western detection reagent.

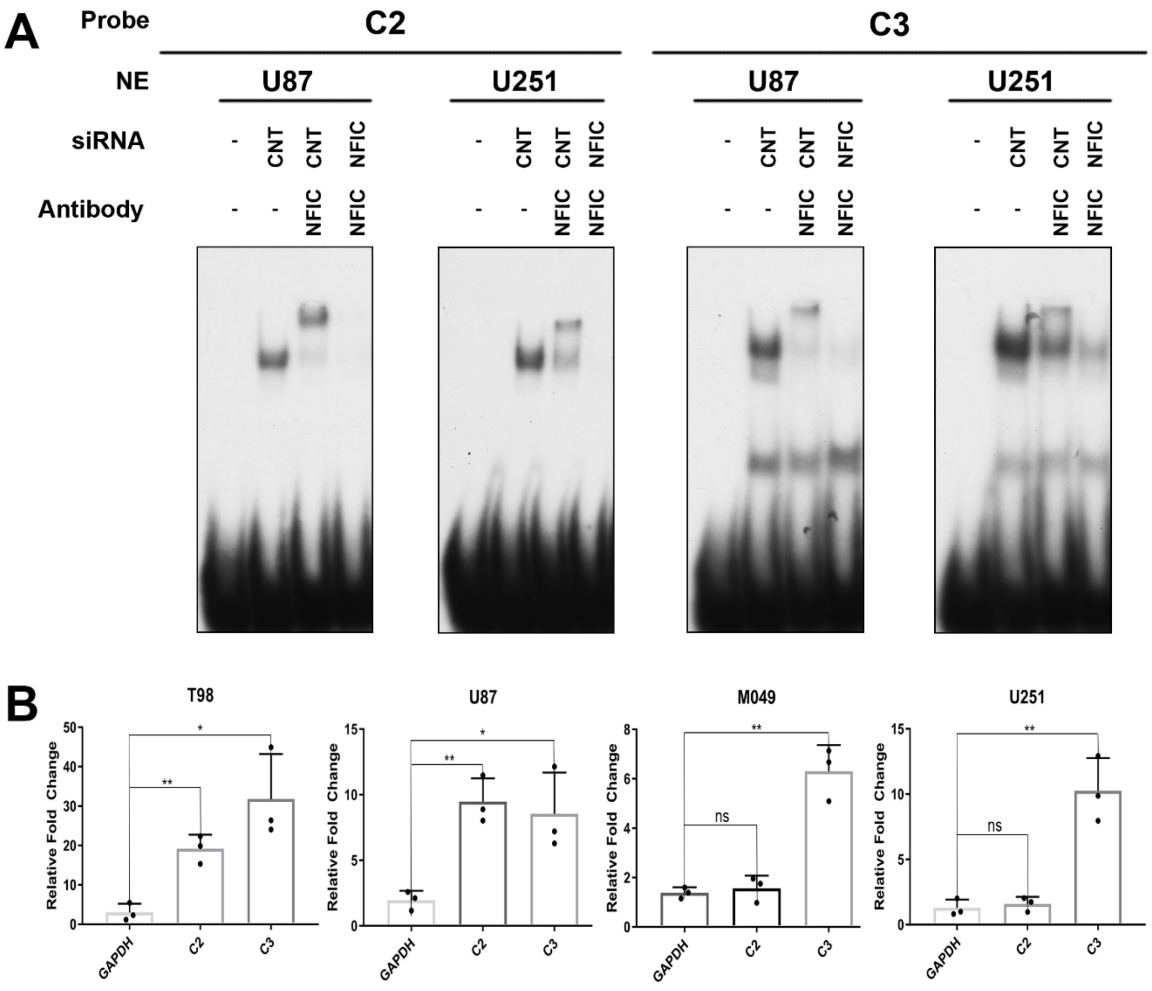
A
Probe
C2
C3
NE
U87
U251
U87
U251
siRNA
- CNT CNT NFIC
Antibody
- - NFIC NFIC
B
T98
U87
M049
U251
Relative Fold Change
GAPDH
C2
C3
ns

Figure 2.10. Binding of *CAST* by NFIC and quantification of ChIP results

(A) Nuclear extracts were prepared from U87 and U251 MG cells transiently transfected with either scrambled or NFIC-specific siRNA. Four μg nuclear extracts were incubated with ^{32}P-labelled C2 and C3 oligonucleotides and GenScript anti-NFIC antibody included where indicated. Samples were electrophoresed in a 6% polyacrylamide gel in 0.5X TBE buffer to separate free DNA probes and DNA-protein complexes. Results are representative of two independent experiments. (B) ChIP analyses were performed with 2 μg of a pan-specific anti-NFI (Tanese) using the following cell lines: NFI-hyperphosphorylated T98 and U87 and NFI-hypophosphorylated M049 and U251 MG cell lines. Primers targeting C2 and C3 were used for qPCR amplification of *CAST* NFI binding sites (Table 2.1). Primers to the upstream region of the *GAPDH* promoter served as negative control (Table 2.1). Results were derived from three independent experiments and presented as mean ± S.D. (*p-value<0.05, **p-value <0.01, ***p-value <0.001, ****p-value <0.0001).

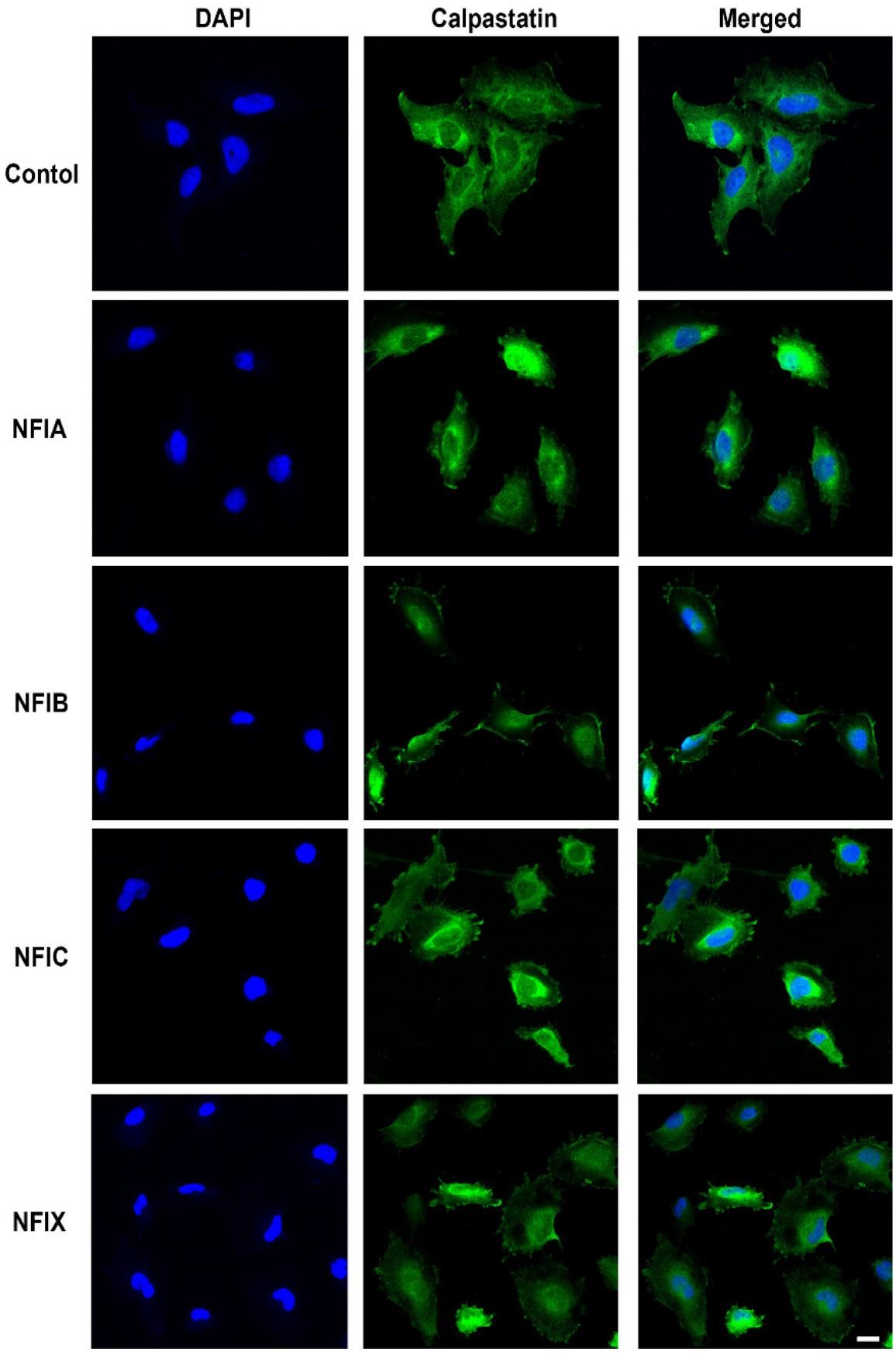
DAPI
Calpastatin
Merged
Contol
NFIA
NFIB
NFIC
NFIX

Figure 2.11. Changes in calpastatin subcellular localization in U251 MG cells upon NFI depletion

Cells were transiently transfected with siRNAs targeting the indicated NFIs then plated on coverslips. After 48 h, cells were fixed with 4% paraformaldehyde and immunostained with a polyclonal anti-calpastatin antibody (1:100, Santa Cruz Biotechnologies) followed by Alexa 488-conjugated secondary antibody. Nuclei were stained with DAPI and images acquired by confocal microscopy using a 40X/1.3 oil immersion lens. Bars, 20 μm. All images are representative of three independent experiments.

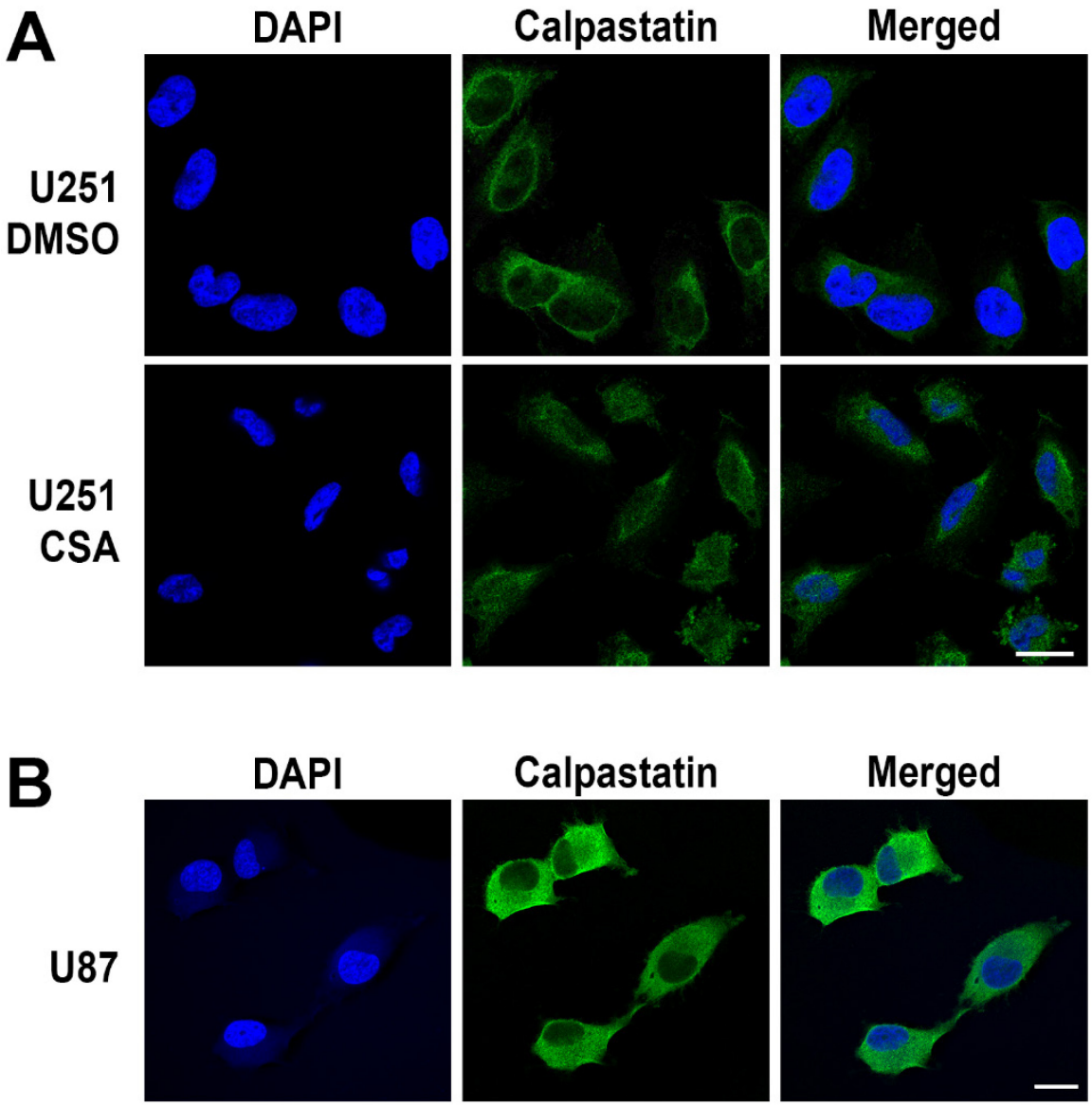
A
DAPI
Calpastatin
Merged
U251
DMSO
U251
CSA
B
DAPI
Calpastatin
Merged
U87

Figure 2.12. Calpastatin subcellular localization upon induction of NFI hyperphosphorylation in U251 MG cells and in NFI-hyperphosphorylated U87 MG cells

(A) U251 MG cells were plated on coverslips. After 24 h, cells were treated with 1 μM CSA at 37ºC. (B) U87 MG cells were transiently transfected with scrambled (control) siRNA and then plated on coverslips. After 1 h (A) or 48 h (B), cells were fixed with 4% paraformaldehyde. Coverslips were immunostained with a polyclonal anti-calpastatin antibody (1:100, Santa Cruz Biotechnologies) followed by Alexa 488-conjugated secondary antibody. Nuclei were stained with DAPI and images acquired by confocal microscopy using a 40X/1.3 oil immersion lens. Bars, 20 μm. All images are representative of three independent experiments.

CHAPTER 3: NUCLEAR FACTOR IB AND CALPAIN 1 POSITIVE FEEDBACK LOOP NEGATIVELY REGULATES GLIOBLASTOMA CELL MIGRATION

3.1 Introduction

Glioblastomas (GBM), classified as WHO grade IV astrocytomas, are the most aggressive form of adult brain tumors (57). Despite recent advances in therapeutic intervention, the prognosis for GBM patients remains dismal, with median survival times of ~15 months (30,55). GBM cells are highly infiltrative, a property that may be driven by expression of neural stem markers. These stem like/infiltrative properties allow GBM cells to evade conventional treatment, including surgery, chemotherapy (usually temozolomide) and radiation therapy (354-356). Without effective second-line treatment, patients often succumb to the disease shortly after tumor recurrence (357-359). Although significant effort has been made to unravel the mechanisms underlying GBM infiltration of normal brain tissue, we still have a poor understanding of what drives infiltration at the molecular level.

The Nuclear Factor I family of four transcription factors (NFIA, NFIB, NFIC and NFIX) plays an integral role in regulating genes involved in neural cell migration and gliogenesis (112,117). We have shown that NFIs regulate the neural progenitor/stem cell marker gene (brain fatty acid-binding protein - *FABP7*) (163,362), whose expression is associated with higher GBM cell migration *in vitro* and infiltration *in vivo* (183,184,361,372). NFI regulation of *FABP7* is dependent on its phosphorylation state, with hypophosphorylated NFI upregulating *FABP7* expression *(362)*. NFIs are dephosphorylated by calcineurin phosphatase in GBM cells (164).

Calcineurin cleavage and activation are mediated by calpain, a family of calcium-dependent neutral proteases (196,282,365). The best characterized calpains, calpain 1 (μ-calpain) and calpain 2 (m-calpain), are named based on the amount of calcium required for their activation *in vitro*: micro (μ)- or milli (m)-molar Ca^{2+} concentrations (196). Both calpains 1 and 2 function as heterodimers, comprised of a distinct large subunit, CAPN1 (for μ-calpain) or CAPN2 (for m-calpain), and a shared smaller subunit (CAPSN1) (218). Calpain can either promote or inhibit cell migration depending on cell type. For example, inhibition of calpain 1 activity results in reduced platelet cell spreading (211). In contrast, inhibition of calpain 1 activity promotes random neutrophil migration (195). In addition, calpain 1 has been shown to prevent endothelial cell spreading as the result of calpain 1-mediated proteolysis of RhoA, a key factor in cell migration (213).

Calpain proteolytic activity is tightly regulated. Soon after its discovery, calpain was shown to undergo autoproteolysis (or autolysis) (196). Autolyzed calpain requires lower calcium to reach half-maximal activity and thus is more active compared to full-length calpain (299). However, autolyzed calpain is also more unstable and prone to degradation and/or aggregation, the latter resulting in its inactivation (299). This instability may protect cells from detrimental effects associated with hyperactive calpain. Calpain activity is also regulated by its highly specific endogenous inhibitor, calpastatin (366). Binding of calpastatin to calpain not only inhibits its activity, but also prevents full autolysis of calpain leading to accumulation of the full-length form (392). Since calpastatin and calpain are

ubiquitously expressed, their ratio and/or subcellular distributions may determine the level of calpain proteolytic activity within a cell.

Calpains can be inhibited by a wide array of exogenous inhibitors, including calpain inhibitor I (ALLN), a membrane-permeable synthetic peptide that specifically targets both calpain 1 and 2 *in vitro* (393). Aclacinomycin a (aclarubicin, ACM), used for the treatment of patients with relapsed or refractory myeloid cancers, is a doxorubicin-like antibiotic that inhibits calpain activity (394-396)

We have previously shown that the *CAST* gene, encoding calpastatin, is a target of NFI in GBM cells. NFI functions through an alternative promoter containing two NFI binding sites located in *CAST* intron 3 (369,397). By differentially regulating the usage of *CAST* canonical and alternative promoters, NFI can alter the relative levels of *CAST* variants encoding full-length versus truncated calpastatin in GBM cells, with accompanying changes in the subcellular localization of calpastatin (397). NFI phosphorylation is an important determinant of *CAST* variant levels in GBM cells (397). Here, we show that NFIB regulation of *CAST* variants, and therefore calpastatin isoforms, affects calpain 1 levels and calpain 1 subcellular distribution in GBM cells. In turn, calpain 1 induces NFIB dephosphorylation through activation of calcineurin. This NFIB-calpain 1 positive feedback loop suppresses GBM cell migration but does not affect GBM cell survival.

3.2 Results

3.2.1 NFI directly regulates CAST but not calpain genes

We have previously shown that the expression of *CAST* variants in GBM cells is dependent on NFI phosphorylation state (397). To examine how differentially phosphorylated NFI affects calpastatin protein levels, we transiently transfected T98 (NFI-hyperphosphorylated) and U251 (NFI-hypophosphorylated) GBM cells (163) with either NFI expression constructs or previously validated siRNAs (362,369,397) targeting each of the four NFIs. Knocking down individual NFIs in NFI-hypophosphorylated U251 cells resulted in increased levels of calpastatin (Figure 3.1A, left panel), with NFI overexpression having no effect on calpastatin (data not shown). In contrast, NFI depletion in NFI-hyperphosphorylated T98 GBM cells had no effect on calpastatin levels (data not shown). However, NFI overexpression reduced calpastatin levels (Figure 3.1, right panel). These data indicate that all four NFIs, through regulation of *CAST* variants, suppress the expression of calpastatin in GBM cells. Of note, the calpastatin antibody used for these experiments is specific to full-length calpastatin (~145 kDa), which has four calpain inhibitory domains (I-IV), the XL and the L N-terminal domains.

Calpastatin is an endogenous inhibitor of calpain. Since NFIs affect levels of calpastatin, we were interested in whether NFIs might also affect calpain activity through a calpastatin feedforward loop. But first, we wanted to ensure that NFI did not directly regulate calpain genes, as this would negate the need for a calpastatin-mediated feedforward loop. To address this possibility, we transiently transfected

U87 and U251 GBM cells with siRNAs targeting each NFI member and carried out RT-qPCR using primers flanking the large subunit of calpain 1 (*CAPN1*), the large subunit of calpain 2 (*CAPN2*) and the small subunit (*CAPSN1*) that is shared by both calpains. Depletion of NFIs did not significantly affect *CAPN1*, *CAPN2*, and *CAPSN1* RNA levels (Figs. 1B and C). Thus, NFI does not appear to regulate the transcription of calpain genes. In line with these results, we did not identify NFI binding sites in the promoter regions of *CAPN1, CAPN2, and CAPSN1,* based on *in silico* analysis.

3.2.2 Differentially phosphorylated NFIB exert distinct effects on the subcellular distribution of calpain 1

Of the 4 NFIs, the role of NFIB in cancer is best documented (171,398,399). Thus, we focused on examining the role of NFIB in the calpastatin/calpain pathway. To determine whether NFIB-mediated regulation of *CAST* affects calpains 1 and 2, we transiently transfected NFI-hyperphosphorylated U87 and NFI-hypophosphorylated U251 GBM cells (163) with two siRNAs targeting different regions of NFIB and carried out western blot analysis using antibodies to either calpain 1 or calpain 2. Since calpain-mediated proteolysis of downstream effectors is dependent on the subcellular location of calpain, we carried out nuclear and cytoplasmic fractionation to investigate whether NFIB differentially affects calpain levels in these two cellular compartments.

Knocking down NFIB in U87 GBM cells had no effect on either the cytoplasmic or nuclear levels of calpain 2 (Figs. 2A and B, left panels), but resulted in increased levels of full-length calpain 1 in the cytoplasm (Figure 3.2A, left panel).

Levels of calpain 1 in the nucleus were not affected (Figure 3.2B, left panel). As depletion of NFIB in GBM cells increased overall levels of calpastatin (Figure 3.1A), and calpastatin binds and inhibits calpain autolysis, our combined results suggest that hyperphosphorylated NFIB in U87 cells prevents activation of cytoplasmic calpain 1.

In contrast, depletion of NFIB in NFI-hypophosphorylated U251 cells had no effect on cytoplasmic calpain 1 (Figure 3.2A, right panel) but led to a decrease in levels of a ~55 kDa autolyzed form of calpain 1 in the nucleus (Figure 3.2B, right panel). Of note, we did not detect full-length calpain 1 in the nucleus of either U87 or U251 cells, suggesting that either autolysis of calpain 1 is required for its nuclear translocation or calpain 1 autolysis occurs with higher efficacy in the nucleus. These data suggest that hypophosphorylated NFIB can indirectly influence levels of nuclear, but not cytoplasmic, calpain 1. We used α-tubulin and lamin A/C as the loading controls for the cytoplasmic and nuclear fractions, respectively. NFIB knockdown efficiency is shown in both cell lines (Figure 3.2C). Since NFIB depletion affected calpain 1, but not calpain 2, we focused on calpain 1 in subsequent experiments.

Next, we used immunostaining analysis to examine the effect of NFIB depletion on the subcellular distribution of calpastatin and calpain 1. In NFI-hyperphosphorylated U87 cells, calpastatin was found throughout the cytoplasm with little to no calpastatin in the nucleus. NFIB depletion resulted in increased aggregation of calpastatin surrounding the nucleus, with no apparent effect on nuclear calpastatin (see arrowhead - Figure 3.3A). These two patterns of

localization have been reported for calpastatin in other systems (351,384). Similarly, NFIB depletion in U87 cells resulted in increased cytoplasmic aggregation of calpain 1 to one side of the cell (see arrowheads - Figure 3.3A and C, left panel). These observations suggest an association between hyperphosphorylated NFIB and disaggregation of cytoplasmic calpastatin and calpain 1.

We have previously shown that calpastatin has a perinuclear distribution in NFI-hypophosphorylated U251 cells, with NFIB depletion resulting in increased levels of nuclear calpastatin (397). Here, we show that calpain 1 is primarily in the nucleus of U251 cells (Figure 3.3B). NFIB knockdown resulted in decreased levels of nuclear calpain 1 (Figure 3.3C, right panel), presumably the autolyzed form of calpain 1 based on our western blots (Figure 3.3B). These results point to a role for hypophosphorylated NFIB in the differential localization of calpastatin (to the cytoplasm) and calpain 1 (to the nucleus).

3.2.3 NFIB depletion decreases calpain activity and GBM cell migration but does not affect GBM cell viability

Whether through accumulation of cytoplasmic full-length calpain 1 (as observed in NFI-hyperphosphorylated U87 cells) or loss of autolyzed nuclear calpain 1 (as observed in NFI-hypophosphorylated U251 cells), our results, taken in light of evidence from the literature, point to reduced calpain 1 activity upon NFIB depletion in GBM cells. To investigate how calpain 1 proteolytic activity changes upon NFIB depletion, we transiently transfected U87 and U251 cells with two siRNAs targeting NFIB and then measured calpain activity using a fluorometric

substrate. NFIB depletion resulted in decreased calpain proteolytic activity in both cell lines. Specifically, NFIB knockdown in U87 cells resulted in lower levels of relative fluorescence intensity, to 0.29-fold (siNFIB-1, $p<0.0001$) and 0.55-fold (siNFIB-2, $p<0.001$), compared to scrambled siRNA-transfected cells (Figure 3.4A, left panel). Similarly, NFIB depletion in U251 cells resulted in reduced levels of relative fluorescence intensity, to 0.51-fold (siNFIB-1, $p<0.0001$) and 0.57-fold (siNFIB-2, $p<0.001$), compared to scrambled siRNA-transfected cells (Figure 3.4A, right panel). While our calpain activity fluorometric assay does not differentiate between calpain 1 and calpain 2, our western blots show that calpain 2 levels are not affected by NFIB knockdown (Figure 3.2A and B). As NFIB depletion reduced total calpain activity to ~50% compared to control cells, we conclude that the effect of NFIB on calpain activity is mediated chiefly through calpain 1.

We used the Transwell assay to examine how reduced calpain 1 proteolytic activity in NFIB-depleted cells affects GBM cell migration. NFIB knockdown in U87 and U251 cells resulted in ~3-fold and ~2-fold increases in numbers of migrating cells, respectively (Figure 3.4B). Specifically, the number of migrated U87 cells increased from 392 to 1179 in control- versus siNFIB-1-treated cells (~3-fold, $p<0.0001$). Likewise, the number of migrated U251 cells increased from 433 to 843 in control- versus siNFIB-1-treated cells (~2-fold, $p<0.0001$). These results suggest that NFIB inhibits GBM cell migration, irrespective of NFI phosphorylation state.

We also examined the effect of NFIB depletion on GBM cell survival using the MTS assay. The MTS assay measures cell metabolism, and is a surrogate

assay for cell viability (400). NFIB knockdown had no effect on cell viability in both U87 ($p>0.65$) and U251 ($p>0.48$) cells (Figure 3.4C). These observations indicate that NFIB-calpastatin-calpain 1 crosstalk may not be important for GBM cell viability.

3.2.4 Calpain 1 depletion induces NFIB phosphorylation

So far, we have shown that NFIB affects calpain 1 levels and activity, with concomitant changes in levels and subcellular distribution of calpastatin. Here, we address the possibility of bidirectional signaling between calcineurin/NFIB and calpain 1 in GBM cells. We transiently transfected NFIB-hypophosphorylated U251 cells with two siRNAs targeting calpain 1 and examined the effect of calpain 1 depletion on the catalytic subunit of calcineurin and NFIB phosphorylation. In keeping with calcineurin being cleaved and activated by calpain 1 (282,365), knocking down calpain 1 resulted in accumulation of the uncleaved form of calcineurin (~60 kDa) in the cytoplasm of U251 cells (Figure 3.5A). Loss of calpain 1 also led to increased levels of full-length calpastatin in U251 cells (Figure 3.5A), which agrees with our previous findings showing that NFI-hyperphosphorylated GBM cells preferentially express full-length calpastatin (397).

As expected, depletion of calpain 1 also resulted in decreased levels of the cleaved forms of calcineurin in U251 cells (Figure 3.5B; indicated by the asterisk). Of note, cleaved calcineurin was only observed in the nucleus of U251 cells, suggesting that the cleavage of calcineurin occurs after its nuclear translocation and thus can be influenced by calpain 1 concentration in the nucleus. This observation may explain how NFI remains hyperphosphorylated in U87 cells

despite increased cytoplasmic calpain 1 levels. Along with reduced calcineurin cleavage, we observed hyperphosphorylation of NFIB in calpain 1-depleted U251 cells compared to control cells (asterisk in Figure 3.5C). It is noteworthy that these hyperphosphorylated forms of NFIB migrate even more slowly than those observed in U87 cells (Figure 3.5C), suggesting that NFIB exists in a basally hyperphosphorylated state in control (i.e. non-calpain 1 depleted) U87 GBM cells. To confirm that the slower-migrating forms of NFIB observed upon calpain 1 depletion are indeed hyperphosphorylated, we treated U251 cell extracts with λ-phosphatase. All the NFIB bands underwent a reduction in size after λ-phosphatase treatment (Figure 3.5D). Of note, the banding patterns of NFIB were different depending on whether phosphatase inhibitors were included (Figure 3.5C) or not (Figure 3.5D). This is likely due to the potent phosphatase activity of calcineurin, which may dephosphorylate NFIB in the absence of phosphatase inhibitors. Together, our data support the second signaling branch of the NFIB-calpain 1 crosstalk in GBM cells: calpain 1 cleaves and activates calcineurin, which in turn dephosphorylates NFIB in U251 cells.

3.2.5 Calpain 1 depletion alters the subcellular distribution of calcineurin and NFIB

We performed immunofluorescence analysis of calpain 1-depleted U251 (NFI-hypophosphorylated) cells to further investigate the effect of calpain 1 on the subcellular localization of calcineurin and NFIB. In control cells, both NFIB and calcineurin had a diffuse nuclear pattern (Figure 3.6A, first row). Calpain 1

knockdown resulted in reduced levels of calcineurin in the nucleus with much higher levels of calcineurin in the cytoplasm (Figure 3.6A, second row and Figure 3.6B, right panel). These results are in agreement with our western blot data (Figure 3.5A). Loss of calpain 1 also led to changes in the immunostaining pattern of NFIB such that NFIB appeared to be excluded from nucleoli compared to control cells (Figure 3.6A, second row and Figure 3.6B, left panel).

It is noteworthy that the subcellular distribution of calcineurin and NFIB in calpain 1-depleted U251 cells was similar to that observed in control U87 (NFI-hyperphosphorylated) cells (Figure 3.6C). These observations suggest that the phosphorylation state of NFIB may influence its subcellular distribution. Thus, calpain 1 may alter NFIB subcellular localization through modulation of calcineurin phosphatase activity. Taken together, our data support a positive feedback loop between NFIB and calpain 1 such that NFIB, through calpastatin, promotes autolysis and activation of calpain 1. In turn, calpain 1 upregulates calcineurin phosphatase activity which results in NFIB dephosphorylation, which has been previously correlated with increased transcriptional activity (163,164,362).

3.2.6 Calpain 1 depletion increases GBM cell migration but does not affect cell survival

To understand the effects of the NFIB-calpain 1 positive feedback loop on GBM cell migration and cell survival, we repeated the Transwell assay using U87 and U251 cells depleted of either calpain 1 or both calpain 1 and NFIB. Similar to NFIB depletion, knocking down calpain 1 resulted in increased cell migration in both cell lines. Specifically, the number of migrated cells increased from 392 in

control to 917 in siCAPN1-transfected U87 cells (~2.34-fold increase, $p<0.0001$) (Figure 3.7A). Likewise, the number of migrated cells increased from 433 in control to 991 in siCAPN1-transfected U251 cells (~2.29-fold, $p<0.0001$) (Figure 3.7B). These data indicate that calpain 1, like NFIB, inhibits GBM cell migration. Co-depletion of NFIB and calpain 1 in U87 cells led to a statistically significant further increase in the number of migrated cells compared to calpain 1 depletion: 1238 cells for the former versus 917 cells for the latter (~1.35-fold, $p<0.01$) (Figure 3.7A). Similar results were obtained with U251 cells: 1965 cells for NFIB/calpain 1 co-depletion compared to 991 cells for calpain 1 depletion alone (~1.98-fold, $p<0.001$) (Figure 3.7B). In agreement with our proposed role for NFIB in the negative regulation of GBM cell migration, NFIB ectopic expression resulted in decreased numbers of migrated cells compared to control (~0.23-fold, $p<0.0001$, Figure 3.7C). Importantly, co-transfection of U251 cells with both a calpain 1-specific siRNA and an NFIB expression construct reversed the NFIB-induced reduction in cell migration observed in NFIB-overexpressing U251 cells ($p<0.01$, Figure 3.7C). These data indicate that the negative effect of NFIB on GBM cell migration is at least partly mediated through calpain 1 signaling, thereby providing functional support for our proposed NFIB-calpain 1 positive feedback loop.

Similar to NFIB knockdown, depletion of either calpain 1 or both NFIB and calpain 1 had no effect on either U87 ($p>0.32$ and $p>0.74$, respectively) or U251 ($p>0.18$ and $p>0.85$, respectively) cell survival as measured by the MTS assay (Figure 3.7F). Our data thus indicate that NFIB and calpain 1 act in concert to dampen GBM cell migration but have no effect on cell proliferation. However, given

the further increases in cell migration observed upon co-depletion of calpain 1 and NFIB compared to calpain 1-depleted GBM cells (Figure 3.7A and B), NFIB and calpain 1 may have target genes and downstream effectors that are independent from NFIB-calpain crosstalk.

3.2.7 Calpain 1 depletion increases levels of RhoA and FABP7, both implicated in GBM cell migration

To gain mechanistic insights into calpain 1's role in the inhibition of GBM cell migration, we examined the levels of the pro-migratory factor RhoA. Cleavage of RhoA by calpain 1 has previously been shown to reduce spreading in bovine aortic endothelial cells (213). Calpain 1-depleted U251 cells showed a 5-7-fold increase in uncleaved RhoA (22 kDa) compared to control cells (Figure 3.7D). These results are in line with RhoA serving as an important regulator of GBM cell migration (401,402). While our antibody did not to detect cleaved RhoA (20 kDa), perhaps due to the labile nature of this truncated form, our results are consistent with calpain 1-mediated proteolysis of RhoA being a downstream mechanism by which the NFIB-calpain 1 feedback loop downregulates GBM cell migration.

Brain fatty acid binding protein (FABP7) is a target of NFI transcription factors that has been directly linked to increased GBM cell migration (163,182,362,372). To examine whether the NFIB-calpain 1 crosstalk exerts its negative regulation on GBM cell migration through FABP7, we transfected U251 cells with calpain 1 siRNAs. Calpain 1 depletion led to a 3-4-fold increase in levels of FABP7 (Figure 3.7D). Next, we ectopically expressed NFIB in U251 cells. A

consistent decrease in FABP7 protein levels was observed in these cells compared to control cells (Figure 3.7E). Finally, by transfecting NFIB-overexpressing U251 cells with calpain 1 siRNAs, we showed recovery of FABP7 protein levels to that observed in control cells (Figure 3.7E). The parallels in the effects NFIB and calpain 1 have on FABP7 expression and GBM cell migration (Figure 3.7C), combined with FABP7's previously demonstrated pro-migratory effects, suggest a central role for our proposed NFIB-calpain 1 positive feedback loop on regulating GBM cell migration through FABP7.

3.2.8 Targeting the NFI-calpain pathway in GBM cells using calpain inhibitors

It is well known that calpains 1 and 2 can functionally compensate for the loss of one another under certain conditions, including the cleavage and activation of calcineurin (282,365). To bypass this compensatory pathway, we examined the effect of two inhibitors targeting both calpains 1 and 2, ACM and ALLN, on GBM cell viability using the colony formation assay. Both T98 (NFI-hyperphosphorylated) and U251 (NFI-hypophosphorylated) cells showed a dose-dependent decrease in colony formation in response to either ACM or ALLN treatment (Figure 3.8A). The LD50 values for ACM and ALLN were ~10 nM and ~10 μM, respectively (Figure 3.8A). At higher doses of ACM (100 nM) and ALLN (10 μM), we observed a significant difference between T98 (NFI-hyperphosphorylated) and U251 (NFI-hypophosphorylated) colony formation, with 10.4% of plated T98 cells forming colonies compared to 1% of plated U251 cells

in the case of ACM ($p<0.0001$), and 18.8% of plated T98 cells forming colonies compared to 11.4% of plated U251 cells in the case of ALLN, ($p<0.0001$) (Figure 3.8A). We also observed differences in cell viability that were dependent on the NFI-phosphorylation state in U87 (NFI-hyperphosphorylated) and U373 (NFI-hypophosphorylated) (163) GBM cells at the higher ACM doses using the MTS assay (Figure 3.8B). Together, these results suggest that: (i) inhibition of combined calpain 1 and 2 activity reduces GBM cell survival/proliferation and (ii) GBM cells with hyperphosphorylated NFI may be more resistant to calpain inhibitors than GBM cells with hypophosphorylated NFI.

3.3 Discussion

Despite extensive research, GBM remains a devastating disease, with low survival time and poor quality of life (403). The lack of improvement in clinical outcome may be attributed to incomplete understanding of biological processes underlying GBM tumorigenesis and progression, particularly how tumor cells infiltrate normal brain parenchyma. Both calpain and NFI pathways have been shown to play key roles in regulating GBM cell migration. Calpain-mediated proteolysis of downstream effectors is critical for all aspects of cell migration (201,404). More specific to GBM, calpain 2 is required for tumor cell invasion and infiltration *in vitro and in vivo* (194,253). NFI regulates genes essential for neural cell migration in developing brain (112,364). In GBM cells, NFI regulates *FABP7* (163,362), a gene associated with increased cell migration and worse clinical outcomes in patients (183,184,361,372).

In light of: (i) the significant intersection of calpain and NFI functions in both normal brain development and GBM and (ii) previous work showing that NFI regulates the gene encoding the endogenous inhibitor of calpain, calpastatin (*CAST*), we hypothesized that cross signaling occurs between the NFI and calpain pathways. The first empirical evidence supporting NFI-calpain crosstalk was our discovery that NFI transcriptional activity is regulated by calcineurin which regulates NFI phosphorylation state (164). Calcineurin is a well-known calpain downstream effector (282,365,374,375). Our subsequent finding that NFI regulates *CAST* which encodes calpastatin, provided further substantiation for NFI-calpain crosstalk in GBM cells (397).

In this manuscript, we present evidence for a positive feedback loop between NFIB and calpain 1 in GBM cells. Both NFIB and calpain 1 play paradoxical roles in different types of malignancies. For example, whereas NFIB acts as an oncogene in small cell lung cancer (398), it functions as a tumor suppressor in cutaneous squamous cell carcinoma (405). Similarly, calpain 1 expression has been correlated with both higher and lower survival in different types of breast cancer (406,407). We found that NFIB can affect calpain 1 activity through two different mechanisms in GBM cells, depending on NFIB phosphorylation state. When NFIB is hyperphosphorylated (Figure 3.9A), it downregulates transcription from an alternative promoter of *CAST* which contains NFI binding elements (397). Consequently, *CAST* transcription is primarily initiated at the canonical promoter, resulting in higher levels of full-length calpastatin which has a diffuse cytoplasmic distribution (397). Diffused cytoplasmic calpastatin has

been correlated with intracellular activation of calpain (346). Induction of calpain autolysis through suppression of calpastatin expression has previously been demonstrated for the c-Myc transcription factor (161). On the other hand, when NFI is hypophosphorylated (Figure 3.9B), NFIB promotes transcription from the alternative *CAST* promoter, resulting in higher levels of a truncated form of calpastatin that lacks the XL domain (397). This XL-less calpastatin preferentially localizes to the perinuclear region of the cell (397) and thus is unable to bind and prevent the activation of calpain 1 in other compartments of the cytoplasm. Moreover, the ~55 kDa autolyzed form of calpain 1 detected in our western blot experiments has been shown to have lower affinity for calpastatin compared to the full-length form (408). As a result, autolyzed calpain 1 can translocate to the nucleus, further insulating itself from the inhibition by calpastatin. Thus, our combined data suggest that while mechanistically different, both hyper- and hypo-phosphorylated NFIB can enhance calpain 1 activity. In support of an NFIB-calpain 1 positive feedback loop in GBM, we also found that calpain 1 can affect NFIB phosphorylation. We have previously shown that NFIB phosphorylation affects its transcriptional activity (163,362). Thus, calpain 1 cleaves and activates calcineurin, which in turn dephosphorylates NFIB and perpetuates the signaling cycle. Whether calpain 1-induced and calcineurin-mediated dephosphorylation can be extended to members of the NFI family other than NFIB remains to be examined.

Evidence from the literature suggests various roles for NFIB in cancer cell migration. For example, NFIB enhances migration of tumor cells by changing

chromatin state and accessibility (173,175). However, NFIB expression can also be inversely correlated with cell migration and invasion, as demonstrated in osteosarcoma (409). In line with the latter observation, we show that NFIB negatively regulates GBM cell migration by downregulating the expression of GBM pro-migratory protein FABP7. Intriguingly, hypophosphorylated NFIs have previously been shown to up-regulate, not down-regulate, *FABP7* expression in GBM cells (362). However, closer examination of the data in this paper shows similar results to those reported here; i.e. upregulation of FABP7 upon NFIB depletion. Brun *et al.* attributed the effect of NFIB on FABP7 to possible interplay between the various members of the NFI family. However, in light of our new data, a more likely explanation is that different members of the NFI family play different roles in GBM cells. Thus, NFIB, as a negative regulator of *FABP7*, may counteract the oncogenic effect of other NFI members. Also, in agreement with our results, there is a correlation between higher levels of NFIB and increased survival in patients with classical and mesenchymal GBM tumors (171). Since both U87 and U251 are of the mesenchymal GBM subtype (410,411), the association between NFIB expression and better clinical outcomes may be explained in part by NFIB-mediated downregulation of FABP7 expression, resulting in reduced GBM cell migration

Similar to NFIB, the role of calpain 1 in regulating cell migration varies depending on the system being analyzed, perhaps due to functional compensation provided by other calpain members. While a number of studies have established calpain 2 as an essential promoter of GBM cell migration, the present work may

be the first to implicate calpain 1 as a negative regulator of cell migration in GBM. A few reports in other systems support an anti-migratory role for calpain 1. For example, in bovine aortic endothelial cells, calpain 1 can cleave and generate a dominant-negative fragment of RhoA that inhibits cell spreading (213). While we were not able to detect the cleaved form of RhoA in GBM cells, possibly due to instability of calpain 1-proteolyzed RhoA, we did observe increased levels of full-length RhoA upon calpain 1 depletion in GBM cells. Calpain 1 depletion in GBM cells also led to an increase in the expression of pro-migratory FABP7. These combined observations support a link between NFIB, calpain 1, and RhoA/FABP7-mediated cell migration.

Over the last few decades, there has been increasing interest in using calpain activators and inhibitors for clinical purposes (218,240,393), with attention focusing on using calpain inhibitors for the treatment of many pathological conditions including neurodegenerative diseases and cancer. Our colony formation assay indicates that calpain inhibitors ACM and ALLN can be used to significantly reduce GBM cell survival. NFIs, like many other transcription factors, remain largely undruggable. Consequently, the existence of crosstalk between NFI and calpain may allow targeting of these key pathways with calpain inhibitors. However, our Transwell and colony formation data suggest that inhibiting both calpains 1 and 2 may also cause increased tumor cell migration, a hallmark of tumor infiltration. As the NFIB-calpain 1 positive feedback loop in GBM cells appears to suppress tumor cell migration, we suggest that a calpain 1-specific agonist holds the most promise for targeting infiltrative GBM cells. Opposite effects

for calpain 1 and calpain 2 have been observed in both neurodegeneration and synaptic plasticity: calpain 1 is neuroprotective and induces long-term potentiation (LTP), in contrast to calpain 2 which promotes neurodegeneration and restricts LTP (214). In the context of brain development, calpain 1 acts to maintain the self-renewing capacity of neural stem cells while calpain 2 promotes the differentiation of these cells (215).

In summary, we report a positive NFIB-calpain 1 feedback loop in GBM cell lines. Our results shed light on the molecular basis of the signaling pathways of this crosstalk, with calpain 1 inducing NFIB dephosphorylation through cleavage and activation of calcineurin and NFIB increasing calpain 1 activity through *CAST*-mediated regulation of calpastatin levels and subcellular localization. We also provide evidence that NFIB, through NFIB-mediated downregulation of *FABP7*, and calpain 1, likely through calpain 1-mediated proteolysis of RhoA into its dominant-negative form (Figure 3.9C), act in concert to suppress GBM cell migration. Finally, our data suggest that inhibitors targeting both calpains 1 and 2, although useful for reducing tumor mass, may not be of benefit in controlling GBM cell migration and infiltration.

3.4 Experimental Procedures

3.4.1 Cell lines, constructs, transfections and treatments

T98, U87, U251 and U373 GBM cell lines have been described elsewhere (181,362). Cells were cultured in Dulbecco's modified Eagle's minimum essential medium supplemented with 8% fetal bovine serum (FBS), streptomycin (50 µg/ml),

and penicillin (50 units/ml). pCH-NFI expression constructs were a generous gift from Dr. R. Gronostajski (Case Western Reserve University). GBM cells were transfected with pCH empty vector or NFI-expression constructs using polyethyleneimine (PEI) (Polysciences) with a ratio of 5:1 (μg PEI: μg DNA). Co-transfection of calpain 1 siRNA and NFIB expression construct (pCH-NFIB) was carried out using the JetPrime reagent (VWR). Cells were harvested 60 h post-transfection.

3.4.2 Knockdown of endogenous NFIs and CAPN1

GBM cells were transfected with the following siRNAs (Life Technologies): scrambled (control) siRNAs (Cat. # 12935-200 and 12935-300); NFIA, NM_005595_stealth_919 (5'-GAAAGUUCUUCAUACUACAGCAUGA-3'); NFIB-1, NM_005596_stealth_1020 (5'-AAGCCACAAUGAUCCUGCCAAGAAU-3'), NFIB-2, NIFBHSS107131 (5'-GCUGGAAGUCGAACAUGGCACGAAA-3'); NFIC, NM_005597_stealth_1045 (5'-CAGAGAUGGACAAGUCACCAUUCAA-3'), NFIX, NM_002501_stealth_752 (5'-GAGAGUAUCACAGACUCCUGUUGCA-3'), CAPN1-1, CAPN1HSS188701 (5'-CAGAGUGGAACAACGUGGACCCAUA-3'), CAPN1-2, CAPN1HSS101345 (5'-CCGUACCACUUGAAGCGUGACUUCUU-3'). Ten nM of each siRNA was introduced into GBM cells using the RNAiMAX Lipofectamine reagent (Invitrogen) according to the manufacturer's instruction. Cells were trypsinized and replated 48 h post-transfection (1:6) for the second round of siRNA. Cells were harvested 60 h after the second transfection.

3.4.3 Reverse transcription (RT) and quantitative polymerase chain reaction (qPCR)

The TRIzol® reagent (ThermoFisher Scientific) was used to isolate total RNA from GBM cells. First-strand cDNA synthesis was carried out with Superscript II® reverse transcriptase (Invitrogen). For RT-PCR, primers specific to *CAPN1*, *CAPN2, CAPSN1* and *ACTB* were used to amplify cDNA (Table 1). For RT-qPCR, cDNAs were amplified using primers flanking a unique region of *CAPN1* with the BrightGreen® qPCR master mix (ABM Scientific). Raw signals were first normalized to *GAPDH* and then to the respective scrambled siRNA control to generate relative fold change data.

3.4.4 Western blot analysis

Whole cell lysates were prepared by lysing cells in modified RIPA buffer [50 mM Tris-HCl pH 7.5, 1% sodium deoxycholate, 1% Triton X-100, 150 mM NaCl, 50 mM sodium fluoride, 1 mM sodium orthovanadate, 10 mM EDTA, 0.1% SDS, 0.5 mM PMSF, 1X cOmplete protease inhibitor (Roche Applied Science), and 1X PhosSTOP phosphatase inhibitor (Roche Applied Science)]. For λ-phosphatase (NEB) treatment, 10 µg of nuclear lysates were incubated with either water (negative control) or 400 units of λ-phosphatase for 1 h at 30°C in the supplied reaction buffer, supplemented with 1 mM $MnCl_2$. Whole cell and nuclear lysates were resolved in polyacrylamide-SDS gels and transferred to nitrocellulose membranes. Blots were then immunostained with rabbit anti-calpastatin antibody (1:5,000, Abcam, cat.# ab5582), mouse anti-calpain 1 antibody (1:500, Santa

Cruz, cat.# sc-271313), rabbit anti-calpain 2 antibody (1:1000, Santa Cruz, cat.# sc-30064), mouse anti-calcineurin antibody (1:1000, Pharmingen, clone G182-1847), rabbit anti-NFIB antibody (1:2500, Invitrogen, cat.# PA5-52032), mouse anti-RhoA antibody (1:500, Santa Cruz, cat#: sc-418), mouse anti-lamin A/C antibody (1:1,000, ThermoFisher Scientific, cat.# MA3-1000), mouse anti-α-tubulin (1:100,000, Hybridoma Bank, clone 12G10), or mouse anti-β-actin antibody (1:100,000, Sigma Aldrich, clone AC-15). Proteins of interest were visualized using horseradish peroxidase-conjugated secondary antibody (Jackson ImmunoResearch Biotech) with the Immobilon (EMD Millipore) or ECL (GE Healthcare) chemiluminescent HRP substrate.

3.4.5 Cytoplasmic and nuclear fractionation

Nuclear and cytoplasmic fractionation was carried out using the NE-PER kit (ThermoFisher Scientific) with modification for nuclear fractionation. Briefly, cytoplasmic lysates were prepared using the supplied reagents supplemented with 1X cOmplete protease inhibitors and 1X PhosSTOP. Nuclei were obtained by centrifugation of cytoplasmic lysates. Purified nuclei were lysed in modified RIPA buffer as described in the previous section. For λ-phosphatase treatment, cytoplasmic and nuclear fractionation was carried out in the absence of EDTA and phosphatase inhibitors (sodium fluoride, sodium orthovanadate and PhosSTOP). To shear chromatin, nuclear lysates were subjected to 20 cycles of sonication at 4°C (high output, 30 s power on and 30 s power off) using a Bioruptor 300®

sonicator (Diagenode). Nuclear debris was pelleted by centrifugation. The supernatant was then removed and used as nuclear lysates.

3.4.6 Calpain activity assay

Calpain proteolytic activity was measured using the fluorogenic Calpain Activity Assay Kit (Calbiochem). Briefly, whole cell lysates were prepared from U87 and U251 GBM cells using the supplied lysis buffer. Changes in fluorescence intensity upon substrate cleavage was measured in buffers that promote (Activation buffer) or suppress (Inhibition buffer) calpain activity using the FLUOstar Optima microplate reader (355 nm excitation and 480 nm emission, BMGLABTECH). Raw data obtained with the Activation buffer were normalized against those obtained with the Inhibition buffer. Relative fold change in fluorescence intensity was generated by normalizing each data point to the respective scrambled siRNA control.

3.4.7 Transwell migration assay

U251 and U87 GBM cells were transfected with the indicated siRNAs and plasmid-based expression constructs. Thirty thousand cells in FBS-free DMEM were seeded in the top chamber of a Falcon Cell Culture Inserts (Fisher Scientific). Cells were allowed to migrate through an 8-μm polyethylene terephthalate (PET) membrane towards a chemoattractant (DMEM +10% fetal calf serum) in the bottom chamber for 20 h. Cells were then fixed with 100% cold methanol for 20 minutes and stained with 1% crystal violet in 20% methanol for 30 minutes. Migrated cells were imaged using a Zeiss Axioskop2 plus microscope using

multiple fields covering the whole surface of the inserts. Cell counting was carried out using MetaMorph software (Molecular Devices).

3.4.8 MTS assay

U87, T98, U251 and U373 GBM cells were transfected with the indicated siRNAs as previously described or treated with the indicated concentrations of ACM. Cell metabolism, a surrogate of cell viability, was measured using the CellTiter 96® Non-Radioactive Cell Proliferation MTS Assay (Promega). Briefly, ~3,500 siRNA-transfected cells were seeded in 96-well plates in triplicate and allowed to grow for 48 h. For ACM treatment, ~3,500 cells were seeded and allowed to recover for 24 h and then incubated with the drug for an additional 36 h. Next, twenty uL of MTS reagent was added to each well and then incubated for an additional 2 h. Absorbance was measured using the FLUOstar OPTIMA microplate reader with the absorbance wavelength of 495 nm. Relative fold change was generated by normalizing absorbance values to their respective scrambled siRNA or DMSO controls.

3.4.9 Colony formation assay

The colony formation assay was carried out as previously described (412). Briefly, ~500 T98 or U251 GMB cells were plated in triplicate and treated with the indicated doses of ACM or ALLN. After 24 h, the medium was changed followed by washing with PBS to remove traces of drug. Cells were allowed to grow for an additional 12 days and then fixed and stained with 1% crystal violet in 70% ethanol. Colonies (>30 cells) were counted.

3.4.10 Immunofluorescence analysis

For immunofluorescence analysis, siRNA-transfected GBM cells were plated onto glass coverslips. Cells were allowed to recover for 24 h and then fixed with 4% paraformaldehyde for 10 min at room temperature. Cells were then permeabilized with 0.25% Triton X-100 for 4 min. To reduce background staining, cells were blocked with 3% BSA for 45 min at room temperature. Cells were then immunostained with rabbit anti-calpastatin (1:100, Santa Cruz, cat.# sc-20779), mouse anti-calpain 1 antibody (1:10, Santa Cruz, cat.# sc-271313), mouse anti-calcineurin antibody (1:50, Pharmingen, clone G182-1847) and rabbit anti-NFIB antibody (1:400, Life Technologies, cat.# PA5-52032). Signals were visualized using Alexa 488-conjugated donkey anti-rabbit or Alexa 555-conjugated donkey anti-mouse secondary antibodies (both at 1:400, Life Technologies). Nuclei were stained with 4′,6-diamidino-2-phenylindole (DAPI, CalBiochem). Images were acquired with a X40/1.3 oil immersion objective lens on a Zeiss LSM 710 confocal microscope using Zeiss ZEN imaging software. For quantification of calpain 1 and calcineurin subcellular localization, fluorescence signal intensity values were calculated for at least 300 cells (100 cells for each biological replicate) using the MetaXpress software (Molecular Devices), with DAPI being used as the marker for the nuclear region. Data are presented as relative percentage of nuclear over cytoplasmic fluorescence intensity. For quantification of NFIB nucleolus localization, at least 300 random cells (100 cells for each biological replicate) were assessed for the absence of NFIB immunostaining in the nucleolus region. Data

are presented as percentage of cells negative for nucleolar NFIB related to total number of cells counted.

Locus	Forward Primer (5' to 3')	Reverse Primer (5' to 3')
GAPDH	ACCAGGGAGGGCTGCAGT	CAGTTCGGAGCCCACACG
CAPN1	CACCACACTCTACGAAGGCA	ACGCTTCAAGTGTACGGCC
CAPN2	TAACGGAAGCCTACAGAAACT	TTTTTGCTGAGGTGGATGTTG
CAPNS1	CCAACGAGAGTGAGGAGGT	TGACCAAGCAGCTGATGAAG
ACTB	CTGGCACCACACCTTCTAC	CATACTCCTGCTTGCTGATC

Table 3.1. Primer Sequences

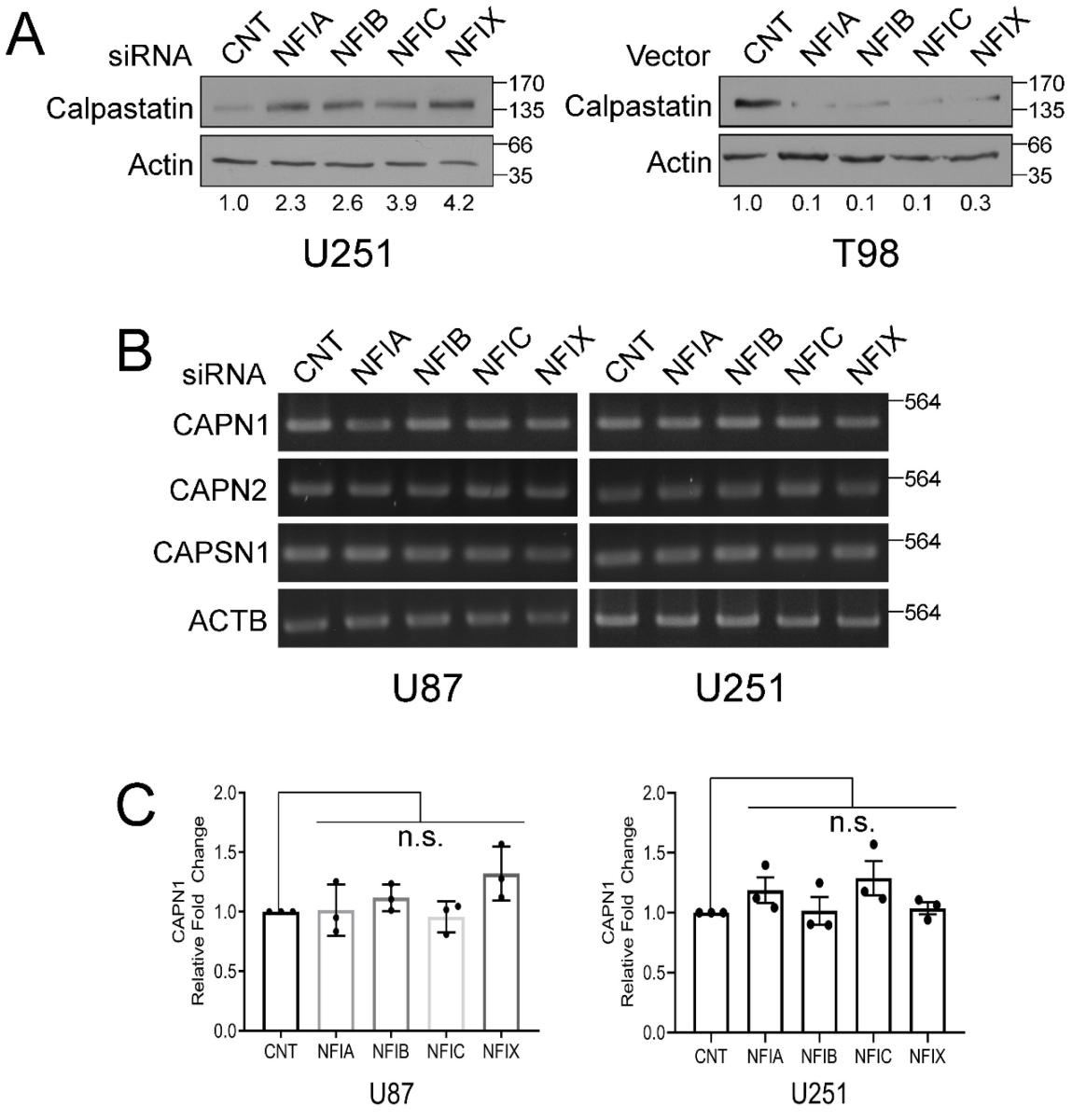
A
siRNA
CNT
NFIA
NFIB
NFIC
NFIX
Calpastatin
Actin
170
135
66
35
1.0 2.3 2.6 3.9 4.2
U251
Vector
1.0 0.1 0.1 0.1 0.3
T98
B
CAPN1
CAPN2
CAPSN1
ACTB
564
U87
U251
C
CAPN1 Relative Fold Change
2.0
1.5
1.0
0.5
0.0
n.s.
U87
U251

Figure 3.1. NFI directly regulates *CAST* but not calpain genes

(A) Whole cell lysates were prepared from T98 and U251 cells transfected with the indicated siRNAs (left) or NFI expression constructs (right). Proteins were separated by SDS-PAGE, electroblotted onto nitrocellulose membranes, immunoblotted with a rabbit anti-calpastatin monoclonal antibody or a mouse anti-β-actin antibody. Numbers underneath each lane represent fold changes in densitometric values relative to actin compared to control transfections (N=2). (B and C) U87 and U251 cells were transfected with siRNAs specific to each NFI member and total RNA extracted using the TRIzol reagent. (B) cDNA was PCR amplified using primers flanking the indicated genes, with actin serving as a loading control. (C) cDNA was amplified by qPCR using CAPN1-specific primers. Relative fold changes were generated by normalizing CAPN1 data to those of GAPDH and then to the internal scrambled siRNA control. Results are representative of three independent experiments.

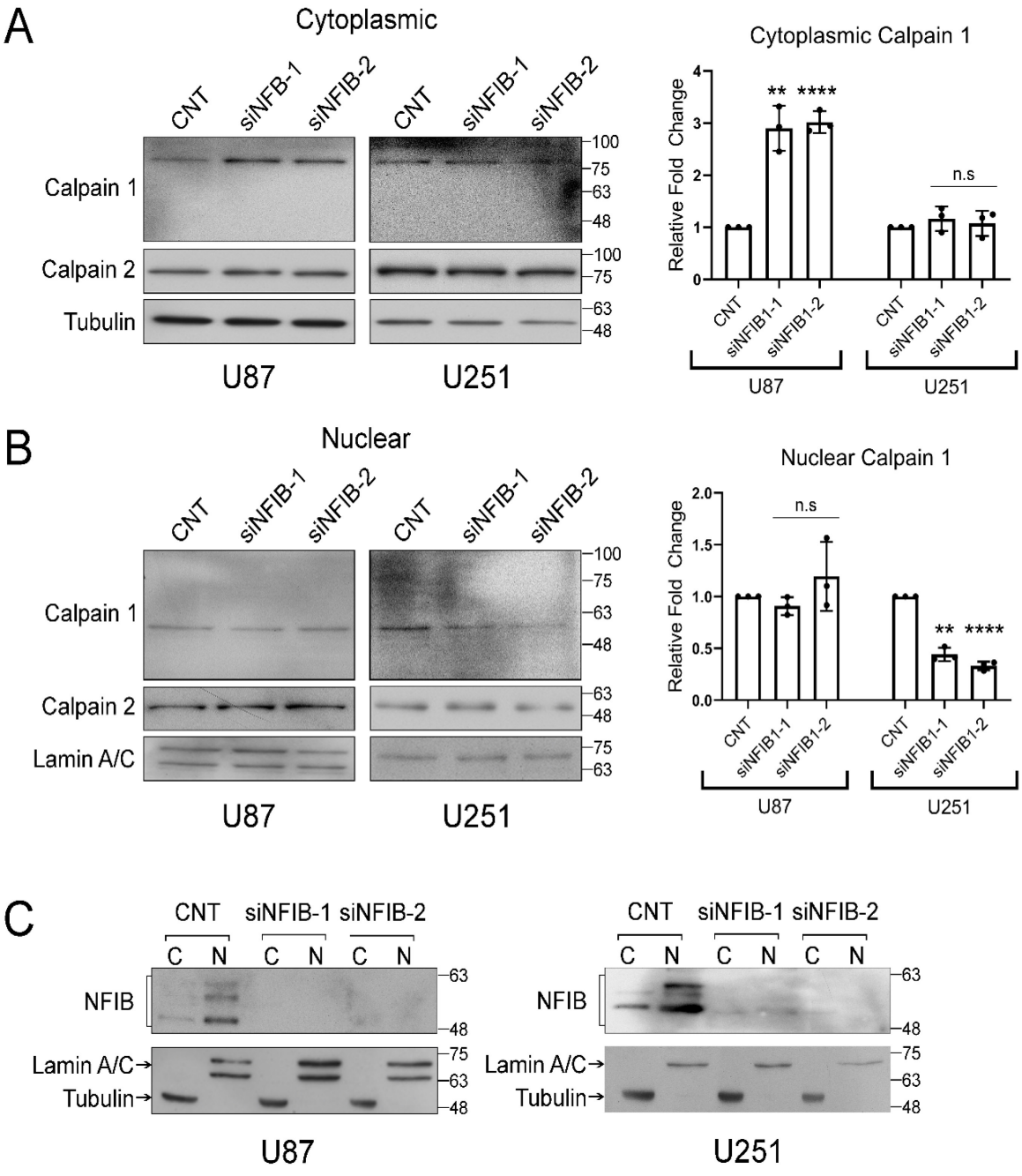
A
Cytoplasmic
CNT
siNFB-1
siNFIB-2
CNT
siNFIB-1
siNFIB-2
Calpain 1
Calpain 2
Tubulin
100
75
63
48
100
75
63
48
U87
U251
Cytoplasmic Calpain 1
Relative Fold Change
**
****
n.s
CNT
siNFIB1-1
siNFIB1-2
CNT
siNFIB1-1
siNFIB1-2
U87
U251
B
Nuclear
CNT
siNFIB-1
siNFIB-2
CNT
siNFIB-1
siNFIB-2
Calpain 1
Calpain 2
Lamin A/C
100
75
63
48
63
48
75
63
U87
U251
Nuclear Calpain 1
Relative Fold Change
n.s
**
****
CNT
siNFIB1-1
siNFIB1-2
CNT
siNFIB1-1
siNFIB1-2
U87
U251
C
CNT
siNFIB-1
siNFIB-2
C
N
C
N
C
N
NFIB
Lamin A/C
Tubulin
63
48
75
63
48
U87
CNT
siNFIB-1
siNFIB-2
C
N
C
N
C
N
NFIB
Lamin A/C
Tubulin
63
48
75
63
48
U251

Figure 3.2. Changes in cytoplasmic and nuclear calpain 1 levels upon NFIB knockdown

U87 and U251 cells were transfected with scrambled (control) siRNAs or two different siRNAs targeting NFIB. Cytoplasmic (A), nuclear (B), or both cytoplasmic and nuclear (C) lysates were prepared using the NE-PER kit, electrophoresed on polyacrylamide gel and transferred to nitrocellulose membranes. Blots were immunostained with mouse anti-calpain 1 and rabbit anti-calpain 2 antibodies. α-tubulin and lamin A/C served as loading controls for the cytoplasmic and nuclear fractions, respectively. Histograms represent relative fold changes in densitometric values compared to scrambled siRNA control (N=3) (n.s, p-value >0.05, **p-value <0.01, and ****p-value <0.0001). (C) Blots are representative of three independent experiments. Abbreviations: C - cytoplasmic; N - nuclear.

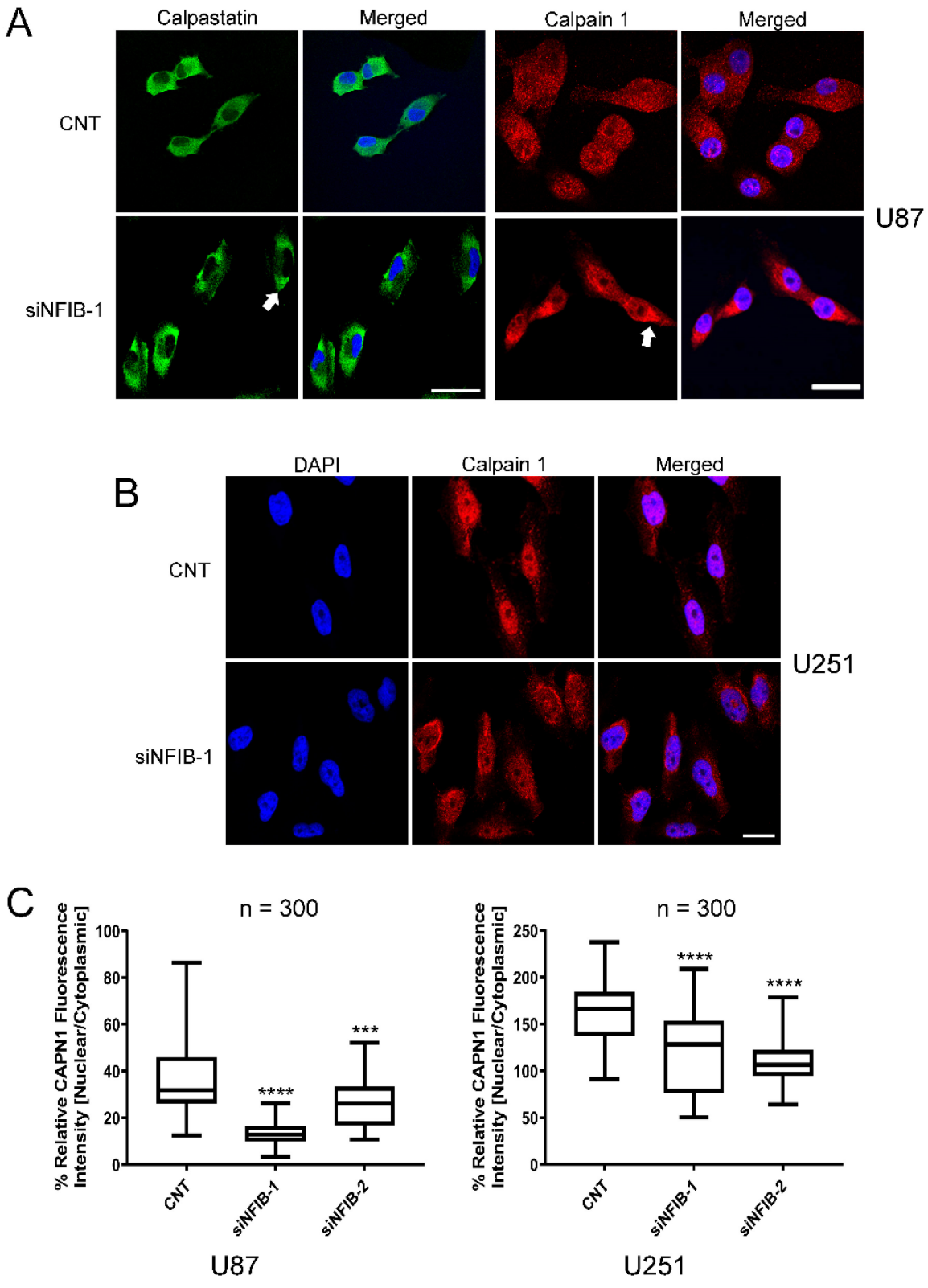
A
Calpastatin
Merged
Calpain 1
Merged
CNT
siNFIB-1
U87
B
DAPI
Calpain 1
Merged
CNT
siNFIB-1
U251
C
n = 300
% Relative CAPN1 Fluorescence Intensity [Nuclear/Cytoplasmic]
100
80
60
40
20
0
****
***
CNT
siNFIB-1
siNFIB-2
U87
n = 300
% Relative CAPN1 Fluorescence Intensity [Nuclear/Cytoplasmic]
250
200
150
100
50
0
****
****
CNT
siNFIB-1
siNFIB-2
U251

Figure 3.3. Changes in calpastatin and calpain 1 subcellular localization upon NFIB depletion

U87 (A) or U251 (B) cells were transiently transfected with scrambled (control) siRNAs or an NFIB-specific siRNA and then plated on coverslips. Cells were cultured for 24 h and then fixed with 4% paraformaldehyde and immunostained with either rabbit anti-calpastatin (A) or mouse anti-calpain 1 (A and B) antibodies followed by Alexa 488 (rabbit, green)- or Alexa 555 (mouse, red)-conjugated secondary antibodies, respectively. Nuclei were visualized with DAPI (blue) and images acquired with a 40X/1.3 oil immersion lens using the Zeiss LSM 710 confocal microscope and Zeiss ZEN imaging software. Bars, 20 μm. Images are representative of the majority of cells observed under each condition and are derived from three independent experiments. (C) For quantification of calpain 1 subcellular localization, fluorescence intensity values in the red channel (calpain 1) were generated for nuclear (DAPI as marker) and cytoplasmic fractions using 300 random U251 cells (100 cells for each biological replicate). Data are presented as percent nuclear fluorescence intensity relative to cytoplasmic fluorescence intensity. (***p-value <0.001, and ****p-value <0.0001).

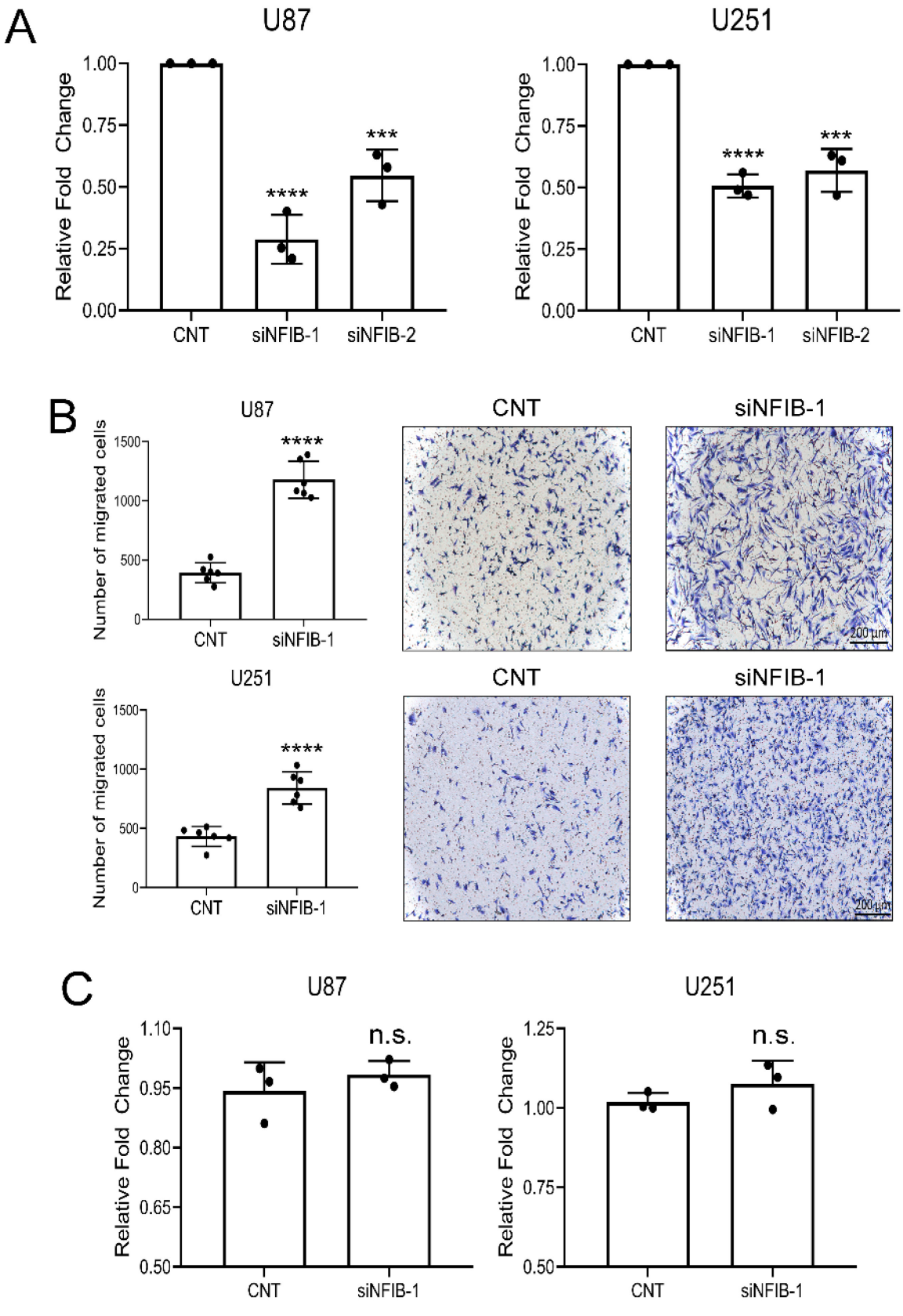
A
U87
U251
Relative Fold Change
1.00
0.75
0.50
0.25
0.00
****
***
CNT
siNFIB-1
siNFIB-2
B
U87
U251
Number of migrated cells
1500
1000
500
0
CNT
siNFIB-1
200 µm
C
U87
U251
n.s.
1.10
0.95
0.80
0.65
0.50
1.25
1.00
0.75

Figure 3.4. Effects of NFIB depletion on calpain activity and GBM cell migration and viability

(A-C) U87 and U251 cells were transfected with scrambled siRNAs or siRNAs targeting NFIB. (A) Calpain activity was assessed by measuring the cleavage of a synthetic substrate provided in the Calpain Activity Fluorometric Assay Kit (CalBiochem). Fluorescent signals obtained in a buffer that activates calpain activity was normalized against fluorescent signals obtained in a buffer that inhibits calpain activity. Relative fold change was obtained by normalizing the scrambled siRNA control to 1. (B) Thirty thousand cells in FBS-free DMEM were seeded in the top chambers of Falcon Cell Culture Inserts in a 24-well plate. Directional migration was induced by supplementing the medium in the bottom chamber with 10% FBS. After 20 h, cells that had migrated through the porous membrane of the inserts were fixed with methanol and stained with crystal violet. Migrated cells were imaged with the Zeiss Axioskop2 plus microscope. Cells were counted using MetaMorph software. Bars, 200 μm. (C) Cell metabolism, used as a surrogate for cell viability, was measured using the MTS assay. Thirty-five hundred cells were seeded in 96-well plates. After 48 h, cells were incubated with the MTS reagent for 2 h. Fluorescence emission (495 nm) was measured using the FLUOstar Optima plate reader and then normalized to the scrambled siRNA control. Each experiment was repeated at least three times. (n.s., p-value>0.05, ***p-value <0.001 and ****p-value <0.0001).

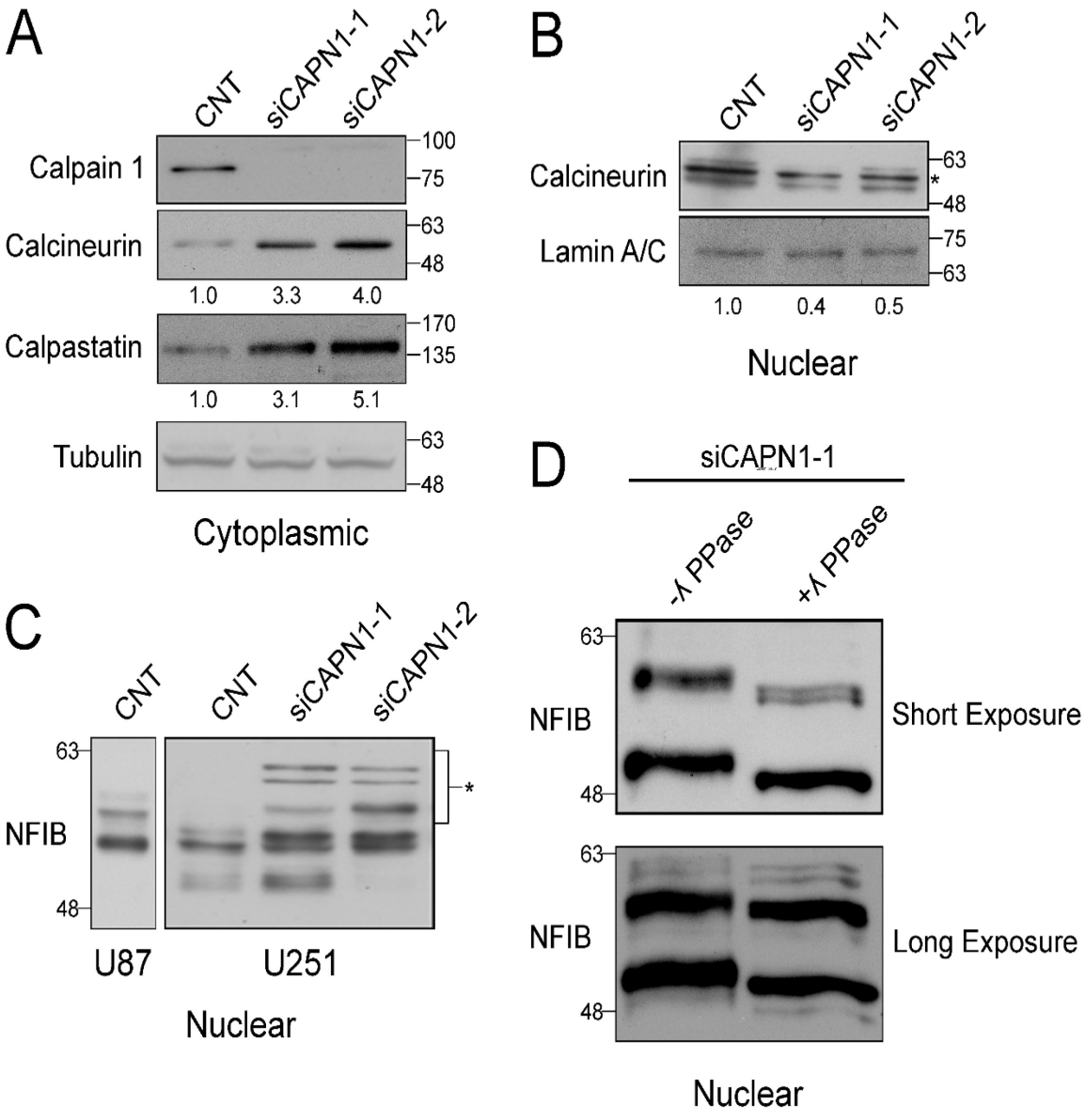
A
CNT
siCAPN1-1
siCAPN1-2
Calpain 1
100
75
Calcineurin
63
48
1.0
3.3
4.0
Calpastatin
170
135
1.0
3.1
5.1
Tubulin
63
48
Cytoplasmic
B
CNT
siCAPN1-1
siCAPN1-2
Calcineurin
63
*
48
Lamin A/C
75
63
1.0
0.4
0.5
Nuclear
C
CNT
CNT
siCAPN1-1
siCAPN1-2
63
NFIB
48
*
U87
U251
Nuclear
D
siCAPN1-1
-λ PPase
+λ PPase
63
NFIB
48
Short Exposure
63
NFIB
48
Long Exposure
Nuclear

Figure 3.5. Calpain 1 depletion affects levels of calpastatin and calcineurin as well as NFIB dephosphorylation

(A) Cytoplasmic and (B) nuclear lysates were prepared from U251 cells transiently transfected with scrambled siRNAs or siRNAs targeting calpain 1 (siCAPN1-1 and siCAPN1-2). Numbers represent relative fold changes in densitometric values compared to control transfections (N=2). The asterisk indicates the cleaved form of calcineurin. (C) Nuclear fractions were prepared from U87 and U251 cells transfected with scrambled siRNAs (CNT) or siRNAs targeting calpain 1 (siCAPN1-1 and siCAPN1-2). Blots are representative of three independent experiments. The asterisk indicates the hyperphosphorylated forms of NFIB. (D) Nuclear extracts were prepared from U251 cells transfected with CAPN1-1 siRNA in the absence of phosphatase inhibitors and then treated with λ-phosphatase for 1 h at 30°C. Blots are representative of two independent experiments. (A-D) Proteins were electrophoresed on SDS-polyacrylamide gels and transferred to nitrocellulose membranes. Blots were immunostained with mouse anti-calpain 1, mouse anti-calcineurin, rabbit anti-calpastatin and rabbit anti-NFIB antibodies. α-tubulin and lamin A/C were used as loading controls for cytoplasmic and nuclear fractions, respectively.

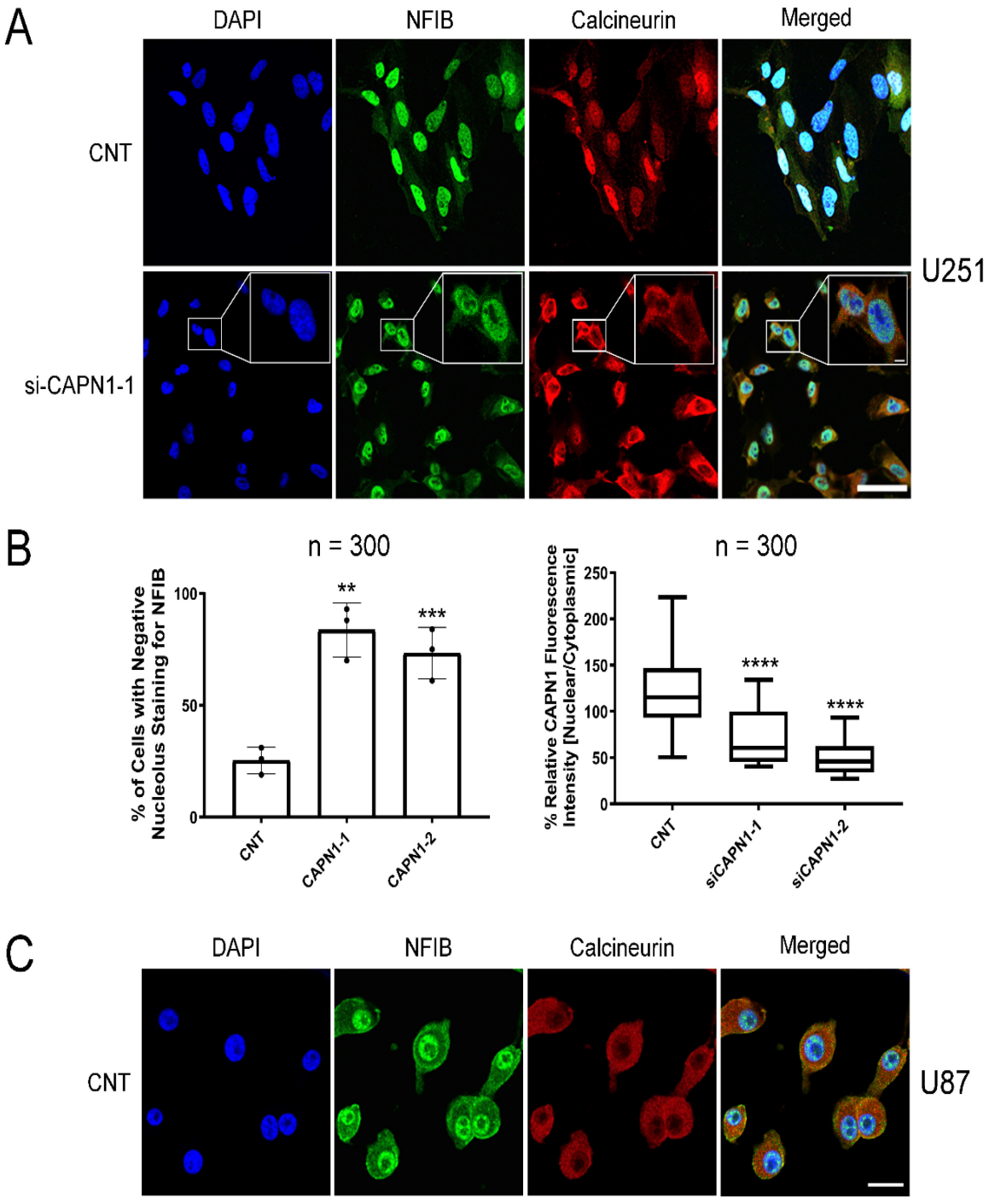
A
DAPI
NFIB
Calcineurin
Merged
CNT
si-CAPN1-1
U251
B
n = 300
% of Cells with Negative Nucleolus Staining for NFIB
100
50
0
**
***
CNT
CAPN1-1
CAPN1-2
n = 300
% Relative CAPN1 Fluorescence Intensity [Nuclear/Cytoplasmic]
250
200
150
100
50
0
****
****
CNT
siCAPN1-1
siCAPN1-2
C
DAPI
NFIB
Calcineurin
Merged
CNT
U87

Figure 3.6. Changes in calcineurin and NFIB subcellular localization upon calpain 1 depletion

U251 (A,B) or U87 (C) cells were transiently transfected with scrambled siRNAs or a calpain 1-specific siRNAs and then plated on coverslips. Cells were cultured for 24 h and then fixed with 4% paraformaldehyde and immunostained with rabbit anti-NFIB and mouse anti-calcineurin antibodies followed by Alexa 488 rabbit (green)- or Alexa 555 mouse (red)-conjugated secondary antibodies, respectively. Nuclei were visualized with DAPI (blue) and images acquired with a 40X/1.3 oil immersion lens using the Zeiss LSM 710 confocal microscope and Zeiss ZEN imaging software. Bars, 50 μm (A) and 5 μm (insets); 20 μm (C). Images are representative of the majority of cells observed under each condition and are derived from three independent experiments. (B) Three hundred random U251 cells (100 cells for each biological replicate) were used for NFIB and calcineurin quantification. For NFIB nucleolus localization, cells showing absence of nucleolar staining in the green channel (NFIB) were manually counted. Data are presented as percent of cells negative for nucleolar NFIB immunostaining relative to total number of cells counted. For calcineurin subcellular localization, fluorescence intensity values in the red channel (calcineurin) were generated for nuclear (DAPI as marker) and cytoplasmic fractions. Data are presented as percent nuclear fluorescence intensity relative to cytoplasmic fluorescence intensity. (**p-value <0.01, ***p-value <0.001, and ****p-value <0.0001).

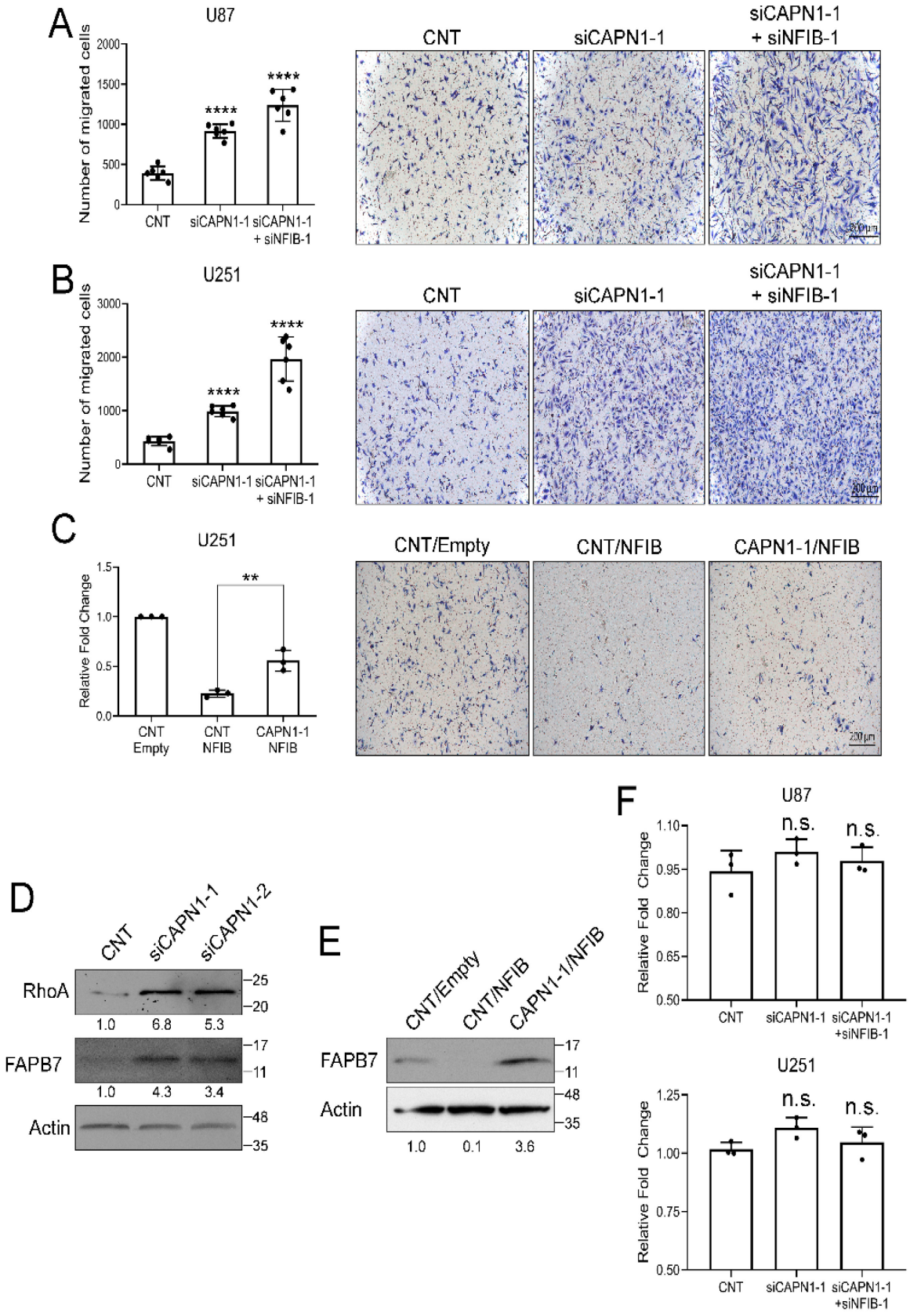
A
U87
Number of migrated cells
2000
1500
1000
500
0
****
****
CNT
siCAPN1-1
siCAPN1-1 + siNFIB-1
CNT
siCAPN1-1
siCAPN1-1 + siNFIB-1
B
U251
Number of migrated cells
3000
2000
1000
0
****
****
CNT
siCAPN1-1
siCAPN1-1 + siNFIB-1
CNT
siCAPN1-1
siCAPN1-1 + siNFIB-1
C
U251
Relative Fold Change
1.5
1.0
0.5
0.0
**
CNT Empty
CNT NFIB
CAPN1-1 NFIB
CNT/Empty
CNT/NFIB
CAPN1-1/NFIB
D
CNT
siCAPN1-1
siCAPN1-2
RhoA
25
20
1.0
6.8
5.3
FAPB7
17
11
1.0
4.3
3.4
Actin
48
35
E
CNT/Empty
CNT/NFIB
CAPN1-1/NFIB
FAPB7
17
11
Actin
48
35
1.0
0.1
3.6
F
U87
Relative Fold Change
1.10
0.95
0.80
0.65
0.50
n.s.
n.s.
CNT
siCAPN1-1
siCAPN1-1 +siNFIB-1
U251
Relative Fold Change
1.25
1.00
0.75
0.50
n.s.
n.s.
CNT
siCAPN1-1
siCAPN1-1 +siNFIB-1

Figure 3.7. Effects of calpain 1 depletion on GBM cell migration and viability

U87 (A) and U251 (B) cells were transfected with scrambled (CNT) siRNAs or siRNAs targeting either calpain 1 alone or both calpain 1 and NFIB. (C) U251 cells were co-transfected with siRNAs (CNT: scrambled siRNAs or CAPN1-1: calpain 1-specific siRNA) and DNA construct (Empty: parent pCH vector; NFIB: pCH-NFIB expression construct) using the JetPrime reagent. Thirty thousand U87 (A) or U251 (B and C) cells in fetal calf serum-free DMEM were seeded in the top chambers of Falcon Cell Culture Inserts in a 24-well plate. Directional migration was induced, imaged, and quantified as described in Figure 3.4B. Bars, 200 μm. (A, B) CNT panels are shared with Figure 3.4B as these transfections were carried out at the same time, but are reported separately to focus on the effect of NFIB depletion (Figure 3.4B) or calpain 1 depletion (Figs. 7A, B) on glioblastoma cell migration. (D) Whole cell lysates were prepared from U251 cells transiently transfected with scrambled siRNAs or siRNAs targeting calpain 1 (siCAPN1-1 and siCAPN1-2). (E) Whole cell lysates were prepared from U251 cells transfected with an NFIB expression construct or co-transfected with calpain 1 siRNA and an NFIB expression construct. (D, E) Cell lysates were electrophoresed in SDS-polyacrylamide gels and transferred to nitrocellulose membranes. Blots were immunostained with mouse anti-RhoA, rabbit anti-FABP7 and mouse anti-actin antibodies. Numbers represent relative fold changes in densitometric values compared to control transfections (N=2). (F) U87 and U251 cells were transfected with the indicated siRNAs as outlined in panels A and B, respectively. Cell viability was measured using the MTS assay as described in Figure 3.4C. Each experiment

(except for D and E) was repeated at least three times. (n.s., p-value>0.05, **p-value<0.01, and ****p-value <0.0001).

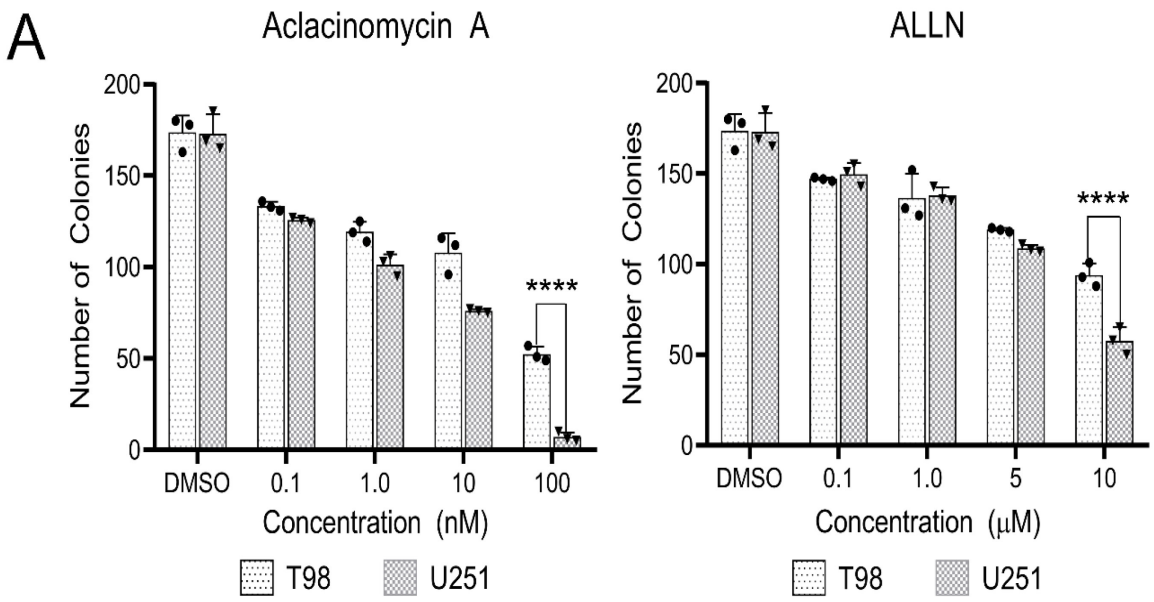
A
Aclacinomycin A
ALLN
Number of Colonies
200
150
100
50
0
DMSO
0.1
1.0
10
100
5
****
Concentration (nM)
Concentration (μM)
T98
U251

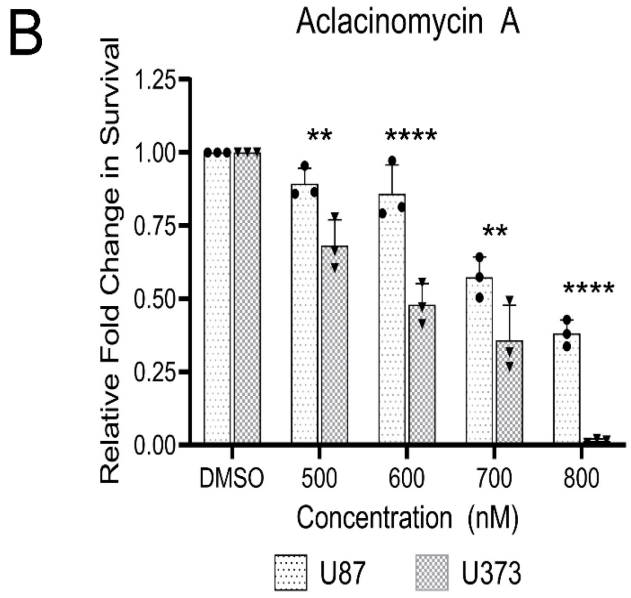
B
Aclacinomycin A
Relative Fold Change in Survival
1.25
1.00
0.75
0.50
0.25
0.00
**
****
DMSO
500
600
700
800
Concentration (nM)
U87
U373

Figure 3.8. Effects of calpain inhibitors on GBM cell clonogenic survival

(A) Five hundred T98 (NFI-hyperphosphorylated) or U251 (NFI-hypophosphorylated) cells were treated with increasing doses of aclacinomycin A (ACM) or calpain inhibitor I (ALLN). After 24 h, the drugs were removed, and cells allowed to grow for another 12 days. Cells were then fixed and stained with 1% crystal violet in 70% ethanol. Colonies (colony defined as >30 cells) were counted. (B) Cell metabolism, a surrogate for cell viability, was measured using the MTS assay. Thirty-five hundred U87 (NFI-hyperphosphorylated) or U373 (NFI-hypophosphorylated) cells were seeded in triplicate in 96-well plates. After 24 h, cells were treated with indicated concentrations of ACM. At 36 h post treatment, cells were incubated with the MTS reagent for an additional 2 h. Fluorescence emission (495 nm) was measured using the FLUOstar Optima plate reader and then normalized to the scrambled siRNA control. Each experiment was repeated three times. (**p-value <0.01 and ****p-value <0.0001).

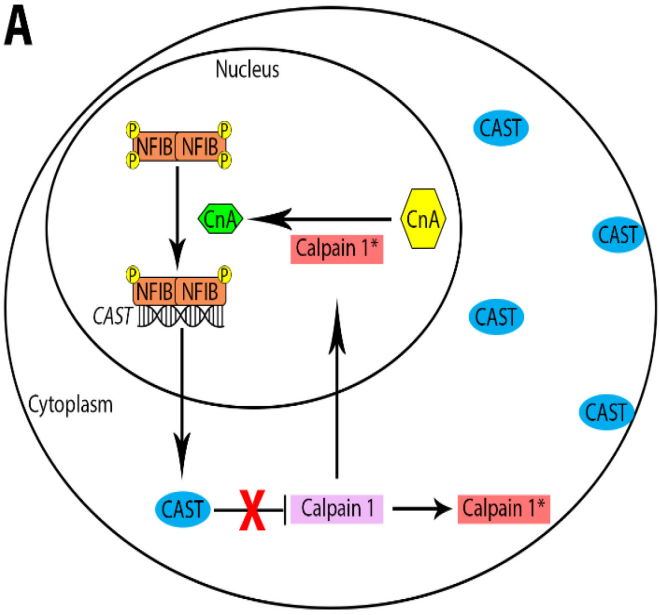

NFI-hyperphosphorylated GBM cells

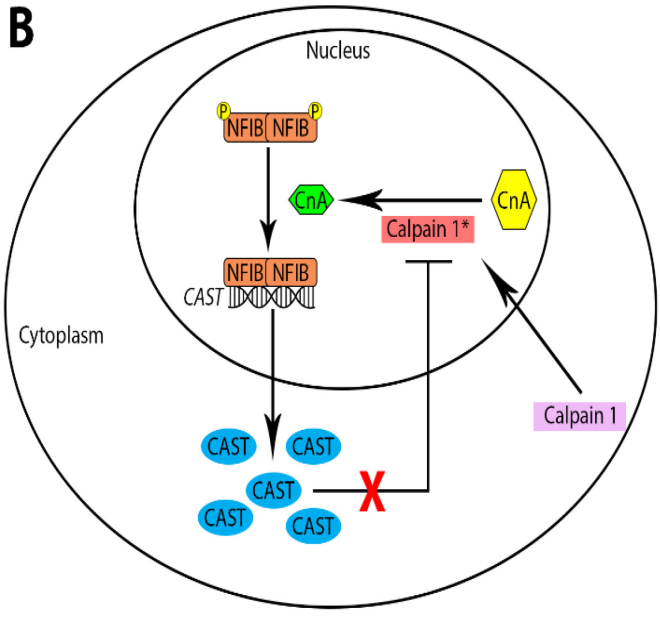

NFI-hypophosphorylated GBM cells

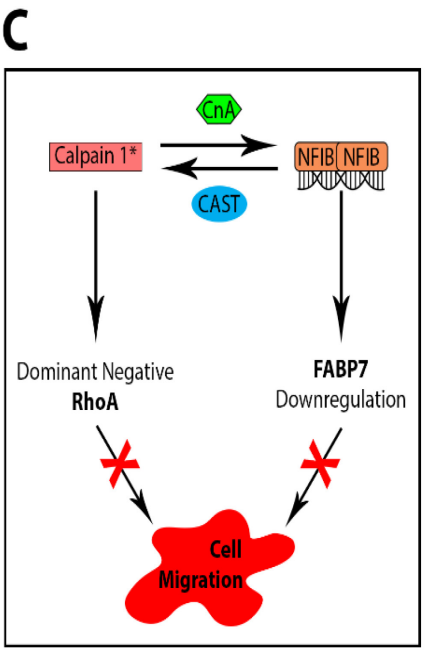

Figure 3.9. Proposed models for the NFIB-calpain 1 positive feedback loop and how it negatively regulates GBM cell migration.

(A) In NFI-hyperphosphorylated GBM cells, low levels of calcineurin (CnA) result in basally-hyperphosphorylated NFIB. CnA, in turn, is cleaved and activated by autolyzed calpain 1 in the nucleus. Hyperphosphorylated NFIB does not upregulate the alternative promoter containing NFI binding sites, resulting in higher levels of full-length calpastatin which has a diffuse distribution in the cytoplasm. Diffused calpastatin is unable to effectively prevent the autolysis and activation of full-length calpain 1, resulting in a small amount of autolyzed calpain 1. This autolyzed calpain 1, with low affinity for calpastatin, translocates into the nucleus resulting in low levels of CnA activation, repeating the signaling cycle. (B) In NFI-hypophosphorylated GBM cells, NFIB is dephosphorylated by high levels of CnA in the nucleus. Hypophosphorylated NFIB upregulates the alternative *CAST* promoter, resulting in increased levels of a truncated form of calpastatin that lacks the XL domain. This XL-less calpastatin preferentially localizes to the perinuclear region of the cell. As a result, calpastatin is unable to bind calpain 1 in other compartments of the cytoplasm. The majority of free cytoplasmic calpain 1 undergoes autolysis, producing high levels of autolyzed calpain 1. The latter accumulates in the nucleus, resulting in increased levels of cleaved and activated CnA, which in turn further dephosphorylates NFIB, perpetuating the positive feedback loop. (C) The calpain 1-NFIB positive feedback loop negatively regulates GBM cell migration through calpain 1-mediated proteolysis of RhoA (generating a

dominant-negative fragment) and NFIB-mediated downregulation of *FABP7* expression.

CHAPTER 4: NUCLEAR FACTOR IA AND CALPAIN 2 POSITIVE FEEDBACK LOOP POSITIVELY REGULATES GLIOBLASTOMA CELL MIGRATION AND CELL SURVIVAL

4.1 Introduction

WHO grade IV astrocytoma, also known as glioblastoma (GBM), is the most common and lethal form of adult brain tumours (57). Despite aggressive standard-of-care, including surgical resection, radiation and chemotherapy, GBM remains virtually incurable, with low survival times (~15 months) and poor quality of life (30,55). Failure of local and systemic therapies, resulting in inevitable tumour recurrence, can be attributed, at least in part, to the highly infiltrative nature of GBM cells (354-356). Although second-line treatment is available for GBM, it is primarily of palliative nature, with most patients succumbing to the disease soon after recurrence (357-359). As a result, targeting infiltrative GBM cells may be of clinical benefit; however, the molecular mechanisms underlying GBM cell migration/infiltration remain largely unknown.

We and others have implicated the Nuclear Factor I (NFI) family of transcription factors in the regulation of genes critical for gliogenesis and neural cell migration (112,117). There are four members of the NFI family, including NFIA, NFIB, NFIC and NFIX (413). NFIs bind as homodimers or heterodimers, with similar affinities, to the palindromic consensus sequence 5'-TTGGCN(3-6)GCCAA-3' through their highly conserved N-terminal DNA-binding domains (117). However, because of their variable C-terminal transactivation domain, NFI members can exert specific effects on the same promoter depending on tissue context (117,362). We have previously demonstrated that NFI regulates the expression of *FABP7* (brain fatty acid-binding protein) (362,364). As a neural stem cell marker, FABP7 expression has been correlated with both increased GBM cell

migration and worse clinical prognoses for GBM patients (183,184,361,372). In addition, NFI also regulates *GFAP* (glial fibrillary acidic protein), a marker of glial cell differentiation in GBM cells (117,362,364). We have shown that NFI is differentially phosphorylated in GBM cells, with the hypophosphorylated form of NFI associated with *GFAP* and *FABP7* expression (362). Dephosphorylation of NFI is mediated by the calcineurin phosphatase (164).

Calcineurin is a well-known target of calpain, a family of calcium-dependent proteases, with calpain-mediated proteolysis of calcineurin resulting in higher activity of this phosphatase (196,282,365). To date, at least 15 members of the calpain family have been identified. Amongst these are calpain 1 (μ-calpain) and calpain 2 (m-calpain), named after the *in vitro* calcium concentrations (micro (μ)- or milli (m)-molar) required for their proteolytic activity (196). Both calpains 1 and 2 are comprised of two subunits: a common small subunit (CAPSN1) and a large subunit that is unique to each calpain (CAPN1 for μ-calpain or CAPN2 for m-calpain) (218). Calpain is an important regulator of cell migration (195). Importantly, calpain 2 has been reported to be essential for *in vitro* and *in vivo* infiltration of GBM cells (249,253).

Dysregulation of calpain is associated with many pathological conditions including neurodegeneration, cardiomyopathy, and cancer (196,218). As a result, calpain proteolytic activity is tightly regulated by a variety of intra- and inter-molecular mechanisms. Calpain activation occurs concomitant with autoproteolysis, hereafter abbreviated as autolysis (196). This process lowers the amount of calcium needed for calpain to reach half-maximal proteolytic activity, but

also results in reduction of calpain stability by aggregation (299). In vertebrate cells, however, calpain activity is primarily regulated by its endogenous inhibitor, calpastatin (366). Calpastatin is highly specific to calpain and does not inhibit any other proteases tested so far (366). Calpastatin inhibits calpain proteolytic activity as well as its autolysis (392).

Interestingly, the *CAST* gene, encoding calpastatin, is regulated by NFI in GBM cells (397). We have shown that NFI, through the use of different *CAST* promoters, can alter the relative ratio of full-length to truncated calpastatin isoforms, with accompanying changes in calpastatin subcellular localization (369,397). NFI-mediated regulation of *CAST* is dependent on NFI's phosphorylation state (397). Building upon previous findings, we have also established a positive feedback loop between NFIB and calpain 1 in GBM cells. We demonstrated that this positive feedback loop functions to suppress GBM cell migration but appears to have little to no role in GBM cell viability. Here, we show that NFIA also forms a positive feedback loop with calpain 2 in GBM cells. Unlike the NFIB-calpain 1 positive feedback loop, however, NFIA and calpain 2 may act in concert to promote both GBM cell migration and survival.

4.2 Results

4.2.1 NFIA does not transcriptionally regulate calpain 2 gene

We have previously shown that all members of the NFI family negatively regulate the expression of calpastatin through the transcriptional regulation of *CAST* in GBM cells (Chapter 2 and 3). We also demonstrated that the effect of

NFIB on calpain 1 is primarily mediated through calpastatin, rather than being a consequence of the transcriptional regulation of calpain 1 by NFIB (Chapter 3). We were interested in whether NFIs might also play a role in calpain 2 activation. To address the possibility that calpain 2 might be a target of NFI, we transiently depleted each NFI in U87 and U251 GBM cells using NFI-specific siRNAs and carried out RT-qPCR with primers flanking the large (*CAPN2*) and small (*CAPSN1*) subunits of calpain 2. Knocking down NFIs had no effect on the RNA levels of either *CAPN2* or *CAPSN1* (Figure 4.1A and B). The efficacy of these NFI siRNAs to knockdown NFIs has been demonstrated in our previous studies (362,397). These results suggest that, similar to calpain 1, NFI does not transcriptionally regulate the expression of calpain 2.

4.2.2 NFIA induces increased levels of autolyzed calpain 2 in the nucleus of GBM cells.

Although NFIB forms a positive feedback loop with calpain 1, it does not appear to affect levels of calpain 2 (Chapter 3). As a result, we were interested to see if other members of the NFI family could cross signal with calpain 2. Of the three remaining NFIs, the role of NFIA in cancer, specifically GBM, is best documented (126,127,170). For this reason, we decided to focus our investigations on NFIA. Since a direct interaction is required for calpain 2 to proteolyze its downstream effectors and calpain 2 is found in both the cytoplasm and nucleus, we asked whether NFIA can affect the subcellular distribution of calpain 2. We carried out cytoplasmic and nuclear fractionation experiments using U87 and U251

GBM cells transiently transfected with either scrambled siRNAs (control) or NFIA-specific siRNAs. Cytoplasmic and nuclear fractions were electrophoresed on SDS-polyacrylamide gels and immunoblotted with an antibody specific to either calpain 1 or calpain 2. Depletion of NFIA had no consistent effects on levels of cytoplasmic or nuclear calpain 1 (Figure 4.1C).

We detected two forms of calpain 2 in the cytoplasmic extracts of both U87 and U251 GBM cell lines, with molecular weights of ~80 kDa and ~60 kDa (Figure 4.1C). The higher molecular weight band is full-length calpain 2 and the smaller fragment is an autolyzed form of calpain 2 previously described in chicken (285,414). NFIA knockdown had little to no effect on cytoplasmic calpain 2 in either U87 or U251 GBM cells (Figure 4.1C). In contrast, we observed only one form of calpain 2, with a molecular mass of ~55 kDa, in the nuclear extracts of GBM cells, suggesting that either autolysis is required for the nuclear translocation of calpain 2 or calpain 2 autolysis occurs with high efficacy in the nucleus (Figure 4.1C). A ~55 kDa autolyzed calpain 2 isoform has previously been described in both neuronal and muscle cells (415,416). Interestingly depletion of NFIA resulted in decreased levels of the ~55 kDa form of calpain 2 in both U87 and U251 GBM cells, with a more noticeable reduction observed in U251 cells (Figure 4.1C). Lamin A/C and α-tubulin were used as loading controls for the nuclear and cytoplasmic fractions, respectively. Together, our results indicate that NFIA expression is associated with higher levels of autolyzed calpain 2 in the nucleus but has little to no effect on cytoplasmic calpain 2.

4.2.3 NFIA depletion does not affect calpastatin subcellular localization but induces loss of nuclear calpain 2 and calcineurin

Knocking down NFIB in NFI-hyperphosphorylated GBM cells results in the aggregation of calpastatin in the cytoplasm, whereas knockdown of NFIB in NFI-hypophosphorylated GBM cells leads to increased levels of calpastatin in the nucleus (Chapter 3). To examine whether NFIA has similar effects on calpastatin subcellular distribution, we transfected NFI-hyperphosphorylated U87 GBM cells and NFI-hypophosphorylated U251 GBM cells with control and NFIA-specific siRNAs and examined the subcellular distribution of calpastatin by immunofluorescence microscopy. Surprisingly, NFIA depletion had no noticeable effect on the subcellular distribution of calpastatin in either cell line (Figure 4.2). These results suggest that, unlike NFIB and calpain 1, the subcellular location of calpastatin may not play a significant role in the crosstalk between NFIA and calpain 2.

To determine whether loss of NFIA causes any changes in the subcellular distribution of calpain 2 and its target, calcineurin, we repeated the aforementioned transfection experiments and immunofluorescence analysis with antibodies to calpain 2 and calcineurin. In agreement with our western blot data, loss of NFIA in either U87 or U251 cells resulted in reduced levels of nuclear calpain 2, with a stronger effect observed in U251 cells (Figure 4.3). Similarly, knocking down NFIA also led to reduced levels of nuclear calcineurin in both cell lines, with a more noticeable decrease in U251 compared to U87 cells (Figure 4.3). These results

suggest that NFIA induces the accumulation of calpain 2 and calcineurin in the nucleus of GBM cells.

4.2.4 NFIA enhances calpain proteolytic activity, GBM cell survival and migration

We have previously shown that depletion of NFIB in GBM cells results in reduced calpain proteolytic activity (Chapter 3). To determine if calpain proteolytic activity is also affected by NFIA, we transiently transfected U87 and U251 GBM cells with two NFIA-specific siRNAs and then measured calpain-specific cleavage of a fluorometric substrate. NFIA knockdown in both cell lines led to reduced calpain proteolytic activity (Figure 4.4A). Specifically, NFIA depletion in U87 cells resulted in decreased levels of fluorescence intensity, to 0.37-fold (siNFIA-1, $p<0.01$) and 0.43-fold (siNFIA-2, $p<0.001$), compared to control cells (Figure 4.4A, left panel). Similarly, NFIA knockdown in U251 cells led to decreased levels of fluorescence intensity, to 0.34-fold (siNFIA-1, $p<0.0001$) and 0.42-fold (siNFIA-2, $p<0.001$), compared to control cells (Figure 4.4A, right panel).

We also investigated the consequence of reduced calpain proteolytic activity, induced by NFIA depletion, on GBM cell migration using the Transwell assay. Knocking down NFIA in U251 cells resulted in a 0.67-fold decrease in numbers of migrating cells compared to control-transfected U251 cells (Figure 4.4B). These results suggest that NFIA promotes GBM cell migration. Finally, we examined the effect of NFIA depletion on GBM cell viability using the MTT assay, which measures metabolism and is a surrogate assay for cell viability (400). NFIA

depletion resulted in decreased cell viability in both U87 (0.59-fold $p<0.0001$) and U251 (0.54-fold, $p<0.001$) cells (Figure 4.4C). Together, these findings indicate that, unlike NFIB, NFIA appears to enhance GBM cell survival, and the effect of NFIA on cell survival is independent of NFI phosphorylation status.

4.2.5 Calpain 2 increases NFI transcriptional activity through calcineurin

Calpain 2 has been shown to cleave calcineurin in a wide variety of biological contexts (282,365,374,375). To examine whether calpain 2 can also affect calcineurin subcellular localization in GBM cells, we transiently transfected NFI-hypophosphorylated U251 cells with siRNAs targeting calpain 2. We examined calcineurin distribution by immunofluorescence microscopy. Similar to calpain 1 knockdown, depletion of calpain 2 also resulted in loss of calcineurin in the nucleus of U251 cells (Figure 4.5B).

We have previously demonstrated that NFI is hypophosphorylated by calcineurin in U251 cells, with hypophosphorylated NFI upregulating *FABP7* expression. To indirectly investigate the consequence of loss of nuclear calcineurin on NFI transcriptional activity, we depleted NFIA in U251 GBM cells using two NFIA-specific siRNAs and examined FABP7 levels by western blotting. We observed a reduction in the levels of FABP7 in U251 cells, suggesting that NFI transcriptional activity may have been reduced upon loss of calpain 2 (Figure 4.5, left panels). Efficiency of calpain 2 knockdown is shown in Figure 4.5A. Actin was used as loading control.

4.2.6 Calpain 2 enhances GBM cell survival and migration

To examine whether our proposed NFIA and calpain 2 crosstalk affects GBM cell migration and cell survival, we transfected U87 and/or U251 GBM cells with siRNAs targeting either calpain 2 alone or both calpain 2 and NFIA. Like NFIA knockdown, calpain 2 depletion led to a 0.54-fold reduction ($p<0.05$) in U251 cell migration (Figure 4.6A). Co-depletion of NFIA and calpain 2 in U251 GBM cells did not lead to a statistically significant decrease in the number of migrated cells compared to calpain 2 depletion alone (Figure 4.6A). These results suggest that: (i) calpain 2, similar to NFIA, enhances GBM cell migration and (ii) these two proteins are likely to function in a common pathway that positively regulates GBM cell migration. Also, knocking down either calpain 2 or both NFIA and calpain 2 resulted in decreased U87 (0.61-fold, $p<0.001$) and U251 (0.45-fold, $p<0.0001$) cell survival compared to control cells as measured by the MTS assay (Figure 4.6B). In addition, compared to calpain 2 single knockdown, co-depletion of both calpain 2 and NFIA resulted in a minor but statistically significant reduction in the survival of both U87 cells (0.61-fold for single knockdown versus 0.41-fold for co-depletion, $p<0.05$, both relative to scrambled siRNA transfected cells) and U251 cells (0.45-fold for single knockdown versus 0.27-fold for co-depletion, $p<0.05$, both relative to scrambled siRNA transfected cells) (Figure 4.6B). These results suggest that NFIA and calpain 2 may act in concert to enhance GBM cell survival. However, unlike the regulation of GBM cell migration, it is most likely that NFIA and calpain 2 function in multiple independent pathways that positively regulate GBM cell survival.

4.3 Discussion

Since FDA approval of temozolomide in 1999, there has been little improvement in GBM clinical outcomes despite recent advances on both the biological and technological fronts. On the one hand, intra- and inter-tumour heterogeneity, together with the anatomical location of the brain, pose significant barriers to the development of new anti-GBM therapeutics. On the other hand, early and extensive tumour infiltration severely limits the ability of current standard-of-care approaches to fully eradicate GBM cells, leading to inevitable tumour recurrence. In previous attempts to unravel the molecular mechanisms underlying GBM infiltration, we showed that the NFI family of transcription factors play key roles in regulating expression of genes involved in GBM cell migration. Specifically, we found that NFI regulates *FABP7* (362), the expression of which correlates with GBM cell invasion *in vitro* and a worse patient prognosis (163,184). In this regard, the role of NFI in GBM is closely related to its role in normal embryogenesis, particularly as related to the regulation of genes involved in neural cell migration and glial cell differentiation (112,364).

We then linked NFI transcriptional activity to its phosphorylation state, with NFI dephosphorylation mediated by calcineurin phosphatase. As calcineurin is a well-known target of calpain proteases, we provided the first empirical evidence for the regulation of NFI activity by calpain. Calpain proteolytic activity is required for all major steps of cell migration (201,404). Recently, we identified *CAST*, encoding calpastatin, the endogenous inhibitor of calpain, as a target gene of NFI

thereby providing the foundation for a bidirectional signaling between the NFI and calpain pathway.

In Chapter 3, we showed that NFIB forms a positive feedback loop with calpain 1 in GBM cells, resulting in the negative regulation of GBM cell migration. In this chapter, we present evidence supporting crosstalk between NFIA and calpain 2 in GBM cells. Although NFI members have similar apparent affinities toward NFI binding elements, they may elicit distinct effects from the same promoter depending on cellular context (117). As a result, different NFIs may have unique, or even opposing, roles depending on cancer type and subtype (129). For example, NFIA has been shown to promote GBM growth and survival (170), whereas NFIB was found to have tumour suppressing roles in certain subtypes of GBM (171). Similarly, calpains 1 and 2 are known to compensate for the activity of one another in a variety of biological contexts, including the cleavage of calcineurin (282,365,375). However, calpains 1 and 2 also have specific functions. For example, calpain 1 promotes the self-renewing capacity of neural stem cells (NSCs), whereas calpain 2 induces neural stem cell differentiation (215). Here, using a variety of techniques including immunoblotting and immunofluorescence analyses, as well as cell metabolism/survival and invasion assays, we provide mechanistic insight into the putative NFIA-calpain 2 crosstalk in GBM cells and demonstrate that this crosstalk has opposite effects on GBM properties compared to NFIB-calpain 1 crosstalk.

Based on our previous work, hypophosphorylated NFIB regulates *CAST* variant expression by binding to NFI regulatory elements located in a *CAST*

alternative promoter. As a result, levels of a truncated form of calpastatin which preferentially localizes to perinuclear aggregates are increased (Chapters 2 and 3). This form of calpastatin therefore cannot bind and prevent the autolysis of calpain 1 in other cytosolic compartments. Autolyzed calpain 1 then translocates to the nucleus and further isolates itself from calpastatin inhibition. Thus, knockdown of hypophosphorylated NFIB results in the loss of nuclear calpain 1. In contrast, NFIA increases calpain 2 activity by downregulating the expression of *CAST*. NFIA, unlike NFIB, has no effect on the subcellular localization of calpastatin. Thus, NFIA appears to be able to increase calpain 2 autolysis and activation simply by lowering levels of calpastatin.

We have previously shown that there are two *de novo* NFI binding sites (C2 and C3) located in *CAST* intron 3 (Chapter 2). While only hyperphosphorylated NFI can bind to C2, NFI can interact with C3 irrespective of its phosphorylation status (Chapter 2). Consequently, NFIA may only exert its regulatory effects on *CAST* through C3. Although this allows for a less restricted interaction between NFIA and *CAST*, it also means that NFIA may not be able to regulate different *CAST* variants like NFIB. As a result, NFIA is unable to alter calpastatin subcellular localization through isoform switching. Together, these observations help explain mechanistic differences between the NFIA-calpain 2 crosstalk and the NFIB-calpain 1 positive feedback loop.

Like autolyzed calpain 1 in NFIB-hypophosphorylated cells (Chapter 3), autolyzed calpain 2 translocates into the nucleus of either NFI-hyper- or hypo-phosphorylated GBM cells. By immunofluorescence analysis, calpain 2 has been

shown to preferentially localize to the nucleus of cultured neurons, in which it cleaves and activates nuclear Ca2+/Calmodulin-dependent Protein Kinase Type IV (CaMKIV) (388). CaMKIV, together with CaMKII, are important pro-survival mediators of neuronal cells (417). Unlike the ~55 kDa form of calpain 1, the affinity of autolyzed calpain 2 toward calpastatin is currently unknown. However, given the relatively high levels of homology (55%-65% depending on species) between the two calpains, it is possible that autolyzed calpain 2, similar to autolyzed calpain 1, may also have low affinity toward calpastatin (196). As a result, calpastatin may not be able to prevent nuclear translocation of autolyzed calpain 2, leading to increased levels of calpain 2 proteolytic activity in the nucleus. Our proposed mechanism for increasing calpain 2 activity by NFIA-mediated downregulation of calpastatin expression has previously been observed for the c-Myc transcription factor (161).

Unlike the paradoxical roles reported for NFIB and calpain 1 depending on cancer type and subtype, reports to date indicate that NFIA and calpain 2 have exclusively oncogenic properties regardless of tumour type, with both NFIA and calpain 2 promoting GBM tumorigenesis and progression. NFIA is highly expressed in GBM tumours compared to normal brain (169). Loss of NFIA in GBM cells results in reduced growth and increased tumour cell death by apoptosis (169). NFIA's oncogenic role is mediated by the transcriptional repression of tumour suppressor genes including *TP53* (encoding p53) and *CDKN1A* (encoding p21) (169). To date, there have been no reports on the role of calpain 2 in the control of GBM cell survival, although calpain functions in cancer cell death and survival are

well characterized (218). In breast cancer, for example, calpain 2, together with calpain 1, promote tumour cell apoptosis upon trastuzumab treatment (418). However, calpain can also promote lung cancer cell survival through the proteolytic degradation of IκBα and subsequent activation of NF-κB transcriptional activity (419). Interestingly, NFIA has also been shown to form a feed-forward loop with another nuclear factor, NF-κB, to promote GBM cell survival (170). These findings provide further support for our proposed NFIA-calpain 2 crosstalk in GBM cells. In keeping with evidence from the literature, our data confirm that both NFIA and calpain 2 independently promote GBM cell viability. However, given the minor reduction in GBM cell viability when NFIA and calpain 2 are co-depleted compared to single knockdowns, it appears that these two proteins act predominantly in concert to enhance GBM cell viability, in agreement with our proposed NFIA-calpain 2 crosstalk model.

The role of NFIA in promoting GBM cell migration has also been investigated although specific mechanisms have yet to be reported (169). For example, Lee *et al.* showed that ectopic expression of NFIA correlates with increased GBM cell migration and invasion *in vitro* (169). The role of calpain 2 in regulating GBM cell migration/infiltration is better understood and has been confirmed in animal models (249,253). In response to integrin-mediated signaling, calpain 2 upregulates the expression of matrix metalloproteinase (MMP) 2 leading to increased GBM cell migration (194). In support of these observations, our data indicate that both NFIA and calpain 2 can enhance GBM cell migration.

Even though calcineurin likely dephosphorylates all four NFI members, we were not able to confirm calpain 2-induced and calcineurin-mediated dephosphorylation of NFIA due to our inability to find an antibody specific to NFIA. As a result, the second branch of the crosstalk, from calpain 2 to NFIA, could not be verified. We are in the process of purchasing additional anti-NFIA antibodies to carry out confirmatory experiments.

In summary, our results are in line with crosstalk between NFIA and calpain 2 in GBM cell lines. We provide mechanistic insight into the forward branch of the crosstalk, from NFIA to calpain 2. However, the backward branch, from calpain 2 to NFIA, needs to be further investigated. In Chapter 4, we also show that NFIA and calpain 2 act chiefly in concert to enhance GBM cell survival and cell migration although the latter needs to be confirmed with more biological replicates.

4.4 Experimental Procedures

4.4.1 Cell lines, constructs, transfections and treatments

The origins of U87 and U251 GBM cell lines have previously been described (181,362). Cells were cultured in Dulbecco's modified Eagle's minimum essential medium supplemented with 8% fetal bovine serum (FBS), streptomycin (50 µg/ml), and penicillin (50 units/ml).

4.4.2 Knockdown of endogenous NFIs and CAPN2

GBM cells were transiently transfected with the following Stealth® siRNAs (Life Technologies): scrambled (control) siRNAs (Cat. # 12935-200 and 12935-

300); NFIA-1, NM_207685.1_stealth_335 (5'-CCAACCACUGUAAACAACAACUGCU-3');NFIA-2, NM_005595_stealth_919 (5'-GAAAGUUCUUCAUACUACAGCAUGA-3 of NFIA'); NFIA-3, NIFAHSS181500 (5'-UUCACUUAGCAAUUCAUCCUUCACG-3'); NFIB, NM_005596_stealth_1020 (5'-AAGCCACAAUGAUCCUGCCAAGAAU-3'), NFIC, NM_005597_stealth_1045 (5'-CAGAGAUGGACAAGUCACCAUUCAA-3'), NFIX, NM_002501_stealth_752 (5'-GAGAGUAUCACAGACUCCUGUUGCA-3'), CAPN2-1, CAPN2HSS101347 (5'-GCUGCUCUUUGUGCAUUCAGCCGAA-3'), CAPN2-2, CAPN2HSS101348 (5'-GCAUUGCUGAGUGGUAUGAGUUGAA-3'). Cells were transfected with 10 nM of each siRNA using the RNAiMAX Lipofectamine reagent (Invitrogen) according to the manufacturer's instruction. Scrambled siRNAs (low and medium GC content) served as the control for these experiments. After 48 h, cells were trypsinized and replated for a second round of siRNA transfection and then harvested 60 h after the last transfection. Of note, cells were only transfected with one round of siRNA for immunofluorescence experiments.

4.4.3 Reverse transcription (RT) and quantitative polymerase chain reaction (qPCR)

Total RNA was isolated from GBM cells depleted of specific NFIs using the TRIzol® reagent (ThermoFisher Scientific). First-strand cDNA synthesis was generated using Superscript II® reverse transcriptase (Invitrogen). RT-qPCR was performed on cDNAs with primers flanking either *CAPN2, CAPNS1,* or *GAPDH* using the BrightGreen® qPCR master mix (ABM Scientific). Fluorescence

intensities obtained with *CAPN2* primers were first normalized to that of *GAPDH* and then to the scrambled siRNA control to generate relative fold change results.

4.4.4 Western blot analysis

Whole cell extracts (WCEs) were prepared by lysing cells in modified RIPA buffer [50 mM Tris-HCl pH 7.5, 1% sodium deoxycholate, 1% Triton X-100, 150 mM NaCl, 50 mM sodium fluoride, 1 mM sodium orthovanadate, 10 mM EDTA, 0.1% SDS, 0.5 mM PMSF, 1X cOmplete protease inhibitor (Roche Applied Science), and 1X PhosSTOP phosphatase inhibitor (Roche Applied Science)]. WCEs were electrophoresed in polyacrylamide-SDS gels and transferred to nitrocellulose membranes and then immunostained with rabbit anti-calpain 2 antibody (1:1000, Santa Cruz, cat.# sc-30064), mouse anti-calcineurin antibody (1:1000, Pharmingen, clone G182-1847), mouse anti-lamin A/C antibody (1:1,000, ThermoFisher Scientific, cat.# MA3-1000), mouse anti-α-tubulin (1:100,000, Hybridoma Bank, clone 12G10), or mouse anti-β-actin antibody (1:100,000, Sigma Aldrich, clone AC-15). Proteins were detected with horseradish peroxidase-conjugated secondary antibody (Jackson ImmunoResearch Biotech) using the Immobilon (EMD Millipore) or ECL (GE Healthcare) chemiluminescent HRP substrate.

4.4.5 Cytoplasmic and nuclear fractionation

Nuclear and cytoplasmic fractionation was carried out as previously described (Chapter 3). Briefly, cytoplasmic extracts were prepared using reagents supplied with the NE-PER kit (ThermoFisher Scientific), supplemented with 1X

cOmplete protease inhibitors and 1X PhosSTOP. Nuclei were isolated by centrifugation of cytoplasmic extracts and then lysed in modified RIPA buffer (described in the previous section). Chromatin was sheared by sonication (20 cycles at 4°C, high output, 30 s power on and 30 s power off) in a Bioruptor 300® sonicator (Diagenode).

4.4.6 Calpain activity assay

Calpain proteolytic activity was measured with the Calpain Activity Assay Kit (Calbiochem). Briefly, whole cell extracts were prepared from GBM cells with the supplied lysis buffer. Substrate cleavage was measured by changes in fluorescence intensity in buffers that promote (Activation buffer) or suppress (Inhibition buffer) calpain activity using the FLUOstar Optima microplate reader (355 nm excitation and 480 nm emission, BMGLABTECH). Raw data obtained with the Activation buffer were first normalized against the Inhibition buffer and then the scrambled siRNA control to generate relative fold change.

4.4.7 Transwell migration assay

U251 GBM cells were depleted of NFIA and/or calpain 2. Thirty thousand cells in FBS-free DMEM were plated in the top chamber of Falcon Cell Culture Inserts (Fisher Scientific) and then allowed to migrate through an 8-µm polyethylene terephthalate (PET) membrane towards a chemoattractant (DMEM +10% fetal calf serum) in the bottom chamber for 20 h. Cells were fixed with 100% cold methanol for 20 minutes and then stained with 1% crystal violet in 20%

methanol for 30 minutes. Migrated cells were imaged using a Zeiss Axioskop2 plus microscope using multiple fields covering the whole surface of the inserts. Cell counting was carried out using Metamorph software (Molecular Devices).

4.4.8 MTS assay

U251 and U87 GBM cells were depleted of NFIA and/or calpain 2. Cell metabolism, a surrogate assay for cell viability, was measured using the CellTiter 96® Non-Radioactive Cell Proliferation MTs Assay (Promega). Briefly, ~3,500 cells were plated in triplicate in 96-well plates and then allowed to grow for 48 h. Cells were incubated in culture medium supplemented with 20 μL MTS reagent for an additional 2 h. Absorbance values were measured using the FLUOstar OPTIMA microplate reader (495 nm). Relative fold change was generated by normalizing absorbance values to that of scrambled siRNA controls.

4.4.9 Immunofluorescence analysis

GBM cells were transfected with scrambled siRNAs or siRNAs targeting either NFIA or calpain 2 and then plated on coverslips. After 24 h, cells were fixed with 4% paraformaldehyde for 10 min at room temperature and then permeabilized with 0.25% Triton X-100 for 4 min. Cells were blocked with 3% BSA for 45 min at room temperature to reduce background signal. Cells were then immunostained with rabbit anti-calpain 2 antibody (1:50, Santa Cruz, cat.# sc-30064), or mouse anti-calcineurin antibody (1:50, Pharmingen, clone G182-1847). Signals were visualized using Alexa 488-conjugated donkey anti-rabbit or Alexa 555-conjugated

donkey anti-mouse secondary antibodies (1:400, Life Technologies). Nuclei were stained with 4′,6-diamidino-2-phenylindole (DAPI, CalBiochem). Images were acquired with a X40/1.3 oil immersion objective lens on a Zeiss LSM 710 confocal microscope using Zeiss ZEN imaging software.

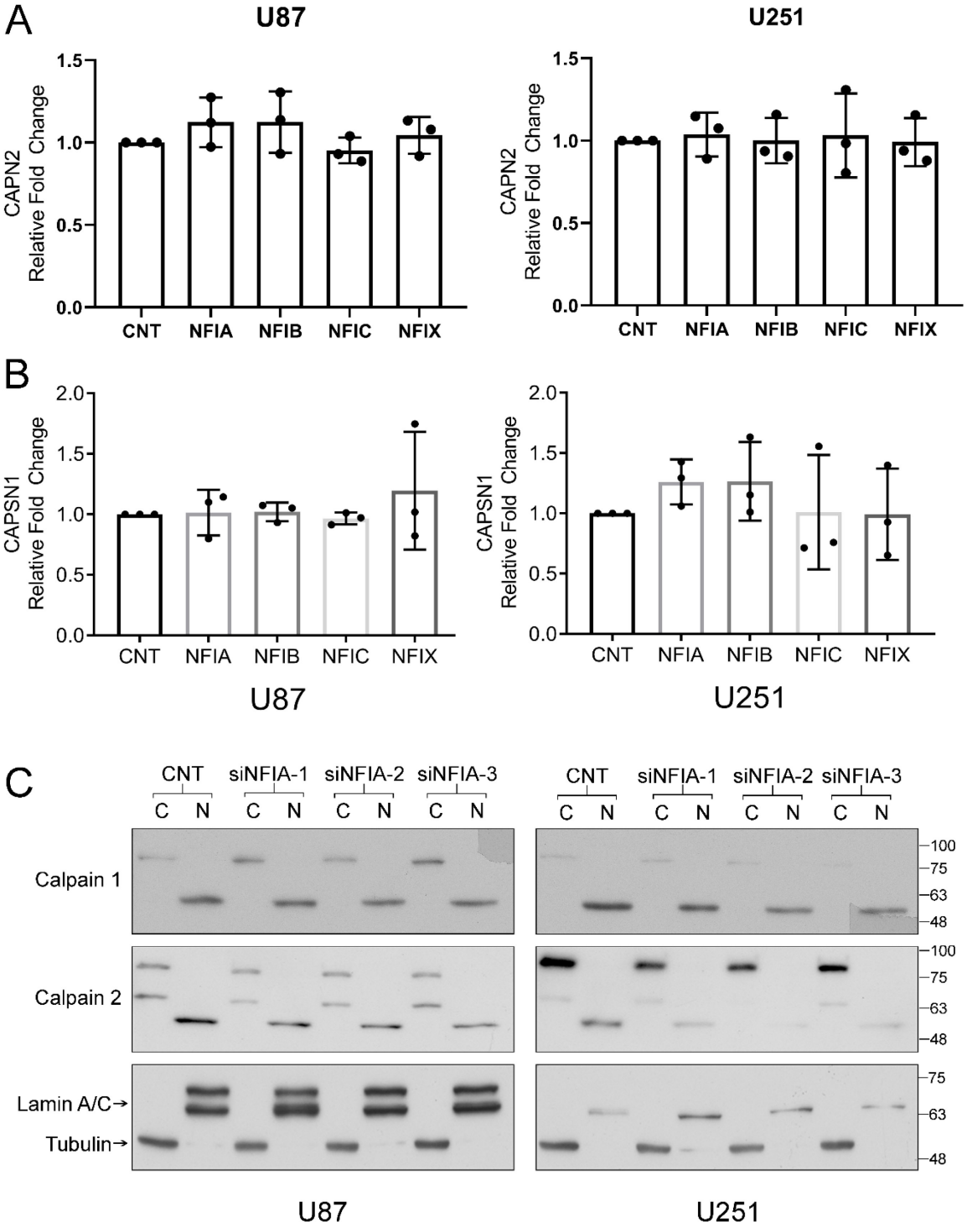
A
U87
U251
CAPN2
Relative Fold Change
1.5
1.0
0.5
0.0
CNT
NFIA
NFIB
NFIC
NFIX
B
CAPSN1
Relative Fold Change
2.0
1.5
1.0
0.5
0.0
U87
U251
C
CNT
siNFIA-1
siNFIA-2
siNFIA-3
C
N
Calpain 1
Calpain 2
Lamin A/C→
Tubulin→
100
75
63
48

Figure 4.1. NFIA indirectly upregulates nuclear calpain 2 levels

(A) U87 and U251 cells were transfected with siRNAs specific to each NFI family member and total RNA extracted using the TRIzol reagent. cDNAs were amplified by RT-qPCR using *CAPN2*-specific primers. Relative fold changes were generated by normalizing *CAPN2* data to those of *GAPDH* and then to the internal scrambled siRNA control. Results are representative of three independent experiments. (B) Cytoplasmic (abbreviated as C) and nuclear (abbreviated as N) lysates were prepared from U87 and U251 cells transfected with siRNAs specific to NFIA. Proteins were separated by SDS-PAGE, transferred to nitrocellulose membranes, and immunoblotted with mouse anti-calpain 1 or rabbit anti-calpain 2 antibodies. α-tubulin and lamin A/C served as loading controls for the cytoplasmic and nuclear fractions, respectively.

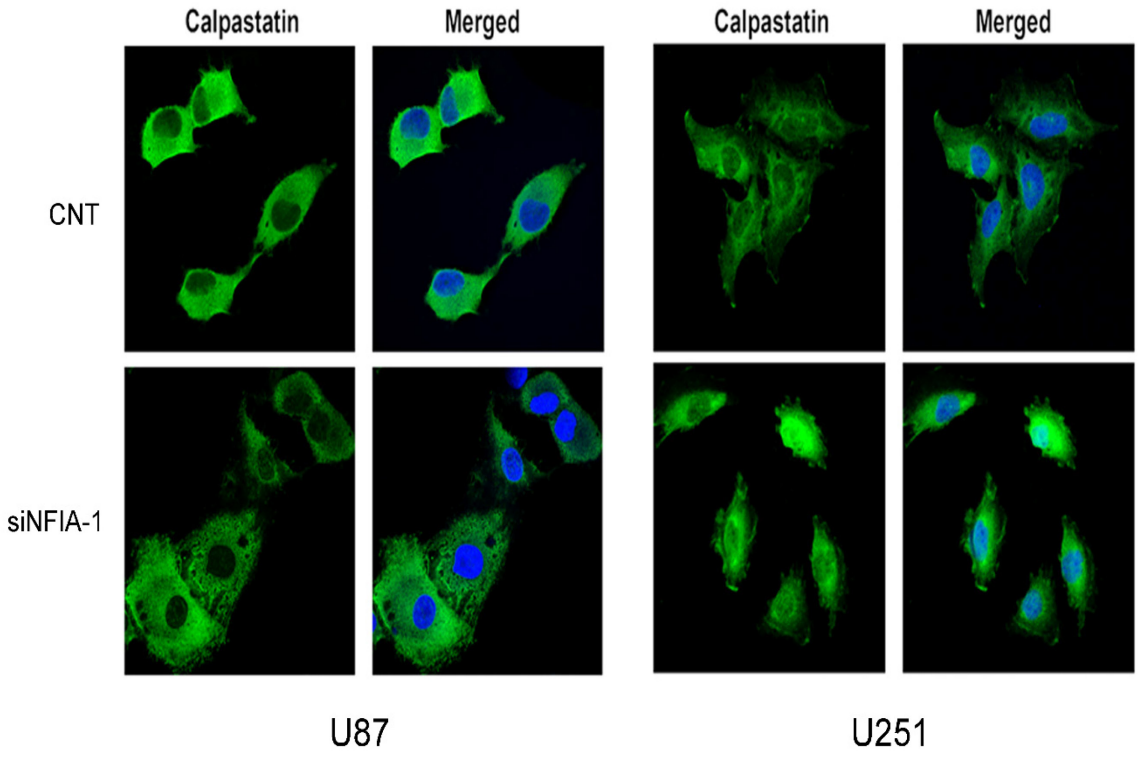
Calpastatin
Merged
Calpastatin
Merged
CNT
siNFIA-1
U87
U251

Figure 4.2. NFIA does not regulate calpastatin subcellular distribution

U87 and U251 cells were transiently transfected with scrambled or an NFIA-specific siRNAs and then plated on coverslips. Cells were cultured for 24 h and then fixed with 4% paraformaldehyde and immunostained with a rabbit anti-calpastatin antibody followed by Alexa 488-conjugated secondary antibody. Nuclei were visualized with DAPI (blue) and images acquired with a 40X/1.3 oil immersion lens using a Zeiss LSM 710 confocal microscope and Zeiss ZEN imaging software. Images are representative of the majority of cells observed under each condition and are derived from three independent experiments.

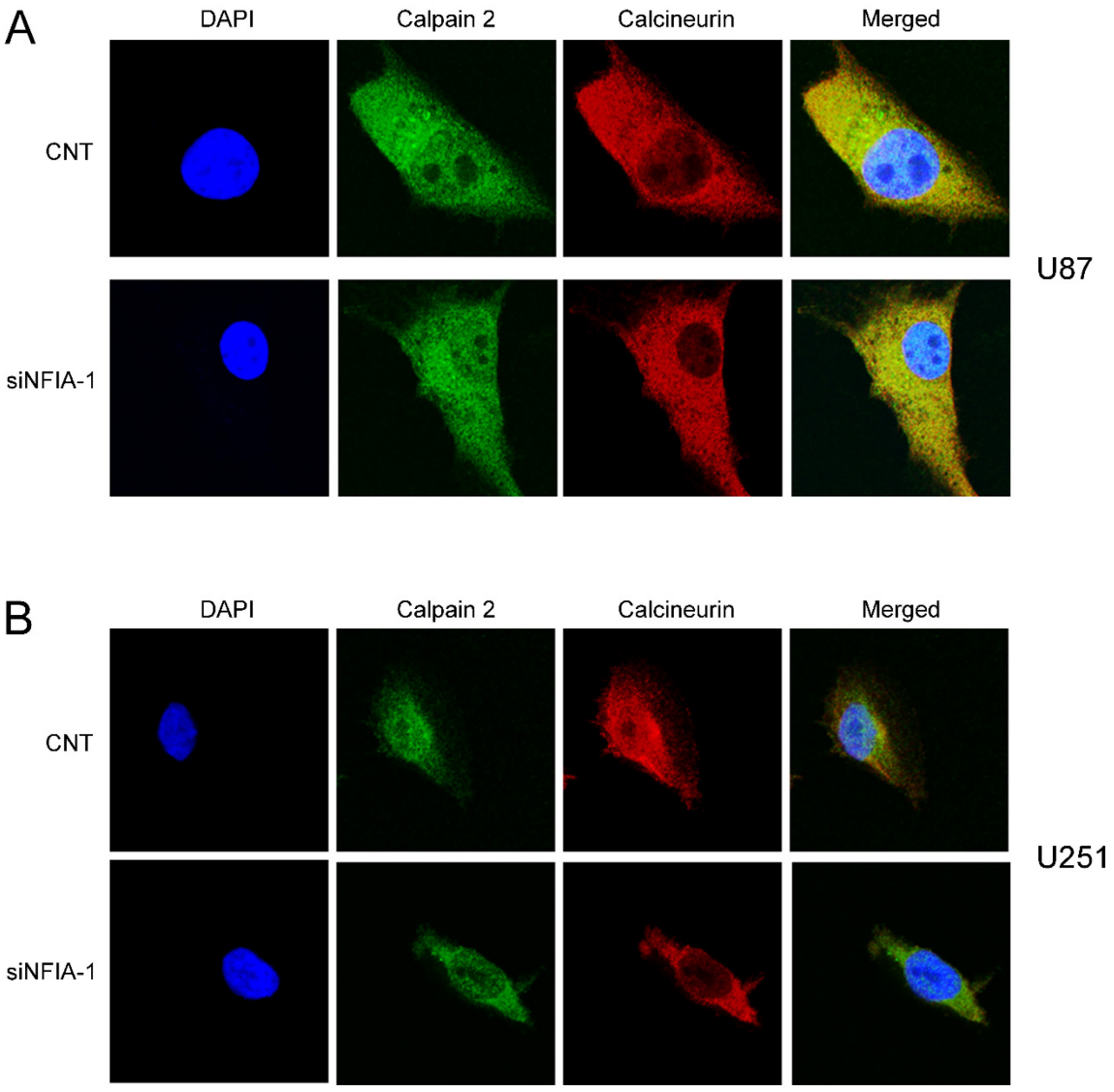
A
DAPI
Calpain 2
Calcineurin
Merged
CNT
siNFIA-1
U87
B
DAPI
Calpain 2
Calcineurin
Merged
CNT
siNFIA-1
U251

Figure 4.3. Changes in calpain 2 and calcineurin subcellular localization upon NFIA depletion

U87 (A) or U251 (B) cells were transiently transfected with scrambled or NFIA-specific siRNAs and then plated on coverslips. Cells were cultured for 24 h and then fixed with 4% paraformaldehyde and immunostained with either rabbit anti-calpain 2 (A) or mouse anti-calcineurin (A and B) antibodies followed by Alexa 488 (rabbit, green)- or Alexa 555 (mouse, red)-conjugated secondary antibodies, respectively. Nuclei were visualized with DAPI (blue) and images acquired with a 40X/1.3 oil immersion lens using a Zeiss LSM 710 confocal microscope and Zeiss ZEN imaging software. Bars, 20 μm. Images are representative of the majority of cells observed under each condition and are derived from three independent experiments.

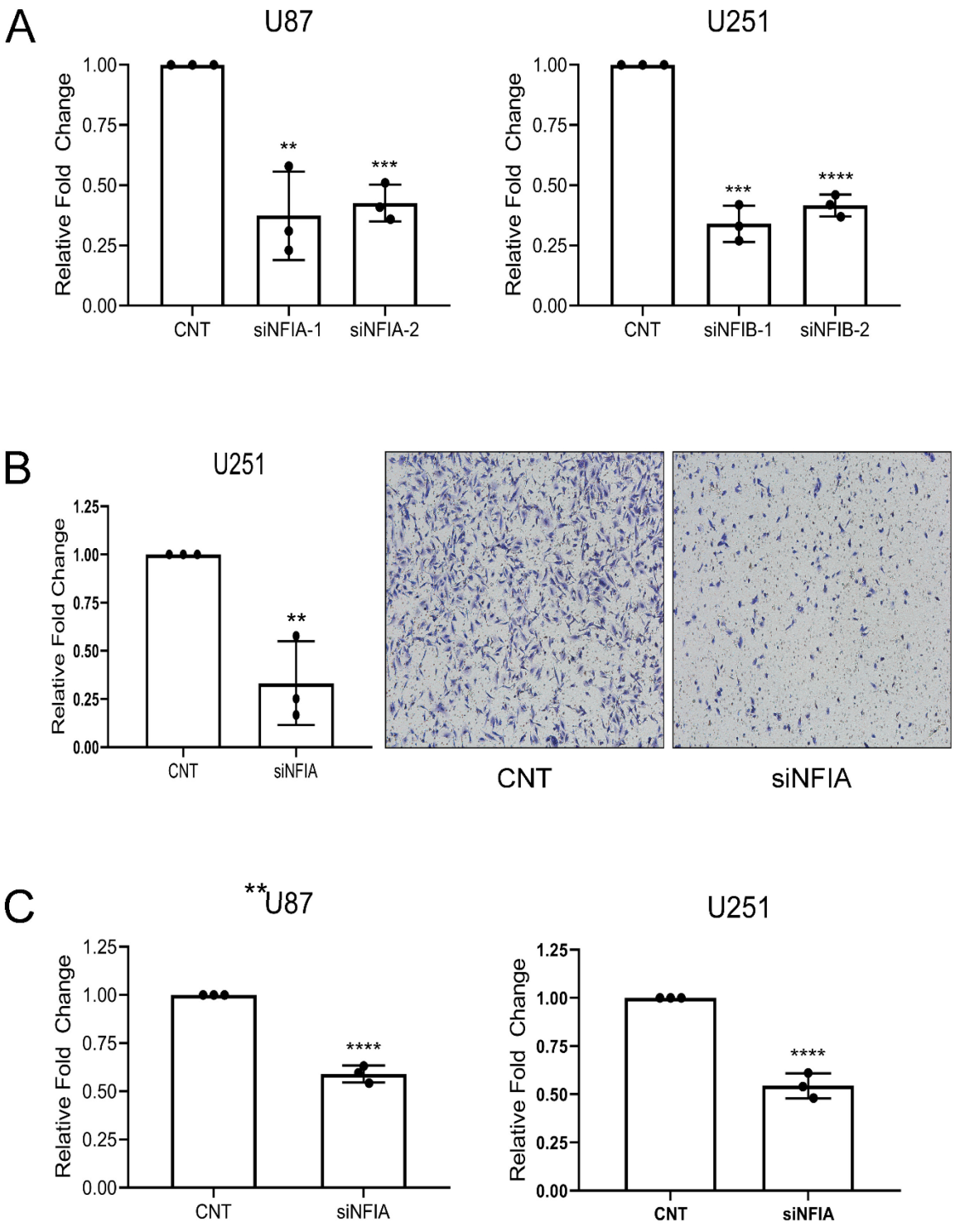
A
U87
U251
Relative Fold Change
1.00
0.75
0.50
0.25
0.00
**
***
***
****
CNT
siNFIA-1
siNFIA-2
siNFIB-1
siNFIB-2
B
U251
Relative Fold Change
1.25
1.00
0.75
0.50
0.25
0.00
**
CNT
siNFIA
CNT
siNFIA
C
**U87
U251
Relative Fold Change
1.25
1.00
0.75
0.50
0.25
0.00
****
****
CNT
siNFIA
CNT
siNFIA

Figure 4.4. Effects of NFIA depletion on calpain activity and GBM cell migration and viability

(A-C) U87 and/or U251 cells were transfected with scrambled siRNAs or siRNAs targeting NFIA. (A) Calpain activity was assessed by measuring the cleavage of a synthetic substrate provided in the Calpain Activity Fluorometric Assay Kit (CalBiochem). Fluorescence signals obtained in a buffer that activates calpain activity was normalized against fluorescence signals obtained in a buffer that inhibits calpain activity. Relative fold change was obtained by normalizing the scrambled siRNA control to 1. (B) Thirty thousand U251 cells in FBS-free DMEM were seeded in the top chambers of Falcon Cell Culture Inserts in a 24-well plate. Directional migration was induced by supplementing the medium in the bottom chamber with 10% FBS. After 20 h, cells that had migrated through the porous membrane of the inserts were fixed with methanol and stained with crystal violet. Migrated cells were imaged with a Zeiss Axioskop2 plus microscope. Cells were counted using MetaMorph software. (C) Cell metabolism, used as a surrogate for cell viability, was measured using the MTS assay. Thirty-five hundred cells were seeded in 96-well plates. After 48 h, cells were incubated with the MTS reagent for 2 h. Fluorescence emission (495 nm) was measured using the FLUOstar Optima plate reader and then normalized to the scrambled siRNA control. (A and C) Each experiment was repeated at least three times. (**p-value<0.01, ***p-value <0.001 and ****p-value <0.0001).

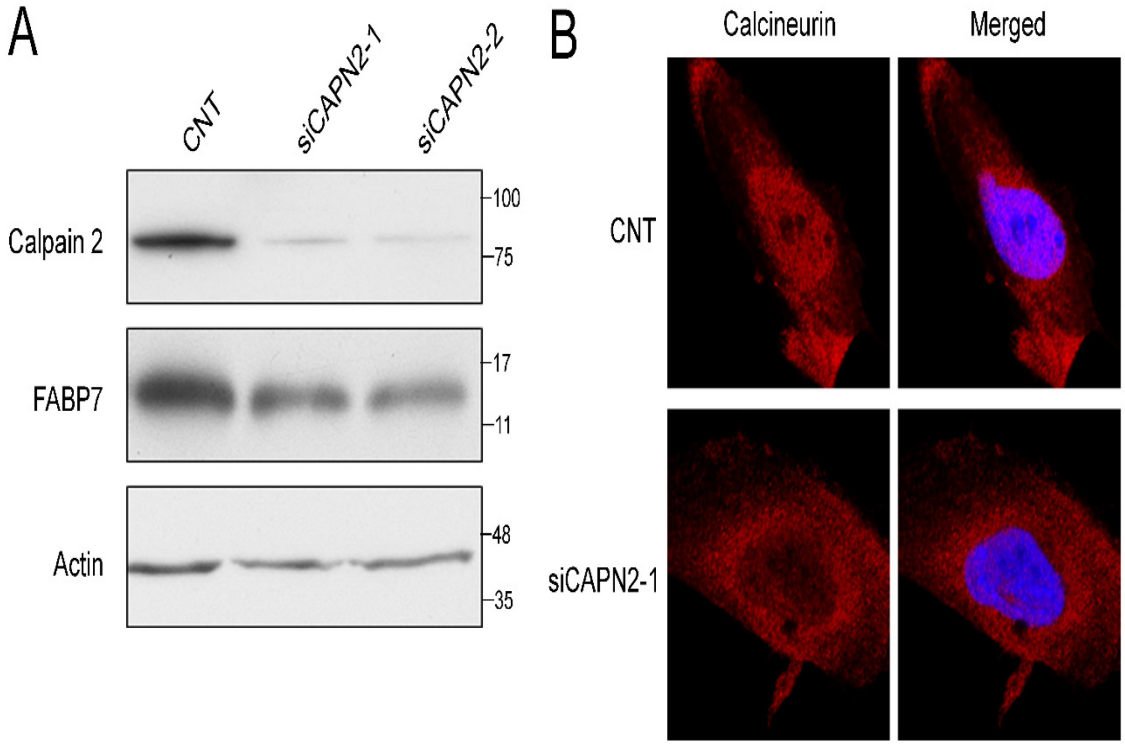
A
CNT
siCAPN2-1
siCAPN2-2
Calpain 2
100
75
FABP7
17
11
Actin
48
35
B
Calcineurin
Merged
CNT
siCAPN2-1

Figure 4.5. Calpain 2 depletion affects calcineurin subcellular localization and NFI transcriptional activity

(A) Whole cell lysates were prepared from U251 cells transiently transfected with scrambled siRNAs or siRNAs targeting calpain 2 (siCAPN2-1 and siCAPN2-2). Proteins were electrophoresed in SDS-polyacrylamide gels and transferred to nitrocellulose membranes. Membranes were immunostained with rabbit anti-calpain 2 and rabbit anti-FABP7 antibodies. Actin was used as loading control. (B) U251 cells were transiently transfected with scrambled or calpain 2-specific siRNAs and then plated on coverslips. Cells were cultured for 24 h and then fixed with 4% paraformaldehyde and immunostained with mouse anti-calcineurin antibody followed by Alexa 555-conjugated secondary antibody. Nuclei were visualized with DAPI (blue) and images acquired with a 40X/1.3 oil immersion lens using a Zeiss LSM 710 confocal microscope and Zeiss ZEN imaging software. Images are representative of the majority of cells observed under each condition and are derived from three independent experiments.

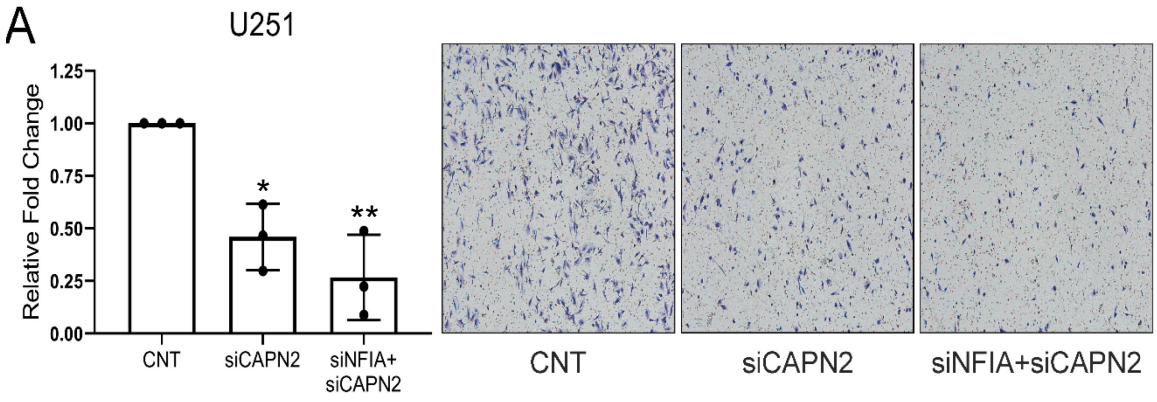
A
U251
Relative Fold Change
1.25
1.00
0.75
0.50
0.25
0.00
*
**
CNT
siCAPN2
siNFIA+
siCAPN2
CNT
siCAPN2
siNFIA+siCAPN2

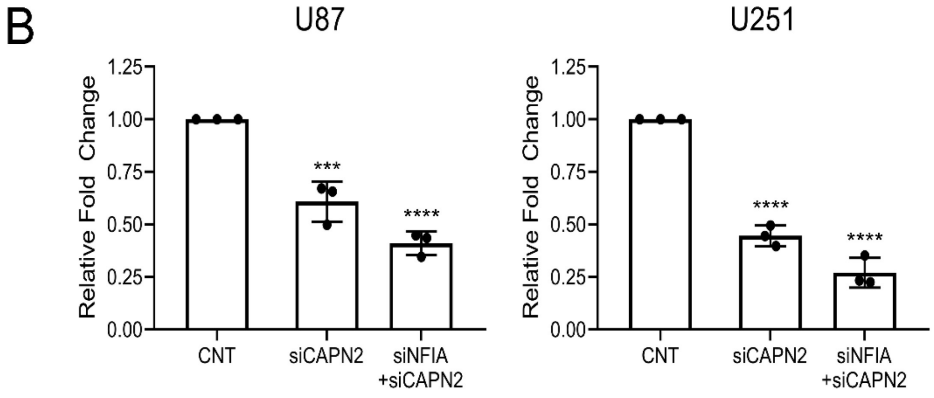
B
U87
U251
Relative Fold Change
1.25
1.00
0.75
0.50
0.25
0.00
***
****
****
CNT
siCAPN2
siNFIA
+siCAPN2
CNT
siCAPN2
siNFIA
+siCAPN2

Figure 4.6. Effects of calpain 2 depletion on GBM cell migration and viability

U251 (A) or U87 and U251 (B) cells were transfected with scrambled (CNT) siRNAs or siRNAs targeting either calpain 2 alone or both calpain 2 and NFIA. (A) Thirty thousand U251 cells in FBS-free DMEM were seeded in the top chambers of Falcon Cell Culture Inserts in a 24-well plate. Directional migration was induced by supplementing the medium in the bottom chamber with 10% FBS. After 20 h, cells were fixed with methanol and then stained with crystal violet. Migrated cells were imaged with a Zeiss Axioskop2 plus microscope. Quantitative data were obtained by counting the number of migrated cells using MetaMorph software. (B) Cell metabolism, a surrogate for cell viability, was measured using the MTS assay. Thirty-five hundred cells were seeded in 96-well plates. After 48 h, cells were incubated with the MTS reagent for 2 h. Fluorescence emission (495 nm) was measured using the FLUOstar Optima plate reader and then normalized to the scrambled siRNA control. (B only) Each experiment was repeated at least three times. (n.s. p-value>0.05, *p-value<0.05, **p-value<0.01, ***p-value<0.001 and ****p-value <0.0001).

CHAPTER 5: DISCUSSION

5.1 Discussion

5.1.1 Tumour infiltration: a major obstacle in curing GBM

Despite decades of intense research and clinical innovation, GBM remains a mostly incurable disease with short survival times and poor quality of life. Many aggravating factors, including inter- and intra-tumoural heterogeneity in addition to acquired drug resistance and therapy-induced adverse side effects, undermine the effectiveness of the aggressive therapeutic regimens used to treat GBM tumours. Amongst these, however, early tumour infiltration poses a virtually insurmountable barrier to a curative treatment for GBM.

Surgery is often the first stage in the treatment of GBM. It has been demonstrated that resection of at least 98% of the tumour volume is associated with increased survival in GBM patients (~13 months vs ~11.5 months) (420). However, the anatomical location of the tumour together with vital functions of the brain often limit the extent of tumour resection or, in some instances, preclude surgical intervention altogether. In addition, GBM cells have been found to extensively infiltrate the normal parenchyma both adjacent to and distal from the main tumour mass in early stages of the disease (356). Advances in surgical techniques, including fluorescence dye-assisted visualization of the tumour margins, have led to improvement in the gross tumour resection volume and thus clinical outcomes (421). Yet, real-time detection and tracking of infiltrating GBM cells at the microscopic level have yet to be realized. As a result, benefits of surgery are severely compromised in the case of GBM, reflected by the minimal increase in patient survival time.

Whether surgery is prescribed or not, GBM patients are treated with radiation therapy, which can increase survival time by ~2X (43). In a similar manner to surgical resection, early and distal tumour infiltration also undermines the efficacy of this local/regional therapy (359). Consequently, following radiation therapy, GBM patients are often prescribed chemotherapeutic drugs (usually TMZ) and, in some recurrent cases, the antiangiogenic agent bevacizumab (52). TMZ can induce cell death through DNA alkylation and sensitize tumour cells to radiation therapy (422). However, GBM cells can gain resistance to TMZ through a variety of mechanisms, including the expression of MGMT and disruption of genes involved in DNA mismatch repair (423-426). The exact contribution of infiltrative tumour cells to the resistance of GBM cells to TMZ is currently unknown. However, it has been proposed that by putting selective pressure on GBM cells, TMZ treatment enriches the stem-like population of tumour cells that can invade neighbouring tissue (427). With respect to bevacizumab, the efficacy and safety of this drug are controversial, with recent studies demonstrating that bevacizumab treatment may promote GBM cell infiltration while offering little to no improvement in patient prognosis (357,428,429).

The process of normal cell migration is complex and, understandably, influenced by a wide array of signaling pathways, some of which are yet to be identified. Similarly, in the context of GBM, myriads of molecular mechanisms contribute to the initiation, execution and termination of tumour cell migration/infiltration. Amongst these are classical pro-migration signaling pathways including the PI3K/Akt/mTOR and NF-κB (430). As the PI3K/Akt/mTOR

pathway is one of the most commonly altered signaling axis in GBM, a plethora of targeted therapies have been designed to target key proteins of this signaling cascade (81). Although clinical trials involving the first generation of PI3K inhibitors were halted due to their high toxicity and low selectivity, several second-generation pan-PI3K inhibitors, including BKM120 and PX-866, have been demonstrated to have anti-invasive properties in GBM animal models (431,432). Having passed phase I safety study, their efficacy is being tested in both *de novo* and recurrent GBM (81). However, recent phase II results indicate that while some anti-tumour activity is observed, the overall response rate is minimal for both agents, whether used as a monotherapy or in combination with bevacizumab (433,434). Perifosine, a promising Akt inhibitor under clinical investigation for recurrent GBM, only provided marginal improvement in patient outcomes due to its limited blood-brain-barrier penetration (81). Similarly, rapamycin, a well-known mTOR allosteric inhibitor, and their analogs, also failed to deliver promising phase II results (435). It is well recognized that aberrant NF-κB signaling is an important hallmark for tumourigenesis and progression (436). However, owing to its essential role in immunity amongst other cellular processes, no drugs specific to the NF-κB have been clinically approved in the last 30 years (437,438).

Although it appears that targeting infiltrating GBM cells may lead to therapeutic breakthrough, this avenue of research has unfortunately failed to yield any fruitful clinical result. However, these efforts were not in vain as they have shed light into the molecular mechanisms underlying GBM cell migration and thus fuel renewed hope for novel anti-infiltration therapies for this disease.

5.1.2 Novel pathways underlying infiltrative GBM cells: Nuclear Factor I

Previous findings highlight the difficulties in targeting traditional signaling pathways that govern GBM cell migration and thus new approaches and/or targets are required to control GBM infiltration. To this end, our group and others have demonstrated that expression of FABP7 correlates with increased GBM cell invasion and proliferation *in vitro* (361,372). During neurogenesis, FABP7 is expressed in radial glial cells, a population of neural stem cells that can give rise to neurons and glial cells including astrocytes and oligodendrocytes (439-442). In adult brain, FABP7 expression is detected in the subventricular zone, where neural stem cells reside (443). As a result, FAPB7 is considered to be a neural/progenitor cell marker and thus its expression is often associated with higher infiltration and poor prognosis in GBM patients (183,184).

We subsequently showed that *FABP7* expression is regulated by the NFI family of four transcription factors: NFIA, NFIB, NFIC and NFIX (362). In addition, NFI also regulates the expression of *GFAP*, a marker of astrocytes (362). During normal brain development, NFI regulates genes involved in the onset of gliogenesis (143,145). For example, NFIA has been shown to upregulate the expression of *GFAP* in neural progenitor cells (NPCs), presumably leading to the differentiation of these cells into the astrocytic lineage (142,145). Similar to FABP7, NFIA is preferentially detected in the subventricular zone (167). These findings suggest that NFIA may also be a marker of astrocytes that retain stem-like characteristics. This notion is supported by the observation that upon transduction of oncogenes, unlike *Nfia+/-* neural stem cells*, Nfia-/-* neural stem cells are unable

to form tumours in mouse model (168). Furthermore, NFIA has been shown to enhance GBM cell migration *in vitro* and in orthotopic models (169). NFIA is also important for GBM tumourigenesis as expression of NFIA in oligodendroglioma tumours leads to a phenotypic switch that resembles astrocytic gliomas (127). Together, these observations indicate a role for NFI, specifically NFIA, in regulating stem-like properties that may be essential for GBM oncogenesis and infiltration. Our data provide empirical evidence confirming the tumour promoting role of NFIA in GBM, with loss of NFIA resulting in decreased GBM cell survival and migration (Chapter 4).

Compared to the well-defined oncogenic properties of NFIA, the exact role of NFIB in GBM is still under debate. *NFIB* haploinsufficiency, caused by the loss of one *NFIB* allele on chromosome 9p, is detected in 39% of GBM patients (444,445). *Nfib*-directed mutagenesis also increased the probability of GBM tumour formation relative to other CNS tumours (446-449). In addition, ectopic expression of NFIB represses the oncogenic transformation of chicken embryonic fibroblasts induced by *Myc* and *Jun* nuclear oncogenes (450). In GBM, *NFIB* expression is inversely associated with astrocytic tumour grade and positively correlated with patient survival (171). However, the tumour suppressing properties of NFIB only extend to certain subtypes of GBM including mesenchymal and classical tumours (171). Furthermore, *Nfib*-/- mice show increased numbers of NPCs and delayed differentiation of astrocytes (134,137,451). Mechanistically, NFIB represses the expression of histone methyltransferase *Ezh2*, a component of the polycomb repressive complex 2 (135). This complex is expressed by NPCs

and is gradually downregulated as NPCs differentiate (452,453). These findings suggest that NFIB promotes differentiation of NPCs during embryogenesis and thus may have a tumour suppressing role in the context of GBM. Our data support this conclusion, with loss of NFIB resulting in increased GBM migration/invasion (Chapter 3).

However, NFIB has also been shown to act as an oncogene in a wide range of malignancies including melanoma, small cell lung cancer and breast cancer (172-175,399). In gastric cancer, NFIB appears to promote malignant phenotypes through the activation of the Akt/STAT3 signaling pathway, resulting in increased levels of phospho-STAT3 (454). STAT3 signaling is a well-known tumour promoting pathway which, upon activation, can promote cell proliferation, invasion, survival and immunosuppression (455). Yet, recent studies have indicated that STAT3, in addition to its oncogenic role, can also function as a tumour suppressor (456). Although the mechanisms underlying this dual function of STAT3 are the subject of ongoing investigations, two different isoforms of STAT3 have been proposed to be responsible for the dichotomic roles of STAT3 in esophageal squamous cell carcinoma (ESCC) (457). Whereas STAT3α promotes tumourigenesis of ESCC, STAT3β (a truncated form of STAT3) inhibits the oncogenic properties of the other isoform (457). Interestingly, the tumour suppressing properties of NFIB in certain GBM subtypes are also associated with increased levels of phospho-STAT3 and thus activation of STAT3 signaling (171). It is possible that NFIB upregulates the levels of STAT3β in these GBM cells,

resulting in the repression of tumour migration (Chapter 2) concomitant with the induction of tumour cell differentiation (171).

The NFI family has also been shown to be involved in the cross-signaling of all three core pathways underlying GBM tumourigenesis and progression: p53 (458), pRB (459) and RTK\PI3K (460). As a result, it appears that NFI, mirroring its role as a regulator of neurogenesis, is positioned at a relatively high level in the signaling cascades that may drive/sustain or inhibit/attenuate malignancy in GBM cells. Thus, treating all four NFIs as a homogenous family of transcription factors may result in the omission of member-specific functions and egregious interpretation of the role of NFIs in the context of cancer. For this reason, we tried to incorporate all four members of the NFI family in our studies whenever possible, with particular attention paid to downstream regulatory networks.

5.1.3 NFI-mediated regulation of *CAST* variants and calpastatin isoforms

Our efforts in identifying putative NFI target genes in GBM cells led us to a fascinating but largely uncharted research area: calpastatin and its encoding genes, *CAST* (Chapter 2). At the time that this thesis was written, there were fewer than 10 peer-reviewed articles describing the usage of alternative *CAST* promoters, with a similar number of papers connecting the expression of *CAST* variants to that of calpastatin isoforms, and an even fewer number of papers investigating the physiological functions of different forms of calpastatin. Although a detailed description of calpastatin was provided in Section 1.4.1, it is important to reiterate a couple of facts about this complex protein family, with ≥44 *CAST*

transcript variants (Ensembl database, gene ID: ENSG00000153113) and ≥21 calpastatin isoforms (NCBI database, gene ID: 831) identified in humans so far, with the significance of most of these variants and isoforms being unknown. One would posit that there are few publications in this field not because calpastatin is biologically inconsequential, but because investigative efforts are often deterred by the complex expression profile of *CAST* and calpastatin, manifested as confusing or inexplicable results.

A major drawback to the calpastatin field is that investigators often treat all calpastatin isoforms as a single protein in order to extract some conclusions from their studies (461-464). However, alternative splicing of *CAST* is clearly important, with most alternative splicing events involving domain L of calpastatin (322,324,350). For example, exclusion of the amino acid sequence of calpastatin domain L encoded by exon 6 of *CAST* leads to the loss of several phosphorylation sites (350). Reversible phosphorylation of calpastatin at exon 6-encoded amino acid sequence can change its cytoplasmic distribution from soluble to aggregated, and vice versa (350). Although additional domain L functions in an intact calpastatin molecule remain to be identified, the domain L polypeptide by itself has been shown to have some independent functions, most of which are related to the priming of Ca^{2+}- channels (352,353).

Compared to domain L, the functions of domain XL remain a complete mystery. Besides being phosphorylated by PKA/C, nothing else is known about this domain except for its nucleotide and amino acid sequences (325). In fact, domain XL has not been directly shown to be expressed by human calpastatin.

Our study is amongst a few to provide indirect evidence for the existence of domain XL in human calpastatin and to implicate the putative role of this domain in the regulation of calpastatin subcellular distribution (Chapter 2). Even then, we could not provide a direct causal link between the inclusion of domain XL and calpastatin localization as a plethora of other factors can influence the latter, including but not limited to calcium concentration, phosphorylation, binding to its targets, and alternative splicing downstream of domain XL (196).

The most significant finding of Chapter 2 is the transcriptional regulation of *CAST* by differentially phosphorylated NFI through a novel alternative promoter located in *CAST* intron 3. We were able to directly link the expression of two types of *CAST* transcript variants to their corresponding types of calpastatin isoform. Although this may seem to be a small discovery, it provides the first mechanistic insight into the regulation of different *CAST* promoters at the transcriptional level. In addition, our data confirmed that the subcellular distribution of calpastatin is important for its functions (326,350,351) and demonstrated that transcription factors, including NFI (Chapter 2) and cMyc (221), may alter calpastatin activity through transcription-mediated isoform switching. However, it is safe to say that Chapter 2 raised more questions than it answered. For example, are other alternative promoters of *CAST* active in GBM cells? If yes, how might NFIs be involved in their regulation? Does domain XL indeed play a key role in regulating calpastatin subcellular localization? If so, is it mediated by phosphorylation or through other post-translation modifications? What is the significance of domain L in the regulation of calpastatin in GBM cells?

Irrespective of remaining unanswered questions, Chapter 2, together with previous findings (164,282,365), provided us with an invaluable piece of information: NFI cross-signaling with the calpain pathway. This finding alone shifts the course of this project from basic science to translational research as NFI, like other transcription factors, remains undruggable whereas calpain proteolytic activity can be inhibited by a wide range of synthetic compounds (393,465). Furthermore, while NFI is located far upstream of any signaling cascades that may regulate GBM cell migration/infiltration, calpain is the integrative hub to which virtually all pro- and anti-migration signals converge (201) and thus may serve as a potential target for a novel therapeutic approach to GBM management.

5.1.4 Regulation and function of calpain in GBM

To target the calpain pathway in GBM, one must first understand its physiological significance and regulation in tumour cells. The important roles of the calpain pathway in both normal and diseased states have long been appreciated as calpain-mediated proteolysis of its downstream effectors can be observed in many ordinary and pathological cellular processes (196,218). Despite intense research efforts, however, two perplexing issues remain largely unaddressed in virtually all investigations of calpain activity: (i) how calpain proteolytic activity is controlled by the cell and (ii) whether any specific effect under observation is mediated by one or multiple calpain members.

To date, the mechanisms underlying calpain activation during the normal operation of the cell remain unclear. However, the following facts are known: (i)

the amount of Ca^{2+} required for calpain to reach half-maximal activity lie far above physiological Ca^{2+} concentrations (299), (ii) calpastatin and calpain are co-expressed in virtually all cell types (366), and (iii) calpastatin can bind calpain at lower Ca^{2+} concentration than what is needed for calpain activation (197). Together, these findings suggest that calpain activity is tightly controlled to the point that activation seems rather impossible. Yet, calpain-mediated proteolysis occurs on a regular basis inside any given cell. Clearly, the cell must have mechanisms to transiently induce calpain activity.

It has been proposed that autolysis, which lowers Ca^{2+} concentration required for half-maximal activity of calpain, may be the main method through which calpain can achieve activation (286). In the 1980s and 1990s, calpain was believed to be synthesized as a proenzyme, like many other cysteine proteases, and subsequently activated by autolysis (466-468). However, this notion was quickly proven to be inaccurate as full-length calpain also habours proteolytic activity, albeit at lower levels compared to autolyzed calpain (469). Since autolysis always occurs in parallel with calpain activation, autolysis has been commonly used as a marker of calpain activation (285,286,469). Our data support this view as the loss of calpain 1 activity was observed in concurrence with the accumulation of full-length calpain 1 in the cytoplasm of GBM cells (Chapter 3). Furthermore, we noticed that only the autolyzed forms of calpains 1 and 2 were found in the nucleus of GBM cells, suggesting that autolysis of calpain may have functions other than simply acting as a rheostat for Ca^{2+} concentration.

Another well-known way for the cell to regulate calpain activity is to alter levels and subcellular localization of calpastatin. As calpastatin requires direct interaction to inhibit calpain and, in turn, calpain needs to physically bind its substrates to carry out proteolysis, the compartmentalization of calpastatin and calpain is vital to their functions (345,366). Our results indicate that NFI, specifically NFIA and NFIB, can increase calpain activity by: (i) downregulating the global expression of calpastatin and (ii) inducing changes in calpastatin subcellular distribution that may limit its availability for binding and inhibiting calpain (Chapters 2-4). In addition, we also showed that the cell can control calpain activity by modulating levels of autolyzed calpain in the nucleus of GBM cells although we could not identify the exact mechanism underlying this observation (Chapters 3 and 4). Neither calpain 1 nor calpain 2 has been reported to carry a nuclear localization signal (NLS). However, calpain 5 – a non-conventional calpain – has two NLSs: one is found near the N-terminus and the other near the C-terminus (470). Given that both calpains 1 and 2 can localize to the nucleus (Chapters 3 and 4) (471,472), it is reasonable to speculate that they may harbour at least one, potentially concealed, NLS. Thus, autolysis of these ubiquitous calpains may expose a hidden NLS and enhance their nuclear translocation. Notwithstanding the molecular mechanism, we demonstrated that NFI, through the regulation of *CAST* variants and calpastatin isoforms, can increase calpain activity.

Various *in silico* and *in vitro* analyses have been performed to elucidate the consensus amino acid sequence for calpain-mediated proteolysis (473-476). Although such efforts have led to the synthesis of peptides that are faithfully

recognized and cleaved by calpain (476), they did not shed much light on the specificity of endogenous calpain substrates. Indeed, most studies suggest that the primary amino acid sequence of a polypeptide is of little significance for calpain-mediated cleavage, with calpain recognition largely depending on the target's higher structural order (473,474). Furthermore, little is known about the substrate specificity of each calpain member. As a result, knowledge about calpain activity is largely derived from gain- or loss-of-function studies and their accompanied physiological effects. Three possible scenarios can occur in regard to calpains 1 and 2 biological activity, ranging from the most to the least frequently encountered in the literature. First, calpains 1 and 2 can cleave the same target, effectively compensating for one another if the activity of one is disrupted or lost. For example, both calpains 1 and 2 have been shown to cleave focal adhesion kinase (FAK) protein (376,477), amongst other shared substrates. Second, calpains 1 and 2 have specific functions such that the loss of one activity cannot be rescued by the other. Studies with calpain-specific siRNAs demonstrate that loss of calpain 2, but not calpain 1, results in limited membrane protrusions and lamellipodial dynamics (194). Vice versa, the spreading of bovine aortic endothelial cells is dependent on calpain 1, but not calpain 2 (478). Third, in a few biological systems, calpains 1 and 2 can counteract the effect of one another. An illustration of this has been reported in the context of synaptic plasticity and neurodegeneration, with calpain 1 promoting long-term potentiation (LTP) and neuronal cell survival, whereas calpain 2 inhibits LTP and induces neurodegeneration (214). Adding to the small body of literature supporting the third

scenario, the most significant finding of this project demonstrates that calpain 1 and calpain 2, in crosstalk with NFIB and NFIA, respectively, appear to have opposing roles in regulating the malignant phenotypes of GBM cells. Thus, calpain 1 inhibits tumour cell migration whereas calpain 2 promotes both GBM cell migration and survival (Chapters 3 and 4). Our findings suggest that while calpain is an attractive target for GBM treatment, concurrent inhibition of both calpains 1 and 2 may not be an appropriate approach for GBM as it may create a futile cycle at best, or undesired effects, including increased GBM infiltration, at worst.

5.1.5 Targeting the NFI-calpain crosstalk with calpain inhibitors in GBM: potential benefits and challenges

The idea of targeting calpain for therapeutic benefits is not new. Pre-clinical investigations with calpain inhibitors have been explored for multiple pathological conditions, including cancer (218,393). *In vitro* disruption of calpain activity, whether by siRNA-mediated depletion, or chemical-induced inhibition or overexpression of calpastatin, has been shown to repress tumour cell viability (419,479), migration/invasion (226,235) and therapeutic resistance (480,481). Our Chapter 4 data echo these observations as depletion of calpain 2 resulted in decreased GBM cell migration and viability. At the molecular level, calpain 2 has been shown to be a mediator and regulator of the RTK/Akt/PI3K/mTOR signaling pathway (482-485). In addition, calpain 2 can cleave and induce p53 instability (486). pRB, another key protein underlying GBM oncogenesis and progression, is also cleaved and degraded by calpain 2. Our own results suggest that calpain 2

may increase the transcriptional activity of NFI, most likely NFIA, which in turn forms a feedforward loop with NF-κB (170). As mentioned earlier, NFI can also cross signal with p53, pRB and PI3K, the three core signaling pathways in GBM. Consequently, targeting calpain, specifically calpain 2, may inhibit oncogenic signaling far beyond the boundaries of the NFI-calpain crosstalk.

Despite the proven and potential benefits of calpain inhibition, none of the available calpain antagonists have advanced to clinical trials for cancer. However, dosing and tolerability of calpain inhibitors have or are currently being evaluated in a few phase I trials for other diseases. In 2016, patients with Alzheimer's disease were recruited for a phase 1 clinical trial with the calpain inhibitor ABT-957 (NCT02220738). Unfortunately, this study had to be cancelled due to slow patient enrollment. There is currently an ongoing phase 1 clinical trial to test the safety and toxicity of the calpain inhibitor BLD-2660 in patients with lung or liver fibrosis (NCT03559166). While these phase I studies advocate the possibility of using calpain inhibitors as therapeutic agents, the lack of phase II/III trials, together with the absence of clinically approved calpain inhibitors, demonstrate the profound difficulties in moving the first generation of calpain antagonists into the clinical settings.

Nearly all calpain inhibitors are of peptidyl nature and all share an important feature in that they can inhibit both calpains 1 and 2 (393). These inhibitors are often regarded as 'pan-specific' although their effects on other members of the calpain family have not been evaluated. Since calpains 1 and 2 dominate the field of calpain research and are the focus of this project, we will use the term 'pan-

specific' to describe the dual specificity of these agents towards calpains 1 and 2. As previously discussed, calpains 1 and 2 can compensate for the loss of one another in multiple biological contexts. Therefore, pan-specific calpain inhibitors are beneficial when concurrent inhibition of both calpains is desired: e.g., to prevent the cleavage and activation of calcineurin (282,365,375). These inhibitors may also be useful in any pathological condition that is caused by hyperactivation of either calpain 1 or calpain 2, but not both (235,487). However, in situations where both calpains are present and perform opposing roles, as demonstrated by our data (Chapters 3 and 4), pan-specific calpain inhibitors may not deliver the expected therapeutic effects. This issue is well-recognized in contemporary calpain research, and it is clear that more attention needs to be placed on the development of member-specific calpain inhibitors. Another issue of targeting calpain is potential cytotoxic side effects as calpain is central to a wide array of signaling pathways and cellular processes. Surprisingly, calpain inhibitors have been shown to have excellent safety profiles in mouse models of neurodegeneration or brain ischemic injuries (488-491). Whether humans have similar tolerance toward these calpain inhibitors is a subject for future investigation.

As suggested by our calpain 1 data, inhibition of calpain activity is not always beneficial to a specific pathological condition. Sometimes, activation of calpain is desired; e.g., to promote tumour cell death by apoptosis (492-494). Synthetic calpain activators, including dibucaine, have been generated (495-497). However, similar to calpain inhibitors, no current synthetic calpain activators can differentiate between calpains 1 and 2. Unfortunately, these agents failed to

capture research interest, reflected by the limited number of synthetic calpain activators. As a result, little is known about their efficacy and safety in disease models although calpain activators may also have therapeutic benefits.

5.2 Future Directions

5.2.1 Establish NFIA-calpain 2 as a positive feedback loop

Although our data strongly point to the existence of a positive feedback loop between NFIA and calpain 2, the effects of calpain 2 on NFIA have not yet been established due to the lack of a working anti-NFIA antibody. We are in the process of obtaining other antibodies to NFIA to examine whether NFIA is indeed not dephosphorylated upon the loss of calpain 2. Based on our previous findings of hypophosphorylated NFI being able to induce the transcription of *FABP7* (163,362), we concluded that reduced FABP7 levels upon calpain 2 depletion is mediated by the phosphorylation of NFI. Even though no link between calpain 2 and FABP7 has been reported in the literature, the former is involved in multiple signaling pathways and thus its downstream effectors could have influenced the expression of FABP7 at the protein level. Therefore, we will design a luciferase reporter construct with a promoter harbouring an NFI binding consensus to provide a more direct readout for changes in NFI transcriptional activity upon calpain 2 knockdown.

For both Chapters 3 and 4, we used the MTS assay to examine GBM cell viability. Although this assay is commonly used as a surrogate for cell viability, some concerns have been raised about the universal equivalence of these two

physiological states (400). More importantly, calpain has been linked to the metabolism of endogenous NADPH, which is an essential reagent for the MTS assay (498,499). As a result, we will use more stringent techniques to assess GBM cell survival, including colony formation and cell count assays. We also used the Transwell assay to examine the migration of GBM cells through a synthetic membrane in response to a chemoattractant. However, GBM cells have been shown to use preexisting blood vessels or white matter tracts to infiltrate normal brain parenchyma (430,500). The Transwell assay does not recapitulate these complex processes. To address this issue, we will visualize and quantify GBM cell migration along blood vessels using the chick embryo chorioallantoic membrane model, which is routinely used to study metastatic potential of cells from solid tumours (501).

5.2.2 Explore potential crosstalk between NIFC (or NFIX) and calpain

In Chapter 2, our EMSA results suggested that NFIC and NFIX have stronger *in vitro* binding affinity for the NFI-responsive elements located in *CAST* intron 3. Surprisingly, the loss of NFIC and NFIX did not lead to meaningful changes in the expression of *CAST* variants as determined by RT-qPCR (Chapter 2). It is possible that NFIC and NFIX may not be involved in the regulation of *CAST* in intact GBM cells and that the binding of these two NFIs to *CAST* intron 3 is an *in vitro* artifact. However, given that loss of NFIC and NFIX led to increased calpastatin levels and changes in its subcellular distribution (Chapter 3), it is more likely that our primers, which were designed to examine alternative promoters but

not alternative splicing, did not fully capture the complex mRNA profile of *CAST* transcript variants, resulting in limited detection sensitivity for effects induced by NFIC and NFIX knockdowns. Consequently, we will design additional sets of primers that can differentiate between different *CAST* variants generated by selected alternative splicing events, including exons 3, 5 and 6, and repeat RT-qPCR experiments to examine whether NFIC and NFIX have any regulatory effects on specific transcript variants of *CAST*. In parallel, we will also investigate whether depletion of NFIC or NFIX, similar to knocking down NFIA and NFIB, can lead to changes in cytoplasmic or nuclear levels of calpain 1 or calpain 2 as well as their subcellular localization and proteolytic activity.

Previous data obtained with a pan-specific NFI antibody indicate that calcineurin-mediated dephosphorylation likely affects all NFI family members (164). We are therefore interested in whether calpain 1 or 2 also forms a positive feedback loop or crosstalk with NFIC and NFIX via calcineurin. If such crosstalk indeed exists, we will examine its effects on GBM cell migration and survival using previously described methodologies. We and others have demonstrated that, depending on tissue context, both compensatory and antagonistic pathways exist for the four NFIs (133,137,362). In addition, since NFIs bind DNA as either homodimers or heterodimers, concurrent depletion of different NFIs may magnify the effects observed by single NFI knockdowns and, in some instances, result in novel regulatory effects on NFI target genes (362). To address the latter, we will expand our knockdown study to include a range of NFI combinations and examine how NFI-mediated regulation of *CAST* variants is affected compared to single NFI

depletion. Importantly, we will investigate whether compensatory or antagonistic effects observed for different NFIs extends to their ability to crosstalk with the calpain/calpastatin pathway.

5.2.3 Calpastatin isoform expression and subcellular localization

Despite decades of research, little is known about the physiological significance of calpastatin isoforms or how their expression is regulated by the cell. Our results suggest that different isoforms of calpastatin have different patterns of subcellular distribution and thus varied ability to interact with calpain. For example, the full-length calpastatin may assume a more diffuse cytoplasmic distribution, whereas the XL-less isoform appears to localize predominantly to regions surrounding the nucleus (Chapter 2). Knockdown of NFI results in changes in subcellular localization of calpastatin, presumably caused by transcription-mediated isoform switching. The latter statement requires verification and elucidation. To do so, we will generate constructs expressing either full-length (XL-containing) or XL-less calpastatin and transfect them into GBM cells and investigate whether altered ratios of these two forms of calpastatin does indeed lead to changes in calpastatin subcellular distribution. If yes, we will also examine the changes in localization and proteolytic activity of calpain in response to ectopic expression of these calpastatin isoforms to further understand their physiological significance.

To date, the functions of domain XL of calpastatin still remain a conundrum. Data obtained from our experiments suggest that this domain may play a role in

calpastatin subcellular localization. This notion is supported by prior findings showing that domain XL is phosphorylated by PKA, resulting in increased association between calpastatin and biological membranes (196). The putative phosphorylation sites of domain XL have previously been described (325). We will carry out site-directed mutagenesis at these sites to generate single, double or triple phospho-mutants of full-length calpastatin. We will also knockout full-length calpastatin in GBM cells using the CRISPR-Cas9 system. Next, we will transfect calpastatin-negative cells with constructs expressing either the wildtype full-length calpastatin or one of the phospho-mutant derivatives and examine their subcellular distribution and ability to inhibit calpain.

5.2.4 Testing synthetic and clinically available calpain modulators

Our group and others have provided evidence suggesting independent roles for NFI (163,164,362) and the calpain/calpastatin pathway (218,492,502,503) in promoting GBM cell migration and survival. In this thesis, we show that crosstalk between NFI and calpain can result in either the promotion or inhibition of GBM malignant properties. Since no targeted therapy is available for NFI, calpain inhibitors and activators (collectively referred to as calpain modulators) may have an exclusive advantage in that they can directly modulate calpain signaling and indirectly affect NFI transcriptional activity. With the synthetic calpain inhibitor I (ALLN), we demonstrated the feasibility of using calpain modulators to control GBM clonogenic cell survival (Chapter 3). We also investigated the efficacy of a clinically active calpain inhibitor: ACM (Chapter 3)

(504). Although ACM has other mechanisms of action besides calpain inhibition (505-507), its pharmacokinetic, pharmacodynamic, and toxicological profiles have previously been established (396) and thus could be fast-tracked through animal and human trials. However, due to their size and chemical nature, ALLN and ACM are unlikely to cross the blood-brain-barrier, severely limiting their efficacy if administered systemically. However, it is feasible to bypass the blood-brain-barrier and deliver ACM directly to GBM tumours by means of liposomal encapsulation, which has been successfully achieved for doxorubicin (508), another member of the anthracycline antibiotic to which ACM belongs. We are therefore interested in pursuing this line of investigation with experts in chemotherapeutic liposomes. We will also obtain blood-brain-barrier-permeable calpain inhibitors, such as MDL-28170 (509-512), and examine their safety and efficacy in GBM orthotopic mouse model.

Our Chapter 3 results strongly suggest that calpain activators may have similar therapeutic potentials to that of calpain inhibitors. In keeping with this suggestion, activation of calpain, induced by chemotherapeutic agents, has been linked to increased tumour cell death by apoptosis or apoptosis-like processes (513,514). However, there have been no studies examining the effects of calpain activators on GBM malignant properties including cell migration/infiltration, survival, death and chemoresistance. As a result, we plan to perform extensive pre-clinical investigations to address these questions. Another major finding of this project is that pan-specific calpain modulators may have unintended effects given that calpains 1 and 2 appear to perform opposite roles in GBM cells. It would be

important then to identify/develop member-specific calpain modulators and test their efficacy against GBM cells. We are planning to team up with Drs. Jack Tuszynski (*in silico* drug screening, University of Alberta) and Dennis Hall (drug synthesis, University of Alberta) to pursue this line of investigation.

5.3 Significance

Both calpain and NFI are independent regulators of GBM cell migration and survival. Here, we identify and confirm that *CAST*, encoding calpastatin, the endogenous inhibitor of calpain, is a target of NFI. Using a novel alternative promoter located in *CAST* intron 3, NFI, depending on its phosphorylation state, differentially regulates *CAST* transcript variants encoding calpastatin isoforms that either contain or don't contain the XL domain, leading to changes in calpastatin subcellular distribution. Our findings are amongst a few demonstrating the physiological significance of the transcriptional regulation of different *CAST* transcript variants. Building upon previous findings, we demonstrate crosstalk between NFI and calpain in GBM cells. Through the regulation of *CAST* variants and calpastatin isoforms, NFIB forms a positive feedback loop with calpain 1. Our results provide molecular mechanisms underlying both the forward and backward signaling branches of the NFIB-calpain 1 crosstalk. This positive feedback loop appears to act in concert to dampen GBM cell migration. Furthermore, we provide evidence for crosstalk between NFIA and calpain 2 in GBM cells. Unlike the NFIB-calpain 1 positive feedback loop, the NFIA-calpain 2 crosstalk promotes both GBM cell migration and survival. Thus, this thesis presents the first and only empirical

evidence to date for opposing functions of calpains 1 and 2 in regulating the malignant properties of GBM cells. Our data underscore the clinical potential of calpain inhibitors in controlling GBM cell survival and advocate for the development of member-specific calpain inhibitors, and potentially activators, as a novel class of therapeutic agents for the treatment of GBM.

REFERENCE

1. Kandel, E. R. (2013) *Principles of neural science*,
2. Louis, D. N., and International Agency for Research on Cancer. (2007) *WHO classification of tumours of the central nervous system*, 4th ed., International Agency for Research on Cancer, Lyon
3. Ostrom, Q. T., Bauchet, L., Davis, F. G., Deltour, I., Fisher, J. L., Langer, C. E., Pekmezci, M., Schwartzbaum, J. A., Turner, M. C., Walsh, K. M., Wrensch, M. R., and Barnholtz-Sloan, J. S. (2014) The epidemiology of glioma in adults: a "state of the science" review. *Neuro Oncol* **16**, 896-913
4. Ahmed, R., Oborski, M. J., Hwang, M., Lieberman, F. S., and Mountz, J. M. (2014) Malignant gliomas: current perspectives in diagnosis, treatment, and early response assessment using advanced quantitative imaging methods. *Cancer Manag Res* **6**, 149-170
5. Forst, D. A., Nahed, B. V., Loeffler, J. S., and Batchelor, T. T. (2014) Low-grade gliomas. *Oncologist* **19**, 403-413
6. Ohgaki, H., and Kleihues, P. (2005) Epidemiology and etiology of gliomas. *Acta neuropathologica* **109**, 93-108
7. Cancer Genome Atlas Research, N., Brat, D. J., Verhaak, R. G., Aldape, K. D., Yung, W. K., Salama, S. R., Cooper, L. A., Rheinbay, E., Miller, C. R., Vitucci, M., Morozova, O., Robertson, A. G., Noushmehr, H., Laird, P. W., Cherniack, A. D., Akbani, R., Huse, J. T., Ciriello, G., Poisson, L. M., Barnholtz-Sloan, J. S., Berger, M. S., Brennan, C., Colen, R. R., Colman, H., Flanders, A. E., Giannini, C., Grifford, M., Iavarone, A., Jain, R., Joseph, I., Kim, J., Kasaian, K., Mikkelsen, T., Murray, B. A., O'Neill, B. P., Pachter, L., Parsons, D. W., Sougnez, C., Sulman, E. P., Vandenberg, S. R., Van Meir, E. G., von Deimling, A., Zhang, H., Crain, D., Lau, K., Mallery, D., Morris, S., Paulauskis, J., Penny, R., Shelton, T., Sherman, M., Yena, P., Black, A., Bowen, J., Dicostanzo, K., Gastier-Foster, J., Leraas, K. M., Lichtenberg, T. M., Pierson, C. R., Ramirez, N. C., Taylor, C., Weaver, S., Wise, L., Zmuda, E., Davidsen, T., Demchok, J. A., Eley, G., Ferguson, M. L., Hutter, C. M., Mills Shaw, K. R., Ozenberger, B. A., Sheth, M., Sofia, H. J., Tarnuzzer, R., Wang, Z., Yang, L., Zenklusen, J. C., Ayala, B., Baboud, J., Chudamani, S., Jensen, M. A., Liu, J., Pihl, T., Raman, R., Wan, Y., Wu, Y., Ally, A., Auman, J. T., Balasundaram, M., Balu, S., Baylin, S. B., Beroukhim, R., Bootwalla, M. S., Bowlby, R., Bristow, C. A., Brooks, D., Butterfield, Y., Carlsen, R., Carter, S., Chin, L., Chu, A., Chuah, E., Cibulskis, K., Clarke, A., Coetzee, S. G., Dhalla, N., Fennell, T., Fisher, S., Gabriel, S., Getz, G., Gibbs, R., Guin, R., Hadjipanayis, A., Hayes, D. N., Hinoue, T., Hoadley, K., Holt, R. A., Hoyle, A. P., Jefferys, S. R., Jones, S., Jones, C. D., Kucherlapati, R., Lai, P. H., Lander, E., Lee, S., Lichtenstein, L., Ma, Y., Maglinte, D. T., Mahadeshwar, H. S., Marra, M. A., Mayo, M., Meng, S., Meyerson, M. L., Mieczkowski, P. A., Moore, R. A., Mose, L. E., Mungall, A. J., Pantazi, A., Parfenov, M., Park, P. J., Parker, J. S., Perou, C. M., Protopopov, A., Ren,

X., Roach, J., Sabedot, T. S., Schein, J., Schumacher, S. E., Seidman, J. G., Seth, S., Shen, H., Simons, J. V., Sipahimalani, P., Soloway, M. G., Song, X., Sun, H., Tabak, B., Tam, A., Tan, D., Tang, J., Thiessen, N., Triche, T., Jr., Van Den Berg, D. J., Veluvolu, U., Waring, S., Weisenberger, D. J., Wilkerson, M. D., Wong, T., Wu, J., Xi, L., Xu, A. W., Yang, L., Zack, T. I., Zhang, J., Aksoy, B. A., Arachchi, H., Benz, C., Bernard, B., Carlin, D., Cho, J., DiCara, D., Frazer, S., Fuller, G. N., Gao, J., Gehlenborg, N., Haussler, D., Heiman, D. I., Iype, L., Jacobsen, A., Ju, Z., Katzman, S., Kim, H., Knijnenburg, T., Kreisberg, R. B., Lawrence, M. S., Lee, W., Leinonen, K., Lin, P., Ling, S., Liu, W., Liu, Y., Liu, Y., Lu, Y., Mills, G., Ng, S., Noble, M. S., Paull, E., Rao, A., Reynolds, S., Saksena, G., Sanborn, Z., Sander, C., Schultz, N., Senbabaoglu, Y., Shen, R., Shmulevich, I., Sinha, R., Stuart, J., Sumer, S. O., Sun, Y., Tasman, N., Taylor, B. S., Voet, D., Weinhold, N., Weinstein, J. N., Yang, D., Yoshihara, K., Zheng, S., Zhang, W., Zou, L., Abel, T., Sadeghi, S., Cohen, M. L., Eschbacher, J., Hattab, E. M., Raghunathan, A., Schniederjan, M. J., Aziz, D., Barnett, G., Barrett, W., Bigner, D. D., Boice, L., Brewer, C., Calatozzolo, C., Campos, B., Carlotti, C. G., Jr., Chan, T. A., Cuppini, L., Curley, E., Cuzzubbo, S., Devine, K., DiMeco, F., Duell, R., Elder, J. B., Fehrenbach, A., Finocchiaro, G., Friedman, W., Fulop, J., Gardner, J., Hermes, B., Herold-Mende, C., Jungk, C., Kendler, A., Lehman, N. L., Lipp, E., Liu, O., Mandt, R., McGraw, M., McLendon, R., McPherson, C., Neder, L., Nguyen, P., Noss, A., Nunziata, R., Ostrom, Q. T., Palmer, C., Perin, A., Pollo, B., Potapov, A., Potapova, O., Rathmell, W. K., Rotin, D., Scarpace, L., Schilero, C., Senecal, K., Shimmel, K., Shurkhay, V., Sifri, S., Singh, R., Sloan, A. E., Smolenski, K., Staugaitis, S. M., Steele, R., Thorne, L., Tirapelli, D. P., Unterberg, A., Vallurupalli, M., Wang, Y., Warnick, R., Williams, F., Wolinsky, Y., Bell, S., Rosenberg, M., Stewart, C., Huang, F., Grimsby, J. L., Radenbaugh, A. J., and Zhang, J. (2015) Comprehensive, Integrative Genomic Analysis of Diffuse Lower-Grade Gliomas. *The New England journal of medicine* **372**, 2481-2498

8. Louis, D. N., Perry, A., Reifenberger, G., von Deimling, A., Figarella-Branger, D., Cavenee, W. K., Ohgaki, H., Wiestler, O. D., Kleihues, P., and Ellison, D. W. (2016) The 2016 World Health Organization Classification of Tumors of the Central Nervous System: a summary. *Acta neuropathologica* **131**, 803-820
9. Yan, H., Parsons, D. W., Jin, G., McLendon, R., Rasheed, B. A., Yuan, W., Kos, I., Batinic-Haberle, I., Jones, S., Riggins, G. J., Friedman, H., Friedman, A., Reardon, D., Herndon, J., Kinzler, K. W., Velculescu, V. E., Vogelstein, B., and Bigner, D. D. (2009) IDH1 and IDH2 mutations in gliomas. *The New England journal of medicine* **360**, 765-773
10. Louis, D. N. (1994) The p53 gene and protein in human brain tumors. *J Neuropathol Exp Neurol* **53**, 11-21
11. Cairncross, G., and Jenkins, R. (2008) Gliomas with 1p/19q codeletion: a.k.a. oligodendroglioma. *Cancer J* **14**, 352-357

12. Zhu, H., Acquaviva, J., Ramachandran, P., Boskovitz, A., Woolfenden, S., Pfannl, R., Bronson, R. T., Chen, J. W., Weissleder, R., Housman, D. E., and Charest, A. (2009) Oncogenic EGFR signaling cooperates with loss of tumor suppressor gene functions in gliomagenesis. *Proc Natl Acad Sci U S A* **106**, 2712-2716
13. Ohgaki, H. (2009) Epidemiology of brain tumors. *Methods Mol Biol* **472**, 323-342
14. Neglia, J. P., Meadows, A. T., Robison, L. L., Kim, T. H., Newton, W. A., Ruymann, F. B., Sather, H. N., and Hammond, G. D. (1991) Second neoplasms after acute lymphoblastic leukemia in childhood. *The New England journal of medicine* **325**, 1330-1336
15. Deltour, I., Auvinen, A., Feychting, M., Johansen, C., Klaeboe, L., Sankila, R., and Schuz, J. (2012) Mobile phone use and incidence of glioma in the Nordic countries 1979-2008: consistency check. *Epidemiology* **23**, 301-307
16. Rice, T., Lachance, D. H., Molinaro, A. M., Eckel-Passow, J. E., Walsh, K. M., Barnholtz-Sloan, J., Ostrom, Q. T., Francis, S. S., Wiemels, J., Jenkins, R. B., Wiencke, J. K., and Wrensch, M. R. (2016) Understanding inherited genetic risk of adult glioma - a review. *Neurooncol Pract* **3**, 10-16
17. Hottinger, A. F., and Khakoo, Y. (2009) Neurooncology of familial cancer syndromes. *Journal of child neurology* **24**, 1526-1535
18. Kleihues, P., Soylemezoglu, F., Schauble, B., Scheithauer, B. W., and Burger, P. C. (1995) Histopathology, classification, and grading of gliomas. *Glia* **15**, 211-221
19. Il'yasova, D., McCarthy, B., Marcello, J., Schildkraut, J. M., Moorman, P. G., Krishnamachari, B., Ali-Osman, F., Bigner, D. D., and Davis, F. (2009) Association between glioma and history of allergies, asthma, and eczema: a case-control study with three groups of controls. *Cancer Epidemiol Biomarkers Prev* **18**, 1232-1238
20. Dolecek, T. A., Propp, J. M., Stroup, N. E., and Kruchko, C. (2012) CBTRUS statistical report: primary brain and central nervous system tumors diagnosed in the United States in 2005-2009. *Neuro Oncol* **14 Suppl 5**, v1-49
21. Marko, N. F., and Weil, R. J. (2012) The molecular biology of WHO grade I astrocytomas. *Neuro Oncol* **14**, 1424-1431
22. Dunham, C. (2010) Pediatric brain tumors: a histologic and genetic update on commonly encountered entities. *Seminars in diagnostic pathology* **27**, 147-159
23. Louis, D. N., Deutsches Krebsforschungszentrum Heidelberg., International Agency for Research on Cancer., and World Health Organization. (2007) WHO classification of tumours of the central nervous system. in *World Health Organization classification of tumours*, 4th Ed., Distributed by WHO Press, World Health Organization, Geneva, Switzerland
24. Reuss, D. E., Kratz, A., Sahm, F., Capper, D., Schrimpf, D., Koelsche, C., Hovestadt, V., Bewerunge-Hudler, M., Jones, D. T., Schittenhelm, J.,

Mittelbronn, M., Rushing, E., Simon, M., Westphal, M., Unterberg, A., Platten, M., Paulus, W., Reifenberger, G., Tonn, J. C., Aldape, K., Pfister, S. M., Korshunov, A., Weller, M., Herold-Mende, C., Wick, W., Brandner, S., and von Deimling, A. (2015) Adult IDH wild type astrocytomas biologically and clinically resolve into other tumor entities. *Acta neuropathologica* **130**, 407-417

25. Reuss, D. E., Mamatjan, Y., Schrimpf, D., Capper, D., Hovestadt, V., Kratz, A., Sahm, F., Koelsche, C., Korshunov, A., Olar, A., Hartmann, C., Reijneveld, J. C., Wesseling, P., Unterberg, A., Platten, M., Wick, W., Herold-Mende, C., Aldape, K., and von Deimling, A. (2015) IDH mutant diffuse and anaplastic astrocytomas have similar age at presentation and little difference in survival: a grading problem for WHO. *Acta neuropathologica* **129**, 867-873
26. Olar, A., Wani, K. M., Alfaro-Munoz, K. D., Heathcock, L. E., van Thuijl, H. F., Gilbert, M. R., Armstrong, T. S., Sulman, E. P., Cahill, D. P., Vera-Bolanos, E., Yuan, Y., Reijneveld, J. C., Ylstra, B., Wesseling, P., and Aldape, K. D. (2015) IDH mutation status and role of WHO grade and mitotic index in overall survival in grade II-III diffuse gliomas. *Acta neuropathologica* **129**, 585-596
27. Ohgaki, H., and Kleihues, P. (2013) The definition of primary and secondary glioblastoma. *Clinical cancer research : an official journal of the American Association for Cancer Research* **19**, 764-772
28. DeAngelis, L. M. (2001) Brain tumors. *The New England journal of medicine* **344**, 114-123
29. Kleihues, P., and Sobin, L. H. (2000) World Health Organization classification of tumors. *Cancer* **88**, 2887
30. Ostrom, Q. T., Gittleman, H., Fulop, J., Liu, M., Blanda, R., Kromer, C., Wolinsky, Y., Kruchko, C., and Barnholtz-Sloan, J. S. (2015) CBTRUS Statistical Report: Primary Brain and Central Nervous System Tumors Diagnosed in the United States in 2008-2012. *Neuro Oncol* **17 Suppl 4**, iv1-iv62
31. Tamimi, A. F., and Juweid, M. (2017) Epidemiology and Outcome of Glioblastoma. in *Glioblastoma* (De Vleeschouwer, S. ed.), Brisbane (AU). pp
32. Smoll, N. R., and Hamilton, B. (2014) Incidence and relative survival of anaplastic astrocytomas. *Neuro Oncol* **16**, 1400-1407
33. Hanif, F., Muzaffar, K., Perveen, K., Malhi, S. M., and Simjee Sh, U. (2017) Glioblastoma Multiforme: A Review of its Epidemiology and Pathogenesis through Clinical Presentation and Treatment. *Asian Pac J Cancer Prev* **18**, 3-9
34. Nelson, S. J., and Cha, S. (2003) Imaging glioblastoma multiforme. *Cancer J* **9**, 134-145
35. Lara-Velazquez, M., Al-Kharboosh, R., Jeanneret, S., Vazquez-Ramos, C., Mahato, D., Tavanaiepour, D., Rahmathulla, G., and Quinones-Hinojosa, A. (2017) Advances in Brain Tumor Surgery for Glioblastoma in Adults. *Brain Sci* **7**

36. Hardesty, D. A., and Sanai, N. (2012) The value of glioma extent of resection in the modern neurosurgical era. *Frontiers in neurology* **3**, 140
37. Sanai, N., and Berger, M. S. (2008) Glioma extent of resection and its impact on patient outcome. *Neurosurgery* **62**, 753-764; discussion 264-756
38. Simpson, J. R., Horton, J., Scott, C., Curran, W. J., Rubin, P., Fischbach, J., Isaacson, S., Rotman, M., Asbell, S. O., Nelson, J. S., and et al. (1993) Influence of location and extent of surgical resection on survival of patients with glioblastoma multiforme: results of three consecutive Radiation Therapy Oncology Group (RTOG) clinical trials. *International journal of radiation oncology, biology, physics* **26**, 239-244
39. Stummer, W., Reulen, H. J., Meinel, T., Pichlmeier, U., Schumacher, W., Tonn, J. C., Rohde, V., Oppel, F., Turowski, B., Woiciechowsky, C., Franz, K., and Pietsch, T. (2008) Extent of resection and survival in glioblastoma multiforme: identification of and adjustment for bias. *Neurosurgery* **62**, 564-576; discussion 564-576
40. Lun, M., Lok, E., Gautam, S., Wu, E., and Wong, E. T. (2011) The natural history of extracranial metastasis from glioblastoma multiforme. *J Neurooncol* **105**, 261-273
41. Walker, M. D., Green, S. B., Byar, D. P., Alexander, E., Jr., Batzdorf, U., Brooks, W. H., Hunt, W. E., MacCarty, C. S., Mahaley, M. S., Jr., Mealey, J., Jr., Owens, G., Ransohoff, J., 2nd, Robertson, J. T., Shapiro, W. R., Smith, K. R., Jr., Wilson, C. B., and Strike, T. A. (1980) Randomized comparisons of radiotherapy and nitrosoureas for the treatment of malignant glioma after surgery. *The New England journal of medicine* **303**, 1323-1329
42. Walker, M. D., Alexander, E., Jr., Hunt, W. E., Leventhal, C. M., Mahaley, M. S., Jr., Mealey, J., Norrell, H. A., Owens, G., Ransohoff, J., Wilson, C. B., and Gehan, E. A. (1976) Evaluation of mithramycin in the treatment of anaplastic gliomas. *Journal of neurosurgery* **44**, 655-667
43. Walker, M. D., Alexander, E., Jr., Hunt, W. E., MacCarty, C. S., Mahaley, M. S., Jr., Mealey, J., Jr., Norrell, H. A., Owens, G., Ransohoff, J., Wilson, C. B., Gehan, E. A., and Strike, T. A. (1978) Evaluation of BCNU and/or radiotherapy in the treatment of anaplastic gliomas. A cooperative clinical trial. *Journal of neurosurgery* **49**, 333-343
44. Mason, W. P., Maestro, R. D., Eisenstat, D., Forsyth, P., Fulton, D., Laperriere, N., Macdonald, D., Perry, J., and Thiessen, B. (2007) Canadian recommendations for the treatment of glioblastoma multiforme. *Curr Oncol* **14**, 110-117
45. Onoyama, Y., Abe, M., Yabumoto, E., Sakamoto, T., and Nishidai, T. (1976) Radiation therapy in the treatment of glioblastoma. *AJR. American journal of roentgenology* **126**, 481-492
46. Phillips, C., Guiney, M., Smith, J., Hughes, P., Narayan, K., and Quong, G. (2003) A randomized trial comparing 35Gy in ten fractions with 60Gy in 30 fractions of cerebral irradiation for glioblastoma multiforme and older patients with anaplastic astrocytoma. *Radiotherapy and oncology : journal*

of the European Society for Therapeutic Radiology and Oncology **68**, 23-26

47. Walker, M. D., Strike, T. A., and Sheline, G. E. (1979) An analysis of dose-effect relationship in the radiotherapy of malignant gliomas. *International journal of radiation oncology, biology, physics* **5**, 1725-1731
48. Nelson, D. F., Diener-West, M., Horton, J., Chang, C. H., Schoenfeld, D., and Nelson, J. S. (1988) Combined modality approach to treatment of malignant gliomas--re-evaluation of RTOG 7401/ECOG 1374 with long-term follow-up: a joint study of the Radiation Therapy Oncology Group and the Eastern Cooperative Oncology Group. *NCI monographs : a publication of the National Cancer Institute*, 279-284
49. Roa, W., Brasher, P. M., Bauman, G., Anthes, M., Bruera, E., Chan, A., Fisher, B., Fulton, D., Gulavita, S., Hao, C., Husain, S., Murtha, A., Petruk, K., Stewart, D., Tai, P., Urtasun, R., Cairncross, J. G., and Forsyth, P. (2004) Abbreviated course of radiation therapy in older patients with glioblastoma multiforme: a prospective randomized clinical trial. *Journal of clinical oncology : official journal of the American Society of Clinical Oncology* **22**, 1583-1588
50. Wachowicz, K., Murray, B., and Fallone, B. G. (2018) On the direct acquisition of beam's-eye-view images in MRI for integration with external beam radiotherapy. *Phys Med Biol* **63**, 125002
51. Shapiro, W. R., Green, S. B., Burger, P. C., Mahaley, M. S., Jr., Selker, R. G., VanGilder, J. C., Robertson, J. T., Ransohoff, J., Mealey, J., Jr., Strike, T. A., and et al. (1989) Randomized trial of three chemotherapy regimens and two radiotherapy regimens and two radiotherapy regimens in postoperative treatment of malignant glioma. Brain Tumor Cooperative Group Trial 8001. *Journal of neurosurgery* **71**, 1-9
52. Stupp, R., Mason, W. P., van den Bent, M. J., Weller, M., Fisher, B., Taphoorn, M. J., Belanger, K., Brandes, A. A., Marosi, C., Bogdahn, U., Curschmann, J., Janzer, R. C., Ludwin, S. K., Gorlia, T., Allgeier, A., Lacombe, D., Cairncross, J. G., Eisenhauer, E., Mirimanoff, R. O., European Organisation for, R., Treatment of Cancer Brain, T., Radiotherapy, G., and National Cancer Institute of Canada Clinical Trials, G. (2005) Radiotherapy plus concomitant and adjuvant temozolomide for glioblastoma. *The New England journal of medicine* **352**, 987-996
53. Stupp, R., Hegi, M. E., Mason, W. P., van den Bent, M. J., Taphoorn, M. J., Janzer, R. C., Ludwin, S. K., Allgeier, A., Fisher, B., Belanger, K., Hau, P., Brandes, A. A., Gijtenbeek, J., Marosi, C., Vecht, C. J., Mokhtari, K., Wesseling, P., Villa, S., Eisenhauer, E., Gorlia, T., Weller, M., Lacombe, D., Cairncross, J. G., and Mirimanoff, R. O. (2009) Effects of radiotherapy with concomitant and adjuvant temozolomide versus radiotherapy alone on survival in glioblastoma in a randomised phase III study: 5-year analysis of the EORTC-NCIC trial. *The Lancet. Oncology* **10**, 459-466
54. Easaw, J. C., Mason, W. P., Perry, J., Laperriere, N., Eisenstat, D. D., Del Maestro, R., Belanger, K., Fulton, D., and Macdonald, D. (2011) Canadian

recommendations for the treatment of recurrent or progressive glioblastoma multiforme. *Curr Oncol* **18**, e126-136
55. Mason, W. P., Maestro, R. D., Eisenstat, D., Forsyth, P., Fulton, D., Laperriere, N., Macdonald, D., Perry, J., Thiessen, B., and Canadian, G. B. M. R. C. (2007) Canadian recommendations for the treatment of glioblastoma multiforme. *Curr Oncol* **14**, 110-117
56. Hegi, M. E., Diserens, A. C., Gorlia, T., Hamou, M. F., de Tribolet, N., Weller, M., Kros, J. M., Hainfellner, J. A., Mason, W., Mariani, L., Bromberg, J. E., Hau, P., Mirimanoff, R. O., Cairncross, J. G., Janzer, R. C., and Stupp, R. (2005) MGMT gene silencing and benefit from temozolomide in glioblastoma. *The New England journal of medicine* **352**, 997-1003
57. Omuro, A., and DeAngelis, L. M. (2013) Glioblastoma and other malignant gliomas: a clinical review. *Jama* **310**, 1842-1850
58. Chinot, O. L., Wick, W., and Cloughesy, T. (2014) Bevacizumab for newly diagnosed glioblastoma. *The New England journal of medicine* **370**, 2049
59. Jordan, J. T., and Wen, P. Y. (2015) Novel chemotherapeutic approaches in adult high-grade gliomas. *Cancer treatment and research* **163**, 117-142
60. Hamza, M. A., and Gilbert, M. (2014) Targeted therapy in gliomas. *Current oncology reports* **16**, 379
61. Jackson, C., Ruzevick, J., Phallen, J., Belcaid, Z., and Lim, M. (2011) Challenges in immunotherapy presented by the glioblastoma multiforme microenvironment. *Clin Dev Immunol* **2011**, 732413
62. Masson, F., Calzascia, T., Di Berardino-Besson, W., de Tribolet, N., Dietrich, P. Y., and Walker, P. R. (2007) Brain microenvironment promotes the final functional maturation of tumor-specific effector CD8+ T cells. *J Immunol* **179**, 845-853
63. Calzascia, T., Masson, F., Di Berardino-Besson, W., Contassot, E., Wilmotte, R., Aurrand-Lions, M., Ruegg, C., Dietrich, P. Y., and Walker, P. R. (2005) Homing phenotypes of tumor-specific CD8 T cells are predetermined at the tumor site by crosspresenting APCs. *Immunity* **22**, 175-184
64. Huang, B., Zhang, H., Gu, L., Ye, B., Jian, Z., Stary, C., and Xiong, X. (2017) Advances in Immunotherapy for Glioblastoma Multiforme. *J Immunol Res* **2017**, 3597613
65. Verhaak, R. G., Hoadley, K. A., Purdom, E., Wang, V., Qi, Y., Wilkerson, M. D., Miller, C. R., Ding, L., Golub, T., Mesirov, J. P., Alexe, G., Lawrence, M., O'Kelly, M., Tamayo, P., Weir, B. A., Gabriel, S., Winckler, W., Gupta, S., Jakkula, L., Feiler, H. S., Hodgson, J. G., James, C. D., Sarkaria, J. N., Brennan, C., Kahn, A., Spellman, P. T., Wilson, R. K., Speed, T. P., Gray, J. W., Meyerson, M., Getz, G., Perou, C. M., and Hayes, D. N. (2010) Integrated genomic analysis identifies clinically relevant subtypes of glioblastoma characterized by abnormalities in PDGFRA, IDH1, EGFR, and NF1. *Cancer cell* **17**, 98-110
66. (2008) Comprehensive genomic characterization defines human glioblastoma genes and core pathways. *Nature* **455**, 1061-1068

67. Brennan, C. W., Verhaak, R. G., McKenna, A., Campos, B., Noushmehr, H., Salama, S. R., Zheng, S., Chakravarty, D., Sanborn, J. Z., Berman, S. H., Beroukhim, R., Bernard, B., Wu, C. J., Genovese, G., Shmulevich, I., Barnholtz-Sloan, J., Zou, L., Vegesna, R., Shukla, S. A., Ciriello, G., Yung, W. K., Zhang, W., Sougnez, C., Mikkelsen, T., Aldape, K., Bigner, D. D., Van Meir, E. G., Prados, M., Sloan, A., Black, K. L., Eschbacher, J., Finocchiaro, G., Friedman, W., Andrews, D. W., Guha, A., Iacocca, M., O'Neill, B. P., Foltz, G., Myers, J., Weisenberger, D. J., Penny, R., Kucherlapati, R., Perou, C. M., Hayes, D. N., Gibbs, R., Marra, M., Mills, G. B., Lander, E., Spellman, P., Wilson, R., Sander, C., Weinstein, J., Meyerson, M., Gabriel, S., Laird, P. W., Haussler, D., Getz, G., and Chin, L. (2013) The somatic genomic landscape of glioblastoma. *Cell* **155**, 462-477
68. Noushmehr, H., Weisenberger, D. J., Diefes, K., Phillips, H. S., Pujara, K., Berman, B. P., Pan, F., Pelloski, C. E., Sulman, E. P., Bhat, K. P., Verhaak, R. G., Hoadley, K. A., Hayes, D. N., Perou, C. M., Schmidt, H. K., Ding, L., Wilson, R. K., Van Den Berg, D., Shen, H., Bengtsson, H., Neuvial, P., Cope, L. M., Buckley, J., Herman, J. G., Baylin, S. B., Laird, P. W., and Aldape, K. (2010) Identification of a CpG island methylator phenotype that defines a distinct subgroup of glioma. *Cancer cell* **17**, 510-522
69. Chen, J., McKay, R. M., and Parada, L. F. (2012) Malignant glioma: lessons from genomics, mouse models, and stem cells. *Cell* **149**, 36-47
70. Dunn, G. P., Rinne, M. L., Wykosky, J., Genovese, G., Quayle, S. N., Dunn, I. F., Agarwalla, P. K., Chheda, M. G., Campos, B., Wang, A., Brennan, C., Ligon, K. L., Furnari, F., Cavenee, W. K., Depinho, R. A., Chin, L., and Hahn, W. C. (2012) Emerging insights into the molecular and cellular basis of glioblastoma. *Genes Dev* **26**, 756-784
71. Vousden, K. H., and Prives, C. (2009) Blinded by the Light: The Growing Complexity of p53. *Cell* **137**, 413-431
72. Kubbutat, M. H., Jones, S. N., and Vousden, K. H. (1997) Regulation of p53 stability by Mdm2. *Nature* **387**, 299-303
73. Honda, R., Tanaka, H., and Yasuda, H. (1997) Oncoprotein MDM2 is a ubiquitin ligase E3 for tumor suppressor p53. *FEBS letters* **420**, 25-27
74. Riemenschneider, M. J., Buschges, R., Wolter, M., Reifenberger, J., Bostrom, J., Kraus, J. A., Schlegel, U., and Reifenberger, G. (1999) Amplification and overexpression of the MDM4 (MDMX) gene from 1q32 in a subset of malignant gliomas without TP53 mutation or MDM2 amplification. *Cancer research* **59**, 6091-6096
75. Reifenberger, G., Ichimura, K., Reifenberger, J., Elkahloun, A. G., Meltzer, P. S., and Collins, V. P. (1996) Refined mapping of 12q13-q15 amplicons in human malignant gliomas suggests CDK4/SAS and MDM2 as independent amplification targets. *Cancer research* **56**, 5141-5145
76. Tortosa, A., Ino, Y., Odell, N., Swilley, S., Sasaki, H., Louis, D. N., and Henson, J. W. (2000) Molecular genetics of radiographically defined de novo glioblastoma multiforme. *Neuropathol Appl Neurobiol* **26**, 544-552

77. Mao, H., Lebrun, D. G., Yang, J., Zhu, V. F., and Li, M. (2012) Deregulated signaling pathways in glioblastoma multiforme: molecular mechanisms and therapeutic targets. *Cancer Invest* **30**, 48-56
78. Dick, F. A., and Rubin, S. M. (2013) Molecular mechanisms underlying RB protein function. *Nature reviews. Molecular cell biology* **14**, 297-306
79. Knudsen, E. S., and Wang, J. Y. (2010) Targeting the RB-pathway in cancer therapy. *Clinical cancer research : an official journal of the American Association for Cancer Research* **16**, 1094-1099
80. Janku, F., Yap, T. A., and Meric-Bernstam, F. (2018) Targeting the PI3K pathway in cancer: are we making headway? *Nat Rev Clin Oncol* **15**, 273-291
81. Li, X., Wu, C., Chen, N., Gu, H., Yen, A., Cao, L., Wang, E., and Wang, L. (2016) PI3K/Akt/mTOR signaling pathway and targeted therapy for glioblastoma. *Oncotarget* **7**, 33440-33450
82. Parsons, D. W., Jones, S., Zhang, X., Lin, J. C., Leary, R. J., Angenendt, P., Mankoo, P., Carter, H., Siu, I. M., Gallia, G. L., Olivi, A., McLendon, R., Rasheed, B. A., Keir, S., Nikolskaya, T., Nikolsky, Y., Busam, D. A., Tekleab, H., Diaz, L. A., Jr., Hartigan, J., Smith, D. R., Strausberg, R. L., Marie, S. K., Shinjo, S. M., Yan, H., Riggins, G. J., Bigner, D. D., Karchin, R., Papadopoulos, N., Parmigiani, G., Vogelstein, B., Velculescu, V. E., and Kinzler, K. W. (2008) An integrated genomic analysis of human glioblastoma multiforme. *Science* **321**, 1807-1812
83. Frederick, L., Wang, X. Y., Eley, G., and James, C. D. (2000) Diversity and frequency of epidermal growth factor receptor mutations in human glioblastomas. *Cancer research* **60**, 1383-1387
84. Huang, H. S., Nagane, M., Klingbeil, C. K., Lin, H., Nishikawa, R., Ji, X. D., Huang, C. M., Gill, G. N., Wiley, H. S., and Cavenee, W. K. (1997) The enhanced tumorigenic activity of a mutant epidermal growth factor receptor common in human cancers is mediated by threshold levels of constitutive tyrosine phosphorylation and unattenuated signaling. *J Biol Chem* **272**, 2927-2935
85. Narita, Y., Nagane, M., Mishima, K., Huang, H. J., Furnari, F. B., and Cavenee, W. K. (2002) Mutant epidermal growth factor receptor signaling down-regulates p27 through activation of the phosphatidylinositol 3-kinase/Akt pathway in glioblastomas. *Cancer research* **62**, 6764-6769
86. Liu, A., Hou, C., Chen, H., Zong, X., and Zong, P. (2016) Genetics and Epigenetics of Glioblastoma: Applications and Overall Incidence of IDH1 Mutation. *Front Oncol* **6**, 16
87. Reitman, Z. J., Parsons, D. W., and Yan, H. (2010) IDH1 and IDH2: not your typical oncogenes. *Cancer cell* **17**, 215-216
88. Cohen, A. L., Holmen, S. L., and Colman, H. (2013) IDH1 and IDH2 mutations in gliomas. *Current neurology and neuroscience reports* **13**, 345
89. Ward, P. S., Patel, J., Wise, D. R., Abdel-Wahab, O., Bennett, B. D., Coller, H. A., Cross, J. R., Fantin, V. R., Hedvat, C. V., Perl, A. E., Rabinowitz, J. D., Carroll, M., Su, S. M., Sharp, K. A., Levine, R. L., and Thompson, C. B. (2010) The common feature of leukemia-associated

IDH1 and IDH2 mutations is a neomorphic enzyme activity converting alpha-ketoglutarate to 2-hydroxyglutarate. *Cancer cell* **17**, 225-234
90. Xu, W., Yang, H., Liu, Y., Yang, Y., Wang, P., Kim, S. H., Ito, S., Yang, C., Wang, P., Xiao, M. T., Liu, L. X., Jiang, W. Q., Liu, J., Zhang, J. Y., Wang, B., Frye, S., Zhang, Y., Xu, Y. H., Lei, Q. Y., Guan, K. L., Zhao, S. M., and Xiong, Y. (2011) Oncometabolite 2-hydroxyglutarate is a competitive inhibitor of alpha-ketoglutarate-dependent dioxygenases. *Cancer cell* **19**, 17-30
91. Turcan, S., Rohle, D., Goenka, A., Walsh, L. A., Fang, F., Yilmaz, E., Campos, C., Fabius, A. W., Lu, C., Ward, P. S., Thompson, C. B., Kaufman, A., Guryanova, O., Levine, R., Heguy, A., Viale, A., Morris, L. G., Huse, J. T., Mellinghoff, I. K., and Chan, T. A. (2012) IDH1 mutation is sufficient to establish the glioma hypermethylator phenotype. *Nature* **483**, 479-483
92. Jones, K. A., Yamamoto, K. R., and Tjian, R. (1985) Two distinct transcription factors bind to the HSV thymidine kinase promoter in vitro. *Cell* **42**, 559-572
93. Cohen, R. B., Sheffery, M., and Kim, C. G. (1986) Partial purification of a nuclear protein that binds to the CCAAT box of the mouse alpha 1-globin gene. *Mol Cell Biol* **6**, 821-832
94. Jones, K. A., Kadonaga, J. T., Rosenfeld, P. J., Kelly, T. J., and Tjian, R. (1987) A cellular DNA-binding protein that activates eukaryotic transcription and DNA replication. *Cell* **48**, 79-89
95. Santoro, C., Mermod, N., Andrews, P. C., and Tjian, R. (1988) A family of human CCAAT-box-binding proteins active in transcription and DNA replication: cloning and expression of multiple cDNAs. *Nature* **334**, 218-224
96. Gronostajski, R. M., Adhya, S., Nagata, K., Guggenheimer, R. A., and Hurwitz, J. (1985) Site-specific DNA binding of nuclear factor I: analyses of cellular binding sites. *Mol Cell Biol* **5**, 964-971
97. Gronostajski, R. M. (1986) Analysis of nuclear factor I binding to DNA using degenerate oligonucleotides. *Nucleic Acids Res* **14**, 9117-9132
98. Leegwater, P. A., van der Vliet, P. C., Rupp, R. A., Nowock, J., and Sippel, A. E. (1986) Functional homology between the sequence-specific DNA-binding proteins nuclear factor I from HeLa cells and the TGGCA protein from chicken liver. *The EMBO journal* **5**, 381-386
99. Borgmeyer, U., Nowock, J., and Sippel, A. E. (1984) The TGGCA-binding protein: a eukaryotic nuclear protein recognizing a symmetrical sequence on double-stranded linear DNA. *Nucleic Acids Res* **12**, 4295-4311
100. Messina, G., Biressi, S., Monteverde, S., Magli, A., Cassano, M., Perani, L., Roncaglia, E., Tagliafico, E., Starnes, L., Campbell, C. E., Grossi, M., Goldhamer, D. J., Gronostajski, R. M., and Cossu, G. (2010) Nfix regulates fetal-specific transcription in developing skeletal muscle. *Cell* **140**, 554-566

101. Hebbar, P. B., and Archer, T. K. (2007) Chromatin-dependent cooperativity between site-specific transcription factors in vivo. *J Biol Chem* **282**, 8284-8291
102. Amemiya, K., Traub, R., Durham, L., and Major, E. O. (1992) Adjacent nuclear factor-1 and activator protein binding sites in the enhancer of the neurotropic JC virus. A common characteristic of many brain-specific genes. *J Biol Chem* **267**, 14204-14211
103. Lajoie, M., Hsu, Y. C., Gronostajski, R. M., and Bailey, T. L. (2014) An overlapping set of genes is regulated by both NFIB and the glucocorticoid receptor during lung maturation. *BMC genomics* **15**, 231
104. Murtagh, J., Martin, F., and Gronostajski, R. M. (2003) The Nuclear Factor I (NFI) gene family in mammary gland development and function. *Journal of mammary gland biology and neoplasia* **8**, 241-254
105. Rupp, R. A., Kruse, U., Multhaup, G., Gobel, U., Beyreuther, K., and Sippel, A. E. (1990) Chicken NFI/TGGCA proteins are encoded by at least three independent genes: NFI-A, NFI-B and NFI-C with homologues in mammalian genomes. *Nucleic Acids Res* **18**, 2607-2616
106. Kruse, U., Qian, F., and Sippel, A. E. (1991) Identification of a fourth nuclear factor I gene in chicken by cDNA cloning: NFI-X. *Nucleic Acids Res* **19**, 6641
107. Kruse, U., and Sippel, A. E. (1994) The genes for transcription factor nuclear factor I give rise to corresponding splice variants between vertebrate species. *Journal of molecular biology* **238**, 860-865
108. Grunder, A., Qian, F., Ebel, T. T., Mincheva, A., Lichter, P., Kruse, U., and Sippel, A. E. (2003) Genomic organization, splice products and mouse chromosomal localization of genes for transcription factor Nuclear Factor One. *Gene* **304**, 171-181
109. Apt, D., Liu, Y., and Bernard, H. U. (1994) Cloning and functional analysis of spliced isoforms of human nuclear factor I-X: interference with transcriptional activation by NFI/CTF in a cell-type specific manner. *Nucleic Acids Res* **22**, 3825-3833
110. Prado, F., Vicent, G., Cardalda, C., and Beato, M. (2002) Differential role of the proline-rich domain of nuclear factor 1-C splice variants in DNA binding and transactivation. *J Biol Chem* **277**, 16383-16390
111. Mermod, N., O'Neill, E. A., Kelly, T. J., and Tjian, R. (1989) The proline-rich transcriptional activator of CTF/NF-I is distinct from the replication and DNA binding domain. *Cell* **58**, 741-753
112. Mason, S., Piper, M., Gronostajski, R. M., and Richards, L. J. (2009) Nuclear factor one transcription factors in CNS development. *Molecular neurobiology* **39**, 10-23
113. Armentero, M. T., Horwitz, M., and Mermod, N. (1994) Targeting of DNA polymerase to the adenovirus origin of DNA replication by interaction with nuclear factor I. *Proc Natl Acad Sci U S A* **91**, 11537-11541
114. Kruse, U., and Sippel, A. E. (1994) Transcription factor nuclear factor I proteins form stable homo- and heterodimers. *FEBS letters* **348**, 46-50

115. Osada, S., Matsubara, T., Daimon, S., Terazu, Y., Xu, M., Nishihara, T., and Imagawa, M. (1999) Expression, DNA-binding specificity and transcriptional regulation of nuclear factor 1 family proteins from rat. *The Biochemical journal* **342 (Pt 1)**, 189-198
116. Chaudhry, A. Z., Vitullo, A. D., and Gronostajski, R. M. (1998) Nuclear factor I (NFI) isoforms differentially activate simple versus complex NFI-responsive promoters. *J Biol Chem* **273**, 18538-18546
117. Gronostajski, R. M. (2000) Roles of the NFI/CTF gene family in transcription and development. *Gene* **249**, 31-45
118. Wendler, W., Altmann, H., and Ludwig-Winnacker, E. (1994) Transcriptional activation of NFI/CTF1 depends on a sequence motif strongly related to the carboxyterminal domain of RNA polymerase II. *Nucleic Acids Res* **22**, 2601-2603
119. Xiao, H., Lis, J. T., Greenblatt, J., and Friesen, J. D. (1994) The upstream activator CTF/NF1 and RNA polymerase II share a common element involved in transcriptional activation. *Nucleic Acids Res* **22**, 1966-1973
120. Kim, T. K., and Roeder, R. G. (1994) Involvement of the basic repeat domain of TATA-binding protein (TBP) in transcription by RNA polymerases I, II, and III. *J Biol Chem* **269**, 4891-4894
121. Altmann, H., Wendler, W., and Winnacker, E. L. (1994) Transcriptional activation by CTF proteins is mediated by a bipartite low-proline domain. *Proc Natl Acad Sci U S A* **91**, 3901-3905
122. Dusserre, Y., and Mermod, N. (1992) Purified cofactors and histone H1 mediate transcriptional regulation by CTF/NF-I. *Mol Cell Biol* **12**, 5228-5237
123. Alevizopoulos, A., Dusserre, Y., Tsai-Pflugfelder, M., von der Weid, T., Wahli, W., and Mermod, N. (1995) A proline-rich TGF-beta-responsive transcriptional activator interacts with histone H3. *Genes Dev* **9**, 3051-3066
124. Grabowska, M. M., Elliott, A. D., DeGraff, D. J., Anderson, P. D., Anumanthan, G., Yamashita, H., Sun, Q., Friedman, D. B., Hachey, D. L., Yu, X., Sheehan, J. H., Ahn, J. M., Raj, G. V., Piston, D. W., Gronostajski, R. M., and Matusik, R. J. (2014) NFI transcription factors interact with FOXA1 to regulate prostate-specific gene expression. *Mol Endocrinol* **28**, 949-964
125. Bachurski, C. J., Yang, G. H., Currier, T. A., Gronostajski, R. M., and Hong, D. (2003) Nuclear factor I/thyroid transcription factor 1 interactions modulate surfactant protein C transcription. *Mol Cell Biol* **23**, 9014-9024
126. Kang, P., Lee, H. K., Glasgow, S. M., Finley, M., Donti, T., Gaber, Z. B., Graham, B. H., Foster, A. E., Novitch, B. G., Gronostajski, R. M., and Deneen, B. (2012) Sox9 and NFIA coordinate a transcriptional regulatory cascade during the initiation of gliogenesis. *Neuron* **74**, 79-94
127. Glasgow, S. M., Zhu, W., Stolt, C. C., Huang, T. W., Chen, F., LoTurco, J. J., Neul, J. L., Wegner, M., Mohila, C., and Deneen, B. (2014) Mutual antagonism between Sox10 and NFIA regulates diversification of glial lineages and glioma subtypes. *Nature neuroscience* **17**, 1322-1329

128. Chaudhry, A. Z., Lyons, G. E., and Gronostajski, R. M. (1997) Expression patterns of the four nuclear factor I genes during mouse embryogenesis indicate a potential role in development. *Developmental dynamics : an official publication of the American Association of Anatomists* **208**, 313-325
129. Chen, K. S., Lim, J. W. C., Richards, L. J., and Bunt, J. (2017) The convergent roles of the nuclear factor I transcription factors in development and cancer. *Cancer Lett* **410**, 124-138
130. das Neves, L., Duchala, C. S., Tolentino-Silva, F., Haxhiu, M. A., Colmenares, C., Macklin, W. B., Campbell, C. E., Butz, K. G., and Gronostajski, R. M. (1999) Disruption of the murine nuclear factor I-A gene (Nfia) results in perinatal lethality, hydrocephalus, and agenesis of the corpus callosum. *Proceedings of the National Academy of Sciences of the United States of America* **96**, 11946-11951
131. Shu, T., Butz, K. G., Plachez, C., Gronostajski, R. M., and Richards, L. J. (2003) Abnormal development of forebrain midline glia and commissural projections in Nfia knock-out mice. *The Journal of neuroscience : the official journal of the Society for Neuroscience* **23**, 203-212
132. Driller, K., Pagenstecher, A., Uhl, M., Omran, H., Berlis, A., Grunder, A., and Sippel, A. E. (2007) Nuclear factor I X deficiency causes brain malformation and severe skeletal defects. *Mol Cell Biol* **27**, 3855-3867
133. Wong, Y. W., Schulze, C., Streichert, T., Gronostajski, R. M., Schachner, M., and Tilling, T. (2007) Gene expression analysis of nuclear factor I-A deficient mice indicates delayed brain maturation. *Genome biology* **8**, R72
134. Barry, G., Piper, M., Lindwall, C., Moldrich, R., Mason, S., Little, E., Sarkar, A., Tole, S., Gronostajski, R. M., and Richards, L. J. (2008) Specific glial populations regulate hippocampal morphogenesis. *The Journal of neuroscience : the official journal of the Society for Neuroscience* **28**, 12328-12340
135. Piper, M., Barry, G., Harvey, T. J., McLeay, R., Smith, A. G., Harris, L., Mason, S., Stringer, B. W., Day, B. W., Wray, N. R., Gronostajski, R. M., Bailey, T. L., Boyd, A. W., and Richards, L. J. (2014) NFIB-mediated repression of the epigenetic factor Ezh2 regulates cortical development. *The Journal of neuroscience : the official journal of the Society for Neuroscience* **34**, 2921-2930
136. Betancourt, J., Katzman, S., and Chen, B. (2014) Nuclear factor one B regulates neural stem cell differentiation and axonal projection of corticofugal neurons. *The Journal of comparative neurology* **522**, 6-35
137. Steele-Perkins, G., Plachez, C., Butz, K. G., Yang, G., Bachurski, C. J., Kinsman, S. L., Litwack, E. D., Richards, L. J., and Gronostajski, R. M. (2005) The transcription factor gene Nfib is essential for both lung maturation and brain development. *Mol Cell Biol* **25**, 685-698
138. Heng, Y. H., McLeay, R. C., Harvey, T. J., Smith, A. G., Barry, G., Cato, K., Plachez, C., Little, E., Mason, S., Dixon, C., Gronostajski, R. M., Bailey, T. L., Richards, L. J., and Piper, M. (2014) NFIX regulates neural

progenitor cell differentiation during hippocampal morphogenesis. *Cereb Cortex* **24**, 261-279
139. Piper, M., Harris, L., Barry, G., Heng, Y. H., Plachez, C., Gronostajski, R. M., and Richards, L. J. (2011) Nuclear factor one X regulates the development of multiple cellular populations in the postnatal cerebellum. *The Journal of comparative neurology* **519**, 3532-3548
140. Campbell, C. E., Piper, M., Plachez, C., Yeh, Y. T., Baizer, J. S., Osinski, J. M., Litwack, E. D., Richards, L. J., and Gronostajski, R. M. (2008) The transcription factor Nfix is essential for normal brain development. *BMC developmental biology* **8**, 52
141. Steele-Perkins, G., Butz, K. G., Lyons, G. E., Zeichner-David, M., Kim, H. J., Cho, M. I., and Gronostajski, R. M. (2003) Essential role for NFI-C/CTF transcription-replication factor in tooth root development. *Mol Cell Biol* **23**, 1075-1084
142. Cebolla, B., and Vallejo, M. (2006) Nuclear factor-I regulates glial fibrillary acidic protein gene expression in astrocytes differentiated from cortical precursor cells. *Journal of neurochemistry* **97**, 1057-1070
143. Deneen, B., Ho, R., Lukaszewicz, A., Hochstim, C. J., Gronostajski, R. M., and Anderson, D. J. (2006) The transcription factor NFIA controls the onset of gliogenesis in the developing spinal cord. *Neuron* **52**, 953-968
144. Pringle, N. P., Yu, W. P., Howell, M., Colvin, J. S., Ornitz, D. M., and Richardson, W. D. (2003) Fgfr3 expression by astrocytes and their precursors: evidence that astrocytes and oligodendrocytes originate in distinct neuroepithelial domains. *Development* **130**, 93-102
145. Namihira, M., Kohyama, J., Semi, K., Sanosaka, T., Deneen, B., Taga, T., and Nakashima, K. (2009) Committed neuronal precursors confer astrocytic potential on residual neural precursor cells. *Dev Cell* **16**, 245-255
146. Stolt, C. C., Rehberg, S., Ader, M., Lommes, P., Riethmacher, D., Schachner, M., Bartsch, U., and Wegner, M. (2002) Terminal differentiation of myelin-forming oligodendrocytes depends on the transcription factor Sox10. *Genes Dev* **16**, 165-170
147. Plachez, C., Cato, K., McLeay, R. C., Heng, Y. H., Bailey, T. L., Gronostajski, R. M., Richards, L. J., Puche, A. C., and Piper, M. (2012) Expression of nuclear factor one A and -B in the olfactory bulb. *The Journal of comparative neurology* **520**, 3135-3149
148. Wang, W., Stock, R. E., Gronostajski, R. M., Wong, Y. W., Schachner, M., and Kilpatrick, D. L. (2004) A role for nuclear factor I in the intrinsic control of cerebellar granule neuron gene expression. *J Biol Chem* **279**, 53491-53497
149. Wang, W., Shin, Y., Shi, M., and Kilpatrick, D. L. (2011) Temporal control of a dendritogenesis-linked gene via REST-dependent regulation of nuclear factor I occupancy. *Mol Biol Cell* **22**, 868-879
150. Ding, B., Wang, W., Selvakumar, T., Xi, H. S., Zhu, H., Chow, C. W., Horton, J. D., Gronostajski, R. M., and Kilpatrick, D. L. (2013) Temporal regulation of nuclear factor one occupancy by calcineurin/NFAT governs a

voltage-sensitive developmental switch in late maturing neurons. *The Journal of neuroscience : the official journal of the Society for Neuroscience* **33**, 2860-2872
151. Wang, W., Mullikin-Kilpatrick, D., Crandall, J. E., Gronostajski, R. M., Litwack, E. D., and Kilpatrick, D. L. (2007) Nuclear factor I coordinates multiple phases of cerebellar granule cell development via regulation of cell adhesion molecules. *The Journal of neuroscience : the official journal of the Society for Neuroscience* **27**, 6115-6127
152. Wang, W., Crandall, J. E., Litwack, E. D., Gronostajski, R. M., and Kilpatrick, D. L. (2010) Targets of the nuclear factor I regulon involved in early and late development of postmitotic cerebellar granule neurons. *J Neurosci Res* **88**, 258-265
153. Kilpatrick, D. L., Wang, W., Gronostajski, R., and Litwack, E. D. (2012) Nuclear factor I and cerebellar granule neuron development: an intrinsic-extrinsic interplay. *Cerebellum* **11**, 41-49
154. Ohtsuka, T., Sakamoto, M., Guillemot, F., and Kageyama, R. (2001) Roles of the basic helix-loop-helix genes Hes1 and Hes5 in expansion of neural stem cells of the developing brain. *J Biol Chem* **276**, 30467-30474
155. Mateo, J. L., van den Berg, D. L., Haeussler, M., Drechsel, D., Gaber, Z. B., Castro, D. S., Robson, P., Crawford, G. E., Flicek, P., Ettwiller, L., Wittbrodt, J., Guillemot, F., and Martynoga, B. (2015) Characterization of the neural stem cell gene regulatory network identifies OLIG2 as a multifunctional regulator of self-renewal. *Genome research* **25**, 41-56
156. Martynoga, B., Mateo, J. L., Zhou, B., Andersen, J., Achimastou, A., Urban, N., van den Berg, D., Georgopoulou, D., Hadjur, S., Wittbrodt, J., Ettwiller, L., Piper, M., Gronostajski, R. M., and Guillemot, F. (2013) Epigenomic enhancer annotation reveals a key role for NFIX in neural stem cell quiescence. *Genes Dev* **27**, 1769-1786
157. Harris, L., Dixon, C., Cato, K., Heng, Y. H., Kurniawan, N. D., Ullmann, J. F., Janke, A. L., Gronostajski, R. M., Richards, L. J., Burne, T. H., and Piper, M. (2013) Heterozygosity for nuclear factor one x affects hippocampal-dependent behaviour in mice. *PLoS One* **8**, e65478
158. Jackson, S. P., and Tjian, R. (1988) O-glycosylation of eukaryotic transcription factors: implications for mechanisms of transcriptional regulation. *Cell* **55**, 125-133
159. Jackson, S. P., MacDonald, J. J., Lees-Miller, S., and Tjian, R. (1990) GC box binding induces phosphorylation of Sp1 by a DNA-dependent protein kinase. *Cell* **63**, 155-165
160. Kawamura, H., Nagata, K., Masamune, Y., and Nakanishi, Y. (1993) Phosphorylation of NF-I in vitro by cdc2 kinase. *Biochem Biophys Res Commun* **192**, 1424-1431
161. Yang, B. S., Gilbert, J. D., and Freytag, S. O. (1993) Overexpression of Myc suppresses CCAAT transcription factor/nuclear factor 1-dependent promoters in vivo. *Mol Cell Biol* **13**, 3093-3102

162. Nilsson, J., Bjursell, G., and Kannius-Janson, M. (2006) Nuclear Jak2 and transcription factor NF1-C2: a novel mechanism of prolactin signaling in mammary epithelial cells. *Mol Cell Biol* **26**, 5663-5674
163. Bisgrove, D. A., Monckton, E. A., Packer, M., and Godbout, R. (2000) Regulation of brain fatty acid-binding protein expression by differential phosphorylation of nuclear factor I in malignant glioma cell lines. *J Biol Chem* **275**, 30668-30676
164. Brun, M., Glubrecht, D. D., Baksh, S., and Godbout, R. (2013) Calcineurin regulates nuclear factor I dephosphorylation and activity in malignant glioma cell lines. *J Biol Chem* **288**, 24104-24115
165. Alevizopoulos, A., and Mermod, N. (1996) Antagonistic regulation of a proline-rich transcription factor by transforming growth factor beta and tumor necrosis factor alpha. *J Biol Chem* **271**, 29672-29681
166. Scrideli, C. A., Carlotti, C. G., Jr., Okamoto, O. K., Andrade, V. S., Cortez, M. A., Motta, F. J., Lucio-Eterovic, A. K., Neder, L., Rosemberg, S., Oba-Shinjo, S. M., Marie, S. K., and Tone, L. G. (2008) Gene expression profile analysis of primary glioblastomas and non-neoplastic brain tissue: identification of potential target genes by oligonucleotide microarray and real-time quantitative PCR. *J Neurooncol* **88**, 281-291
167. Song, H. R., Gonzalez-Gomez, I., Suh, G. S., Commins, D. L., Sposto, R., Gilles, F. H., Deneen, B., and Erdreich-Epstein, A. (2010) Nuclear factor IA is expressed in astrocytomas and is associated with improved survival. *Neuro Oncol* **12**, 122-132
168. Glasgow, S. M., Laug, D., Brawley, V. S., Zhang, Z., Corder, A., Yin, Z., Wong, S. T., Li, X. N., Foster, A. E., Ahmed, N., and Deneen, B. (2013) The miR-223/nuclear factor I-A axis regulates glial precursor proliferation and tumorigenesis in the CNS. *The Journal of neuroscience : the official journal of the Society for Neuroscience* **33**, 13560-13568
169. Lee, J. S., Xiao, J., Patel, P., Schade, J., Wang, J., Deneen, B., Erdreich-Epstein, A., and Song, H. R. (2014) A novel tumor-promoting role for nuclear factor IA in glioblastomas is mediated through negative regulation of p53, p21, and PAI1. *Neuro-oncology* **16**, 191-203
170. Lee, J., Hoxha, E., and Song, H. R. (2017) A novel NFIA-NFkappaB feed-forward loop contributes to glioblastoma cell survival. *Neuro Oncol* **19**, 524-534
171. Stringer, B. W., Bunt, J., Day, B. W., Barry, G., Jamieson, P. R., Ensbey, K. S., Bruce, Z. C., Goasdoue, K., Vidal, H., Charmsaz, S., Smith, F. M., Cooper, L. T., Piper, M., Boyd, A. W., and Richards, L. J. (2016) Nuclear factor one B (NFIB) encodes a subtype-specific tumour suppressor in glioblastoma. *Oncotarget* **7**, 29306-29320
172. Moon, H. G., Hwang, K. T., Kim, J. A., Kim, H. S., Lee, M. J., Jung, E. M., Ko, E., Han, W., and Noh, D. Y. (2011) NFIB is a potential target for estrogen receptor-negative breast cancers. *Molecular oncology* **5**, 538-544
173. Denny, S. K., Yang, D., Chuang, C. H., Brady, J. J., Lim, J. S., Gruner, B. M., Chiou, S. H., Schep, A. N., Baral, J., Hamard, C., Antoine, M., Wislez,

M., Kong, C. S., Connolly, A. J., Park, K. S., Sage, J., Greenleaf, W. J., and Winslow, M. M. (2016) Nfib Promotes Metastasis through a Widespread Increase in Chromatin Accessibility. *Cell* **166**, 328-342
174. Semenova, E. A., Kwon, M. C., Monkhorst, K., Song, J. Y., Bhaskaran, R., Krijgsman, O., Kuilman, T., Peters, D., Buikhuisen, W. A., Smit, E. F., Pritchard, C., Cozijnsen, M., van der Vliet, J., Zevenhoven, J., Lambooij, J. P., Proost, N., van Montfort, E., Velds, A., Huijbers, I. J., and Berns, A. (2016) Transcription Factor NFIB Is a Driver of Small Cell Lung Cancer Progression in Mice and Marks Metastatic Disease in Patients. *Cell Rep* **16**, 631-643
175. Fane, M. E., Chhabra, Y., Hollingsworth, D. E. J., Simmons, J. L., Spoerri, L., Oh, T. G., Chauhan, J., Chin, T., Harris, L., Harvey, T. J., Muscat, G. E. O., Goding, C. R., Sturm, R. A., Haass, N. K., Boyle, G. M., Piper, M., and Smith, A. G. (2017) NFIB Mediates BRN2 Driven Melanoma Cell Migration and Invasion Through Regulation of EZH2 and MITF. *EBioMedicine* **16**, 63-75
176. Lee, H. K., Lee, D. S., and Park, J. C. (2015) Nuclear factor I-C regulates E-cadherin via control of KLF4 in breast cancer. *BMC cancer* **15**, 113
177. Rahman, N. I. A., Abdul Murad, N. A., Mollah, M. M., Jamal, R., and Harun, R. (2017) NFIX as a Master Regulator for Lung Cancer Progression. *Front Pharmacol* **8**, 540
178. Gopalan, S. M., Wilczynska, K. M., Konik, B. S., Bryan, L., and Kordula, T. (2006) Nuclear factor-1-X regulates astrocyte-specific expression of the alpha1-antichymotrypsin and glial fibrillary acidic protein genes. *J Biol Chem* **281**, 13126-13133
179. Singh, S. K., Bhardwaj, R., Wilczynska, K. M., Dumur, C. I., and Kordula, T. (2011) A complex of nuclear factor I-X3 and STAT3 regulates astrocyte and glioma migration through the secreted glycoprotein YKL-40. *J Biol Chem* **286**, 39893-39903
180. Feng, L., Hatten, M. E., and Heintz, N. (1994) Brain lipid-binding protein (BLBP): a novel signaling system in the developing mammalian CNS. *Neuron* **12**, 895-908
181. Godbout, R., Bisgrove, D. A., Shkolny, D., and Day, R. S., 3rd. (1998) Correlation of B-FABP and GFAP expression in malignant glioma. *Oncogene* **16**, 1955-1962
182. Mita, R., Coles, J. E., Glubrecht, D. D., Sung, R., Sun, X., and Godbout, R. (2007) B-FABP-expressing radial glial cells: the malignant glioma cell of origin? *Neoplasia* **9**, 734-744
183. Liang, Y., Bollen, A. W., Aldape, K. D., and Gupta, N. (2006) Nuclear FABP7 immunoreactivity is preferentially expressed in infiltrative glioma and is associated with poor prognosis in EGFR-overexpressing glioblastoma. *BMC cancer* **6**, 97
184. Kaloshi, G., Mokhtari, K., Carpentier, C., Taillibert, S., Lejeune, J., Marie, Y., Delattre, J. Y., Godbout, R., and Sanson, M. (2007) FABP7 expression in glioblastomas: relation to prognosis, invasion and EGFR status. *J Neurooncol* **84**, 245-248

185. Guroff, G. (1964) A Neutral, Calcium-Activated Proteinase from the Soluble Fraction of Rat Brain. *J Biol Chem* **239**, 149-155
186. Dayton, W. R., Goll, D. E., Zeece, M. G., Robson, R. M., and Reville, W. J. (1976) A Ca2+-activated protease possibly involved in myofibrillar protein turnover. Purification from porcine muscle. *Biochemistry* **15**, 2150-2158
187. Sorimachi, H., Hata, S., and Ono, Y. (2011) Calpain chronicle--an enzyme family under multidisciplinary characterization. *Proc Jpn Acad Ser B Phys Biol Sci* **87**, 287-327
188. Ono, Y., and Sorimachi, H. (2012) Calpains: an elaborate proteolytic system. *Biochimica et biophysica acta* **1824**, 224-236
189. Sorimachi, H., Hata, S., and Ono, Y. (2011) Impact of genetic insights into calpain biology. *J Biochem* **150**, 23-37
190. Maki, M., Narayana, S. V., and Hitomi, K. (1997) A growing family of the Ca2+-binding proteins with five EF-hand motifs. *The Biochemical journal* **328 (Pt 2)**, 718-720
191. Croall, D. E., Chacko, S., and Wang, Z. (1996) Cleavage of caldesmon and calponin by calpain: substrate recognition is not dependent on calmodulin binding domains. *Biochimica et biophysica acta* **1298**, 276-284
192. Fischer, S., Vandekerckhove, J., Ampe, C., Traub, P., and Weber, K. (1986) Protein-chemical identification of the major cleavage sites of the Ca2+ proteinase on murine vimentin, the mesenchymal intermediate filament protein. *Biol Chem Hoppe Seyler* **367**, 1147-1152
193. Stabach, P. R., Cianci, C. D., Glantz, S. B., Zhang, Z., and Morrow, J. S. (1997) Site-directed mutagenesis of alpha II spectrin at codon 1175 modulates its mu-calpain susceptibility. *Biochemistry* **36**, 57-65
194. Franco, S., Perrin, B., and Huttenlocher, A. (2004) Isoform specific function of calpain 2 in regulating membrane protrusion. *Exp Cell Res* **299**, 179-187
195. Lokuta, M. A., Nuzzi, P. A., and Huttenlocher, A. (2003) Calpain regulates neutrophil chemotaxis. *Proc Natl Acad Sci U S A* **100**, 4006-4011
196. Goll, D. E., Thompson, V. F., Li, H., Wei, W., and Cong, J. (2003) The calpain system. *Physiol Rev* **83**, 731-801
197. Hanna, R. A., Campbell, R. L., and Davies, P. L. (2008) Calcium-bound structure of calpain and its mechanism of inhibition by calpastatin. *Nature* **456**, 409-412
198. Moldoveanu, T., Hosfield, C. M., Lim, D., Elce, J. S., Jia, Z., and Davies, P. L. (2002) A Ca(2+) switch aligns the active site of calpain. *Cell* **108**, 649-660
199. Tompa, P., Emori, Y., Sorimachi, H., Suzuki, K., and Friedrich, P. (2001) Domain III of calpain is a ca2+-regulated phospholipid-binding domain. *Biochem Biophys Res Commun* **280**, 1333-1339
200. Arthur, J. S., Elce, J. S., Hegadorn, C., Williams, K., and Greer, P. A. (2000) Disruption of the murine calpain small subunit gene, Capn4: calpain is essential for embryonic development but not for cell growth and division. *Mol Cell Biol* **20**, 4474-4481

201. Franco, S. J., and Huttenlocher, A. (2005) Regulating cell migration: calpains make the cut. *J Cell Sci* **118**, 3829-3838
202. Huttenlocher, A., Palecek, S. P., Lu, Q., Zhang, W., Mellgren, R. L., Lauffenburger, D. A., Ginsberg, M. H., and Horwitz, A. F. (1997) Regulation of cell migration by the calcium-dependent protease calpain. *J Biol Chem* **272**, 32719-32722
203. Palecek, S. P., Huttenlocher, A., Horwitz, A. F., and Lauffenburger, D. A. (1998) Physical and biochemical regulation of integrin release during rear detachment of migrating cells. *J Cell Sci* **111 (Pt 7)**, 929-940
204. Calderwood, D. A., Zent, R., Grant, R., Rees, D. J., Hynes, R. O., and Ginsberg, M. H. (1999) The Talin head domain binds to integrin beta subunit cytoplasmic tails and regulates integrin activation. *J Biol Chem* **274**, 28071-28074
205. Yan, B., Calderwood, D. A., Yaspan, B., and Ginsberg, M. H. (2001) Calpain cleavage promotes talin binding to the beta 3 integrin cytoplasmic domain. *J Biol Chem* **276**, 28164-28170
206. Calderwood, D. A., Yan, B., de Pereda, J. M., Alvarez, B. G., Fujioka, Y., Liddington, R. C., and Ginsberg, M. H. (2002) The phosphotyrosine binding-like domain of talin activates integrins. *J Biol Chem* **277**, 21749-21758
207. Bhatt, A., Kaverina, I., Otey, C., and Huttenlocher, A. (2002) Regulation of focal complex composition and disassembly by the calcium-dependent protease calpain. *J Cell Sci* **115**, 3415-3425
208. Paulhe, F., Bogyo, A., Chap, H., Perret, B., and Racaud-Sultan, C. (2001) Vascular smooth muscle cell spreading onto fibrinogen is regulated by calpains and phospholipase C. *Biochem Biophys Res Commun* **288**, 875-881
209. Parnaud, G., Hammar, E., Rouiller, D. G., and Bosco, D. (2005) Inhibition of calpain blocks pancreatic beta-cell spreading and insulin secretion. *Am J Physiol Endocrinol Metab* **289**, E313-321
210. Rock, M. T., Dix, A. R., Brooks, W. H., and Roszman, T. L. (2000) Beta1 integrin-mediated T cell adhesion and cell spreading are regulated by calpain. *Exp Cell Res* **261**, 260-270
211. Croce, K., Flaumenhaft, R., Rivers, M., Furie, B., Furie, B. C., Herman, I. M., and Potter, D. A. (1999) Inhibition of calpain blocks platelet secretion, aggregation, and spreading. *J Biol Chem* **274**, 36321-36327
212. Potter, D. A., Tirnauer, J. S., Janssen, R., Croall, D. E., Hughes, C. N., Fiacco, K. A., Mier, J. W., Maki, M., and Herman, I. M. (1998) Calpain regulates actin remodeling during cell spreading. *J Cell Biol* **141**, 647-662
213. Kulkarni, S., Goll, D. E., and Fox, J. E. (2002) Calpain cleaves RhoA generating a dominant-negative form that inhibits integrin-induced actin filament assembly and cell spreading. *J Biol Chem* **277**, 24435-24441
214. Baudry, M., and Bi, X. (2016) Calpain-1 and Calpain-2: The Yin and Yang of Synaptic Plasticity and Neurodegeneration. *Trends Neurosci* **39**, 235-245

215. Santos, D. M., Xavier, J. M., Morgado, A. L., Sola, S., and Rodrigues, C. M. (2012) Distinct regulatory functions of calpain 1 and 2 during neural stem cell self-renewal and differentiation. *PLoS One* **7**, e33468
216. Gonen, H., Shkedy, D., Barnoy, S., Kosower, N. S., and Ciechanover, A. (1997) On the involvement of calpains in the degradation of the tumor suppressor protein p53. *FEBS letters* **406**, 17-22
217. Atencio, I. A., Ramachandra, M., Shabram, P., and Demers, G. W. (2000) Calpain inhibitor 1 activates p53-dependent apoptosis in tumor cell lines. *Cell Growth Differ* **11**, 247-253
218. Storr, S. J., Carragher, N. O., Frame, M. C., Parr, T., and Martin, S. G. (2011) The calpain system and cancer. *Nature reviews. Cancer* **11**, 364-374
219. Conacci-Sorrell, M., Ngouenet, C., and Eisenman, R. N. (2010) Myc-nick: a cytoplasmic cleavage product of Myc that promotes alpha-tubulin acetylation and cell differentiation. *Cell* **142**, 480-493
220. Small, G. W., Chou, T. Y., Dang, C. V., and Orlowski, R. Z. (2002) Evidence for involvement of calpain in c-Myc proteolysis in vivo. *Archives of biochemistry and biophysics* **400**, 151-161
221. Niapour, M., Yu, Y., and Berger, S. A. (2008) Regulation of calpain activity by c-Myc through calpastatin and promotion of transformation in c-Myc-negative cells by calpastatin suppression. *J Biol Chem* **283**, 21371-21381
222. Gafni, J., Cong, X., Chen, S. F., Gibson, B. W., and Ellerby, L. M. (2009) Calpain-1 cleaves and activates caspase-7. *J Biol Chem* **284**, 25441-25449
223. Tan, Y., Dourdin, N., Wu, C., De Veyra, T., Elce, J. S., and Greer, P. A. (2006) Ubiquitous calpains promote caspase-12 and JNK activation during endoplasmic reticulum stress-induced apoptosis. *J Biol Chem* **281**, 16016-16024
224. Mandic, A., Viktorsson, K., Strandberg, L., Heiden, T., Hansson, J., Linder, S., and Shoshan, M. C. (2002) Calpain-mediated Bid cleavage and calpain-independent Bak modulation: two separate pathways in cisplatin-induced apoptosis. *Mol Cell Biol* **22**, 3003-3013
225. Gao, G., and Dou, Q. P. (2000) N-terminal cleavage of bax by calpain generates a potent proapoptotic 18-kDa fragment that promotes bcl-2-independent cytochrome C release and apoptotic cell death. *J Cell Biochem* **80**, 53-72
226. Braun, C., Engel, M., Seifert, M., Theisinger, B., Seitz, G., Zang, K. D., and Welter, C. (1999) Expression of calpain I messenger RNA in human renal cell carcinoma: correlation with lymph node metastasis and histological type. *Int J Cancer* **84**, 6-9
227. Kimura, Y., Koga, H., Araki, N., Mugita, N., Fujita, N., Takeshima, H., Nishi, T., Yamashima, T., Saido, T. C., Yamasaki, T., Moritake, K., Saya, H., and Nakao, M. (1998) The involvement of calpain-dependent proteolysis of the tumor suppressor NF2 (merlin) in schwannomas and meningiomas. *Nat Med* **4**, 915-922

228. Yu, L. M., Zhu, Y. S., Xu, C. Z., Zhou, L. L., Xue, Z. X., and Cai, Z. Z. (2018) High calpain-1 expression predicts a poor clinical outcome and contributes to tumor progression in pancreatic cancer patients. *Clin Transl Oncol*
229. Lakshmikuttyamma, A., Selvakumar, P., Kanthan, R., Kanthan, S. C., and Sharma, R. K. (2004) Overexpression of m-calpain in human colorectal adenocarcinomas. *Cancer Epidemiol Biomarkers Prev* **13**, 1604-1609
230. Xu, F., Gu, J., Lu, C., Mao, W., Wang, L., Zhu, Q., Liu, Z., Chu, Y., Liu, R., and Ge, D. (2019) Calpain-2 Enhances Non-Small Cell Lung Cancer Progression and Chemoresistance to Paclitaxel via EGFR-pAKT Pathway. *Int J Biol Sci* **15**, 127-137
231. Lee, S. J., Kim, B. G., Choi, Y. L., and Lee, J. W. (2008) Increased expression of calpain 6 during the progression of uterine cervical neoplasia: immunohistochemical analysis. *Oncol Rep* **19**, 859-863
232. Lee, S. J., Choi, Y. L., Lee, E. J., Kim, B. G., Bae, D. S., Ahn, G. H., and Lee, J. H. (2007) Increased expression of calpain 6 in uterine sarcomas and carcinosarcomas: an immunohistochemical analysis. *Int J Gynecol Cancer* **17**, 248-253
233. Moretti, D., Del Bello, B., Cosci, E., Biagioli, M., Miracco, C., and Maellaro, E. (2009) Novel variants of muscle calpain 3 identified in human melanoma cells: cisplatin-induced changes in vitro and differential expression in melanocytic lesions. *Carcinogenesis* **30**, 960-967
234. Yoshikawa, Y., Mukai, H., Hino, F., Asada, K., and Kato, I. (2000) Isolation of two novel genes, down-regulated in gastric cancer. *Jpn J Cancer Res* **91**, 459-463
235. Mamoune, A., Luo, J. H., Lauffenburger, D. A., and Wells, A. (2003) Calpain-2 as a target for limiting prostate cancer invasion. *Cancer research* **63**, 4632-4640
236. Fan, D. G., Dai, J. Y., Tang, J., Wu, M. M., Sun, S. G., Jiang, J. L., and Fan, Q. Y. (2009) Silencing of calpain expression reduces the metastatic potential of human osteosarcoma cells. *Cell Biol Int* **33**, 1263-1267
237. Liu, L., Xing, D., Chen, W. R., Chen, T., Pei, Y., and Gao, X. (2008) Calpain-mediated pathway dominates cisplatin-induced apoptosis in human lung adenocarcinoma cells as determined by real-time single cell analysis. *Int J Cancer* **122**, 2210-2222
238. Liu, L., Xing, D., and Chen, W. R. (2009) Micro-calpain regulates caspase-dependent and apoptosis inducing factor-mediated caspase-independent apoptotic pathways in cisplatin-induced apoptosis. *Int J Cancer* **125**, 2757-2766
239. Tonnetti, L., Netzel-Arnett, S., Darnell, G. A., Hayes, T., Buzza, M. S., Anglin, I. E., Suhrbier, A., and Antalis, T. M. (2008) SerpinB2 protection of retinoblastoma protein from calpain enhances tumor cell survival. *Cancer research* **68**, 5648-5657
240. Leloup, L., and Wells, A. (2011) Calpains as potential anti-cancer targets. *Expert Opin Ther Targets* **15**, 309-323

241. Karmakar, S., Banik, N. L., and Ray, S. K. (2007) Curcumin suppressed anti-apoptotic signals and activated cysteine proteases for apoptosis in human malignant glioblastoma U87MG cells. *Neurochem Res* **32**, 2103-2113
242. Rajgopal, Y., and Vemuri, M. C. (2002) Calpain activation and alpha-spectrin cleavage in rat brain by ethanol. *Neuroscience letters* **321**, 187-191
243. Jeong, J. C., Shin, W. Y., Kim, T. H., Kwon, C. H., Kim, J. H., Kim, Y. K., and Kim, K. H. (2011) Silibinin induces apoptosis via calpain-dependent AIF nuclear translocation in U87MG human glioma cell death. *J Exp Clin Cancer Res* **30**, 44
244. Gutcher, I., Webb, P. R., and Anderson, N. G. (2003) The isoform-specific regulation of apoptosis by protein kinase C. *Cell Mol Life Sci* **60**, 1061-1070
245. Deng, J. Y., Chen, S. J., Jow, G. M., Hsueh, C. W., and Jeng, C. J. (2009) Dehydroeburicoic acid induces calcium- and calpain-dependent necrosis in human U87MG glioblastomas. *Chem Res Toxicol* **22**, 1817-1826
246. Stupp, R., Mason, W. P., van den Bent, M. J., Weller, M., Fisher, B., Taphoorn, M. J., Belanger, K., Brandes, A. A., Marosi, C., Bogdahn, U., Curschmann, J., Janzer, R. C., Ludwin, S. K., Gorlia, T., Allgeier, A., Lacombe, D., Cairncross, J. G., Eisenhauer, E., and Mirimanoff, R. O. (2005) Radiotherapy plus concomitant and adjuvant temozolomide for glioblastoma. *The New England journal of medicine* **352**, 987-996
247. Sontheimer, H. (2008) A role for glutamate in growth and invasion of primary brain tumors. *Journal of neurochemistry* **105**, 287-295
248. Lyons, S. A., Chung, W. J., Weaver, A. K., Ogunrinu, T., and Sontheimer, H. (2007) Autocrine glutamate signaling promotes glioma cell invasion. *Cancer research* **67**, 9463-9471
249. Jang, H. S., Lal, S., and Greenwood, J. A. (2010) Calpain 2 is required for glioblastoma cell invasion: regulation of matrix metalloproteinase 2. *Neurochem Res* **35**, 1796-1804
250. Nabeshima, K., Inoue, T., Shimao, Y., and Sameshima, T. (2002) Matrix metalloproteinases in tumor invasion: role for cell migration. *Pathol Int* **52**, 255-264
251. Ramachandran, R. K., Sorensen, M. D., Aaberg-Jessen, C., Hermansen, S. K., and Kristensen, B. W. (2017) Expression and prognostic impact of matrix metalloproteinase-2 (MMP-2) in astrocytomas. *PLoS One* **12**, e0172234
252. Wang, M., Wang, T., Liu, S., Yoshida, D., and Teramoto, A. (2003) The expression of matrix metalloproteinase-2 and -9 in human gliomas of different pathological grades. *Brain tumor pathology* **20**, 65-72
253. Lal, S., La Du, J., Tanguay, R. L., and Greenwood, J. A. (2012) Calpain 2 is required for the invasion of glioblastoma cells in the zebrafish brain microenvironment. *J Neurosci Res* **90**, 769-781

254. Su, Y., Cui, Z., Li, Z., and Block, E. R. (2006) Calpain-2 regulation of VEGF-mediated angiogenesis. *FASEB journal : official publication of the Federation of American Societies for Experimental Biology* **20**, 1443-1451
255. Kwak, H. I., Kang, H., Dave, J. M., Mendoza, E. A., Su, S. C., Maxwell, S. A., and Bayless, K. J. (2012) Calpain-mediated vimentin cleavage occurs upstream of MT1-MMP membrane translocation to facilitate endothelial sprout initiation. *Angiogenesis* **15**, 287-303
256. Yuen, E. Y., Gu, Z., and Yan, Z. (2007) Calpain regulation of AMPA receptor channels in cortical pyramidal neurons. *J Physiol* **580**, 241-254
257. Rich, D. P., Schworer, C. M., Colbran, R. J., and Soderling, T. R. (1990) Proteolytic activation of calcium/calmodulin-dependent protein kinase II: Putative function in synaptic plasticity. *Molecular and cellular neurosciences* **1**, 107-116
258. Watt, F., and Molloy, P. L. (1993) Specific cleavage of transcription factors by the thiol protease, m-calpain. *Nucleic Acids Res* **21**, 5092-5100
259. Kakkar, R., Raju, R. V., and Sharma, R. K. (1998) In vitro generation of an active calmodulin-independent phosphodiesterase from brain calmodulin-dependent phosphodiesterase (PDE1A2) by m-calpain. *Archives of biochemistry and biophysics* **358**, 320-328
260. Deshpande, R. V., Goust, J. M., Hogan, E. L., and Banik, N. L. (1995) Calpain secreted by activated human lymphoid cells degrades myelin. *J Neurosci Res* **42**, 259-265
261. Hogan, P. G., and Li, H. (2005) Calcineurin. *Current biology : CB* **15**, R442-443
262. Klee, C. B., Crouch, T. H., and Krinks, M. H. (1979) Calcineurin: a calcium- and calmodulin-binding protein of the nervous system. *Proc Natl Acad Sci U S A* **76**, 6270-6273
263. Jain, J., McCaffrey, P. G., Miner, Z., Kerppola, T. K., Lambert, J. N., Verdine, G. L., Curran, T., and Rao, A. (1993) The T-cell transcription factor NFATp is a substrate for calcineurin and interacts with Fos and Jun. *Nature* **365**, 352-355
264. Li, H., Rao, A., and Hogan, P. G. (2011) Interaction of calcineurin with substrates and targeting proteins. *Trends in cell biology* **21**, 91-103
265. Serfling, E., Berberich-Siebelt, F., Chuvpilo, S., Jankevics, E., Klein-Hessling, S., Twardzik, T., and Avots, A. (2000) The role of NF-AT transcription factors in T cell activation and differentiation. *Biochimica et biophysica acta* **1498**, 1-18
266. Hogan, P. G., Chen, L., Nardone, J., and Rao, A. (2003) Transcriptional regulation by calcium, calcineurin, and NFAT. *Genes Dev* **17**, 2205-2232
267. Shaw, K. T., Ho, A. M., Raghavan, A., Kim, J., Jain, J., Park, J., Sharma, S., Rao, A., and Hogan, P. G. (1995) Immunosuppressive drugs prevent a rapid dephosphorylation of transcription factor NFAT1 in stimulated immune cells. *Proc Natl Acad Sci U S A* **92**, 11205-11209
268. Liu, J., Farmer, J. D., Jr., Lane, W. S., Friedman, J., Weissman, I., and Schreiber, S. L. (1991) Calcineurin is a common target of cyclophilin-cyclosporin A and FKBP-FK506 complexes. *Cell* **66**, 807-815

269. Matsuda, S., Shibasaki, F., Takehana, K., Mori, H., Nishida, E., and Koyasu, S. (2000) Two distinct action mechanisms of immunophilin-ligand complexes for the blockade of T-cell activation. *EMBO reports* **1**, 428-434
270. Klee, C. B., Ren, H., and Wang, X. (1998) Regulation of the calmodulin-stimulated protein phosphatase, calcineurin. *J Biol Chem* **273**, 13367-13370
271. Yang, S. A., and Klee, C. B. (2000) Low affinity Ca2+-binding sites of calcineurin B mediate conformational changes in calcineurin A. *Biochemistry* **39**, 16147-16154
272. Kissinger, C. R., Parge, H. E., Knighton, D. R., Lewis, C. T., Pelletier, L. A., Tempczyk, A., Kalish, V. J., Tucker, K. D., Showalter, R. E., Moomaw, E. W., and et al. (1995) Crystal structures of human calcineurin and the human FKBP12-FK506-calcineurin complex. *Nature* **378**, 641-644
273. Vega, R. B., Rothermel, B. A., Weinheimer, C. J., Kovacs, A., Naseem, R. H., Bassel-Duby, R., Williams, R. S., and Olson, E. N. (2003) Dual roles of modulatory calcineurin-interacting protein 1 in cardiac hypertrophy. *Proc Natl Acad Sci U S A* **100**, 669-674
274. Sanna, B., Brandt, E. B., Kaiser, R. A., Pfluger, P., Witt, S. A., Kimball, T. R., van Rooij, E., De Windt, L. J., Rothenberg, M. E., Tschop, M. H., Benoit, S. C., and Molkentin, J. D. (2006) Modulatory calcineurin-interacting proteins 1 and 2 function as calcineurin facilitators in vivo. *Proc Natl Acad Sci U S A* **103**, 7327-7332
275. Kingsbury, T. J., and Cunningham, K. W. (2000) A conserved family of calcineurin regulators. *Genes Dev* **14**, 1595-1604
276. Martinez-Martinez, S., Genesca, L., Rodriguez, A., Raya, A., Salichs, E., Were, F., Lopez-Maderuelo, M. D., Redondo, J. M., and de la Luna, S. (2009) The RCAN carboxyl end mediates calcineurin docking-dependent inhibition via a site that dictates binding to substrates and regulators. *Proc Natl Acad Sci U S A* **106**, 6117-6122
277. Shibasaki, F., and McKeon, F. (1995) Calcineurin functions in Ca(2+)-activated cell death in mammalian cells. *J Cell Biol* **131**, 735-743
278. Hallhuber, M., Burkard, N., Wu, R., Buch, M. H., Engelhardt, S., Hein, L., Neyses, L., Schuh, K., and Ritter, O. (2006) Inhibition of nuclear import of calcineurin prevents myocardial hypertrophy. *Circulation research* **99**, 626-635
279. Shibasaki, F., Price, E. R., Milan, D., and McKeon, F. (1996) Role of kinases and the phosphatase calcineurin in the nuclear shuttling of transcription factor NF-AT4. *Nature* **382**, 370-373
280. Liu, F., Grundke-Iqbal, I., Iqbal, K., Oda, Y., Tomizawa, K., and Gong, C. X. (2005) Truncation and activation of calcineurin A by calpain I in Alzheimer disease brain. *J Biol Chem* **280**, 37755-37762
281. Burkard, N., Becher, J., Heindl, C., Neyses, L., Schuh, K., and Ritter, O. (2005) Targeted proteolysis sustains calcineurin activation. *Circulation* **111**, 1045-1053
282. Wu, H. Y., Tomizawa, K., Oda, Y., Wei, F. Y., Lu, Y. F., Matsushita, M., Li, S. T., Moriwaki, A., and Matsui, H. (2004) Critical role of calpain-mediated

cleavage of calcineurin in excitotoxic neurodegeneration. *J Biol Chem* **279**, 4929-4940
283. Brun, M., and Godbout, R. (2016) Activation of calcineurin in cancer: many paths, one hub. *Translational Cancer Research*, S497-S506
284. Maravall, M., Mainen, Z. F., Sabatini, B. L., and Svoboda, K. (2000) Estimating intracellular calcium concentrations and buffering without wavelength ratioing. *Biophys J* **78**, 2655-2667
285. Suzuki, K., Tsuji, S., Ishiura, S., Kimura, Y., Kubota, S., and Imahori, K. (1981) Autolysis of calcium-activated neutral protease of chicken skeletal muscle. *J Biochem* **90**, 1787-1793
286. Suzuki, K., Tsuji, S., Kubota, S., Kimura, Y., and Imahori, K. (1981) Limited autolysis of Ca2+-activated neutral protease (CANP) changes its sensitivity to Ca2+ ions. *J Biochem* **90**, 275-278
287. Edmunds, T., Nagainis, P. A., Sathe, S. K., Thompson, V. F., and Goll, D. E. (1991) Comparison of the autolyzed and unautolyzed forms of mu- and m-calpain from bovine skeletal muscle. *Biochimica et biophysica acta* **1077**, 197-208
288. Kuboki, M., Ishii, H., and Kazama, M. (1987) Procalpain is activated on the plasma membrane and the calpain acts on the membrane. *Biochimica et biophysica acta* **929**, 164-172
289. Hayashi, M., Saito, Y., and Kawashima, S. (1992) Calpain activation is essential for membrane fusion of erythrocytes in the presence of exogenous Ca2+. *Biochem Biophys Res Commun* **182**, 939-946
290. Cottin, P., Poussard, S., Desmazes, J. P., Georgescauld, D., and Ducastaing, A. (1991) Free calcium and calpain I activity. *Biochimica et biophysica acta* **1079**, 139-145
291. Goll, D. E., Thompson, V. F., Taylor, R. G., and Zalewska, T. (1992) Is calpain activity regulated by membranes and autolysis or by calcium and calpastatin? *Bioessays* **14**, 549-556
292. Crawford, C., Brown, N. R., and Willis, A. C. (1993) Studies of the active site of m-calpain and the interaction with calpastatin. *The Biochemical journal* **296 (Pt 1)**, 135-142
293. Molinari, M., Anagli, J., and Carafoli, E. (1994) Ca(2+)-activated neutral protease is active in the erythrocyte membrane in its nonautolyzed 80-kDa form. *J Biol Chem* **269**, 27992-27995
294. Zimmerman, U. J., and Schlaepfer, W. W. (1991) Two-stage autolysis of the catalytic subunit initiates activation of calpain I. *Biochimica et biophysica acta* **1078**, 192-198
295. Saido, T. C., Nagao, S., Shiramine, M., Tsukaguchi, M., Sorimachi, H., Murofushi, H., Tsuchiya, T., Ito, H., and Suzuki, K. (1992) Autolytic transition of mu-calpain upon activation as resolved by antibodies distinguishing between the pre- and post-autolysis forms. *J Biochem* **111**, 81-86
296. Saido, T. C., Suzuki, H., Yamazaki, H., Tanoue, K., and Suzuki, K. (1993) In situ capture of mu-calpain activation in platelets. *J Biol Chem* **268**, 7422-7426

297. Fox, J. E., Goll, D. E., Reynolds, C. C., and Phillips, D. R. (1985) Identification of two proteins (actin-binding protein and P235) that are hydrolyzed by endogenous Ca2+-dependent protease during platelet aggregation. *J Biol Chem* **260**, 1060-1066
298. Fox, J. E., Reynolds, C. C., Morrow, J. S., and Phillips, D. R. (1987) Spectrin is associated with membrane-bound actin filaments in platelets and is hydrolyzed by the Ca2+-dependent protease during platelet activation. *Blood* **69**, 537-545
299. Li, H., Thompson, V. F., and Goll, D. E. (2004) Effects of autolysis on properties of mu- and m-calpain. *Biochimica et biophysica acta* **1691**, 91-103
300. Coolican, S. A., and Hathaway, D. R. (1984) Effect of L-alpha-phosphatidylinositol on a vascular smooth muscle Ca2+-dependent protease. Reduction of the Ca2+ requirement for autolysis. *J Biol Chem* **259**, 11627-11630
301. Pontremoli, S., Viotti, P. L., Michetti, M., Sparatore, B., Salamino, F., and Melloni, E. (1990) Identification of an endogenous activator of calpain in rat skeletal muscle. *Biochem Biophys Res Commun* **171**, 569-574
302. Pontremoli, S., Melloni, E., Michetti, M., Salamino, F., Sparatore, B., and Horecker, B. L. (1988) An endogenous activator of the Ca2+-dependent proteinase of human neutrophils that increases its affinity for Ca2+. *Proc Natl Acad Sci U S A* **85**, 1740-1743
303. Melloni, E., Michetti, M., Salamino, F., and Pontremoli, S. (1998) Molecular and functional properties of a calpain activator protein specific for mu-isoforms. *J Biol Chem* **273**, 12827-12831
304. Glading, A., Bodnar, R. J., Reynolds, I. J., Shiraha, H., Satish, L., Potter, D. A., Blair, H. C., and Wells, A. (2004) Epidermal growth factor activates m-calpain (calpain II), at least in part, by extracellular signal-regulated kinase-mediated phosphorylation. *Mol Cell Biol* **24**, 2499-2512
305. Glading, A., Uberall, F., Keyse, S. M., Lauffenburger, D. A., and Wells, A. (2001) Membrane proximal ERK signaling is required for M-calpain activation downstream of epidermal growth factor receptor signaling. *J Biol Chem* **276**, 23341-23348
306. Leloup, L., Shao, H., Bae, Y. H., Deasy, B., Stolz, D., Roy, P., and Wells, A. (2010) m-Calpain activation is regulated by its membrane localization and by its binding to phosphatidylinositol 4,5-bisphosphate. *J Biol Chem* **285**, 33549-33566
307. Shiraha, H., Glading, A., Chou, J., Jia, Z., and Wells, A. (2002) Activation of m-calpain (calpain II) by epidermal growth factor is limited by protein kinase A phosphorylation of m-calpain. *Mol Cell Biol* **22**, 2716-2727
308. Yoshizawa, T., Sorimachi, H., Tomioka, S., Ishiura, S., and Suzuki, K. (1995) A catalytic subunit of calpain possesses full proteolytic activity. *FEBS letters* **358**, 101-103
309. Nishiura, I., Tanaka, K., and Murachi, T. (1979) A high molecular weight inhibitor of Ca2+ -dependent neutral protease in rat brain. *Experientia* **35**, 1006-1007

310. Takano, E., and Murachi, T. (1982) Purification and some properties of human erythrocyte calpastatin. *J Biochem* **92**, 2021-2028
311. Imajoh, S., Kawasaki, H., Kisaragi, M., Mukai, M., Sugita, H., and Suzuki, K. (1984) *A 107-kDa INHIBITOR FOR CALCIUM-ACTIVATED NEUTRAL PROTEASE (CANP): PURIFICATION FROM THE HUMAN LIVER*,
312. Mellgren, R. L., and Carr, T. C. (1983) The protein inhibitor of calcium-dependent proteases: purification from bovine heart and possible mechanisms of regulation. *Archives of biochemistry and biophysics* **225**, 779-786
313. Takahashi-Nakamura, M., Tsuji, S., Suzuki, K., and Imahori, K. (1981) Purification and characterization of an inhibitor of calcium-activated neutral protease from rabbit skeletal muscle. *J Biochem* **90**, 1583-1589
314. Lepley, R. A., Pampusch, M., and Dayton, W. R. (1985) Purification of a high-molecular-weight inhibitor of the calcium-activated proteinase. *Biochimica et biophysica acta* **828**, 95-103
315. Otsuka, Y., and Goll, D. E. (1987) Purification of the Ca2+-dependent proteinase inhibitor from bovine cardiac muscle and its interaction with the millimolar Ca2+-dependent proteinase. *J Biol Chem* **262**, 5839-5851
316. Mohan, P. S., and Nixon, R. A. (1995) Purification and properties of high molecular weight calpastatin from bovine brain. *Journal of neurochemistry* **64**, 859-866
317. Konno, T., Tanaka, N., Kataoka, M., Takano, E., and Maki, M. (1997) A circular dichroism study of preferential hydration and alcohol effects on a denatured protein, pig calpastatin domain I. *Biochimica et biophysica acta* **1342**, 73-82
318. Uemori, T., Shimojo, T., Asada, K., Asano, T., Kimizuka, F., Kato, I., Maki, M., Hatanaka, M., Murachi, T., Hanzawa, H., and et al. (1990) Characterization of a functional domain of human calpastatin. *Biochem Biophys Res Commun* **166**, 1485-1493
319. Emori, Y., Kawasaki, H., Imajoh, S., Minami, Y., and Suzuki, K. (1988) All four repeating domains of the endogenous inhibitor for calcium-dependent protease independently retain inhibitory activity. Expression of the cDNA fragments in Escherichia coli. *J Biol Chem* **263**, 2364-2370
320. Takano, E., Maki, M., Mori, H., Hatanaka, M., Marti, T., Titani, K., Kannagi, R., Ooi, T., and Murachi, T. (1988) Pig heart calpastatin: identification of repetitive domain structures and anomalous behavior in polyacrylamide gel electrophoresis. *Biochemistry* **27**, 1964-1972
321. Inazawa, J., Nakagawa, H., Misawa, S., Abe, T., Minoshima, S., Fukuyama, R., Maki, M., Murachi, T., Hatanaka, M., and Shimizu, N. (1990) Assignment of the human calpastatin gene (CAST) to chromosome 5 at region q14----q22. *Cytogenetics and cell genetics* **54**, 156-158
322. De Tullio, R., Averna, M., Stifanese, R., Parr, T., Bardsley, R. G., Pontremoli, S., and Melloni, E. (2007) Multiple rat brain calpastatin forms are produced by distinct starting points and alternative splicing of the N-terminal exons. *Archives of biochemistry and biophysics* **465**, 148-156

323. Takano, J., Watanabe, M., Hitomi, K., and Maki, M. (2000) Four types of calpastatin isoforms with distinct amino-terminal sequences are specified by alternative first exons and differentially expressed in mouse tissues. *J Biochem* **128**, 83-92
324. Lee, W. J., Ma, H., Takano, E., Yang, H. Q., Hatanaka, M., and Maki, M. (1992) Molecular diversity in amino-terminal domains of human calpastatin by exon skipping. *J Biol Chem* **267**, 8437-8442
325. Cong, M., Thompson, V. F., Goll, D. E., and Antin, P. B. (1998) The bovine calpastatin gene promoter and a new N-terminal region of the protein are targets for cAMP-dependent protein kinase activity. *J Biol Chem* **273**, 660-666
326. Li, S., and Goldberg, E. (2000) A novel N-terminal domain directs membrane localization of mouse testis-specific calpastatin. *Biology of reproduction* **63**, 1594-1600
327. Parr, T., Sensky, P. L., Bardsley, R. G., and Buttery, P. J. (2001) Calpastatin expression in porcine cardiac and skeletal muscle and partial gene structure. *Archives of biochemistry and biophysics* **395**, 1-13
328. De Tullio, R., Sparatore, B., Salamino, F., Melloni, E., and Pontremoli, S. (1998) Rat brain contains multiple mRNAs for calpastatin. *FEBS letters* **422**, 113-117
329. Lee, W. J., Hatanaka, M., and Maki, M. (1992) Multiple forms of rat calpastatin cDNA in the coding region of functionally unknown amino-terminal domain. *Biochimica et biophysica acta* **1129**, 251-253
330. Melloni, E., De Tullio, R., Averna, M., Tedesco, I., Salamino, F., Sparatore, B., and Pontremoli, S. (1998) Properties of calpastatin forms in rat brain. *FEBS letters* **431**, 55-58
331. Mellgren, R. L. (2017) *Intracellular calcium-dependent proteolysis*, CRC Press, [Place of publication not identified]
332. Kawasaki, H., Emori, Y., Imajoh-Ohmi, S., Minami, Y., and Suzuki, K. (1989) Identification and characterization of inhibitory sequences in four repeating domains of the endogenous inhibitor for calcium-dependent protease. *J Biochem* **106**, 274-281
333. Maki, M., Takano, E., Mori, H., Kannagi, R., Murachi, T., and Hatanaka, M. (1987) Repetitive region of calpastatin is a functional unit of the proteinase inhibitor. *Biochem Biophys Res Commun* **143**, 300-308
334. Maki, M., Takano, E., Mori, H., Sato, A., Murachi, T., and Hatanaka, M. (1987) All four internally repetitive domains of pig calpastatin possess inhibitory activities against calpains I and II. *FEBS letters* **223**, 174-180
335. Salamino, F., De Tullio, R., Michetti, M., Mengotti, P., Melloni, E., and Pontremoli, S. (1994) Modulation of calpastatin specificity in rat tissues by reversible phosphorylation and dephosphorylation. *Biochem Biophys Res Commun* **199**, 1326-1332
336. Maki, M., Takano, E., Osawa, T., Ooi, T., Murachi, T., and Hatanaka, M. (1988) Analysis of structure-function relationship of pig calpastatin by expression of mutated cDNAs in Escherichia coli. *J Biol Chem* **263**, 10254-10261

337. Maki, M., Bagci, H., Hamaguchi, K., Ueda, M., Murachi, T., and Hatanaka, M. (1989) Inhibition of calpain by a synthetic oligopeptide corresponding to an exon of the human calpastatin gene. *J Biol Chem* **264**, 18866-18869
338. Cottin, P., Vidalenc, P. L., and Ducastaing, A. (1981) Ca2+-dependent association between a Ca2+-activated neutral proteinase (CaANP) and its specific inhibitor. *FEBS letters* **136**, 221-224
339. Imajoh, S., and Suzuki, K. (1985) Reversible interaction between Ca2+-activated neutral protease (CANP) and its endogenous inhibitor. *FEBS letters* **187**, 47-50
340. Kapprell, H. P., and Goll, D. E. (1989) Effect of Ca2+ on binding of the calpains to calpastatin. *J Biol Chem* **264**, 17888-17896
341. Takano, E., Ma, H., Yang, H. Q., Maki, M., and Hatanaka, M. (1995) Preference of calcium-dependent interactions between calmodulin-like domains of calpain and calpastatin subdomains. *FEBS letters* **362**, 93-97
342. Yang, H. Q., Ma, H., Takano, E., Hatanaka, M., and Maki, M. (1994) Analysis of calcium-dependent interaction between amino-terminal conserved region of calpastatin functional domain and calmodulin-like domain of mu-calpain large subunit. *J Biol Chem* **269**, 18977-18984
343. Kawasaki, H., Emori, Y., and Suzuki, K. (1993) Calpastatin has two distinct sites for interaction with calpain--effect of calpastatin fragments on the binding of calpain to membranes. *Archives of biochemistry and biophysics* **305**, 467-472
344. Adachi, Y., Ishida-Takahashi, A., Takahashi, C., Takano, E., Murachi, T., and Hatanaka, M. (1991) Phosphorylation and subcellular distribution of calpastatin in human hematopoietic system cells. *J Biol Chem* **266**, 3968-3972
345. Gil-Parrado, S., Popp, O., Knoch, T. A., Zahler, S., Bestvater, F., Felgentrager, M., Holloschi, A., Fernandez-Montalvan, A., Auerswald, E. A., Fritz, H., Fuentes-Prior, P., Machleidt, W., and Spiess, E. (2003) Subcellular localization and in vivo subunit interactions of ubiquitous mu-calpain. *J Biol Chem* **278**, 16336-16346
346. Stifanese, R., Averna, M., De Tullio, R., Pedrazzi, M., Beccaria, F., Salamino, F., Milanese, M., Bonanno, G., Pontremoli, S., and Melloni, E. (2010) Adaptive modifications in the calpain/calpastatin system in brain cells after persistent alteration in Ca2+ homeostasis. *J Biol Chem* **285**, 631-643
347. Geesink, G. H., Nonneman, D., and Koohmaraie, M. (1998) An improved purification protocol for heart and skeletal muscle calpastatin reveals two isoforms resulting from alternative splicing. *Archives of biochemistry and biophysics* **356**, 19-24
348. De Tullio, R., Franchi, A., Martines, A., Averna, M., Pedrazzi, M., Melloni, E., and Sparatore, B. (2018) Unexpected role of the L-domain of calpastatin during the autoproteolytic activation of human erythrocyte calpain. *Biosci Rep* **38**
349. Melloni, E., Averna, M., Stifanese, R., De Tullio, R., Defranchi, E., Salamino, F., and Pontremoli, S. (2006) Association of calpastatin with

inactive calpain: a novel mechanism to control the activation of the protease? *J Biol Chem* **281**, 24945-24954
350. De Tullio, R., Cantoni, C., Broggio, C., Prato, C., Stifanese, R., Averna, M., Antolini, R., Pontremoli, S., and Melloni, E. (2009) Involvement of exon 6-mediated calpastatin intracellular movements in the modulation of calpain activation. *Biochimica et biophysica acta* **1790**, 182-187
351. Averna, M., de Tullio, R., Passalacqua, M., Salamino, F., Pontremoli, S., and Melloni, E. (2001) Changes in intracellular calpastatin localization are mediated by reversible phosphorylation. *The Biochemical journal* **354**, 25-30
352. Minobe, E., Asmara, H., Saud, Z. A., and Kameyama, M. (2011) Calpastatin domain L is a partial agonist of the calmodulin-binding site for channel activation in Cav1.2 Ca2+ channels. *J Biol Chem* **286**, 39013-39022
353. Hao, L. Y., Kameyama, A., Kuroki, S., Takano, J., Takano, E., Maki, M., and Kameyama, M. (2000) Calpastatin domain L is involved in the regulation of L-type Ca2+ channels in guinea pig cardiac myocytes. *Biochem Biophys Res Commun* **279**, 756-761
354. Claes, A., Idema, A. J., and Wesseling, P. (2007) Diffuse glioma growth: a guerilla war. *Acta neuropathologica* **114**, 443-458
355. de Groot, J. F., Fuller, G., Kumar, A. J., Piao, Y., Eterovic, K., Ji, Y., and Conrad, C. A. (2010) Tumor invasion after treatment of glioblastoma with bevacizumab: radiographic and pathologic correlation in humans and mice. *Neuro Oncol* **12**, 233-242
356. Kallenberg, K., Goldmann, T., Menke, J., Strik, H., Bock, H. C., Stockhammer, F., Buhk, J. H., Frahm, J., Dechent, P., and Knauth, M. (2013) Glioma infiltration of the corpus callosum: early signs detected by DTI. *J Neurooncol* **112**, 217-222
357. Norden, A. D., Young, G. S., Setayesh, K., Muzikansky, A., Klufas, R., Ross, G. L., Ciampa, A. S., Ebbeling, L. G., Levy, B., Drappatz, J., Kesari, S., and Wen, P. Y. (2008) Bevacizumab for recurrent malignant gliomas: efficacy, toxicity, and patterns of recurrence. *Neurology* **70**, 779-787
358. Ogura, K., Mizowaki, T., Arakawa, Y., Ogura, M., Sakanaka, K., Miyamoto, S., and Hiraoka, M. (2013) Initial and cumulative recurrence patterns of glioblastoma after temozolomide-based chemoradiotherapy and salvage treatment: a retrospective cohort study in a single institution. *Radiation oncology* **8**, 97
359. Shankar, A., Kumar, S., Iskander, A. S., Varma, N. R., Janic, B., deCarvalho, A., Mikkelsen, T., Frank, J. A., Ali, M. M., Knight, R. A., Brown, S., and Arbab, A. S. (2014) Subcurative radiation significantly increases cell proliferation, invasion, and migration of primary glioblastoma multiforme in vivo. *Chinese journal of cancer* **33**, 148-158
360. Liang, Y., Diehn, M., Watson, N., Bollen, A. W., Aldape, K. D., Nicholas, M. K., Lamborn, K. R., Berger, M. S., Botstein, D., Brown, P. O., and Israel, M. A. (2005) Gene expression profiling reveals molecularly and

clinically distinct subtypes of glioblastoma multiforme. *Proc Natl Acad Sci U S A* **102**, 5814-5819
361. De Rosa, A., Pellegatta, S., Rossi, M., Tunici, P., Magnoni, L., Speranza, M. C., Malusa, F., Miragliotta, V., Mori, E., Finocchiaro, G., and Bakker, A. (2012) A radial glia gene marker, fatty acid binding protein 7 (FABP7), is involved in proliferation and invasion of glioblastoma cells. *PLoS One* **7**, e52113
362. Brun, M., Coles, J. E., Monckton, E. A., Glubrecht, D. D., Bisgrove, D., and Godbout, R. (2009) Nuclear factor I regulates brain fatty acid-binding protein and glial fibrillary acidic protein gene expression in malignant glioma cell lines. *Journal of molecular biology* **391**, 282-300
363. Roulet, E., Bucher, P., Schneider, R., Wingender, E., Dusserre, Y., Werner, T., and Mermod, N. (2000) Experimental analysis and computer prediction of CTF/NFI transcription factor DNA binding sites. *Journal of molecular biology* **297**, 833-848
364. Heng, Y. H., Barry, G., Richards, L. J., and Piper, M. (2012) Nuclear factor I genes regulate neuronal migration. *Neurosignals* **20**, 159-167
365. Kim, M. J., Jo, D. G., Hong, G. S., Kim, B. J., Lai, M., Cho, D. H., Kim, K. W., Bandyopadhyay, A., Hong, Y. M., Kim, D. H., Cho, C., Liu, J. O., Snyder, S. H., and Jung, Y. K. (2002) Calpain-dependent cleavage of cain/cabin1 activates calcineurin to mediate calcium-triggered cell death. *Proc Natl Acad Sci U S A* **99**, 9870-9875
366. Wendt, A., Thompson, V. F., and Goll, D. E. (2004) Interaction of calpastatin with calpain: a review. *Biological chemistry* **385**, 465-472
367. Lane, R. D., Allan, D. M., and Mellgren, R. L. (1992) A comparison of the intracellular distribution of mu-calpain, m-calpain, and calpastatin in proliferating human A431 cells. *Exp Cell Res* **203**, 5-16
368. Perrin, B. J., and Huttenlocher, A. (2002) Calpain. *Int J Biochem Cell Biol* **34**, 722-725
369. Brun, M., Jain, S., Monckton, E. A., and Godbout, R. (2018) Nuclear Factor I Represses the Notch Effector HEY1 in Glioblastoma. *Neoplasia* **20**, 1023-1037
370. Komarnitsky, P., Cho, E. J., and Buratowski, S. (2000) Different phosphorylated forms of RNA polymerase II and associated mRNA processing factors during transcription. *Genes Dev* **14**, 2452-2460
371. Shao, H., Chou, J., Baty, C. J., Burke, N. A., Watkins, S. C., Stolz, D. B., and Wells, A. (2006) Spatial localization of m-calpain to the plasma membrane by phosphoinositide biphosphate binding during epidermal growth factor receptor-mediated activation. *Mol Cell Biol* **26**, 5481-5496
372. Mita, R., Beaulieu, M. J., Field, C., and Godbout, R. (2010) Brain fatty acid-binding protein and omega-3/omega-6 fatty acids: mechanistic insight into malignant glioma cell migration. *J Biol Chem* **285**, 37005-37015
373. Alevizopoulos, A., Dusserre, Y., Ruegg, U., and Mermod, N. (1997) Regulation of the transforming growth factor beta-responsive transcription factor CTF-1 by calcineurin and calcium/calmodulin-dependent protein kinase IV. *J Biol Chem* **272**, 23597-23605

374. Wu, H. Y., Tomizawa, K., and Matsui, H. (2007) Calpain-calcineurin signaling in the pathogenesis of calcium-dependent disorder. *Acta Med Okayama* **61**, 123-137
375. Ding, F., Li, X., Li, B., Guo, J., Zhang, Y., and Ding, J. (2016) Calpain-Mediated Cleavage of Calcineurin in Puromycin Aminonucleoside-Induced Podocyte Injury. *PLoS One* **11**, e0155504
376. Chan, K. T., Bennin, D. A., and Huttenlocher, A. (2010) Regulation of adhesion dynamics by calpain-mediated proteolysis of focal adhesion kinase (FAK). *J Biol Chem* **285**, 11418-11426
377. Lebart, M. C., and Benyamin, Y. (2006) Calpain involvement in the remodeling of cytoskeletal anchorage complexes. *FEBS J* **273**, 3415-3426
378. Cortesio, C. L., Chan, K. T., Perrin, B. J., Burton, N. O., Zhang, S., Zhang, Z. Y., and Huttenlocher, A. (2008) Calpain 2 and PTP1B function in a novel pathway with Src to regulate invadopodia dynamics and breast cancer cell invasion. *J Cell Biol* **180**, 957-971
379. Tangmansakulchai, K., Abubakar, Z., Kitiyanant, N., Suwanjang, W., Leepiyasakulchai, C., Govitrapong, P., and Chetsawang, B. (2016) Calpastatin overexpression reduces oxidative stress-induced mitochondrial impairment and cell death in human neuroblastoma SH-SY5Y cells by decreasing calpain and calcineurin activation, induction of mitochondrial fission and destruction of mitochondrial fusion. *Mitochondrion* **30**, 151-161
380. Schoch, K. M., Evans, H. N., Brelsfoard, J. M., Madathil, S. K., Takano, J., Saido, T. C., and Saatman, K. E. (2012) Calpastatin overexpression limits calpain-mediated proteolysis and behavioral deficits following traumatic brain injury. *Exp Neurol* **236**, 371-382
381. Nilsson, E., Alafuzoff, I., Blennow, K., Blomgren, K., Hall, C. M., Janson, I., Karlsson, I., Wallin, A., Gottfries, C. G., and Karlsson, J. O. (1990) Calpain and calpastatin in normal and Alzheimer-degenerated human brain tissue. *Neurobiol Aging* **11**, 425-431
382. Gronostajski, R. M. (1987) Site-specific DNA binding of nuclear factor I: effect of the spacer region. *Nucleic Acids Res* **15**, 5545-5559
383. Adachi, Y., Takano, E., Murachi, T., and Hatanaka, M. (1988) Distribution and expression of calpastatin in human hematopoietic system cells. *Biol Chem Hoppe Seyler* **369 Suppl**, 223-227
384. Averna, M., De Tullio, R., Capini, P., Salamino, F., Pontremoli, S., and Melloni, E. (2003) Changes in calpastatin localization and expression during calpain activation: a new mechanism for the regulation of intracellular Ca(2+)-dependent proteolysis. *Cell Mol Life Sci* **60**, 2669-2678
385. Perrin, B. J., Amann, K. J., and Huttenlocher, A. (2006) Proteolysis of cortactin by calpain regulates membrane protrusion during cell migration. *Mol Biol Cell* **17**, 239-250
386. Baek, K. H., Yu, H. V., Kim, E., Na, Y., and Kwon, Y. (2016) Calcium influx-mediated translocation of m-calpain induces Ku80 cleavage and

enhances the Ku80-related DNA repair pathway. *Oncotarget* **7**, 30831-30844
387. Baghdiguian, S., Martin, M., Richard, I., Pons, F., Astier, C., Bourg, N., Hay, R. T., Chemaly, R., Halaby, G., Loiselet, J., Anderson, L. V., Lopez de Munain, A., Fardeau, M., Mangeat, P., Beckmann, J. S., and Lefranc, G. (1999) Calpain 3 deficiency is associated with myonuclear apoptosis and profound perturbation of the IkappaB alpha/NF-kappaB pathway in limb-girdle muscular dystrophy type 2A. *Nat Med* **5**, 503-511
388. Tremper-Wells, B., and Vallano, M. L. (2005) Nuclear calpain regulates Ca2+-dependent signaling via proteolysis of nuclear Ca2+/calmodulin-dependent protein kinase type IV in cultured neurons. *J Biol Chem* **280**, 2165-2175
389. Becker-Santos, D. D., Lonergan, K. M., Gronostajski, R. M., and Lam, W. L. (2017) Nuclear Factor I/B: A Master Regulator of Cell Differentiation with Paradoxical Roles in Cancer. *EBioMedicine* **22**, 2-9
390. O'Brien, R. M., Noisin, E. L., Suwanichkul, A., Yamasaki, T., Lucas, P. C., Wang, J. C., Powell, D. R., and Granner, D. K. (1995) Hepatic nuclear factor 3- and hormone-regulated expression of the phosphoenolpyruvate carboxykinase and insulin-like growth factor-binding protein 1 genes. *Mol Cell Biol* **15**, 1747-1758
391. Pillai, S., Dasgupta, P., and Chellappan, S. P. (2009) Chromatin immunoprecipitation assays: analyzing transcription factor binding and histone modifications in vivo. *Methods Mol Biol* **523**, 323-339
392. Melloni, E., Michetti, M., Salamino, F., Minafra, R., and Pontremoli, S. (1996) Modulation of the calpain autoproteolysis by calpastatin and phospholipids. *Biochem Biophys Res Commun* **229**, 193-197
393. Donkor, I. O. (2011) Calpain inhibitors: a survey of compounds reported in the patent and scientific literature. *Expert Opin Ther Pat* **21**, 601-636
394. Figueiredo-Pereira, M. E., Chen, W. E., Li, J., and Johdo, O. (1996) The antitumor drug aclacinomycin A, which inhibits the degradation of ubiquitinated proteins, shows selectivity for the chymotrypsin-like activity of the bovine pituitary 20 S proteasome. *J Biol Chem* **271**, 16455-16459
395. Staib, P., Lathan, B., Knoppel-Schwark, S., Tesch, H., Voliotis, D., Steinmetz, H. T., Schwonzen, M., Wickramanayake, P. D., and Diehl, V. (1998) Cytosine arabinoside, etoposide and aclarubicin (AVA) for the treatment of acute myeloid leukemia (AML) in elderly patients. *Ann Oncol* **9**, 221-223
396. Rothig, H. J., Kraemer, H. P., and Sedlacek, H. H. (1985) Aclarubicin: experimental and clinical experience. *Drugs Exp Clin Res* **11**, 123-125
397. Vo, T. M., Burchett, R., Brun, M., Monckton, E. A., Poon, H. Y., and Godbout, R. (2018) Effects of nuclear factor I phosphorylation on calpastatin (CAST) gene variant expression and subcellular distribution in malignant glioma cells. *J Biol Chem*
398. Dooley, A. L., Winslow, M. M., Chiang, D. Y., Banerji, S., Stransky, N., Dayton, T. L., Snyder, E. L., Senna, S., Whittaker, C. A., Bronson, R. T., Crowley, D., Barretina, J., Garraway, L., Meyerson, M., and Jacks, T.

(2011) Nuclear factor I/B is an oncogene in small cell lung cancer. *Genes Dev* **25**, 1470-1475
399. Liu, R. Z., Vo, T. M., Jain, S., Choi, W. S., Garcia, E., Monckton, E. A., Mackey, J. R., and Godbout, R. (2019) NFIB promotes cell survival by directly suppressing p21 transcription in TP53-mutated triple-negative breast cancer. *J Pathol* **247**, 186-198
400. Riss, T. L., Moravec, R. A., Niles, A. L., Duellman, S., Benink, H. A., Worzella, T. J., and Minor, L. (2004) Cell Viability Assays. in *Assay Guidance Manual* (Sittampalam, G. S., Coussens, N. P., Brimacombe, K., Grossman, A., Arkin, M., Auld, D., Austin, C., Baell, J., Bejcek, B., Caaveiro, J. M. M., Chung, T. D. Y., Dahlin, J. L., Devanaryan, V., Foley, T. L., Glicksman, M., Hall, M. D., Haas, J. V., Inglese, J., Iversen, P. W., Kahl, S. D., Kales, S. C., Lal-Nag, M., Li, Z., McGee, J., McManus, O., Riss, T., Trask, O. J., Jr., Weidner, J. R., Wildey, M. J., Xia, M., and Xu, X. eds.), Bethesda (MD). pp
401. Talamillo, A., Grande, L., Ruiz-Ontanon, P., Velasquez, C., Mollinedo, P., Torices, S., Sanchez-Gomez, P., Aznar, A., Esparis-Ogando, A., Lopez-Lopez, C., Lafita, C., Berciano, M. T., Montero, J. A., Vazquez-Barquero, A., Segura, V., Villagra, N. T., Pandiella, A., Lafarga, M., Leon, J., Martinez-Climent, J. A., Sanz-Moreno, V., and Fernandez-Luna, J. L. (2017) ODZ1 allows glioblastoma to sustain invasiveness through a Myc-dependent transcriptional upregulation of RhoA. *Oncogene* **36**, 1733-1744
402. Yoshioka, K., Nakamori, S., and Itoh, K. (1999) Overexpression of small GTP-binding protein RhoA promotes invasion of tumor cells. *Cancer research* **59**, 2004-2010
403. Liu, R., Page, M., Solheim, K., Fox, S., and Chang, S. M. (2009) Quality of life in adults with brain tumors: current knowledge and future directions. *Neuro Oncol* **11**, 330-339
404. Sheetz, M. P., Felsenfeld, D., Galbraith, C. G., and Choquet, D. (1999) Cell migration as a five-step cycle. *Biochem Soc Symp* **65**, 233-243
405. Zhou, M., Zhou, L., Zheng, L., Guo, L., Wang, Y., Liu, H., Ou, C., and Ding, Z. (2014) miR-365 promotes cutaneous squamous cell carcinoma (CSCC) through targeting nuclear factor I/B (NFIB). *PLoS One* **9**, e100620
406. Storr, S. J., Zhang, S., Perren, T., Lansdown, M., Fatayer, H., Sharma, N., Gahlaut, R., Shaaban, A., and Martin, S. G. (2016) The calpain system is associated with survival of breast cancer patients with large but operable inflammatory and non-inflammatory tumours treated with neoadjuvant chemotherapy. *Oncotarget* **7**, 47927-47937
407. Pu, X., Storr, S. J., Ahmad, N. S., Chan, S. Y., Moseley, P. M., Televantou, D., Cresti, N., Boddy, A., Ellis, I. O., and Martin, S. G. (2016) Calpain-1 is associated with adverse relapse free survival in breast cancer: a confirmatory study. *Histopathology* **68**, 1021-1029
408. Nishimura, T., and Goll, D. E. (1991) Binding of calpain fragments to calpastatin. *J Biol Chem* **266**, 11842-11850
409. Mirabello, L., Koster, R., Moriarity, B. S., Spector, L. G., Meltzer, P. S., Gary, J., Machiela, M. J., Pankratz, N., Panagiotou, O. A., Largaespada,

D., Wang, Z., Gastier-Foster, J. M., Gorlick, R., Khanna, C., de Toledo, S. R., Petrilli, A. S., Patino-Garcia, A., Sierrasesumaga, L., Lecanda, F., Andrulis, I. L., Wunder, J. S., Gokgoz, N., Serra, M., Hattinger, C., Picci, P., Scotlandi, K., Flanagan, A. M., Tirabosco, R., Amary, M. F., Halai, D., Ballinger, M. L., Thomas, D. M., Davis, S., Barkauskas, D. A., Marina, N., Helman, L., Otto, G. M., Becklin, K. L., Wolf, N. K., Weg, M. T., Tucker, M., Wacholder, S., Fraumeni, J. F., Jr., Caporaso, N. E., Boland, J. F., Hicks, B. D., Vogt, A., Burdett, L., Yeager, M., Hoover, R. N., Chanock, S. J., and Savage, S. A. (2015) A Genome-Wide Scan Identifies Variants in NFIB Associated with Metastasis in Patients with Osteosarcoma. *Cancer Discov* **5**, 920-931

410. Ge, L., Cornforth, A. N., Hoa, N. T., Delgado, C., Chiou, S. K., Zhou, Y. H., and Jadus, M. R. (2012) Differential glioma-associated tumor antigen expression profiles of human glioma cells grown in hypoxia. *PLoS One* **7**, e42661
411. Breznik, B., Motaln, H., Vittori, M., Rotter, A., and Lah Turnsek, T. (2017) Mesenchymal stem cells differentially affect the invasion of distinct glioblastoma cell lines. *Oncotarget* **8**, 25482-25499
412. Franken, N. A., Rodermond, H. M., Stap, J., Haveman, J., and van Bree, C. (2006) Clonogenic assay of cells in vitro. *Nat Protoc* **1**, 2315-2319
413. Sumner, C., Shinohara, T., Durham, L., Traub, R., Major, E. O., and Amemiya, K. (1996) Expression of multiple classes of the nuclear factor-1 family in the developing human brain: differential expression of two classes of NF-1 genes. *Journal of neurovirology* **2**, 87-100
414. Nagainis, P. A., Wolfe, F. H., Sathe, S. K., and Goll, D. E. (1988) Autolysis of the millimolar Ca2+-requiring form of the Ca2+-dependent proteinase from chicken skeletal muscle. *Biochem Cell Biol* **66**, 1023-1031
415. Crawford, C., Willis, A. C., and Gagnon, J. (1987) The effects of autolysis on the structure of chicken calpain II. *The Biochemical journal* **248**, 579-588
416. Nath, R., Raser, K. J., Stafford, D., Hajimohammadreza, I., Posner, A., Allen, H., Talanian, R. V., Yuen, P., Gilbertsen, R. B., and Wang, K. K. (1996) Non-erythroid alpha-spectrin breakdown by calpain and interleukin 1 beta-converting-enzyme-like protease(s) in apoptotic cells: contributory roles of both protease families in neuronal apoptosis. *The Biochemical journal* **319 (Pt 3)**, 683-690
417. Bok, J., Wang, Q., Huang, J., and Green, S. H. (2007) CaMKII and CaMKIV mediate distinct prosurvival signaling pathways in response to depolarization in neurons. *Molecular and cellular neurosciences* **36**, 13-26
418. Kulkarni, S., Reddy, K. B., Esteva, F. J., Moore, H. C., Budd, G. T., and Tubbs, R. R. (2010) Calpain regulates sensitivity to trastuzumab and survival in HER2-positive breast cancer. *Oncogene* **29**, 1339-1350
419. Demarchi, F., Bertoli, C., Greer, P. A., and Schneider, C. (2005) Ceramide triggers an NF-kappaB-dependent survival pathway through calpain. *Cell death and differentiation* **12**, 512-522

420. Lacroix, M., Abi-Said, D., Fourney, D. R., Gokaslan, Z. L., Shi, W., DeMonte, F., Lang, F. F., McCutcheon, I. E., Hassenbusch, S. J., Holland, E., Hess, K., Michael, C., Miller, D., and Sawaya, R. (2001) A multivariate analysis of 416 patients with glioblastoma multiforme: prognosis, extent of resection, and survival. *Journal of neurosurgery* **95**, 190-198
421. Stummer, W., Pichlmeier, U., Meinel, T., Wiestler, O. D., Zanella, F., Reulen, H. J., and Group, A. L.-G. S. (2006) Fluorescence-guided surgery with 5-aminolevulinic acid for resection of malignant glioma: a randomised controlled multicentre phase III trial. *The Lancet. Oncology* **7**, 392-401
422. Chamberlain, M. C., Glantz, M. J., Chalmers, L., Van Horn, A., and Sloan, A. E. (2007) Early necrosis following concurrent Temodar and radiotherapy in patients with glioblastoma. *Journal of neuro-oncology* **82**, 81-83
423. Martinez, R., Schackert, G., Yaya-Tur, R., Rojas-Marcos, I., Herman, J. G., and Esteller, M. (2007) Frequent hypermethylation of the DNA repair gene MGMT in long-term survivors of glioblastoma multiforme. *Journal of neuro-oncology* **83**, 91-93
424. Miyazaki, M., Nishihara, H., Terasaka, S., Kobayashi, H., Yamaguchi, S., Ito, T., Kamoshima, Y., Fujimoto, S., Kaneko, S., Katoh, M., Ishii, N., Mohri, H., Tanino, M., Kimura, T., and Tanaka, S. (2014) Immunohistochemical evaluation of O -methylguanine DNA methyltransferase (MGMT) expression in 117 cases of glioblastoma. *Neuropathology*
425. Yip, S., Miao, J., Cahill, D. P., Iafrate, A. J., Aldape, K., Nutt, C. L., and Louis, D. N. (2009) MSH6 mutations arise in glioblastomas during temozolomide therapy and mediate temozolomide resistance. *Clinical cancer research : an official journal of the American Association for Cancer Research* **15**, 4622-4629
426. Erasimus, H., Gobin, M., Niclou, S., and Van Dyck, E. (2016) DNA repair mechanisms and their clinical impact in glioblastoma. *Mutat Res Rev Mutat Res* **769**, 19-35
427. Jiapaer, S., Furuta, T., Tanaka, S., Kitabayashi, T., and Nakada, M. (2018) Potential Strategies Overcoming the Temozolomide Resistance for Glioblastoma. *Neurol Med Chir (Tokyo)* **58**, 405-421
428. Paez-Ribes, M., Allen, E., Hudock, J., Takeda, T., Okuyama, H., Vinals, F., Inoue, M., Bergers, G., Hanahan, D., and Casanovas, O. (2009) Antiangiogenic therapy elicits malignant progression of tumors to increased local invasion and distant metastasis. *Cancer cell* **15**, 220-231
429. Zuniga, R. M., Torcuator, R., Jain, R., Anderson, J., Doyle, T., Ellika, S., Schultz, L., and Mikkelsen, T. (2009) Efficacy, safety and patterns of response and recurrence in patients with recurrent high-grade gliomas treated with bevacizumab plus irinotecan. *Journal of neuro-oncology* **91**, 329-336
430. Lefranc, F., Brotchi, J., and Kiss, R. (2005) Possible future issues in the treatment of glioblastomas: special emphasis on cell migration and the resistance of migrating glioblastoma cells to apoptosis. *Journal of clinical*

oncology : official journal of the American Society of Clinical Oncology **23**, 2411-2422
431. Speranza, M. C., Nowicki, M. O., Behera, P., Cho, C. F., Chiocca, E. A., and Lawler, S. E. (2016) BKM-120 (Buparlisib): A Phosphatidyl-Inositol-3 Kinase Inhibitor with Anti-Invasive Properties in Glioblastoma. *Sci Rep* **6**, 20189
432. Koul, D., Shen, R., Kim, Y. W., Kondo, Y., Lu, Y., Bankson, J., Ronen, S. M., Kirkpatrick, D. L., Powis, G., and Yung, W. K. (2010) Cellular and in vivo activity of a novel PI3K inhibitor, PX-866, against human glioblastoma. *Neuro Oncol* **12**, 559-569
433. Pitz, M. W., Eisenhauer, E. A., MacNeil, M. V., Thiessen, B., Easaw, J. C., Macdonald, D. R., Eisenstat, D. D., Kakumanu, A. S., Salim, M., Chalchal, H., Squire, J., Tsao, M. S., Kamel-Reid, S., Banerji, S., Tu, D., Powers, J., Hausman, D. F., and Mason, W. P. (2015) Phase II study of PX-866 in recurrent glioblastoma. *Neuro Oncol* **17**, 1270-1274
434. Shih, K. C., Chowdhary, S. A., Becker, K. P., Baehring, J. M., Liggett, W. H., Burris, H. A., and Hainsworth, J. D. (2015) A phase II study of the combination of BKM120 (buparlisib) and bevacizumab in patients with relapsed/refractory glioblastoma multiforme (GBM). *Journal of Clinical Oncology* **33**, 2065-2065
435. Chang, S. M., Wen, P., Cloughesy, T., Greenberg, H., Schiff, D., Conrad, C., Fink, K., Robins, H. I., De Angelis, L., Raizer, J., Hess, K., Aldape, K., Lamborn, K. R., Kuhn, J., Dancey, J., Prados, M. D., North American Brain Tumor, C., and the National Cancer, I. (2005) Phase II study of CCI-779 in patients with recurrent glioblastoma multiforme. *Invest New Drugs* **23**, 357-361
436. Hayden, M. S., and Ghosh, S. (2012) NF-kappaB, the first quarter-century: remarkable progress and outstanding questions. *Genes Dev* **26**, 203-234
437. Begalli, F., Bennett, J., Capece, D., Verzella, D., D'Andrea, D., Tornatore, L., and Franzoso, G. (2017) Unlocking the NF-kappaB Conundrum: Embracing Complexity to Achieve Specificity. *Biomedicines* **5**
438. Gilmore, T. D., and Herscovitch, M. (2006) Inhibitors of NF-kappaB signaling: 785 and counting. *Oncogene* **25**, 6887-6899
439. Anthony, T. E., Klein, C., Fishell, G., and Heintz, N. (2004) Radial glia serve as neuronal progenitors in all regions of the central nervous system. *Neuron* **41**, 881-890
440. Malatesta, P., Hartfuss, E., and Gotz, M. (2000) Isolation of radial glial cells by fluorescent-activated cell sorting reveals a neuronal lineage. *Development* **127**, 5253-5263
441. Malatesta, P., Hack, M. A., Hartfuss, E., Kettenmann, H., Klinkert, W., Kirchhoff, F., and Gotz, M. (2003) Neuronal or glial progeny: regional differences in radial glia fate. *Neuron* **37**, 751-764
442. Casper, K. B., and McCarthy, K. D. (2006) GFAP-positive progenitor cells produce neurons and oligodendrocytes throughout the CNS. *Molecular and cellular neurosciences* **31**, 676-684

443. Giachino, C., Basak, O., Lugert, S., Knuckles, P., Obernier, K., Fiorelli, R., Frank, S., Raineteau, O., Alvarez-Buylla, A., and Taylor, V. (2014) Molecular diversity subdivides the adult forebrain neural stem cell population. *Stem Cells* **32**, 70-84
444. Gao, J., Aksoy, B. A., Dogrusoz, U., Dresdner, G., Gross, B., Sumer, S. O., Sun, Y., Jacobsen, A., Sinha, R., Larsson, E., Cerami, E., Sander, C., and Schultz, N. (2013) Integrative analysis of complex cancer genomics and clinical profiles using the cBioPortal. *Sci Signal* **6**, pl1
445. Cerami, E., Gao, J., Dogrusoz, U., Gross, B. E., Sumer, S. O., Aksoy, B. A., Jacobsen, A., Byrne, C. J., Heuer, M. L., Larsson, E., Antipin, Y., Reva, B., Goldberg, A. P., Sander, C., and Schultz, N. (2012) The cBio cancer genomics portal: an open platform for exploring multidimensional cancer genomics data. *Cancer Discov* **2**, 401-404
446. Genovesi, L. A., Ng, C. G., Davis, M. J., Remke, M., Taylor, M. D., Adams, D. J., Rust, A. G., Ward, J. M., Ban, K. H., Jenkins, N. A., Copeland, N. G., and Wainwright, B. J. (2013) Sleeping Beauty mutagenesis in a mouse medulloblastoma model defines networks that discriminate between human molecular subgroups. *Proc Natl Acad Sci U S A* **110**, E4325-4334
447. Lastowska, M., Al-Afghani, H., Al-Balool, H. H., Sheth, H., Mercer, E., Coxhead, J. M., Redfern, C. P., Peters, H., Burt, A. D., Santibanez-Koref, M., Bacon, C. M., Chesler, L., Rust, A. G., Adams, D. J., Williamson, D., Clifford, S. C., and Jackson, M. S. (2013) Identification of a neuronal transcription factor network involved in medulloblastoma development. *Acta Neuropathol Commun* **1**, 35
448. Johansson, F. K., Brodd, J., Eklof, C., Ferletta, M., Hesselager, G., Tiger, C. F., Uhrbom, L., and Westermark, B. (2004) Identification of candidate cancer-causing genes in mouse brain tumors by retroviral tagging. *Proc Natl Acad Sci U S A* **101**, 11334-11337
449. Vyazunova, I., Maklakova, V. I., Berman, S., De, I., Steffen, M. D., Hong, W., Lincoln, H., Morrissy, A. S., Taylor, M. D., Akagi, K., Brennan, C. W., Rodriguez, F. J., and Collier, L. S. (2014) Sleeping Beauty mouse models identify candidate genes involved in gliomagenesis. *PLoS One* **9**, e113489
450. Schuur, E. R., Kruse, U., Iacovoni, J. S., and Vogt, P. K. (1995) Nuclear factor I interferes with transformation induced by nuclear oncogenes. *Cell Growth Differ* **6**, 219-227
451. Piper, M., Moldrich, R. X., Lindwall, C., Little, E., Barry, G., Mason, S., Sunn, N., Kurniawan, N. D., Gronostajski, R. M., and Richards, L. J. (2009) Multiple non-cell-autonomous defects underlie neocortical callosal dysgenesis in Nfib-deficient mice. *Neural Dev* **4**, 43
452. Hirabayashi, Y., Suzki, N., Tsuboi, M., Endo, T. A., Toyoda, T., Shinga, J., Koseki, H., Vidal, M., and Gotoh, Y. (2009) Polycomb limits the neurogenic competence of neural precursor cells to promote astrogenic fate transition. *Neuron* **63**, 600-613
453. Pereira, J. D., Sansom, S. N., Smith, J., Dobenecker, M. W., Tarakhovsky, A., and Livesey, F. J. (2010) Ezh2, the histone methyltransferase of

PRC2, regulates the balance between self-renewal and differentiation in the cerebral cortex. *Proc Natl Acad Sci U S A* **107**, 15957-15962
454. Wu, C., Zhu, X., Liu, W., Ruan, T., Wan, W., and Tao, K. (2018) NFIB promotes cell growth, aggressiveness, metastasis and EMT of gastric cancer through the Akt/Stat3 signaling pathway. *Oncol Rep* **40**, 1565-1573
455. Yu, H., Lee, H., Herrmann, A., Buettner, R., and Jove, R. (2014) Revisiting STAT3 signalling in cancer: new and unexpected biological functions. *Nature reviews. Cancer* **14**, 736-746
456. Zhang, H. F., and Lai, R. (2014) STAT3 in Cancer-Friend or Foe? *Cancers (Basel)* **6**, 1408-1440
457. Zhang, H. F., Chen, Y., Wu, C., Wu, Z. Y., Tweardy, D. J., Alshareef, A., Liao, L. D., Xue, Y. J., Wu, J. Y., Chen, B., Xu, X. E., Gopal, K., Gupta, N., Li, E. M., Xu, L. Y., and Lai, R. (2016) The Opposing Function of STAT3 as an Oncoprotein and Tumor Suppressor Is Dictated by the Expression Status of STAT3beta in Esophageal Squamous Cell Carcinoma. *Clinical cancer research : an official journal of the American Association for Cancer Research* **22**, 691-703
458. Johansson, E. M., Kannius-Janson, M., Bjursell, G., and Nilsson, J. (2003) The p53 tumor suppressor gene is regulated in vivo by nuclear factor 1-C2 in the mouse mammary gland during pregnancy. *Oncogene* **22**, 6061-6070
459. Ouellet, S., Vigneault, F., Lessard, M., Leclerc, S., Drouin, R., and Guerin, S. L. (2006) Transcriptional regulation of the cyclin-dependent kinase inhibitor 1A (p21) gene by NFI in proliferating human cells. *Nucleic Acids Res* **34**, 6472-6487
460. McClure, C., Ali, E., Youssef, D., Yao, Z. Q., McCall, C. E., and El Gazzar, M. (2016) NFI-A disrupts myeloid cell differentiation and maturation in septic mice. *J Leukoc Biol* **99**, 201-211
461. Liu, R., Lonergan, S., Steadham, E., Zhou, G., Zhang, W., and Huff-Lonergan, E. (2019) Effect of nitric oxide and calpastatin on the inhibition of micro-calpain activity, autolysis and proteolysis of myofibrillar proteins. *Food Chem* **275**, 77-84
462. Du, M., Li, X., Li, Z., Shen, Q., Ren, C., and Zhang, D. (2019) Calpastatin inhibits the activity of phosphorylated mu-calpain in vitro. *Food Chem* **274**, 743-749
463. Wang, S., Huang, Y., Yan, Y., Zhou, H., Wang, M., Liao, L., Wang, Z., Chen, D., Ji, D., Xia, X., Liu, F., Huang, J., and Xiong, K. (2019) Calpain2 but not calpain1 mediated by calpastatin following glutamate-induced regulated necrosis in rat retinal neurons. *Ann Anat* **221**, 57-67
464. Li, S., Ma, J., Li, J. B., Lacefield, J. C., Jones, D. L., Peng, T. Q., and Wei, M. (2018) Over-expression of calpastatin attenuates myocardial injury following myocardial infarction by inhibiting endoplasmic reticulum stress. *J Thorac Dis* **10**, 5283-5297
465. Crawford, C. (1990) Protein and peptide inhibitors of calpains. in *Intracellular Calcium-Dependent Proteolysis* (Ronald L. Mellgren, T. M. ed.), CRC, Boca Raton, Florida. pp 75-89

466. Onizuka, K., Kunimatsu, M., Ozaki, Y., Muramatsu, K., Sasaki, M., and Nishino, H. (1995) Distribution of mu-calpain proenzyme in the brain and other neural tissues in the rat. *Brain research* **697**, 179-186
467. Baki, A., Tompa, P., Alexa, A., Molnar, O., and Friedrich, P. (1996) Autolysis parallels activation of mu-calpain. *The Biochemical journal* **318 (Pt 3)**, 897-901
468. Croall, D. E., and DeMartino, G. N. (1991) Calcium-activated neutral protease (calpain) system: structure, function, and regulation. *Physiol Rev* **71**, 813-847
469. Cottin, P., Thompson, V. F., Sathe, S. K., Szpacenko, A., and Goll, D. E. (2001) Autolysis of mu- and m-calpain from bovine skeletal muscle. *Biological chemistry* **382**, 767-776
470. Singh, R., Brewer, M. K., Mashburn, C. B., Lou, D., Bondada, V., Graham, B., and Geddes, J. W. (2014) Calpain 5 is highly expressed in the central nervous system (CNS), carries dual nuclear localization signals, and is associated with nuclear promyelocytic leukemia protein bodies. *J Biol Chem* **289**, 19383-19394
471. Chang, H., Sheng, J. J., Zhang, L., Yue, Z. J., Jiao, B., Li, J. S., and Yu, Z. B. (2015) ROS-Induced Nuclear Translocation of Calpain-2 Facilitates Cardiomyocyte Apoptosis in Tail-Suspended Rats. *J Cell Biochem* **116**, 2258-2269
472. Mellgren, R. L., and Lu, Q. (1994) Selective nuclear transport of mu-calpain. *Biochem Biophys Res Commun* **204**, 544-550
473. Sorimachi, H., Mamitsuka, H., and Ono, Y. (2012) Understanding the substrate specificity of conventional calpains. *Biological chemistry* **393**, 853-871
474. Shinkai-Ouchi, F., Koyama, S., Ono, Y., Hata, S., Ojima, K., Shindo, M., duVerle, D., Ueno, M., Kitamura, F., Doi, N., Takigawa, I., Mamitsuka, H., and Sorimachi, H. (2016) Predictions of Cleavability of Calpain Proteolysis by Quantitative Structure-Activity Relationship Analysis Using Newly Determined Cleavage Sites and Catalytic Efficiencies of an Oligopeptide Array. *Mol Cell Proteomics* **15**, 1262-1280
475. Cuerrier, D., Moldoveanu, T., and Davies, P. L. (2005) Determination of peptide substrate specificity for mu-calpain by a peptide library-based approach: the importance of primed side interactions. *J Biol Chem* **280**, 40632-40641
476. Tompa, P., Buzder-Lantos, P., Tantos, A., Farkas, A., Szilagyi, A., Banoczi, Z., Hudecz, F., and Friedrich, P. (2004) On the sequential determinants of calpain cleavage. *J Biol Chem* **279**, 20775-20785
477. Liu, W., Ma, K., Kwon, S. H., Garg, R., Patta, Y. R., Fujiwara, T., and Gurtner, G. C. (2017) The Abnormal Architecture of Healed Diabetic Ulcers Is the Result of FAK Degradation by Calpain 1. *J Invest Dermatol* **137**, 1155-1165
478. Kulkarni, S., Saido, T. C., Suzuki, K., and Fox, J. E. (1999) Calpain mediates integrin-induced signaling at a point upstream of Rho family members. *J Biol Chem* **274**, 21265-21275

479. Li, C., Chen, S., Yue, P., Deng, X., Lonial, S., Khuri, F. R., and Sun, S. Y. (2010) Proteasome inhibitor PS-341 (bortezomib) induces calpain-dependent IkappaB(alpha) degradation. *J Biol Chem* **285**, 16096-16104
480. Liu, T. L., Shimada, H., Ochiai, T., Shiratori, T., Lin, S. E., Kitagawa, M., Harigaya, K., Maki, M., Oka, M., Abe, T., Takiguchi, M., and Hiwasa, T. (2006) Enhancement of chemosensitivity toward peplomycin by calpastatin-stabilized NF-kappaB p65 in esophageal carcinoma cells: possible involvement of Fas/Fas-L synergism. *Apoptosis* **11**, 1025-1037
481. Mlynarczuk-Bialy, I., Roeckmann, H., Kuckelkorn, U., Schmidt, B., Umbreen, S., Golab, J., Ludwig, A., Montag, C., Wiebusch, L., Hagemeier, C., Schadendorf, D., Kloetzel, P. M., and Seifert, U. (2006) Combined effect of proteasome and calpain inhibition on cisplatin-resistant human melanoma cells. *Cancer research* **66**, 7598-7605
482. Briz, V., Hsu, Y. T., Li, Y., Lee, E., Bi, X., and Baudry, M. (2013) Calpain-2-mediated PTEN degradation contributes to BDNF-induced stimulation of dendritic protein synthesis. *The Journal of neuroscience : the official journal of the Society for Neuroscience* **33**, 4317-4328
483. Freitas, A. C., Figueiredo, M. J., Campos, E. C., Soave, D. F., Ramos, S. G., Tanowitz, H. B., and Celes, M. R. (2016) Activation of Both the Calpain and Ubiquitin-Proteasome Systems Contributes to Septic Cardiomyopathy through Dystrophin Loss/Disruption and mTOR Inhibition. *PLoS One* **11**, e0166839
484. Abeyrathna, P., Kovacs, L., Han, W., and Su, Y. (2016) Calpain-2 activates Akt via TGF-beta1-mTORC2 pathway in pulmonary artery smooth muscle cells. *Am J Physiol Cell Physiol* **311**, C24-34
485. Ho, W. C., Pikor, L., Gao, Y., Elliott, B. E., and Greer, P. A. (2012) Calpain 2 regulates Akt-FoxO-p27(Kip1) protein signaling pathway in mammary carcinoma. *J Biol Chem* **287**, 15458-15465
486. Kubbutat, M. H., and Vousden, K. H. (1997) Proteolytic cleavage of human p53 by calpain: a potential regulator of protein stability. *Mol Cell Biol* **17**, 460-468
487. Ahmad, F., Das, D., Kommaddi, R. P., Diwakar, L., Gowaikar, R., Rupanagudi, K. V., Bennett, D. A., and Ravindranath, V. (2018) Isoform-specific hyperactivation of calpain-2 occurs presymptomatically at the synapse in Alzheimer's disease mice and correlates with memory deficits in human subjects. *Scientific Reports* **8**, 13119
488. Trinchese, F., Fa, M., Liu, S., Zhang, H., Hidalgo, A., Schmidt, S. D., Yamaguchi, H., Yoshii, N., Mathews, P. M., Nixon, R. A., and Arancio, O. (2008) Inhibition of calpains improves memory and synaptic transmission in a mouse model of Alzheimer disease. *J Clin Invest* **118**, 2796-2807
489. Bartus, R. T., Hayward, N. J., Elliott, P. J., Sawyer, S. D., Baker, K. L., Dean, R. L., Akiyama, A., Straub, J. A., Harbeson, S. L., Li, Z., and et al. (1994) Calpain inhibitor AK295 protects neurons from focal brain ischemia. Effects of postocclusion intra-arterial administration. *Stroke* **25**, 2265-2270

490. Saatman, K. E., Creed, J., and Raghupathi, R. (2010) Calpain as a therapeutic target in traumatic brain injury. *Neurotherapeutics* **7**, 31-42
491. Kawamura, M., Nakajima, W., Ishida, A., Ohmura, A., Miura, S., and Takada, G. (2005) Calpain inhibitor MDL 28170 protects hypoxic-ischemic brain injury in neonatal rats by inhibition of both apoptosis and necrosis. *Brain research* **1037**, 59-69
492. Squier, M. K., Miller, A. C., Malkinson, A. M., and Cohen, J. J. (1994) Calpain activation in apoptosis. *Journal of cellular physiology* **159**, 229-237
493. Smith, M. A., and Schnellmann, R. G. (2012) Calpains, mitochondria, and apoptosis. *Cardiovasc Res* **96**, 32-37
494. Momeni, H. R. (2011) Role of calpain in apoptosis. *Cell J* **13**, 65-72
495. Zhang, W., Liu, J., Sun, R., Zhao, L., Du, J., Ruan, C., and Dai, K. (2011) Calpain activator dibucaine induces platelet apoptosis. *Int J Mol Sci* **12**, 2125-2137
496. Vilagi, I., Kiss, D. S., Farkas, A., Borbely, S., Tarnok, K., Halasy, K., Banoczi, Z., Hudecz, F., and Friedrich, P. (2008) Synthetic calpain activator boosts neuronal excitability without extra Ca2+. *Molecular and cellular neurosciences* **38**, 629-636
497. Banoczi, Z., Tantos, A., Farkas, A., Tompa, P., Friedrich, P., and Hudecz, F. (2007) Synthesis of cell-penetrating conjugates of calpain activator peptides. *Bioconjug Chem* **18**, 130-137
498. Li, Y., Arnold, J. M., Pampillo, M., Babwah, A. V., and Peng, T. (2009) Taurine prevents cardiomyocyte death by inhibiting NADPH oxidase-mediated calpain activation. *Free Radic Biol Med* **46**, 51-61
499. Levesque, S., Wilson, B., Gregoria, V., Thorpe, L. B., Dallas, S., Polikov, V. S., Hong, J. S., and Block, M. L. (2010) Reactive microgliosis: extracellular micro-calpain and microglia-mediated dopaminergic neurotoxicity. *Brain* **133**, 808-821
500. Rao, J. S. (2003) Molecular mechanisms of glioma invasiveness: the role of proteases. *Nature reviews. Cancer* **3**, 489-501
501. Deryugina, E. I., and Quigley, J. P. (2008) Chick embryo chorioallantoic membrane model systems to study and visualize human tumor cell metastasis. *Histochem Cell Biol* **130**, 1119-1130
502. Ma, J., Cui, W., He, S. M., Duan, Y. H., Heng, L. J., Wang, L., and Gao, G. D. (2012) Human U87 astrocytoma cell invasion induced by interaction of betaig-h3 with integrin alpha5beta1 involves calpain-2. *PLoS One* **7**, e37297
503. Demarchi, F., Bertoli, C., Copetti, T., Tanida, I., Brancolini, C., Eskelinen, E. L., and Schneider, C. (2006) Calpain is required for macroautophagy in mammalian cells. *J Cell Biol* **175**, 595-605
504. Lu, Q., and Mellgren, R. L. (1996) Calpain inhibitors and serine protease inhibitors can produce apoptosis in HL-60 cells. *Arch Biochem Biophys* **334**, 175-181

505. Hajji, N., Mateos, S., Pastor, N., Dominguez, I., and Cortes, F. (2005) Induction of genotoxic and cytotoxic damage by aclarubicin, a dual topoisomerase inhibitor. *Mutation research* **583**, 26-35
506. Nitiss, J. L., Pourquier, P., and Pommier, Y. (1997) Aclacinomycin A stabilizes topoisomerase I covalent complexes. *Cancer research* **57**, 4564-4569
507. Chaires, J. B., Herrera, J. E., and Waring, M. J. (1990) Preferential binding of daunomycin to 5'ATCG and 5'ATGC sequences revealed by footprinting titration experiments. *Biochemistry* **29**, 6145-6153
508. Duggan, S. T., and Keating, G. M. (2011) Pegylated liposomal doxorubicin: a review of its use in metastatic breast cancer, ovarian cancer, multiple myeloma and AIDS-related Kaposi's sarcoma. *Drugs* **71**, 2531-2558
509. Li, P. A., Howlett, W., He, Q. P., Miyashita, H., Siddiqui, M., and Shuaib, A. (1998) Postischemic treatment with calpain inhibitor MDL 28170 ameliorates brain damage in a gerbil model of global ischemia. *Neuroscience letters* **247**, 17-20
510. Chen, Z. F., Schottler, F., and Lee, K. S. (1997) Neuronal recovery after moderate hypoxia is improved by the calpain inhibitor MDL28170. *Brain research* **769**, 188-192
511. Thompson, S. N., Carrico, K. M., Mustafa, A. G., Bains, M., and Hall, E. D. (2010) A pharmacological analysis of the neuroprotective efficacy of the brain- and cell-permeable calpain inhibitor MDL-28170 in the mouse controlled cortical impact traumatic brain injury model. *Journal of neurotrauma* **27**, 2233-2243
512. Mehdi, S. (1991) Cell-penetrating inhibitors of calpain. *Trends in biochemical sciences* **16**, 150-153
513. Mathiasen, I. S., Sergeev, I. N., Bastholm, L., Elling, F., Norman, A. W., and Jaattela, M. (2002) Calcium and calpain as key mediators of apoptosis-like death induced by vitamin D compounds in breast cancer cells. *J Biol Chem* **277**, 30738-30745
514. Tagliarino, C., Pink, J. J., Reinicke, K. E., Simmers, S. M., Wuerzberger-Davis, S. M., and Boothman, D. A. (2003) Mu-calpain activation in beta-lapachone-mediated apoptosis. *Cancer Biol Ther* **2**, 141-152